UNCLASSIFIED

AD NUMBER
ADB274493
NEW LIMITATION CHANGE

TO

Approved for public release, distribution
unlimited

FROM

Distribution authorized to U.S. Gov't.
agencies only; Propietary Info.; Sep 2001.
Other requests shall be referred to U.S.
army Medical Research and Materiel
Command, 504 Scott St., Ft. Detrick, MD,
21702-5012.

AUTHORITY

USAMRMC ltr, 26 Aug 2002

THIS PAGE IS UNCLASSIFIED

AD_____

Award Number: DAMD17-97-1-7076

TITLE: Combinatorial Synthesis for the Expedited Discovery of Novel Selective Antiestrogens for Breast Cancer Prevention and Therapy

PRINCIPAL INVESTIGATOR: John A. Katzenellenbogen, Ph.D.

CONTRACTING ORGANIZATION: University of Illinois
Champaign, Illinois 61820-6242

REPORT DATE: September 2001

TYPE OF REPORT: Final

PREPARED FOR: U.S. Army Medical Research and Materiel Command
Fort Detrick, Maryland 21702-5012

DISTRIBUTION STATEMENT: Distribution authorized to U.S. Government agencies only (proprietary information, Sep 01). Other requests for this document shall be referred to U.S. Army Medical Research and Materiel Command, 504 Scott Street, Fort Detrick, Maryland 21702-5012.

20020124 395

NOTICE

USING GOVERNMENT DRAWINGS, SPECIFICATIONS, OR OTHER DATA INCLUDED IN THIS DOCUMENT FOR ANY PURPOSE OTHER THAN GOVERNMENT PROCUREMENT DOES NOT IN ANY WAY OBLIGATE THE U.S. GOVERNMENT. THE FACT THAT THE GOVERNMENT FORMULATED OR SUPPLIED THE DRAWINGS, SPECIFICATIONS, OR OTHER DATA DOES NOT LICENSE THE HOLDER OR ANY OTHER PERSON OR CORPORATION; OR CONVEY ANY RIGHTS OR PERMISSION TO MANUFACTURE, USE, OR SELL ANY PATENTED INVENTION THAT MAY RELATE TO THEM.

LIMITED RIGHTS LEGEND

THIS TECHNICAL REPORT HAS BEEN REVIEWED AND IS APPROVED FOR PUBLICATION.

Earl Hunt Jr. LTC, MS
4 Jan 02

REPORT DOCUMENTATION PAGE

Public reporting burden for this collection of information is estimated to average 1 hour per response, including the time for reviewing instructions, searching existing data sources, gathering and maintaining the data needed, and completing and reviewing this collection of information. Send comments regarding this burden estimate or any other aspect of this collection of information, including suggestions for reducing this burden to Washington Headquarters Services, Directorate for Information Operations and Reports, 1215 Jefferson Davis Highway, Suite 1204, Arlington, VA 22202-4302, and to the Office of Management and Budget, Paperwork Reduction Project (0704-0188), Washington, DC 20503

1. AGENCY USE ONLY (Leave blank)	2. REPORT DATE September 2001	3. REPORT TYPE AND DATES COVERED Final (1 Sep 97 – 31 Aug 01)

4. TITLE AND SUBTITLE
Combinatorial Synthesis for the Expedited Discovery of Novel Selective Antiestrogens for Breast Cancer Prevention and Therapy

5. FUNDING NUMBERS
DAMD17-97-1-7076

6. AUTHOR(S)
John A. Katzenellenbogen, Ph.D.

7. PERFORMING ORGANIZATION NAME(S) AND ADDRESS(ES)
University of Illinois
Champaign, Illinois 61820-6242
E-Mail: jkatzene@uiuc.edu

8. PERFORMING ORGANIZATION REPORT NUMBER

9. SPONSORING / MONITORING AGENCY NAME(S) AND ADDRESS(ES)
U.S. Army Medical Research and Materiel Command
Fort Detrick, Maryland 21702-5012

10. SPONSORING / MONITORING AGENCY REPORT NUMBER

11. SUPPLEMENTARY NOTES
Report contains color

12a. DISTRIBUTION / AVAILABILITY STATEMENT
Distribution authorized to U.S. Government agencies only (proprietary information, Sep 01).
Other requests for this document shall be referred to U.S. Army Medical Research and
Materiel Command, 504 Scott Street, Fort Detrick, Maryland 21702-5012.

12b. DISTRIBUTION CODE

13. Abstract *(Maximum 200 Words)* *(abstract should contain no proprietary or confidential information)*

We have conceived of an approach to prepare by combinatorial methods, libraries of novel ligands for the estrogen receptor, by the creation of simple amide or five-membered ring heterocyclic core structures that display peripheral substituents (phenols, aliphatic groups, etc.) commonly found in non-steroidal estrogens. These novel estrogens might be useful in the treatment or prevention of breast cancer.

We have made excellent progress on the preparation of novel estrogens of the diphenyl carboxamide class, the diphenylsulfonamide class, the phenyl benzylcarboxamide and sulfonamide classes, and the pyrazole, oxazole, thiazole, and imidazole classes. Members of some classes have high affinity for the estrogen receptor, and some of them show high binding and potency selectivity for the estrogen receptor subtype alpha and can be adapted as selective estrogen receptor alpha antagonists. We have also developed a convenient solid phase synthesis of the pyrazole class, so that we can prepare conveniently and rapidly larger libraries of the members of what appear presently to be the most promising of these classes of novel estrogens.

14. SUBJECT TERMS Breast Cancer	15. NUMBER OF PAGES 176
	16. PRICE CODE

17. SECURITY CLASSIFICATION OF REPORT Unclassified	18. SECURITY CLASSIFICATION OF THIS PAGE Unclassified	19. SECURITY CLASSIFICATION OF ABSTRACT Unclassified	20. LIMITATION OF ABSTRACT Unlimited

NSN 7540-01-280-5500

Standard Form 298 (Rev. 2-89)
Prescribed by ANSI Std. Z39-18
298-102

TABLE OF CONTENTS

FINAL REPORT: September 1, 1997 – August 31, 2001

PRINCIPAL INVESTIGATOR: John A. Katzenellenbogen

TITLE: Combinatorial Synthesis For The Expedited Discovery Of Novel Selective Antiestrogens For Breast Cancer Prevention And Therapy

ORGANIZATION: University Of Illinois

++++++++++++++++++++++++++

INTRODUCTION, GOALS OF THE PROJECT AND APPROACH

[NOTE 1: This project was funded for three years, and a final report was submitted September, 2000, covering the progress for the initial three year period. However, I received a one-year no-cost extension on this project, to complete some of the studies that were still ongoing on August 31, 2000. Thus, this "second" final report is largely the same as the previous final report submitted in September, 2000. It has simply been updated to indicate the additional progress that was made during the year of the no-cost extension. To facilitate review of this second final report, those sections that have been added or modified are so indicated with underlining.]

[NOTE 2: For the purpose of continuity, the three Schemes in the attached Appendix have been taken directly from the original proposal. The details of this final report are contained in seven reprints and three manuscripts that are appended. Specific reference is made to these as "Publications No. 1-10".]

Antiestrogens such as tamoxifen are widely used in the treatment of hormone responsive breast cancer and were recently shown to be effective in breast cancer prevention[1-5]. Tamoxifen, however, as well as the pure ICI antiestrogens, are not ideal agents, because they cause vaginal atrophy and menopausal host flashes, induce osteoporosis (pure antiestrogens), and may cause endometrial and liver cancer (tamoxifen)[6-14]. Thus, there is a need for the development of selective antiestrogens with an improved endocrine profile for use in the treatment and prevention of breast cancer[15-16].

Recent advances in our understanding of the molecular pharmacology of estrogens and the development of new selective antiestrogens for menopausal bone maintenance, suggest that new selective antiestrogens of this type can be discovered [16-25]. Up to now, however, this search has not been approached in a systematic fashion [26]. Furthermore, the structures of antiestrogens that have been studied to date are quite complex and their synthesis sufficiently challenging, so as not to be amenable to synthesis by solid-phase combinatorial means. Combinatorial synthesis is the fastest growing new technology in pharmaceutical chemistry, and is proving to be a highly expeditious and promising approach to new drug discovery [27-35].

In preparing for this project, we analyzed the structures of many selective antiestrogens and found that they possess three common peripheral groups (a phenol, a second aromatic group, and a basic side chain) attached to various core structures. Because the core structure appears to function as a scaffold simply to hold these other appendages together, we then designed six novel core structures that will perform the same scaffold function for the peripheral groups, yet are sufficiently simple that they can be readily prepared by solid-phase combinatorial synthesis.

In this project, we proposed to prepare six novel classes of ligands for the estrogen receptor, based on four functional group so far unexplored in the antiestrogen literature: a carboxamide, a sulfonamide, a pyrazole, and an oxazole (and related thiazole and imidazole). Solution-phase syntheses were first to be developed, and then adapted to solid-phase synthesis using an acid-labile linker attached to the common phenol function. Libraries containing larger numbers of the best of these classes were then to be prepared, and all of these compounds then to be assayed for their binding affinity for the estrogen receptor. The estrogen agonist and antagonist activity of those members with high affinity was then later to be determined in cell transfection and proliferation assays, and those with the most appropriate endocrine activity tested in a uterotrophic assay.

The combination of this novel structural insight leading to the design of new core structures for estrogen receptor ligands that can be readily prepared by combinatorial synthesis, together with a set of simple, but effective assays to establish their hormonal activity, should assist in the discovery of novel selective antiestrogens for the treatment and prevention of breast cancer.

+++++++++++++++++++++++++++++

BODY

Experimental Approach

A General Structural Description of Selective Estrogen Receptor Ligands Suggests Alternate Core Structures that Can be Prepared by Solid Phase Combinatorial Chemistry Methods

As a class, selective antiestrogens can be envisioned as having four structural components (Schemes 1 and 2 in attached Appendix [taken from the original proposal]): *a core structure* (**A**) onto which are appended three other structural elements, *a phenol* (**B**), *a second aromatic group* (**C**) and *a basic side chain* (**D**). The achievement of an appropriate balance of estrogenic vs antiestrogenic activities in each of these series of selective antiestrogens appears to involve a delicate interaction between these component parts of their structure. Curiously, whereas components **B**, **C**, and **D** are rather similar in almost all of the selective antiestrogens (cf. Scheme 1, selective antiestrogens), the central core structure **A**, which links together the other three components like a scaffold, is quite variable. This suggests that other core structures could replace this central component in selective antiestrogens.

In the original proposal we proposed to explore new antiestrogens specifically designed to have novel core structures that are readily amenable to solid phase combinatorial synthesis and which may prove to be more tissue selective and efficacious for breast cancer. As explained in Scheme 3 in attached Appendix [taken from the original proposal], we identified three simple structure motifs that are found in ER ligands, around which we designed six new classes of potential ligands for the ER that are based on four new core structures (Scheme 3, right column). We anticipated that these four core structures—a carboxamide, a sulfonamide, a pyrazole, and an oxazole (and a related thiazole and imidazole)—would provide a suitable molecular scaffold for the other three components typically found in selective antiestrogens—the phenol, the second aromatic unit, and the basic side chain—so that these new structural classes would also have selective antiestrogenic activity. The unique feature of these new core structures is that, unlike most antiestrogens develop to date, they can be prepared by combinatorial chemistry means.

The first of the motifs, *motif A is an anti-bibenzyl system*, a structural subunit that is found in the potent estrogen hexestrol, as well as in the antiestrogen hydroxytamoxifen (Scheme 3). The structural analogs of this motif that we planned to explore, the diphenylcarboxamide and diphenylsulfonamide (Classes I and II), are well suited to three-component combinatorial solid phase synthesis methods (see below and Scheme 6). *Motif B is the homolog of the bibenzyl motif*, a substructure that is exemplified in the potent estrogen benzestrol and the selective estrogen raloxifene, but is otherwise largely undeveloped. We planned to explore several structural analogs of the homobibenzyl motif that are better suited for solid phase three-component combinatorial synthesis, benzylic homologs of the carboxamides and sulfonamides (Classes III and IV) and pyrazoles (Class V) (see below and Schemes 6 and 7). Finally, *Motif C, a syn-bibenzyl system* found in tamoxifen and centchroman, is the motivation for the three-

component combinatorial synthesis of a series of heterocyclic analogs, oxazoles, thiazoles, and imidazoles (Class VI; see below and Scheme 8).

As we discuss below, we have made good progress evaluating the synthetic feasibility and ER binding affinity of members of all of these classes, as well as some others.

Results and Discussion for total project, years 1-3, plus one year no-cost extension.

The original statement of work for years 1-3 of this project are listed below.

===
ORIGINAL STATEMENT OF WORK

Project Period: July 1, 1997– June 30, 2000 (3 years)

Year 1
- Synthesis of representative members of Class I-VI ligands by solution phase methods.
- Isolate, purify, and fully characterize these members.
- Measure estrogen receptor binding affinity of representative members of Class I-VI ligands
- Begin to adapt solution phase syntheses to solid phase.

Year 2
- Complete adaptation of solution phase synthesis to solid phase.
- Isolate and fully characterize representative members produced by solid phase synthesis. Determine yield and characterize impurities.
- Compare estrogen receptor binding of representative members of Class I-VI ligands prepared by solution vs solid phase.
- Begin synthesis of full Class I-VI libraries.
- Begin cell proliferation and cell-based transfection assays.

Year 3
- Complete synthesis of full Class I-VI libraries.
- Complete estrogen receptor assay of full libraries at two concentrations.
- Reassay the members with detectable estrogen receptor binding affinity by quantitative titration assay.
- Assay the members with high estrogen receptor binding affinity in the cell proliferation and cell-based transfection assays.

• Assay uterotrophic activity of the most promising members in rats.

===

Summary — Through the work we have engaged in on this project over the past three years, we have completed all of the goals of the original proposal, as summarized in the original Statement of Work. This has involved an exploration of the promise of all of the proposed acyclic amide and 5-membered ring heterocyclic systems, and the development of solid phase synthesis methods and large library synthesis and analysis. In addition, we have discovered in the process that some of the most promising heterocyclic ligands, the pyrazoles, have high affinity and potency selectivity for one of the estrogen receptor subtypes, ERα. Because the development of estrogen receptor subtype selective ligands is a very important issue and one of great current interest, we have devoted considerable efforts in years 2, 3, and 4 to pursue this further. We have completed a careful structure-activity relationship study on the pyrazoles, obtaining ultimately a compound that is almost a completely specific activator of ERα, having essentially no activity on ERβ at doses where it maximally stimulated ERα, and, based on these findings, we have developed a series of pyrazole basic side chain derivatives that hold considerable promise as potency selective antagonists of ERα. Such compounds could be used to block the action of estradiol through this receptor subtype without interfering with its effect on ERβ.

The work that we have done on this project has also spawned several related lines of inquiry that are currently being pursued in my laboratory with independent support. These include investigations of other 5-membered ring heterocyclic systems as estrogen receptor ligands, namely furans, thiophenes, and pyrroles, as well as carbocyclic analogs, cyclopentadienes and related cyclopentadienones. In addition, based on the favorable results of the work under this project, we have begun to synthesize 6-membered ring heterocycles such as pyrazines, pyrimidines, and pyridazines as estrogen receptor ligands. This work is <u>now beginning to mature, and we already</u> know that we have compounds that show high affinity for the receptor, <u>showing high ER subtype selectivity,</u> and are therefore potentially quite interesting, because their structures are unique in the estrogen receptor field.

We certainly appreciate the support that has been provided to our research efforts in this area through this US Army grant. It has served as a stimulus to us to thrust our laboratory research into new directions that have proved to be very fruitful and potentially useful for the prevention and treatment of breast cancer.

The details of this final report are contained in <u>seven</u> reprints and <u>three</u> manuscript that are appended. Specific reference is made to these as "Publications No. 1-<u>10</u>".

Publication No. 1: B. E. Fink, D. S. Mortensen, S. R. Stauffer, Z. D. Aron, J. A. Katzenellenbogen. Novel Structural Templates for Estrogen-Receptor Ligands and Prospects for Combinatorial Synthesis of Estrogens. *Chem. & Biol.*, 1999, *6*, 205-219.

Publication No. 2: S. R. Stauffer, J. Sun, B. S. Katzenellenbogen, J. A. Katzenellenbogen. Acyclic Amides as Estrogen Receptor Ligands: Synthesis, Binding, Activity, and Receptor Interaction. *Bio. Med. Chem.*, 2000, *8*, 1293-1316.

Publication No. 3: S. R. Stauffer, J. A. Katzenellenbogen. Solid-Phase Synthesis of Tetra-Substituted Pyrazoles, Novel Ligands for the Estrogen Receptor. *J. Comb. Chem.*, 2000, *2*, 318-329.

Publication No. 4: S. R. Stauffer, C. J. Coletta, J. Sun, B. S. Katzenellenbogen, J. A. Katzenellenbogen. Pyrazole Ligands: Structure-Affinity/Activity Relationships of Estrogen Receptor-α Selective Agonists. *J. Med. Chem.*, <u>2000, *43*, 4934-4947.</u>

Publication No. 5: S. R. Stauffer, Y. Huang, C. J. Coletta, R. Tedesco, J. A. Katzenellenbogen. Estrogen Pyrazoles: Defining the Pyrazole Core Structure and the Orientation of Substituents in the Ligand Binding Pocket of the Estrogen Receptor. *Bio. Med. Chem.*, <u>2001, *9*, 141-150.</u>

Publication No. 6: S. R. Stauffer, Y. R. Huang, Z. D. Aron, C. J. Coletta, J. Sun, B. S. Katzenellenbogen, J. A. Katzenellenbogen. Triarlpyrazoles with Basic Side Chains: Development of Pyrazole-Based Estrogen Receptor Antagonists. *Bio. Med. Chem.*, <u>2001, *9*, 151-161.</u>

Publication No. 7: Y. R. Huang, J. A. Katzenellenbogen. Regioselective Synthesis of 1,3,5-Triaryl-4-alkylpyrazoles: Novel Ligands for the Estrogen Receptor. *Org. Lett*, 2000, <u>*2*, 2833-2836.</u>

<u>**Publication No. 8:** D. S. Mortensen, A. L. Rodriquez, K. E. Carlson, J. Sun, B. S. Katzenellenbogen, J. A. Katzenellenbogen. Synthesis and Biological Evaluation of a Novel Series of Furans: Ligands Selective for Estrogen Receptor Alpha. *J. Med Chem.*, 2001, In Press.</u>

<u>**Publication No. 9:** D. S. Mortensen, A. L. Rodriquez, J. Sun, B. S. Katzenellenbogen, J. A. Katzenellenbogen. Furans with Basic Side Chains: Synthesis and Biological Evaluation of a Novel Series of Antagonists with Selectivity for the Estrogen Receptor Alpha. *Bioorg. Med. Chem. Letters*, 2001, In Press</u>

Investigation of Novel Core Structures of Estrogen Receptor Ligands [Publications No. 1 and 2]

In the first of these publications [**Publication No. 1**], we surveyed a series of heterocyclic systems to identify which core structure from among those originally proposed (pyrazole, imidazole, oxazole, thiazole, isoxazole and isothiazole classes) were capable of giving ligands with high affinity for the estrogen receptor. This work definitively identified the pyrazole class as the most promising one, and one tetrasubstituted pyrazole, in particular, had a binding affinity that reached 19% that of estradiol, a truly remarkable finding. This compound is numbered **38d** in this publication.

The second of these publications [**Publication No. 2**] we surveyed a series of amides (carboxamides, thiocarboxamides, and sulfonamides) as potential ligands for the estrogen receptor. Again, we found that high affinity for the receptor was restricted to the diphenylcarboxamide class and then only to those analogs having appropriate substituents. The most promising agend, compound **16g** in this publication, has an affinity 15% that of estradiol. This work included extensive analysis of the conformation of these flexible ligands with the aim of understanding how they fit into the ligand binding pocket.

Development of Solid Phase Synthesis Methods to Prepare the Most Promising Ligands [Publication No. 3]

In this publication, we describe the systematic approach that we took to develop an efficient method to synthesize the pyrazole system on a solid phase. In this included a careful determination of the conditions required to attach the precursor to the support and to effect all of the ensuing reactions, including cleavage of the final product. We used NMR and IR analysis directly on the derivatized beads to assess the progress of the reactions. Finally, we used the optimized methods to prepare a small library (12 members) and then a large library (96 members) of the tetrasubstituted pyrazole class. We also measured the receptor binding affinities of these 96 compounds and thereby developed an interesting structure affinity relationship [See Figure 6, **Publication No. 3**]. The highest affinity ligands are those in which at least two of the aromatic rings bear a 4-hydroxy group.

Structure-Activity Relationships of Tetrasubstituted Pyrazoles and Development of an Estrogen Receptor Alpha Specific Ligand [Publication No. 4]

In this publication, we have taken the most favorable results from Publication Nos. 1 and 3 and extended further the structure-activity analysis of the tetrasubstituted pyrazole ligands. In addition, we have assayed their affinity for the estrogen receptor subtypes ERα and ERβ. Remarkably, we find that some of the pyrazoles have especially high affinity for ERα, reaching as high as 75% that of estradiol, yet very low affinity for ERβ. The best of these compounds [numbered **4g (PPT)** in **Publication No. 4**] has a 410-fold affinity preference for ERα. This compound also shows extremely high potency selectivity for ERα in cell-based transcription assays [Figure 2 in **Publication No. 4**]. This compound has proved to be of great interest to the molecular endocrinology community as a probe for assessing the biological roles of ERα and ERβ. We have supplied samples of this ERα selective ligand to more than 20 laboratories who are engaged with use in collaborative studies. In this study we also endeavored to use molecular modeling to supplement the results of our structure-activity study so as to be able to predict the orientational mode with which these rather symmetrical pyrazole core ligands are bound by the estrogen receptor. We also have developed a productive collaboration with Wyeth-Ayerst to evaluate PPT further in a series of biological assays, such as uterotropic, bone mineralization, neuroprotection model, hot flush model, ER-subtype specific gene induction in the brain, etc. PPT functions as a full agonist in most of these assays. This work is still underway and is, so far unpublished. A joint publication is anticipated once the studies have been completed.

Synthesis of Pyrazole Core Isomers in a Further Structure Activity Relationship Study of Tetrasubstituted Pyrazole Estrogen Receptor Ligands [Publication No. 5]

Originally, we explored only one isomeric series of tetrasubstituted pyrazoles as ligands for the estrogen receptor, ones in which the three aryl groups were at N-1, C-3 and C-5, and the alkyl group at C-4. In this publication [**Publication No. 5**] we explore pyrazoles of the isomeric series (i.e., 1,3,4-triaryl-5-alkyl). This required the development of a completely new synthetic method, because the original method, when applied to the corresponding monoaryl 1,3-diones underwent a Fischer indole reaction rather than a pyrazole cyclization. We were able to over come this side reaction by performing the synthesis on a 1,3-dione of lesser substitution and then to introduce the final aryl group by a Suzuki coupling method. The overall process proved to be both regioselective for this series and efficient. The most interesting products from this study were those listed a compounds **10a** and **10b** in **Publication No. 5**.

Investigation of Pyrazoles with Basic Side Chains as Potential Potency-Selective Estrogen Receptor Alpha Antagonists [Publications No. 6 and 10]

Because of the high affinity and potency selectivity of certain of the pyrazoles as agonists for ERα, we were interested in seeing whether we could convert them to ERα potency selective

antagonists by adding a basic side chain to the pyrazole core structure. In this publication [**Publication No. 6**], we attached a basic side chain to the four substituent positions on the tetrasubstituted pyrazoles, and we found that only one of these showed high affinity for the estrogen receptor. This compound showed about a 10-fold potency preference as an antagonist for ERα vs ERβ [see compound **5** and Figure **3** in **Publication No. 6**]. It is the basis for continued studies on pyrazole ligands with basic side chains, which stimulated in part the development of the regioselective method for pyrazole synthesis discussed below. In addition, we have investigated further the biological activity of this series of pyrazoles with basic side chains [**Publication No. 10**], and we have found that one of these, termed methyl-piperidinyl-pyrazole (MPP), is an ERα-selective antagonist. This compound will be a useful pharmacological tool for studying the biological roles of the two ER subtypes.

Development of a Regioselective Synthesis of Pyrazoles [Publication No. 7]

The method we originally devised for the synthesis of the pyrazoles involved the reaction of a hydrazine with a 1,3-diketone and was, therefore, not regioselective. This increasingly became a problem as we wanted to prepare more and more non-symmetrical pyrazoles. In this publication, we have developed an efficient regioselective synthesis of these pyrazoles by the addition of the hydrazine to an enone to give an pyrazoline intermediate. The corresponding anion of this pyrazoline can be alkylated and then oxidized to produce unsymmetrical pyrazoles in high yield and with complete regioselectivity. We have used this method to prepare more than 20 different unsymmetrical pyrazoles, including a variety of ones having different basic side chain substituents on the position where it is most favorable (see discussion above).

Novel Furan Ligands for the Estrogen Receptor [Publication No. 8 and 9]

We have also developed novel ligands for ER based on a different heterocyclic system, furans. In this system we also discovered high affinity ER ligands, some of which are very selective for ERa, as well as basic side chain substituted analogs that are ERa-selective antagonists. This work complements our studies on the pyrazoles.

<p align="center">++++++++++++++++++++++++++</p>

KEY RESEARCH ACCOMPLISHMENTS

Progress in Relation to the Statement of Work

The complete three year Statement of Work, presented in the original proposal of July 1996, is shown below. Our accomplishments are noted in *italics*:

===

ORIGINAL STATEMENT OF WORK

Project Period: September 1, 1997– August 31, 2001 (3 years, with a one-year no-cost extension)

Year 1

- Synthesis of representative members of Class I-VI ligands by solution phase methods. *completed*
- Isolate, purify, and fully characterize these members. *completed*
- Measure estrogen receptor binding affinity of representative members of Class I-VI ligands. *completed*
- Begin to adapt solution phase syntheses to solid phase. *completed for the most promising series (pyrazoles)*

Year 2

- Complete adaptation of solution phase synthesis to solid phase. *completed for the most promising series (pyrazoles)*
- Isolate and fully characterize representative members produced by solid phase synthesis. *completed for the most promising series (pyrazoles)*Determine yield and characterize impurities. *completed for the most promising series (pyrazoles)*
- Compare estrogen receptor binding of representative members of Class I-VI ligands prepared by solution vs solid phase. *completed for the most promising series (pyrazoles)*
- Begin synthesis of full Class I-VI libraries. *completed for the most promising series (pyrazoles)*
- Begin cell proliferation and cell-based transfection assays. *completed for the most promising series (pyrazoles)*

Year 3

- Complete synthesis of full Class I-VI libraries. *completed for the most promising series (pyrazoles)*
- Complete estrogen receptor assay of full libraries at two concentrations. *completed for the most promising series (pyrazoles)*

13

- Reassay the members with detectable estrogen receptor binding affinity by quantitative titration assay. *completed for the most promising series (pyrazoles)*
- Assay the members with high estrogen receptor binding affinity in the cell proliferation and cell-based transfection assays. *completed for the most promising series (pyrazoles)*
- Assay uterotrophic activity of the most promising members in rats. *In vivo assays have been completed through a collaboration with Wyeth-Ayerst.*

Please see **Summary** at the conclusion of the preceeding section that outlines additional accomplishments beyond those outlined in the original Statement of Work.

===

+++++++++++++++++++++++++++

REPORTABLE OUTCOMES

- Seven papers have been published, two manuscripts have been accepted, and one has recently been submitted. These publications are attached as the appendix and are listed as **Publications No. 1-10**.
- Presentations have been made at four American Chemical Society meeting by the PI and principal co-workers, Shaun Stauffer and Deborah Mortensen, and by Stauffer at a meeting on solid phase synthesis. Numerous seminars given by the PI have included work developed under this project.
- A PCT patent has been submitted to the US Patent Office covering the 5-membered ring heterocyclic estrogens.
- Shaun Stauffer, my principal co-worker on this project, has completed his Ph.D. degree in the fall of 1999.
- Deborah Mortensen, another major co-worker on this project, has completed her Ph.D. degree in the fall of 2000.
- After completing a very successful 2-year postdoctoral fellowship with Professor John Hartwig at Yale University, supported by a postdoctoral fellowship from the National Institutes of Health, Shaun Stauffer joined Merck. He had numerous offers from the best pharmaceutical industries. The topic of Shaun's NIH postdoctoral fellowship derived from the experience he developed working on this project.
- On the basis of a presentation that she gave at the ACS meeting in San Francisco, Deborah Mortensen received two job offers. She is now working for Signal Pharmaceuticals in San Diego on a nuclear receptor project.

- Ying Huang, a postdoctoral fellow in my laboratory who worked on this project, has completed her studies and has moved to a job in new drug discovery at Schering-Plough in New Jersey.
- Rosanna Tedesco, a graduate student who has worked on this project, will complete her Ph.D. studies in October, 2000, and she has moved to a position in new drug discovery at SmithKline Beecham.
- Christopher Coletta and Zachary Aron, two undergraduate students who worked on this project for their senior research, have graduated with high honors, based in part on their excellent undergraduate theses. Chris is working as a B. S. Chemist in new drug discovery at Pfizer, in Connecticut, and Zachary is in a Ph.D. graduate program at the University of California, Irvine, working with Professor Larry Overman.

++++++++++++++++++++++++++++

CONCLUSIONS [The Summary, presented earlier, is repeated for convenience]

Summary — Through the work we have engaged in on this project over the past three years, we have completed all of the goals of the original proposal, as summarized in the original Statement of Work. This has involved an exploration of the promise of all of the proposed acyclic amide and 5-membered ring heterocyclic systems, and the development of solid phase synthesis methods and large library synthesis and analysis. In addition, we have discovered in the process that some of the most promising heterocyclic ligands, the pyrazoles, have high affinity and potency selectivity for one of the estrogen receptor subtypes, ERα. Because the development of estrogen receptor subtype selective ligands is a very important issue and one of great current interest, we have devoted considerable efforts in years 2 and 3 to pursue this further. We have completed a careful structure-activity relationship study on the pyrazoles, obtaining ultimately a compound that is almost a completely specific activator of ERα, having essentially no activity on ERβ at doses where it maximally stimulated ERα, and, based on these findings, we have developed a series of pyrazole basic side chain derivatives that hold considerable promise as potency selective antagonists of ERα. Such compounds could be used to block the action of estradiol through this receptor subtype without interfering with its effect on ERβ.

The work that we have done on this project has also spawned several related lines of inquiry that are currently being pursued in my laboratory with independent support. These include investigations of other 5-membered ring heterocyclic systems as estrogen receptor ligands, namely furans, thiophenes, and pyrroles, as well as carbocyclic analogs,

cyclopentadienes and related cyclopentadienones. In addition, based on the favorable results of the work under this project, we have begun to synthesize 6-membered ring heterocycles such as pyrazines, pyrimidines, and pyridazines as estrogen receptor ligands. This work is still in an early state of development, but already we know that we have compounds that show high affinity for the receptor and are therefore potentially quite interesting, because their structures are unique in the estrogen receptor field.

We certainly appreciate the support that has been provided to our research efforts in this area through this US Army grant. It has served as a stimulus to us to thrust our laboratory research into new directions that have proved to be very fruitful and potentially useful for the prevention and treatment of breast cancer.

<div align="center">++++++++++++++++++++++++++++</div>

REFERENCES

1. Katzenellenbogen BS, Montano M, Le Goff P, Schodin DJ, Kraus WL, Bhardwaj B, Fujimoto N. Antiestrogens: Mechanisms and actions in target cells. *J. Steroid Biochem. Molec. Biol.* 1995; 53:387-393.
2. Katzenellenbogen BS, Fang H, Ince BA, Pakdel F, Reese JC, Wooge CH, Wrenn CK. Estrogen receptors: Ligand discrimination and antiestrogen action. *Breast Cancer Res. Treat.* 1993; 27:17-26.
3. Pasqualini JR, Katzenellenbogen BS. Hormone-Dependent Cancer. New York: Marcel Dekker, 1996.
4. Read LD, Katzenellenbogen BS. Characterization and regulation of estrogen and progesterone receptors in breast cancer. In: Dickson RB, Lippman ME, eds. Genes, Oncogenes, and Hormones: Advances in Cellular and Molecular Biology of Breast Cancer. Boston: Kluwer Academic Publishers, 1991; 277-299.
5. Chang JCN, A Review of Breast Cancer Chemoprevention. *Biomedicine & Pharmacotherapy* 1998; 52:133-136.
6. Jordan VC, Morrow M. Should clinicians be concerned about the carcinogenic potential of tamoxifen? *Eur. J. Cancer* 1994; 30A:1714-1721.
7. Katzenellenbogen BS. Antiestrogen resistance: Mechanisms by which breast cancer cells undermine the effectiveness of endocrine therapy. *J. Natl. Cancer Inst.* 1991; 83:1434-1435.
8. Davidson NE. Hormone-replacement therapy—breast versus heart versus bone. *N. Engl. J. Med.* 1995; 332:1638-1639.
9. Nique F, Van de Velde P, Bremaud J, Hardy M, Philibert D, Teutsch G. 11β-Amidoalkoxyphenyl estradiols, a new series of pure antiestrogens. *J. Steroid Biochem. Molec. Biol.* 1994; 50:21-29.
10. Nicholson RI, Gee JMW, Francis AB, Manning DL, Wakeling AE, Katzenellenbogen BS. Observations arising from the use of pure antioestrogens on oestrogen-responsive (MCF-7) and oestrogen growth-independent (K3) human breast cancer cells. *Endocrine Related Cancer* 1995; 2:1-7.
11. Wakeling AE, Bowler J. Biology and mode of action of pure antiestrogens. *J Steroid Biochem* 1988; 30:141-147.
12. Wakeling AE, Dukes M, Bowler J. A potent specific pure antiestrogen with clinical potential. *Cancer Res* 1991; 51:3867-3873.

13. Osborne CK, Coronado-Heinsohn EB, Hilsenbeck SG, McCue BL, Wakeling AE, McClelland RA, Manning DL, Nicholson RI. Comparison of the effects of a pure steroidal antiestrogen with those of tamoxifen in a model of human breast cancer. *J. Natl. Cancer Inst.* 1995; 87:746-750.

14. Howell A, DeFriend D, Robertson J, Blamey R, Walton P. Response to a specific antiestrogen (ICI 182780) in tamoxifen-resistant breast cancer. *Lancet* 1995; 345:29-30.

15. Katzenellenbogen BS. Estrogen receptors: Bioactivities and interactions with cell signaling pathways. *Biol. Reprod.* 1996; 54:287-293.

16. Katzenellenbogen JA, O'Malley BW, Katzenellenbogen BS. Tripartite steroid hormone receptor pharmacology: Interaction with multiple effector sites as a basis for the cell- and promoter-specific action of these hormones. *Mol. Endocrinol.* 1996; 10:119-131.

17. Montano MM, Ekena KE, Krueger KD, Keller AL, Katzenellenbogen BS. Human estrogen receptor ligand activity inversion mutants: Receptors that interpret antiestrogens as estrogens and estrogens as antiestrogens and discriminate among different antiestrogens. *Mol. Endocrinol.* 1996; 10:230-242.

18. Montano MM, Müller V, Trobaugh A, Katzenellenbogen BS. The carboxy-terminal F domain of the human estrogen receptor: Role in the transcriptional activity of the receptor and the effectiveness of antiestrogens as estrogen antagonists. *Mol Endocrinol* 1995; 9:814-825.

19. Tzukerman MT, Esty A, Santiso-Mere D, Danielian P, Parker MG, Stein RB, Pike JW, McDonnell DP. Human estrogen receptor transactivational capacity is determined by both cellular and promoter context and mediated by two functionally distinct intramolecular regions. *Mol Endocrinol* 1994; 8:21-30.

20. Berry M, Metzger D, Chambon P. Role of the two activating domains of the oestrogen receptor in the cell-type and promoter-context dependent agonistic activity of the anti-oestrogen 4-hydroxytamoxifen. *EMBO J.* 1990; 9:2811-2818.

21. McDonnell DP, Clemm DL, Hermann T, Goldman ME, Pike JW. Analysis of estrogen receptor function in vitro reveals three distinct classes of antiestrogens. *Mol Endocrinol* 1995; 9:659-669.

22. Yang NN, Hardikar S, Kim J. Raloxifene, an anti-estrogen, simulates the effects of estrogen on inhibiting bone resorption through regulating TGFβ-3 expression in bone. *J. Bone Miner. Res.* 1993; 8 (Suppl 1):S118.

23. Yang NN, Bryant HU, Hardikar S, Sato M, Galvin RJS, Glasebrook AL, Termine JD. Estrogen and raloxifene stimulate transforming growth factor-β3 gene expression in rat bone: A potential mechanism for estrogen- or raloxifene-mediated bone maintenance. *Endocrinology* 1996; 137:2075-2084.

24. Sato M, Glasebrook AL, Bryant HU. Raloxifene: A selective estrogen receptor modulator. *J Bone Miner Met* 1994; 12 (Suppl 2):S9-S20.

25. Sato M, Rippy MK, Bryant HU. Raloxifene, tamoxifen, nafoxidine, or estrogen effects on reproductive and nonreproductive tisseus in ovariectomized rats. *FASEB J.* 1996; 10:905-912.

26. von Angerer E. The Estrogen Receptor as a Target for Rational Drug Design. Austin: R.G. Landes Company, 1995.

27. Gordon EM, Barrett RW, Dower WJ, Fodor SPA, Gallop MA. Applications of combinatorial technologies to drug discovery. 2. Combinatorial organic synthesis, library screening strategies, and future directions. *J. Med. Chem.* 1994; 37:1385-1401.

28. Gallop MA, Barrett RW, Dower WJ, Fodor SPA, Gordon EM. Applications of combinatorial technologies to drug discovery. 1. Background and peptide combinatorial libraries. *J. Med. Chem.* 1994; 37:1233-1251.

29. Geysen HM, Houghten RA, Kauffman S, Lebl M, Moos WH, Pavia MR, Szostak JW. Molecular diversity comes of age! *Molecular Diversity* 1995; 1:2-3.

30. Murphy MM, Schullek JR, Gordon EM, Gallop MA. Combinatorial organic synthesis of highly functionalized pyrrolidines: Identification of a potent angiotensin converting enzyme inhibitor from a mercaptoacyl proline library. *J. Am. Chem. Soc.* 1995; 117:7029-7030.

31. Terrett NK, Bojanic D, Brown D, Bungay PJ, Gardner M, Gordon DW, Mayers CJ, Steele J. The combinatorial synthesis of a 30,752-compound library: Discovery of SAR around the endothelin antagonist, FR-139,317. *Bioorg. Med. Chem. Lett.* 1995; 5:917-922.

32. Boojamra CG, Burow KM, Ellman JA. An expedient and high-yielding method for the solid-phase synthesis of diverse 1,4-benzodiazepine-2,5-diones. *J. Org. Chem.* 1995; 60:5742-5743.

33. Goff DA, Zuckermann RN. Solid-phase synthesis of defined 1,4-benzodiazepine-2,5-dione mixtures. *J. Org. Chem.* 1995; 60:5744-5745.

34. Plunkett MJ, Ellman JA. Solid-phase synthesis of structurally diverse 1,4-benzodiazepine derivatives using the Stille coupling reaction. *J. Am. Chem. Soc.* 1995; 117:3306-3307.

35. DeWitt SH, Kiely JS, Stankovic CJ, Schroeder MC, Cody DMR, Pavia MR. "Diversomers": An approach to nonpeptide, nonoligomeric chemical diversity. *Proc. Natl. Acad. Sci. U.S.A.* 1993; 90:6909-6913.

Publications, Patents, Meeting Abtracts, and Personnel Supported

Publications:

Publication No. 1: B. E. Fink, D. S. Mortensen, S. R. Stauffer, Z. D. Aron, J. A. Katzenellenbogen. Novel Structural Templates for Estrogen-Receptor Ligands and Prospects for Combinatorial Synthesis of Estrogens. *Chem. & Biol.*, 1999, *6*, 205-219.

Publication No. 2: S. R. Stauffer, J. Sun, B. S. Katzenellenbogen, J. A. Katzenellenbogen. Acyclic Amides as Estrogen Receptor Ligands: Synthesis, Binding, Activity, and Receptor Interaction. *Bio. Med. Chem.*, 2000, *8*, 1293-1316.

Publication No. 3: S. R. Stauffer, J. A. Katzenellenbogen. Solid-Phase Synthesis of Tetra-Substituted Pyrazoles, Novel Ligands for the Estrogen Receptor. *J. Comb. Chem.*, 2000, *2*, 318-329.

Publication No. 4: S. R. Stauffer, C. J. Coletta, J. Sun, B. S. Katzenellenbogen, J. A. Katzenellenbogen. Pyrazole Ligands: Structure-Affinity/Activity Relationships of Estrogen Receptor-α Selective Agonists. *J. Med. Chem.*, 2000, *43*, 4934-4947.

Publication No. 5: S. R. Stauffer, Y. Huang, C. J. Coletta, R. Tedesco, J. A. Katzenellenbogen. Estrogen Pyrazoles: Defining the Pyrazole Core Structure and the Orientation of Substituents in the Ligand Binding Pocket of the Estrogen Receptor. *Bio. Med. Chem.*, 2001, *9*, 141-150.

Publication No. 6: S. R. Stauffer, Y. R. Huang, Z. D. Aron, C. J. Coletta, J. Sun, B. S. Katzenellenbogen, J. A. Katzenellenbogen. Triarlpyrazoles with Basic Side Chains: Development of Pyrazole-Based Estrogen Receptor Antagonists. *Bio. Med. Chem.*, 2001, *9*, 151-161.

Publication No. 7: Y. R. Huang, J. A. Katzenellenbogen. Regioselective Synthesis of 1,3,5-Triaryl-4-alkylpyrazoles: Novel Ligands for the Estrogen Receptor. *Org. Lett,* 2000, *2*, 2833-2836.

Publication No. 8: D. S. Mortensen, A. L. Rodriquez, K. E. Carlson, J. Sun, B. S. Katzenellenbogen, J. A. Katzenellenbogen. Synthesis and Biological Evaluation of a Novel Series of Furans: Ligands Selective for Estrogen Receptor Alpha. *J. Med Chem.*, 2001, In Press.

Publication No. 9: D. S. Mortensen, A. L. Rodriquez, J. Sun, B. S. Katzenellenbogen, J. A. Katzenellenbogen. Furans with Basic Side Chains: Synthesis and Biological Evaluation of a Novel Series of Antagonists with Selectivity for the Estrogen Receptor Alpha *Bioorg. Med. Chem. Letters,* 2001, In Press

Publication No. 10:   J. Sun, Y. R. Huang, W. R. Harrington, S. Sheng, B. S. Katzenellenbogen,[a] J. A. Katzenellenbogen. Antagonists Selective for Estrogen Receptor Alpha. *Endocrinology*. 2001, Submitted

Patents:

PCT Patent Application No. PCT/US99/22747 "Estrogen Receptor Ligands", October 1, 1999.

U. S. Patent Application No. US/09/483,233 "Selective Estrogens and Antiestrogens", January 14, 2000.

Meeting Abstracts:

S. R. Stauffer and J. A. Katzenellenbogen. Conformationally Biased s-cis Anilidoamides as Novel Ligands for the Estrogen Receptor. 216th National Meeting of the American Chemical Society, Boston, August 23-27, **1998.**

D. Mortensen and J. A. Katzenellenbogen, Novel Heterocyclic Ligands for the Estrogen Receptor. 219th ACS National Meeting, San Francisco, CA, March, **2000.**

J. A. Katzenellenbogen, Estrogen Receptor Ligands: Design and Dynamics. Frontiers in Estrogen Action, April, Manalapan, FL, April **2000.**

S. R. Stauffer, K. E. Carlson, J. A. Katzenellenbogen. Solid Phase Synthesis and Relative Binding Affinity Assessment of a Tetrasubstituted Pyrazole Library, Novel Ligands for the Estrogen Receptor. 6th Annual Conference and Exhibition "Screening in the New Millennium". Vancouver, British Columbia, Canada, September 6-9, **2000.**

D. S. Mortensen, B. F. Fink, S. R. Stauffer, Y. Huang, J. Sun, B. S. Katzenellenbogen, J. A. Katzenellenbogen, Heterocyclic Non-Steroidal Ligands for the Estrogen Receptor with Very High Receptor Subtype Specificity. ICE 2000, Sydney, Australia, October 29-November 3, **2000.**

J. A. Katzenellenbogen and S R., Stauffer, Design and Combinatorial Synthesis of Novel Heterocyclic Antiestrogens. Era of Hope, Department of Defense Breast Cancer Research Program Meeting. Atlanta, GA, June 8-11, **2000.**
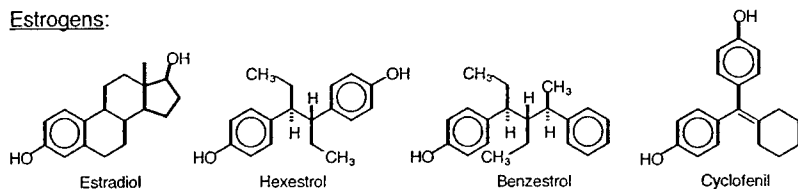
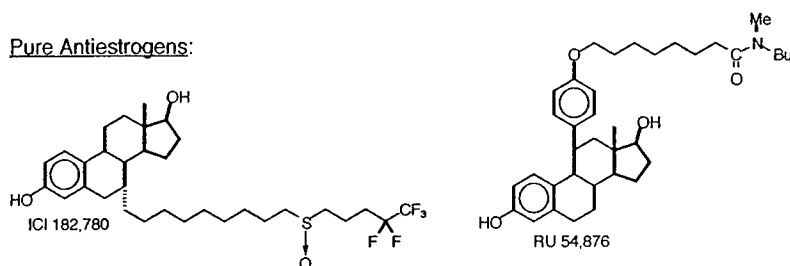<u>Personnel Supported:</u>

Shaun R. Stauffer

<u>Deborah Mortensen</u>

Ying R. Huang

Scheme 1. Estrogens, Pure Antiestrogens, and Selective Antiestrogens – From the Original Proposal

Estrogens:

Estradiol   Hexestrol   Benzestrol   Cyclofenil

Pure Antiestrogens:

ICI 182,780   RU 54,876

Selective Antiestrogens:

Hydroxytamoxifen   Raloxifene   Centchroman   Zindoxifene   Cyclofenil Derivative
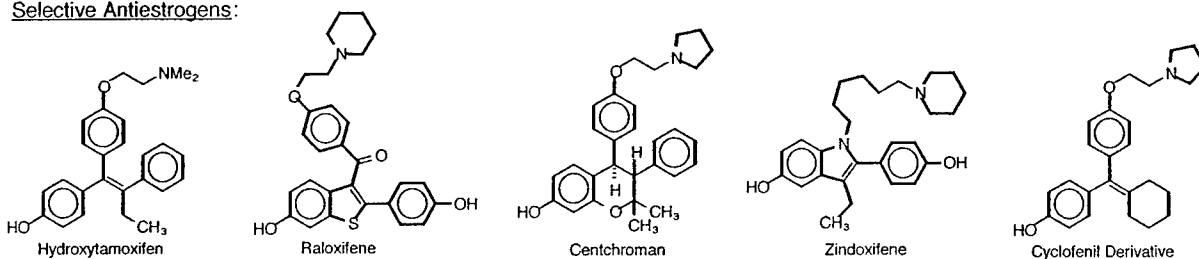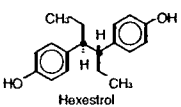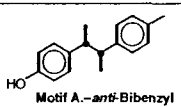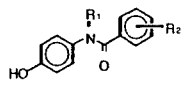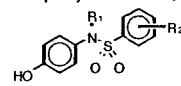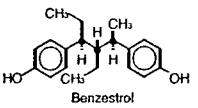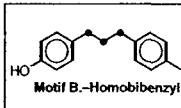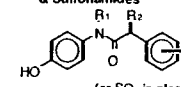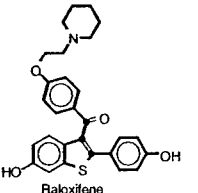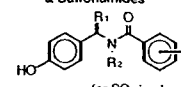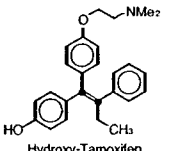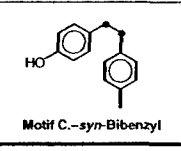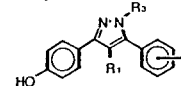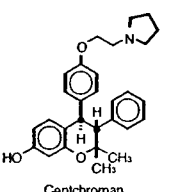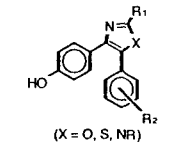
Scheme 2. Structural Components of Selective Antiestrogens – From the Original Proposal

Basic Side Chain **D**

Core Structure **A**

Phenol **B**

Second Aromatic Unit **C**
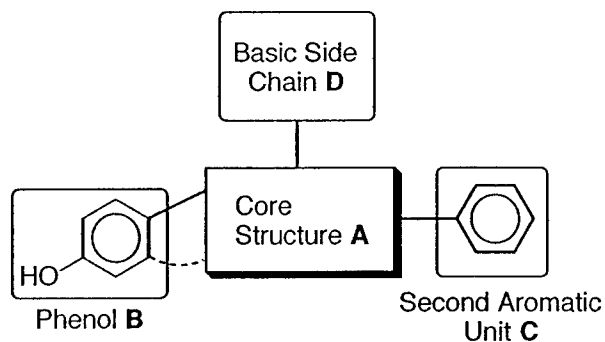
**Scheme 3. Structural Motifs for Estrogen Receptor Ligands
and Their Combinatorial Analogs – From the Original Proposal**

Estrogen Receptor Ligand	Structural Motif	Combinatorial Analog (Class)

I. Diphenyl Carboxamides

II. Diphenyl Sulfonamides

III. Phenyl Benzylcarboxamides & Sulfonamides

(or SO$_2$ in place of CO)

IV. Benzyl Phenylcarboxamides & Sulfonamides

(or SO$_2$ in place of CO)

V. Pyrazoles

VI. Oxazoles, Thiazoles, and Imidazoles

(X = O, S, NR)

Hexestrol — Motif A.–*anti*-Bibenzyl

Hydroxytamoxifen

Benzestrol — Motif B.–Homobibenzyl

Raloxifene

Hydroxy-Tamoxifen — Motif C.–*syn*-Bibenzyl

Centchroman

23

Novel structural templates for estrogen-receptor ligands and prospects for combinatorial synthesis of estrogens

Brian E Fink, Deborah S Mortensen, Shaun R Stauffer, Zachary D Aron and John A Katzenellenbogen

Introduction: The development of estrogen pharmaceutical agents with appropriate tissue-selectivity profiles has not yet benefited substantially from the application of combinatorial synthetic approaches to the preparation of structural classes that are known to be ligands for the estrogen receptor (ER). We have developed an estrogen pharmacophore that consists of a simple heterocyclic core scaffold, amenable to construction by combinatorial methods, onto which are appended 3–4 peripheral substituents that embody substructural motifs commonly found in nonsteroidal estrogens. The issue addressed here is whether these heterocyclic core structures can be used to prepare ligands with good affinity for the ER.

Results: We prepared representative members of various azole core structures. Although members of the imidazole, thiazole or isoxazole classes generally have weak binding for the ER, several members of the pyrazole class show good binding affinity. The high-affinity pyrazoles bear close conformational relationship to the nonsteroidal ligand raloxifene, and they can be fitted into the ligand-binding pocket of the ER–raloxifene X-ray structure.

Conclusions: Compounds such as these pyrazoles, which are novel ER ligands, are well suited for combinatorial synthesis using solid-phase methods.

Address: Department of Chemistry, University of Illinois, 600 S. Mathews Avenue, Urbana, IL 61801, USA.

Correspondence: John A Katzenellenbogen
E-mail: jkatzene@uiuc.edu

Introduction

Estrogens are endocrine regulators of the vertebrate reproductive system that have important effects in many non-reproductive tissues as well (bone, liver, cardiovascular system, CNS and so on). Many estrogen pharmaceuticals, based on both natural and synthetic substances, have been developed as agents for regulating fertility, preventing and controlling hormone-responsive breast cancer, and menopausal hormone replacement. These substances display a spectrum of agonist to antagonist activity that can show remarkable tissue and cell selectivity [1].

The molecular target of estrogens is the estrogen receptor (ER), of which there are now known to be two subtypes, ER-α and ER-β, that have different patterns of tissue expression and somewhat different ligand-binding specificities [2,3]. ER is a transcription factor that binds to specific estrogen-response elements in the promoter region of estrogen-regulated genes and whose activity is modulated by the estrogen ligands [4]. The capacity of ER–ligand complexes to activate gene transcription is mediated by a series of co-regulator proteins [5]. These co-regulators have interaction functions that tether ER to the RNA polymerase II preinitiation complex and enzymatic activities to modify chromatin structure [6]. It is the fact that each cell and each gene presents to an ER(subtype)–ligand complex a unique combination of these effector components—various estrogen-response elements and

co-regulators—that appears to underlie, in part, the cell and gene selectivity of various estrogens [7].

Among known ligands for ER, the natural estrogens are the simplest of the steroidal hormones, distinguished by their phenolic A-ring (Figure 1). Synthetic estrogens, especially those of nonsteroidal nature, generally retain a phenolic function (at least for those of high potency), but otherwise span a remarkable range of structural motifs that encompass simple acyclic core structures of various lengths and sizes, as well as a variety of ring-size fused and nonfused carbocyclic and heterocyclic systems [8–10]. It is clear from many decades of medicinal-chemistry investigations that minor changes in the structure and stereochemistry of these ligands can have profound effects on both their affinity and their biocharacter (i.e. the agonist versus antagonist balance in various tissues). Major efforts have been directed at optimizing ER ligand structure to obtain desired profiles of tissue selectivity, but, even so, the ideal profile for various uses has not yet been achieved [1,11,12].

As currently explored, ER ligands are, by and large, not well suited for synthesis using combinatorial approaches, because their preparation generally involves a series of carbon–carbon bond forming reactions that do not give uniformly high yields, nor are they well adapted to solid-phase-synthesis methods. There are two examples of the preparation of estrogen combinatorial libraries on solid

Figure 1
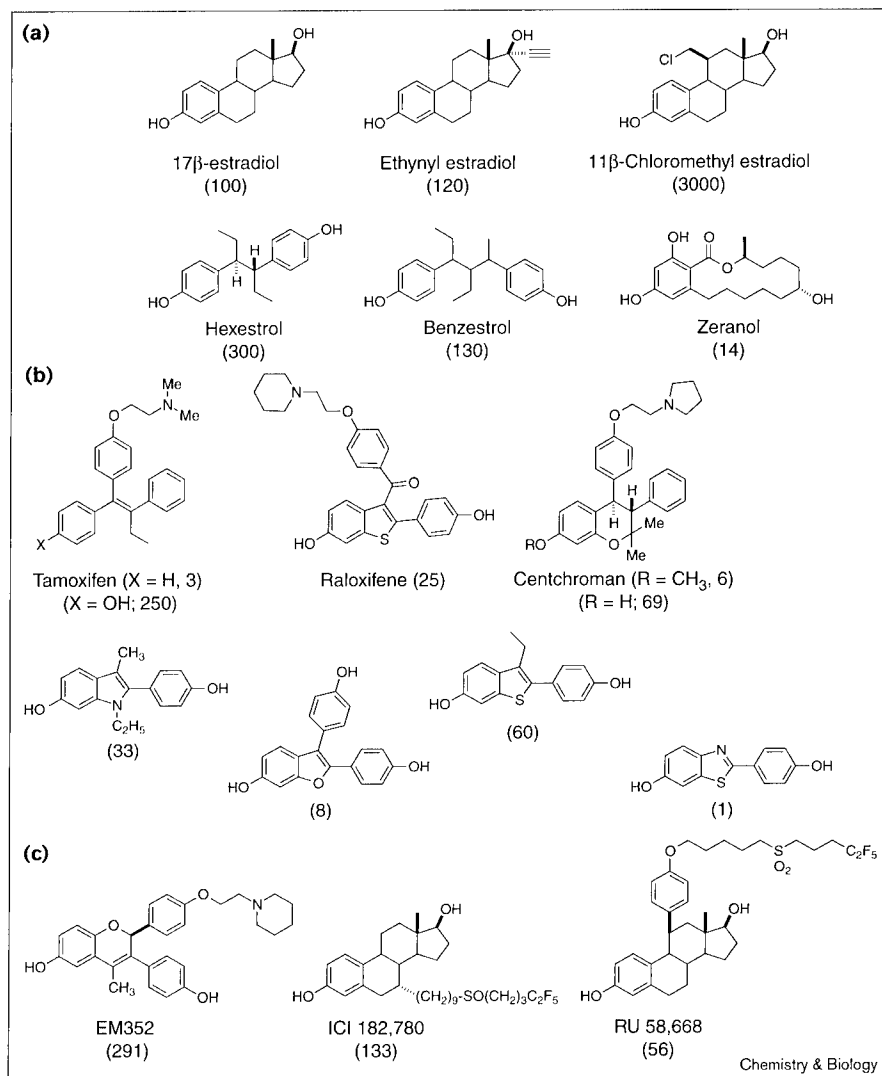
Examples of ligands with high affinity for the estrogen receptor. In each case, the binding affinity relative to that of estradiol (100%) is given in parentheses. The compounds are grouped according to their activity in a standard rat uterine weight gain assay as **(a)** agonists, **(b)** mixed or selective agonist/antagonists or **(c)** pure antagonists.

phase, both involving stilbene-like structures [13,14], but the application of combinatorial approaches for the preparation of ER ligands has, so far, been limited.

To expand possible combinatorial approaches to the synthesis of ER ligands, we have begun investigating simple structural motifs that might be used for the construction of molecules with high affinity for ER. The goal was to identify core structures that could be readily prepared by the types of simple condensation reactions that typify those used in solid-phase combinatorial approaches for the preparation of drug-like molecules, and from these to select ones that would support the development of high-affinity ligands for ER.

Here, we describe the investigation of prototype 1,2- and 1,3-azole systems as potential ligands for the ER. We examine the issue of whether ER ligands can be considered simply as an assembly of a phenol unit together with 2–3 auxiliary peripheral groups linked together by a functionally inert core scaffold, or whether the core scaffold itself plays an integral role in ligand binding. In the process, we have discovered a new class of high-affinity ligands for ER, 4-alkyl-1,3,5-triarylpyrazoles, that bear an unexpected topological resemblance to the nonsteroidal estrogen raloxifene and show an interesting structure-binding affinity pattern.

Results and discussion

Structural motifs found in estrogen-receptor ligands and proposed heterocyclic surrogates

Selected examples of nonsteroidal ligands for the estrogen receptor are shown in Figure 1, together with an indication of their ER-binding affinity and their agonist (Ag) versus antagonist (Antag) character in a standard rat uterine weight gain assay. Collectively, these molecules exemplify a recognizable structural gestalt (Figure 2): a core structure (A) onto

Figure 2
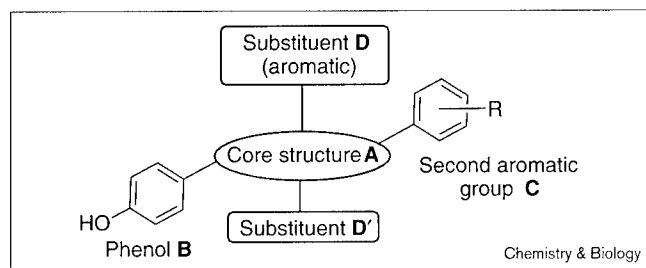
Estrogen ligand pharmacophore model.

which are attached other, peripheral structural elements, a phenolic unit (B) that is always preserved, a second aromatic group (C) that is usually present, and another substituent (D) or two (D′), one of which might be aromatic. In the case of ER antagonists or mixed agonist/antagonists, one of the substituents generally contains a basic or polar function.

Comparisons of the various specific manifestations of this basic structure (Figure 1) suggest that, to achieve high

ER-binding affinity, the peripheral substituents (B–D′) need to be displayed in a certain geometric arrangement, so that they will be 'in register' with their corresponding subsites in the ligand-binding pocket in ER. It seems that this peripheral group 'display function' can be accomplished by using core elements that encompass a considerable structural variety. This raises the interesting question of whether the core element itself plays any direct role in ER binding or whether it serves merely as an inert molecular scaffold whose function is simply to display these peripheral elements with appropriate topology. If the latter is true, it should be possible to replace the core scaffold with a variety of other units, providing they also are able to display the peripheral elements with the appropriate geometry. Some of these core scaffolds, namely small-ring heterocycles, could be assembled by facile condensation reactions from simpler components, a situation that is favorable for the development of large chemical libraries of related compounds by combinatorial synthesis approaches.

In Table 1 we have outlined two (out of many possible) manifestations of this conceptual approach, based on the incorporation of certain substructural motifs into 1,2- and

Table 1

Structural motifs found in ER ligands and proposed surrogates.

Estrogen-receptor ligand	Structural motif	Combinatorial analog (class)
Benzestrol	Motif A. Homobibenzyl*	3,5-Diaryl pyrazoles
Raloxifene		3,5-Diaryl isoxazoles
		2,4-Diaryl imidazoles, thiazoles, oxazoles
Hydroxytamoxifen	Motif B. Bibenzyl*	4,5-Diaryl imidazoles, oxazoles, thiazoles

*These structural motifs are meant to highlight alternative atom connections between the phenol and a second aromatic substituent, without specific consideration of conformational factors. Structural motifs found in ER ligands and proposed surrogates.

Figure 3
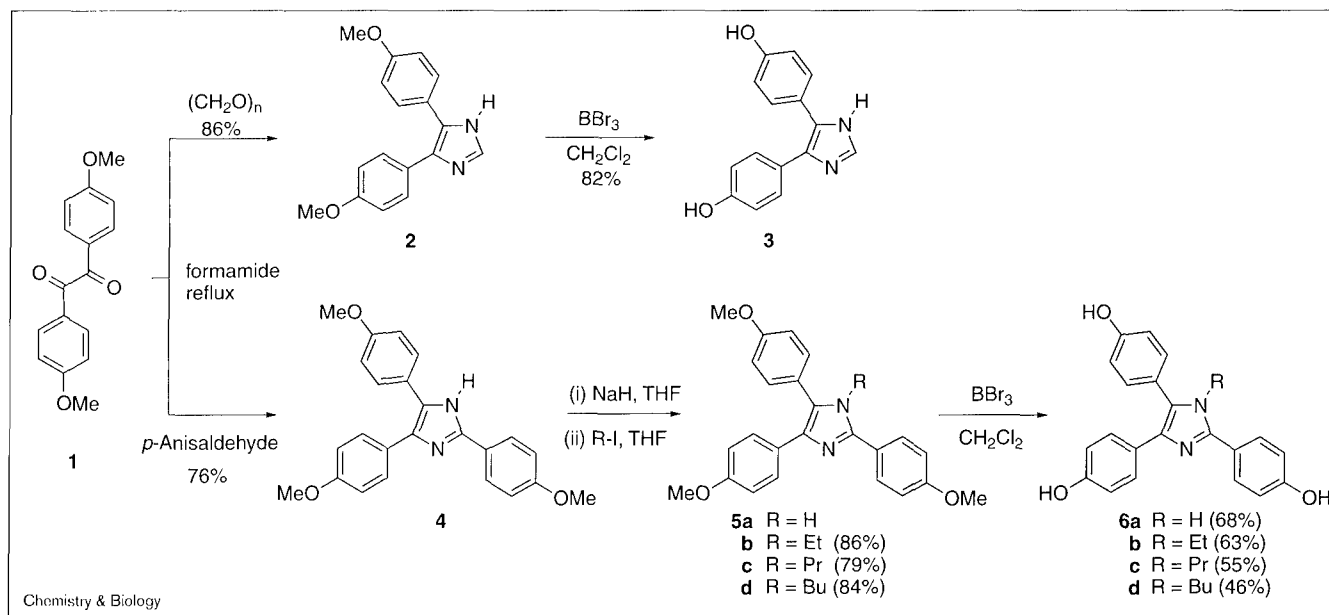
Synthesis of imidazoles **3** and **6a–d**.

1,3-azole systems. Here, the homobibenzyl motif A, exemplified in the nonsteroidal ligands benzestrol and raloxifene, is represented in various 3,5-diaryl-1,2-azoles (pyrazoles and isoxazoles) and 2,4-diaryl-1,3-azoles (imidazoles, thiazoles and oxazoles). Similarly, the bibenzyl motif B is represented in various 4,5-diaryl-1,3-azoles. In each case, the diazole N,N-systems (namely pyrazoles and imidazoles) can accommodate up to four peripheral substituents, whereas the N,O- and N,S-heterocycles (oxazoles, isoxazoles and thiazoles) are limited to three substituents.

Synthesis of representative diaryl and triaryl 1,2- and 1,3-azoles as potential ligands for the estrogen receptor

Imidazoles

The synthesis of representative symmetrical members of the imidazole class and their N-alkyl analogs was accomplished by a well-precedented approach [15] shown in Figure 3. Refluxing 4,4′-dimethoxybenzil (**1**) in formamide in the presence of *para*-formaldehyde afforded the 4,5-disubstituted imidazole **2** [16], which upon deprotection with BBr₃ in CH₂Cl₂ afforded imidazole **3** in good yield. A similar reaction using 4-methoxybenzaldehyde afforded the 2,4,5- tri-substituted imidazole **4** [17–19] in good yield. To prepare tetra-substituted systems, the sodium salt of imidazole **4** was alkylated with ethyl, propyl and butyl iodide, and then deprotected to afford free phenols **6a–d**.

Two additional, unsymmetrical, imidazoles were synthesized as outlined in Figure 4. The top reaction sequence illustrates the synthetic approach to N-ethyl imidazole **12** Reaction of 4-methoxy-deoxybenzoin (**7**) [20] with bromine

Figure 4

Synthesis of imidazoles **12** and **17**.

Figure 5

Synthesis of thiazoles **22a** and **22b**.

Figure 6

Synthesis of oxazoles **29** and **31**.

and a trace of $AlCl_3$ in Et_2O gave α-bromoketone **8** [21], which, upon reaction with sodium azide in acetone, afforded the corresponding azide **9**. The azido-ketone **9** was treated with one equivalent of Et_3N and imine **10** in tetrahydrofuran (THF). Removal of solvent and excess Et_3N followed by treatment of the crude intermediate 2,5-dihydro-2-hydroxyimidazole with TFA in CH_2Cl_2, according to the procedure of Patonay and Hoffman [22], resulted in the formation of *N*-ethyl imidazole **11**. Deprotection with $BF_3 \cdot SMe_2$ in CH_2Cl_2 produced imidazole **12** in good yield.

The synthesis of N-aryl substituted imidazole **17** is also shown in Figure 4. Refluxing 4′-methoxy-α-bromobutyrophenone (**13**) with *p*-anisidine in acetone gave the α-amino-ketone **14**, which was converted into the benzamide **15** upon reaction with benzoyl chloride and base. Cyclization with ammonium acetate in refluxing acetic acid afforded the 1,2,4,5 tetra-substituted imidazole **16**, which upon deprotection with $BF_3 \cdot SMe_2$ in CH_2Cl_2 produced the free phenol **17**.

Thiazoles
The synthesis of representative thiazoles is shown in Figure 5. Thioamide **19**, derived from 4-methoxybenzonitrile (**18**) [23], was condensed with 4′-methoxy-α-bromoacetophenone (**20**) or 4′-methoxy-α-bromobutyrophenone (**13**) in refluxing DMF to give high yields of the 2,4-disubstituted thiazole **21a** [24] or 2,4,5- tri-substituted thiazole **21b**, respectively. Deprotection with BBr_3 afforded moderate yields of the free phenols **22a** and **22b**.

Oxazoles
Two representative oxazoles were synthesized as shown in Figure 6. Reaction of the lithium anion of dithiane **23** with *p*-methoxybenzyl bromide gave the alkylated product **24**, which upon hydrolysis afforded 4′-methoxy-deoxybenzoin (**25**) [25] in excellent yield. Conversion to the

bromide **26** [26] and azide **27** was accomplished as described for analogous compounds **8** and **9** above. The azido-ketone **27** was then treated with one equivalent of Et_3N and *p*-anisaldehyde, and then with TFA to afford oxazole **28** [27]. Oxazole **30** resulted from the condensation of bromo-ketone **26** with *p*-methoxybenzamide in refluxing toluene, analogous to the thiazole synthesis discussed above. Deprotection of **28** and **30** with $BF_3 \cdot SMe_2$ gave oxazoles **29** and **31**, respectively.

Pyrazoles
The synthesis of the pyrazoles involves the condensation of a hydrazine with a 1,3-diketone [28]. Using the method of Beak and coworkers [29], we obtained 1,3-diketone **33** from the reaction of the methyl thioester **32** and lithium tetramethylpiperidide in good yield (Figure 7). Condensation of the diketone with hydrazine hydrochloride or N-substituted hydrazine hydrochlorides in refluxing DMF/THF (3:1) afforded the 3,5-disubstituted pyrazole **34a** or 1,3,5- tri-substituted pyrazoles **34b–d**; yields were higher with aryl-substituted hydrazines than with hydrazine itself. Deprotection of **34a–d** with BBr_3 afforded the free phenols **35a–d** in moderate yield.

The introduction of a 4-alkyl substituent was accomplished through the alkylation of diketone **33** with TBAF and ethyl iodide to afford **36** in moderate yield [30,31]. Attempts to increase the yield of this alkylation were

Figure 7

Synthesis of pyrazoles **35a–d** and **38a–d**.

unsuccessful. Conversion of diketone **36** to the corre-sponding pyrazoles was accomplished as with the unsub-stituted case, to afford pyrazoles **38a–d**.

Isoxazoles
The preparation of a single isoxazole is shown in Figure 8 [32]. Double deprotonation of the ketoxime **39** derived from 4-methoxyacetophenone with nBuLi, followed by addition of methyl 4-methoxybenzoate afforded the 3,5-dis-ubstituted isoxazole **40** in low yield [33]. Deprotection with BBr$_3$ afforded the free phenol **41** in moderate yield [34].

Estrogen-receptor binding
The binding affinities of the heterocycles prepared above for the estrogen receptor are shown in Tables 2–4, organized according to heterocyclic core structure. The binding values were obtained from a competitive radiometric binding assay, using [^{3}H]estradiol as the tracer, dextran-coated charcoal

to adsorb free tracer and lamb uterine cytosol as a source of ER. The values are expressed as relative binding affini-ties (RBA), with estradiol having an affinity of 100% [35]. In replicate assays, these values are reproducible with a coefficient of variation of 30% (K.E. Carlson and J.A.K., unpublished observations).

Imidazoles, oxazoles and thiazoles
The receptor-binding data for the imidazole series are shown in Table 2. Although the members of this series have rather low affinity, there is an increase in RBA with the addition of alkyl substituents at the 1-position (R$_3$; **6a–d**); this trend reaches a maximum for propyl **6c**, revers-ing for the butyl substituent **6d**. Such trends, where affinity
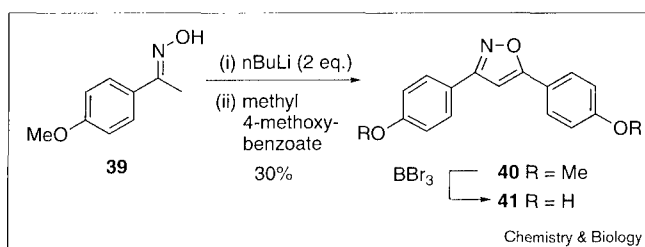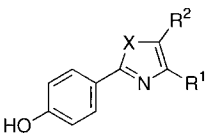
Figure 8

Synthesis of isoxazole **41**.

Table 2

Estrogen receptor binding data for imidazoles 3, 6a–d, 12 and 17.

Compound	R^1	R^2	R^3	R^4	RBA*
3	4′-HO-C$_6$H$_4$	4′-HO-C$_6$H$_4$	H	H	<0.001
6a	4′-HO-C$_6$H$_4$	4′-HO-C$_6$H$_4$	H	4′-HO-C$_6$H$_4$	0.007
6b	4′-HO-C$_6$H$_4$	4′-HO-C$_6$H$_4$	C$_2$H$_5$	4′-HO-C$_6$H$_4$	0.38
6c	4′-HO-C$_6$H$_4$	4′-HO-C$_6$H$_4$	C$_3$H$_7$	4′-HO-C$_6$H$_4$	0.62
6d	4′-HO-C$_6$H$_4$	4′-HO-C$_6$H$_4$	C$_4$H$_9$	4′-HO-C$_6$H$_4$	0.17
12	C$_6$H$_5$	4′-HO-C$_6$H$_4$	C$_2$H$_5$	4′-HO-C$_6$H$_4$	0.25
17	4′-HO-C$_6$H$_4$	C$_2$H$_5$	4′-HO-C$_6$H$_4$	C$_6$H$_5$	0.37

*RBA, relative binding affinity (estradiol = 100%).

Table 3

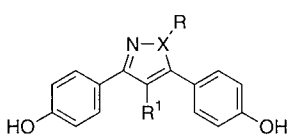Estrogen receptor binding data for thiazoles **22a**, **22b** and oxazoles **29** and **31**.

Compound	X	R¹	R²	RBA
22a	S	4'-HO-C_6H_4	H	0.018
22b	S	4'-HO-C_6H_4	C_2H_5	0.041
29	O	4'-HO-C_6H_4	C_6H_5	<0.001
31	O	C_6H_5	4'-HO-C_6H_4	0.027

increases with substituent size up to a point, are well known both in steroidal systems (11β- and 16α-substituents) [36] and in other non-steroidal ligand series (such as 2-phenylindoles [37], tetrahydrochrysenes [38] and so on), and probably represent the filling of preformed pockets of limited volume in the receptor by these substituents [37]. The principal difference in binding, however, is between the tetra-substituted imidazoles (**6b–d**, **12** and **17**) and the di- or tri-substituted imidazole (**3** and **6a**), the tetra-substituted ones having much higher affinity. There is little difference in binding between imidazoles **12** and **17**, which have a different arrangement of nitrogen atoms in the heterocyclic core but display their four substituents in an identical fashion (Figure 9). The overall low binding affinity of the imidazoles as a class might be the result of the high inherent polarity of this heterocyclic system as compared with the pyrazoles, reflected by their higher chromatographic polarity in both normal and reversed phases systems. It is also of note that the dipole moment for imidazole is very
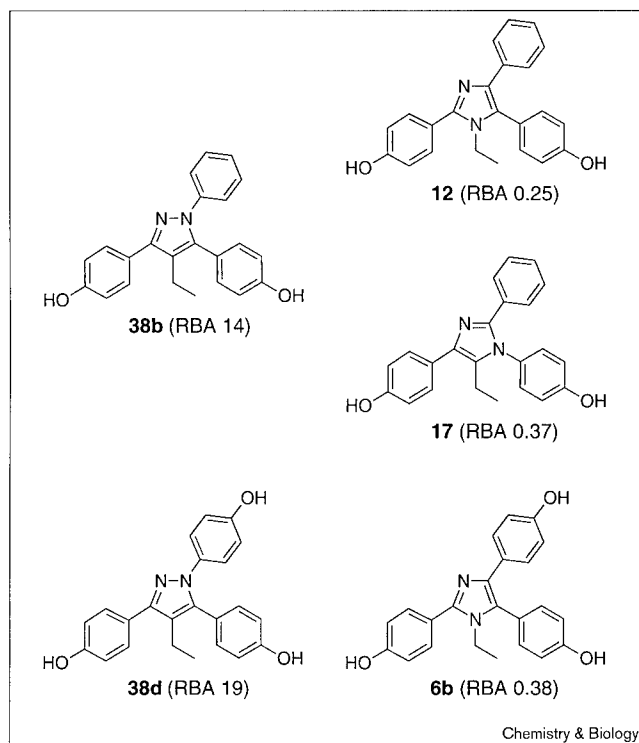
Table 4

Estrogen receptor binding affinity data for pyrazoles and an isoxazole.

| Compound	X	R	R¹	RBA
35a	N	H	H	0.009
35b	N	C_6H_5–	H	0.028
35c	N	$C_6H_5CH_2$–	H	<0.007
35d	N	4'-HO-C_6H_4–	H	0.059
38a	N	H	C_2H_5	0.015
38b	N	C_6H_5–	C_2H_5	14.0
38c	N	$C_6H_5CH_2$–	C_2H_5	0.150
38d	N	4'-HO-C_6H_4–	C_2H_5	19.0
41	O	–	C_2H_5	0.006

Figure 9

Comparisons between ring pyrazoles (**38b**, **38d**) and imidazoles (**6b**, **12** and **17**).

large, 5.56 D [39], and this might be unfavorable for binding to the estrogen receptor.

Table 3 shows the binding data for the two thiazoles and oxazoles. Although affinities are again very low, the more highly substituted thiazole again has the higher affinity (**22a** compared with **22b**). The oxazole **29** has undetectable affinity for ER. The isomer **31**, however, does have measurable, albeit low, binding. In contrast to imidazoles, thiazoles and oxazoles do not have very high dipole moments [39]; so overall polarity is not likely to be the cause of their low ER binding affinity, although heteroatom orientation appears to play a role (**29** compared with **31**). In the imidazole series, the compounds with the highest affinities were all tetra-substituted, however. As it is only possible to trisubstitute a thiazole or oxazole, this core structure might be unable to present sufficient peripheral substituents to afford ligands with good ER binding affinities, at least as far as we have investigated.

The low binding affinities of the imidazoles, thiazoles and oxazoles are disappointing, although not surprising, considering the relatively poor affinity of the most closely related benzothiazole reported by von Angerer [40] (Figure 1). The sparsely substituted monocyclic or polycyclic aromatic systems are also expected to be rather
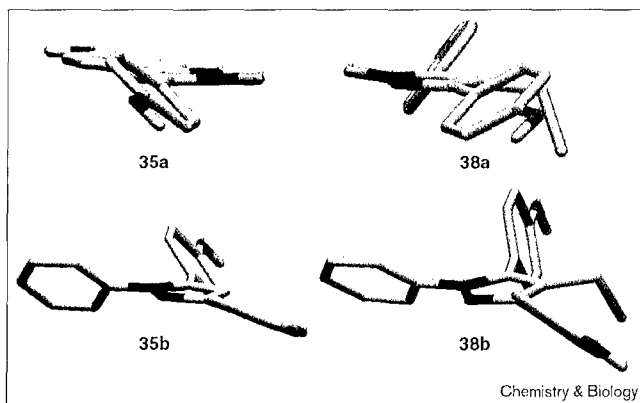
Figure 10
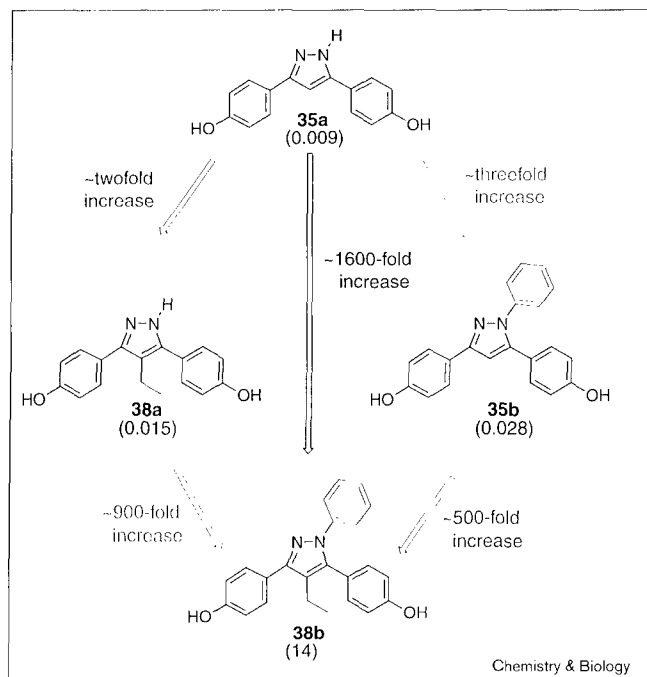
Comparison of the estrogen receptor binding affinity of four related pyrazoles with increasing substitution.

Figure 11

Ab initio calculated conformations for **35a**, **35b**, **38a** and **38b**.

planar. It is generally agreed that good ligands for the estrogen receptor need to have some degree of 'thickness' in the central portion of the ligand [38]. When alkyl substituents are added to either the imidazoles or thiazoles, their RBA increases (Tables 2,3). This increased binding could be due to an increase in steric bulk around the central portion of the molecule, the result, in part, of a twisting of some of the aromatic substituents (see below) or to an increase in lipophilicity. Regardless, the effects are not great, and in general the 1,3-azoles seem to present some special challenges that might best be investigated further by combinatorial approaches.

Pyrazoles and isoxazoles
The RBA data for the 1,2-azoles are presented in Table 4. Immediately apparent is the relatively high binding affinity of pyrazoles **38b** and **38d**. An interesting comparison can be made among compounds **35a**, **35b**, **38a** and **38b** (Figure 10). The disubstituted progenitor **35a** has very low affinity; addition of a third substituent, 1-phenyl in **35b** or 4-ethyl in **38a**, causes only a twofold or threefold increase in binding affinity, respectively. By contrast, addition of the fourth substituent (to give **38b**) causes either an 900- or 500-fold increase in binding affinity, respectively. Clearly, this is not additive behavior—two groups that each alone raise binding affinity twofold and threefold, together raise binding not sixfold but 1600-fold. This suggests that to achieve high binding affinity there needs to be a detailed

and proper match between the peripheral substituents and several subsites on the receptor, and in the azole systems we have explored, it appears that this requires a tetra-substituted ring (see below). Consistent with this is the low affinity of the isoxazole **41**, whose affinity is similar to the most closely related tri-substituted pyrazole **38a**.

There are other interesting trends in the pyrazole series: replacement of the N-phenyl substituent (**38b**) with an N-benzyl group (**38c**) causes a dramatic 100-fold reduction in binding. Both of these compounds are tetra-substituted pyrazoles, and they contain the homobibenzyl motif A that was considered to be an important factor for receptor binding (as do all of the other compounds in Table 1). The decrease in binding affinity in **38b** compared with **38c** again suggests the need for a detailed match between ligand substituents and receptor subsites: the extra 'kink' in the benzyl substituent in **38c** might be repositioning the peripheral substituents in a less favorable geometry. The addition of a hydroxyl group at the *para* position of the N-phenyl substituent (compound **38d** compared with **38b**) causes a minor increase in binding, indicating that polarity is well tolerated in this region of the receptor.

Structural comparisons between high-affinity pyrazole ligands and other nonsteroidal ligands
The conformation of pyrazoles **35a,b** and **38a,b** was determined by *ab initio* calculations at the 3-G21* level (Figure 11). The action of A-strain is evident in these structures: even in the disubstituted system **35a**, the 5-phenyl group is twisted ~60° out of the plane; this twisting increases as the third (**35b**, **38a**) and fourth (**38b**) substituents are added to the pyrazole ring, so that in **38b** the 5-phenyl substituent is nearly perpendicular to the pyrazole core. In this conformation **38b** resembles the general propeller-type conformation of the triarylethylene nonsteroidal estrogens such as tamoxifen [41].

Although the comparison of the conformations of tamoxifen with pyrazole **38b** might give some idea of the reason **38b** binds to ER with high affinity, it does not adequately explain why **35a**, **35b** and **38a** have so much lower binding affinities. When the latter three pyrazoles are compared with **38b**, it is apparent that there is little difference in conformation that could account for the large discrepancy in binding within the series. The reasons for the marked changes in RBA in response to very small changes in structure, noted especially for the pyrazole series, are therefore not intuitively obvious from an examination of the structure of the ligands alone, although they are not entirely unexpected on the basis of the behavior of other nonsteroidal ligands and the detailed fit of these congeners in the ligand-binding pocket of the estrogen receptor (see below).

Analysis of the X-ray structure of the estrogen-receptor ligand-binding domain complexed with estradiol and the nonsteroidal ligand raloxifene

The explanation that was previously proposed — that high-affinity binding to ER derives from a proper match between the peripheral substituents on the ligand and their complementary binding regions on the receptor—can now be considered in some detail, because, recently, the X-ray structures of the estrogen receptor-α bound to estradiol and the nonsteroidal ligand raloxifene have been reported [42].

The ligand-binding pocket in the ER–estradiol structure has a volume of approximately 450 Å^3, which is ~200 Å^3 larger than the volume of estradiol [43] (Figure 12a). As a result, there is a large hydrophobic space around the central portion of the binding pocket, especially in the regions corresponding to the 11β position and, to a lesser degree, 7α position (Figure 12a), which is consistent with the tolerance that ER shows for binding steroids with large substituents at these positions [36]. A view of the ER–raloxifene structure is shown in Figure 12b. The core of this ligand is oriented in the same manner as estradiol and occupies much of the same space in the binding pocket, but the benzoyl substituent projects outward, askew of the ligand core, with the piperidinyl sidechain extending into an upper hydrophobic region, which is much more open due to the displacement of helix 12 [42].

Comparison between raloxifene and the tetra-substituted pyrazole (38b)

The structure of the high-affinity pyrazole (**38b**) can be overlayed onto the structure of raloxifene (Figure 13a). In such a superposition, it is evident that the centroids of all three aromatic rings lie quite close to one another. This structural alignment can be used to place the pyrazole **38b** into the ligand-binding pocket of the ER–raloxifene structure (Figure 13b). With a minimal, energetically reasonable rearrangement of nearby residues (see Figure 13 legend), this ligand can fit quite comfortably in the raloxifene pocket (compare Figure 13b with Figure 12b).
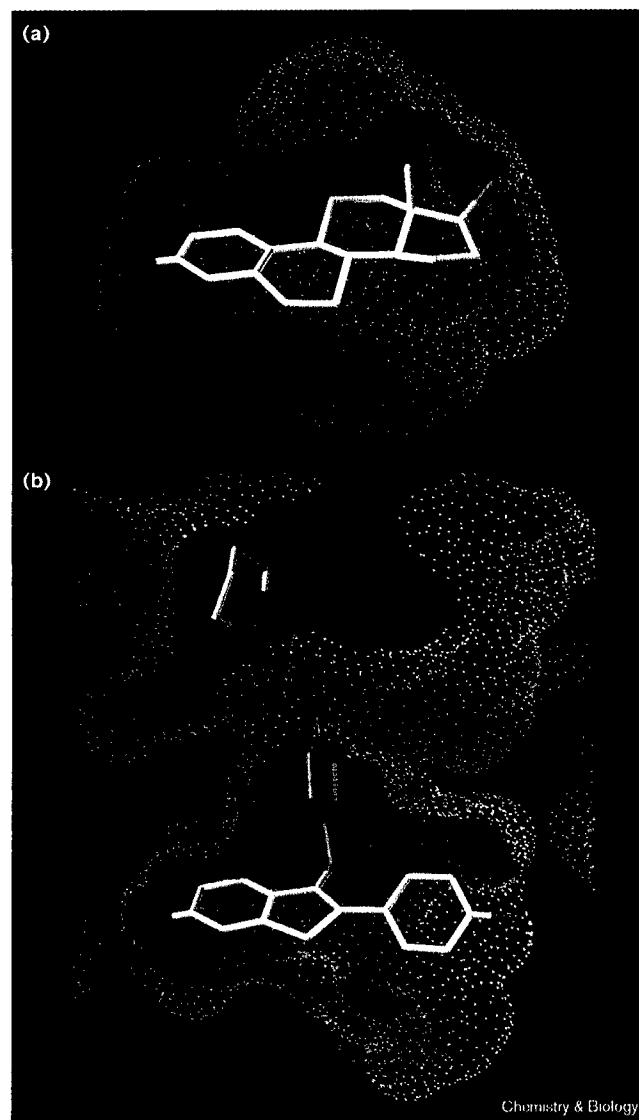
Ligand binding pockets for **(a)** estradiol and **(b)** raloxifene. Structures were prepared from the crystallographic coordinates [43] by generating a solvent-accessible surface for the protein (green–blue dot surface) and for the ligand (purple).

In the arrangement shown in Figure 13b, the two hydroxyl groups are positioned in such a manner that they could engage the same protein hydrogen-bonding partners as do the corresponding hydroxyl groups in raloxifene; the 3-(p-hydroxyphenyl) substituent of **38b** is mimicking the estradiol A-ring surrogate of raloxifene (i.e. the fused phenol of the benzothiophene unit) and the 5-(*p*-hydroxyphenyl) group of **38b** is mimicking the pendant *p*-hydroxyphenyl group at position 2 of the benzothiophene (compare with Figure 12b). The 1-phenyl group of **38b** overlies the benzoyl arene of raloxifene and projects into channel that exists in roughly the 11β direction in the ER–raloxifene

Figure 13
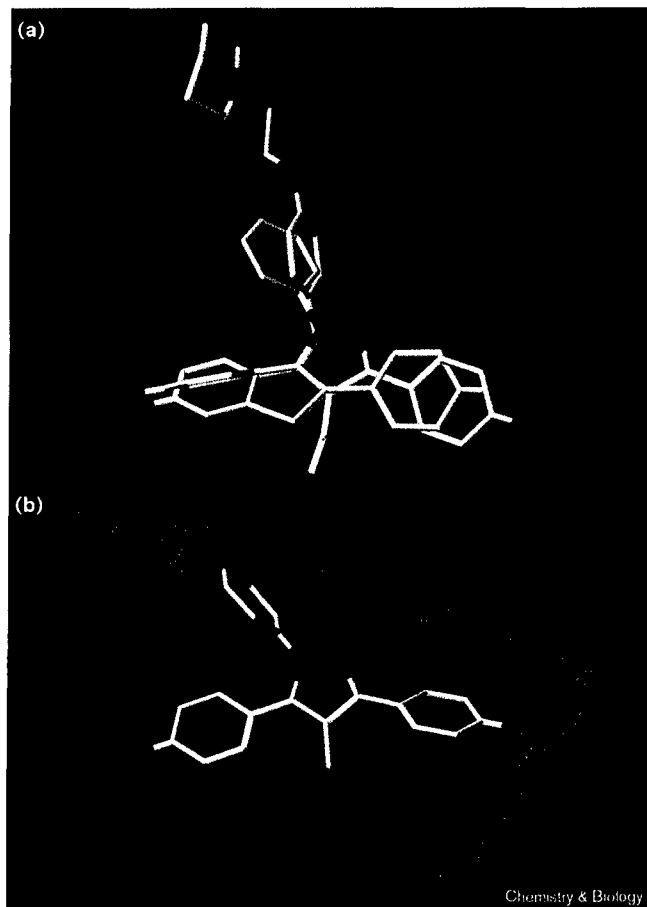
(a) Overlay of pyrazole **38b** with raloxifene and (b) pyrazole **38b** in the binding pocket of the ER–raloxifene structure. (a) The overlay of the two ligands was obtained by a least-squares multifitting seven atoms in each molecule (rms=0.924 Å): in each of the three benzene rings, the two atoms selected were the ones at the site of attachment and the ones *para* to this site; in addition, the *p*-hydroxy group on the 5-phenyl substituent in pyrazole **38b** was overlaid with the benzothiophene hydroxyl group. (b) Pyrazole **38b** was pre-positioned into the ER–raloxifene crystal structure [42] from the overlay shown in (a). From this structure additional docking studies using FlexiDock (Tripos, St Louis, MO) followed by a three-step minimization using the TRIPOS Forcefield were conducted to afford the final model (see the Materials and methods section). This minimization caused only small changes in the protein and ligand, but reduced the ligand–protein interaction energy to a reasonable level.

structure. The 4-ethyl substituent on pyrazole **38b** projects outwards from the heterocycle from a position that corresponds roughly to the sulfur atom of the benzothiophene ring system, and extends into an open pocket in the ER.

When analyzed in this manner, one can appreciate that the pyrazole core can display these four substituents in a manner congruent with the same regions in the binding pocket of the estrogen receptor that accommodate corresponding portions of raloxifene. In addition, the high cost in binding affinity that results from the absence of

either the 1-phenyl or the 4-ethyl substituent (compare with Figure 10) suggests that proper registration of each of the four peripheral substituents into its appropriate binding subsite is supported by the interaction of the other three. By this analysis, it is therefore not surprising that all of the other heterocyclic systems that were only di-substituted or tri-substituted were low affinity ligands, at least with the substituents we have thus far investigated. The low-affinity of the tetra-substituted imidazoles, however, most likely derives from their high polarity, as noted (see below).

The importance of core structural element in ligand binding: passive or active?

The question raised initially—does the core scaffold in these novel ER ligands play only a passive role in their binding, merely displaying the peripheral substituents in an appropriate topology, or is its role more active or functional?—can be answered reasonably definitively from the results we have obtained so far. Clearly, with the substituents we have examined, high-affinity binding was obtained only with those azoles that afforded the possibility of tetra-substitution. But of these, the 1,2-diazoles (pyrazoles) and the 1,3-diazoles (imidazoles), only the pyrazoles gave good binding. Although there are not many direct comparisons that can be made between these two diazole systems, pyrazole **38b** and imidazoles **12** and **17** are, in fact, just ring nitrogen isomers of one another, having otherwise identical peripheral groups and functionality (Figure 9). The same is true for pyrazole **38d** and imidazole **6b**. In both cases, however, the pyrazole partner binds to ER with ~30–36-fold higher affinity than the isomeric imidazole(s). This would suggest that the core structure does play more than a passive role in ER binding, although, as noted before, the high polarity and significant dipole moment of the imidazole might be the principal reason for the difference in this case. The issue of the functional role of the core scaffold in ER binding needs to be investigated further in these and other heterocyclic systems.

Significance

Compounds with a remarkable variety of structures bind with high affinity to the estrogen receptor (ER), and many nonsteroidal ligands have been prepared in the search for agents that have improved tissue-selectivity profiles. The application of combinatorial approaches to the development of selective ER ligands, however, is still in a state of infancy.

Based on a simple pharmacophore model consisting of a core scaffold and various peripheral groups we have designed systems that display the peripheral groups on simple heterocyclic core systems, which are readily prepared by simple condensation reactions. Here, we describe the synthesis and ER-binding affinity of various substituted 1,2- and 1,3-azoles.

No significant binding was found for members of the imidazole, thiazole or isoxazole classes, and this is rationalized either by the inherent polarity of these compounds (imidazoles) or by their inability to carry a sufficient number of the types of peripheral substituents we have explored so far (thiazoles, oxazoles and isoxazoles). Several members of the pyrazole class did show good binding affinity, however, the best being a tetra-substituted pyrazole **38d**. Both **38b** and **38d** bear an unexpectedly close conformational relationship to the nonsteroidal ligand raloxifene.

Compounds such as **38b** and **38d** are well suited to combinatorial synthesis using solid-phase methods. The large differences in binding affinity that result from small structural changes suggest that a thorough investigation of many possible combinations of core structures and peripheral substituents will be needed to identify novel high-affinity ligands for the ER that can be evaluated for their selective biological activity. The solid-phase combinatorial synthesis of pyrazole libraries is currently underway and has yielded other high-affinity ligands for the estrogen receptor (S.R.S. and J.A.K., unpublished observations). Some of these heterocycles have also shown intriguing biological activity [43].

Materials and methods
General methods
All reactions using water- or air-sensitive reagents were conducted under an Ar atmosphere with dry solvents. Solvents were distilled under N_2 as follows: CH_2Cl_2 from CaH_2, tetrahydrofuran (THF) from sodium benzophenone ketyl, dimethylformamide (DMF) from $MgSO_4$, and hexanes from $CaSO_4$. Triethylamine was distilled over CaH_2. All other reagents were purchased from commercial suppliers and used without further purification. Reactions were all monitored using thin-layer chromatography (TLC), performed on 0.25 mm silica gel glass plates containing F-254 indicator. Visualization on TLC was achieved by UV light (254 nm), iodine vapors, or phosphomolybdic acid indicator. Flash chromatography was performed using Woelm 32–63 μm silica gel packing unless otherwise noted.

^{1}H NMR and ^{13}C NMR spectra were recorded on a Varian U400, Varian U500 or Varian INOVA 750. NMR spectra chemical shifts (δ) are reported in parts per million downfield from TMS and referenced with either TMS internal standard for $CDCl_3$, acetone-d_6, MeOD-d_4, or DMSO-d_6 solvent peak. NMR coupling constants are reported in Hertz. Electron ionization (EI) spectra were obtained using a Finnigan–MATCH5 spectrometer at 70 eV. Fast atom bombardment (FAB) were recorded on a VG ZAB-SE spectrometer. High-pressure liquid chromatography (HPLC) was performed on a SpectraPhysics P100 solvent delivery system with ultraviolet detection at 254 nm. Elemental analysis was performed by the Microanalytical Service Laboratory at the University of Illinois. All characterized compounds are chromatographically homogeneous.

Relative binding affinities
Assays were performed as reported previously [44] using lamb uterine cytosol diluted to approximately 1.5 nM of receptor, which was incubated with buffer of several concentrations of unlabeled competitor together with 10 nM [3H]estradiol for 18–24 h. Free ligand was removed by adsorption onto dextran-coated charcoal. Unlabeled competitors were prepared in 1:1 DMF:TEA to ensure solubility.

Molecular modeling and docking studies
Solvent-accessible surfaces were generated (Figures 12 and 13) using the QCPE Connolly Program module (Indiana University) in Sybyl 6.5 (Tripos, St. Louis, MO). Figure 13b: the pre-positioned pyrazole **38b** was used for additional docking studies using the Tripos FlexiDock module. Both hydrogen-bond donors and acceptors within the pocket surrounding the ligand and the ligand itself in addition to select rotatable torsional bonds were defined in order to afford an optimal docked-structure prior to molecular mechanics minimization. With the protein backbone held rigid, the ligand and the protein residues within 8 Å of the ligand were then minimized using a step-wise approach: first torsional bonds about the ligand were minimized holding the receptor fixed, followed by minimization of the receptor holding the ligand fixed, and then minimization of both the ligand and receptor. Minimizations were done using the TRIPOS Forcefield (as implemented in the program Sybyl) with the Powell gradient method and default settings (final RMS < 0.05 kcal/mol-Å).

Representative chemical synthesis
4,5-Di(4-methoxyphenyl)-1H-imidazole (2). To 4,4′-dimethoxybenzil (1) (2.0 g, 7.4 mmol) and *p*-formaldehyde (1.0 g, 11.1 mmol) was added formamide (50 ml). The bright yellow suspension was heated to reflux (220°C) for 2 h. The reaction mixture was then cooled to room temperature then to 0°C. The crystals that formed were filtered and recrystallized from EtOAc to afford 2 (2.4 g, 86%). mp 183–184°C (lit [16] mp 183–184°C); ^{1}H NMR (400 MHz, MeOH-d_4) δ 7.64 (s, 1H), 7.44 (d, 4H, J = 7.50), 6.89 (d, 4H, J = 7.50), 3.79 (s, 6H); ^{13}C NMR (100 MHz, MeOH-d_4) δ 158.4, 135.2, 129.1, 128.9, 122.6, 114.2, 55.3.

General demethylation procedure using BBr_3. To a stirring solution of the methyl-protected heterocycle (1 equiv) in CH_2Cl_2 at −78°C was added a solution of BBr_3 (4–5 equiv) as a 1N solution in CH_2Cl_2. The reaction was allowed to warm to room temperature and stirred for 18 h. After quenching with H_2O, the layers were separated and the aqueous layer extracted with EtOAc (3 × 5 ml). The combined organic layers were dried over Na_2SO_4, fitered and concentrated to afforded the crude phenols. Flash chromatography afforded the demethylated products.

4,5-Di(4-hydroxyphenyl)-1H-imidazole (3). Imidazole 2 (100 mg, 0.35 mmol) afforded 3 (52 mg, 59%) by the general BBr_3 demethylation procedure. ^{1}H NMR (400 MHz, $CDCl_3$) δ 14.56 (br s, 1H), 9.93 (br s, 1H), 9.24 (s, 1H), 7.24 (d, 4H, J = 8.47), 6.82 (d, 4H, J = 8.40); MS (FAB) *m/z* (relative intensity, %) 253.1 (MH+ 24), 169.2 (100).

2,4,5-Tri(4-methoxyphenyl)-1H-imidazole (4). A suspension of 4,4′-dimethoxybenzil (1) (4.0 g, 15 mmol) and *p*-anisaldehyde (20 ml, 164 mmol) and formamide (100 ml) was heated to reflux (220°C) for 2 h, during which time the reaction mixture became homogeneous. The reaction was then cooled to 0°C and the precipitated product 4 was filtered. The light yellow powder was recrystallized from MeOH/H_2O to afford 3.80 g of 4 [19] (66%). mp 89–91°C (lit [19] mp 88–94°C). ^{1}H NMR (400 MHz, Acetone-d_6) δ 7.98 (d, 2H, J = 8.88), 7.42 (d, 4H, J = 8.52), 7.01 (d, 2H, J = 8.83), 6.92 (br s, 4H), 3.79 (s, 3H), 3.75 (s, 6H); ^{13}C NMR (100 MHz, Acetone-d_6) δ 162.4, 159.9, 158.9, 145.4, 131.0, 129.0, 128.9, 126.6, 132.8, 114.0, 113.7, 113.6; MS (EI, 70 eV) *m/z* (relative intensity, %) 386.2 (M+, 100), 371 (30), 280 (100), 265 (30); HRMS calc'd for $C_{21}H_{16}N_2O_3$: 345.123800, found: 345.123918.

General N-alkylation procedure for imidazoles. A solution of imidazole 4 (200 mg, 0.52 mmol) in THF (10 ml) and DMF (1.5 ml) was cooled to 5°C. NaH (31 mg, 0.78 mmol) was added as 60% dispersion in mineral oil. The reaction mixture was warmed to room temperature for 1 h and respective alkyl halide (0.04 ml, 0.62 mmol) was added. The resulting suspension was heated to reflux for 12 h, then cooled to room temperature. The light precipitate was filtered, and the filtrate was concentrated under vacuum to a yellow solid which was flashed on silica (30% EtOAc/Hexanes) to afford alkylated products **5b–d** in 80–90% yields.

1-Ethyl-2,4,5-tri(4-methoxyphenyl)-imidazole (5b). ^{1}H NMR (400 MHz, $CDCl_3$) δ 7.60 (AA'XX', 2H, J_{AX} = 8.88, J_{AA} = 2.51), 7.46 (AA'XX', 2H,

$J_{AX} = 8.97$, $J_{AA} = 2.56$), 7.32 (AA'XX', 2H, $J_{AX} = 8.88$, $J_{AA} = 2.56$),7.00 (AA'XX', 2H, $J_{AX} = 8.88$, $J_{AA} = 2.51$), 6.99 (AA'XX', 2H, $J_{AX} = 8.88$, $J_{AA} = 2.56$), 6.74 (AA'XX', 2H, $J_{AX} = 8.97$, $J_{AA} = 2.56$), 3.87 (q, 2H, $J = 7.32$), 3.87 (s, 3H), 3.85 (s, 3H), 1.00 (t, 3H, $J = 7.14$); ^{13}C NMR (100 MHz, CDCl$_3$) δ 160.0, 159.7, 158.1, 146.8, 137.2, 132.4, 130.5, 127.9, 127.5, 123.8, 123.7, 114.5, 114.0, 113.5, 55.3, 55.2, 55.1, 39.5, 16.2.

2,4,5-Tri(4-hydroxyphenyl)-1H-imidazole (6a). According to the general BBr$_3$ demethylation procedure above, imidazole **4** (3.0 g, 7.8 mmol) afforded **6a** as a green-orange solid that darkened upon exposure to air (1.8 g, 68%). mp 203–205°C; ^{1}H NMR (400 MHz, Acetone-d_6) δ 7.93 (AA'XX', 2H, $J_{AX} = 8.97$, $J_{AA} = 2.47$), 7.40 (AA'XX', 4H, $J_{AX} = 8.60$, $J_{AA} = 2.47$), 6.89 (AA'XX', 2H, $J_{AX} = 8.97$, $J_{AA} = 2.47$), 6.80 (AA'XX', 2H, $J_{AX} = 8.60$, $J_{AA} = 2.47$); ^{13}C NMR (100 MHz, Acetone-d_6) δ 157.9, 156.4, 145.9, 129.0, 126.8, 124.0, 123.4, 121.3, 115.0, 114.7; MS (FAB) *m/z* (relative intensity, %) 345.1 (M+H$^+$, 10), 353 (10), 169 (100); HRMS calc'd for C$_{21}$H$_{16}$N$_2$O$_3$: 345.123800, found: 345.123918.

1-Ethyl-2,4,5-tri(4-hydroxyphenyl)-imidazole (6b). According to the general BBr$_3$ demethylation procedure above, imidazole 5b (185 mg, 0.46 mmol) afforded **5b** (107 mg, 62%). mp 150–153°C; ^{1}H NMR (400 MHz, Acetone-d_6) δ 7.51 (AA'XX', 2H, $J_{AX} = 8.52$, $J_{AA} = 2.42$), 7.34 (AA'XX', 2H, $J_{AX} = 8.71$, $J_{AA} = 2.39$), 7.24 (AA'XX', 2H, $J_{AX} = 8.63$, $J_{AA} = 2.41$), 6.97 (AA'XX', 2H, $J_{AX} = 8.58$, $J_{AA} = 2.31$), 6.90 (AA'XX', 2H, $J_{AX} = 8.75$, $J_{AA} = 2.31$), 6.64 (AA'XX', 2H, $J_{AX} = 8.96$, $J_{AA} = 2.43$), 3.93 (q, 2H, $J = 7.19$), 0.98 (t, 3H, $J = 7.12$); ^{13}C NMR (100 MHz, Acetone-d_6) δ 158.2, 157.9, 155.9, 146.5, 136.8, 132.5, 130.3, 127.9, 127.8, 126.6, 122.5, 122.4, 116.0, 115.4, 114.8, 17.9, 15.4; MS (FAB) *m/z* (relative intensity, %) 372.1 (MH$^+$, 100), 343 (15), 275 (10), 214 (25), 162 (30), 148 (30); HRMS calc'd for C$_{23}$H$_{20}$N$_2$O$_3$: 372.147251, found: 372.147393.

1-Ethyl-2,5-(4-methoxyphenyl)-4-phenyl imidazole (11). Azido-ketone **9** (50.0 mg, 0.187 mmol) and imine **10** (92.0 mg, 0.564 mmol) were dissolved in THF (15 ml). Et$_3$N (29.0 μλ, 0.208 mmol) was added via syringe and reaction stirred at room temperature for 48 h. The reaction mixture was then poured into H$_2$O and extracted with CH$_2$Cl$_2$, organic fractions were pooled, dried over Na$_2$SO$_4$, filtered and solvent removed under reduced pressure. The intermediate, 2,5-dihydro-2-hydroxyimidazole, used in next step without further purification or characterization, was taken up CH$_2$Cl$_2$ (10 ml). Solution was cooled to 0°C and TFA (14.4 μl, 0.187 mmol) was added via syringe. Reaction stirred at 0°C for 36 h. The mixture was diluted with CH$_2$Cl$_2$ (10 ml) and washed with H$_2$O, sat. NaHCO$_3$, and sat. NaCl successively. The organic fraction was dried over Na$_2$SO$_4$, filtered and solvent removed under reduced pressure. Purification by flash column chromatography (1:2 EtOAc:Hexanes) and recrystallization from CH$_2$Cl$_2$/Hexanes afforded imidazole **11** as a white solid (24.6 mg, 34% yield from azide **9**). ^{1}H NMR (500 MHz, CDCl$_3$) δ 7.63 (AA'XX', 2H, $J_{AX} = 8.81$, $J_{XX'} = 2.53$), 7.54 (m, 2H), 7.34 (AA'XX', 2H, $J_{AX} = 8.80$, $J_{XX'} = 2.45$), 7.20 (m, 2H), 7.12 (m, 1H), 7.02 (AA'XX', 2H, $J_{AX} = 8.78$, $J_{AA'} = 2.54$), 7.01 (AA'XX', 2H, $J_{AX} = 8.43$, $J_{AA'} = 2.57$), 3.90 (q, 2H, $J = 7.08$), 3.89 (s, 3H), 3.87 (s, 3H), 1.02 (t, 3H, $J = 7.17$); ^{13}C NMR (125 MHz, CDCl$_3$) δ 200..8, 160.0, 159.8, 147.0, 134.8, 132.3 (2), 130.5 (2), 129.3, 128.9, 128.0 (2), 126.6 (2), 126.0, 123.6, 114.5 (2), 114.0 (2), 55.33, 55.28, 36.4, 16.2; MS (EI, 70 eV) *m/z* 384.2 (M$^+$); Anal. calc'd for C$_{25}$H$_{24}$N$_2$O$_2$, C: 78.10%, H: 6.29%, N: 7.29%, found, C: 77.91%, H:6.28%, N: 7.28%.

General demethylation procedure using BF$_3$•SMe$_2$. To a stirring solution of the methyl protected heterocycle (1 equiv) in CH$_2$Cl$_2$ (8 ml) at room temperature was added BF$_3$•SMe$_2$ complex (75 equiv). After stirring for 24 h, solvent and excess reagent were evaporated under nitrogen stream in hood. Residue was taken up in EtOAc and washed with H$_2$O and sat. NaCl. Organic extract was dried over Na$_2$SO$_4$, filtered and solvent removed under reduced pressure. The resulting residue was purified though a silica plug, eluting with EtOAc. Solvent evaporation afforded the deprotected products.

1-Ethyl-2,5-(4-hydroxyphenyl)-4-phenyl imidazole (12). Imidazole **11** (12.0 mg, 0.031 mmol) was demethylated according to the general BF$_3$•SMe$_2$ procedure to afford imidazole **12** as an off-white powder (10.6 mg, 95%). ^{1}H NMR (500 MHz, Acetone-d_6) δ 7.80 (AA'XX', 2H, $J_{AX} = 8.81$, $J_{XX'} = 2.44$), 7.47–7.49 (m, 2H), 7.44 (AA'XX', 2H, $J_{AX} = 8.65$, $J_{XX'} = 2.44$), 7.37–7.40 (m, 3H), 7.14 (AA'XX', 2H, $J_{AX} = 8.80$, $J_{AA'} = 2.43$), 7.06 (AA'XX', 2H, $J_{AX} = 8.68$, $J_{AA'} = 2.46$), 4.25 (q, 2H, $J = 7.28$), 1.17 (t, 3H, $J = 7.29$); MS (FAB) *m/z* 357.2 (M+H$^+$); HRMS calc'd for C$_{23}$H$_{21}$N$_2$O$_2$: 357.160303, found: 357.160000.

5-Ethyl-1,4-(4-methoxyphenyl)-2-phenyl imidazole (16). Keto-amide **15** (110.0 mg, 0.273 mmol) and ammonium acetate (105.0 mg, 1.362 mmol) were heated to reflux in acetic acid (10 ml) for 48 h. Acetic acid was removed under reduced pressure, resulting residue was taken up in EtOAc, washed with sat. NaHCO$_3$, H$_2$O, and sat. NaCl. Organic extracts were dried over Na$_2$SO$_4$, filtered and solvent removed. Product was purified by flash column chromatography (1:4 EtOAc:Hexanes) and recrystallization from CH$_2$Cl$_2$/Hexanes to give imidazole **16** as a white solid (25.7 mg, 25%). ^{1}H NMR (500 MHz, CDCl$_3$) δ 7.72 (AA'XX', 2H, $J_{AX} = 8.29$, $J_{XX'} = 2.55$), 7.14 (m, 2H), 7.21 (m, 3H), 7.19 (AA'XX', 2H, $J_{AX} = 9.33$, $J_{XX'} = 2.71$), 6.98 (AA'XX', 2H, $J_{AX} = 8.48$, $J_{AA'} = 2.52$), 6.96 (AA'XX', 2H, $J_{AX} = 8.62$, $J_{AA'} = 2.74$), 3.87 (s, 3H), 3.85 (s, 3H), 2.67 (q, 2H, $J = 7.48$), 1.01 (t, 3H, $J = 7.45$); MS (EI, 70 eV) *m/z* 384.2 (M$^+$).

5-Ethyl-1,4-(4-hydroxyphenyl)-2-phenyl imidazole (17). Imidazole **16** (25.0 mg, 0.065 mmol) was demethylated as outlined in general BF$_3$•SMe$_2$ procedure above to give deprotected imidazole **17** as an off-white powder (20.2 mg, 87%). ^{1}H NMR (400 MHz, Acetone-d_6) δ 9.04 (br s, 1H), 8.51 (br s, 1H), 7.64 (AA'XX', 2H, $J_{AX} = 8.73$, $J_{XX'} = 2.51$), 7.50-7.47 (m, 2H), 7.31–7.27 (m, 5H), 7.01 (AA'XX', 2H, $J_{AX} = 8.94$, $J_{AA'} = 2.76$), 6.94 (AA'XX', 2H, $J_{AX} = 8.73$, $J_{AA'} = 2.52$), 2.69 (q, 2H, $J = 7.48$), 1.02 (t, 3H, $J = 7.49$); MS (FAB) *m/z* 357.1 (M+H$^+$); HRMS calc'd. for C$_{23}$H$_{21}$N$_2$O$_2$: 357.1603, found 357.1602.

2,4-Di(4-methoxyphenyl)-thiazole (21a). A suspension of thioamide **19** (1.3 g, 7.9 mmol) and α-bromo-4'-methoxy-acetophenone (**20**) (1.8 g, 7.9 mmol) in DMF (10 ml) was heated to reflux for 1h, until it became homogeneous. The heat was removed and the reaction was stirred for 15 h at room temperature. The reaction mixture was poured into H$_2$O (50 ml) and the solid precipitate was filtered to afford crude **21a**. Recrystallization from CH$_3$NO$_2$ afforded pure **21a** as light yellow crystals (1.8 g, 81%). ^{1}H NMR (400 MHz, CDCl$_3$) δ 7.98 (AA'XX', 2H, $J_{AX} = 8.87$, $J_{AA} = 2.53$), 7.63 (AA'XX', 2H, $J_{AX} = 8.94$, $J_{AA} = 2.48$), 6.86 (AA'XX', 2H, $J_{AX} = 8.87$, $J_{AA} = 2.53$), 6.85 (AA'XX', 2H, $J_{AX} = 8.94$, $J_{AA} = 2.48$), 7.26 (s, 1H), 3.86 (s, 3H), 3.85 (s, 3H); ^{13}C NMR (400 MHz, CDCl$_3$) δ 167.5, 160.9, 159.4, 155.6, 127.9, 127.6, 127.4, 126.6, 114.1, 113.9, 109.9, 55.3, 55.2; MS (EI, 70 eV) *m/z* (relative intensity, %) 297.1 (M$^+$, 100), 282.1 (10), 164.1 (30), 149.1 (55), 133.1 (10), 121.1 (25), 77.1 (15); HRMS calc'd for C$_{17}$H$_{15}$NSO$_2$: 297.082469, found: 297.082351.

2,4-Di(4-hydroxyphenyl)-thiazole (22a). Thiazole **21a** (1.0 g, 3.6 mmol) was demethylated using BBr$_3$ as outlined in the general procedure above to afford **22a** (430 mg, 45%). mp 218–221°C; ^{1}H NMR (400 MHz, Acetone-d_6) δ 8.84 (br s, 2H), 7.92 (AA'XX', 4H, $J_{AX} = 8.57$, $J_{AA} = 2.17$), 7.58 (s, 1H), 6.96 (AA'XX', 2H, $J_{AX} = 8.79$, $J_{AA} = 2.51$), 6.92 (AA'XX', 2H, $J_{AX} = 8.78$, $J_{AA} = 2.44$); ^{13}C NMR (100 MHz, Acetone-d_6) δ 168.2, 159.3, 157.2, 155.8, 127.7, 127.3, 126.2, 125.1, 115.2, 114.9, 109.3; MS (EI, 70 eV) *m/z* (relative intensity, %) 296.1 (M$^+$, 100), 150.1 (27), 121.1 (11), 78.1 (8); HRMS calc'd for C$_{15}$H$_{11}$NSO$_2$: 269.051163, found: 269.051051.

2,4-(4-Methoxyphenyl)-5-phenyl oxazole (28). Azido-ketone 27 (0.18 g, 0.673 mmol) and p-anisaldehyde (0.25 ml, 2.05 mmol) were dissolved in THF (15 ml). Et$_3$N (94.0 μl, 0.674 mmol) was added via syringe and reaction stirred at room temperature for 48 h. The reaction mixture was then poured into H$_2$O and extracted with CH$_2$Cl$_2$, organic fraction was dried over Na$_2$SO$_4$, filtered and solvent removed under reduced pressure. Resulting intermediate 2,5-dihydro-5-hydroxyoxazole, used in next

step without further purification or characterization, was taken up CH_2Cl_2 (10 ml). Solution was cooled to 0°C and TFA (54.0 μl, 0.701 mmol) was added via syringe. Reaction stirred at 0°C for 36 h. The mixture was diluted with CH_2Cl_2 (10 ml) and washed with H_2O, sat. $NaHCO_3$, and sat. NaCl successively. Organic extracts were combined, dried over Na_2SO_4, filtered and solvent removed under reduced pressure. Purification by flash column chromatography (1:2 EtOAc: hexanes) and recrystallization from CH_2Cl_2/Hexanes afforded oxazole **28** as a white solid (72.4 mg, 30% yield from azide 27). mp 125–128°C (lit. [27] mp 126–127°C); ¹H NMR (500 MHz, CDCl₃) δ 7.84 (AA′XX′, 2H, J_{AX} = 8.89, $J_{XX'}$ = 2.47), 7.43 (AA′XX′, 2H, J_{AX} = 8.83, $J_{XX'}$ = 2.48), 7.53 (m, 2H), 7.32 (m, 2H), 7.26 (tt, 1H, *J* = 7.03, 1.42), 6.97 (AA′XX′, 2H, J_{AX} = 8.85, $J_{AA'}$ = 2.53), 6.88 (AA′XX′, 2H, J_{AX} = 8.70, $J_{AA'}$ = 2.53), 3.84 (s, 3H), 3.81 (s, 3H).

2,4-(4-Hydroxyphenyl)-5-phenyl oxazole (29). Oxazole **28** (22.0 mg, 0.062 mmol) was demethylated according to the general BF_3•SMe_2 procedure above to give deprotected oxazole **29** as an off-white powder (18.8 mg, 93%). ¹H NMR (500 MHz, Acetone-*d₆*) δ 9.43 (br s, 1H), 8.90 (br s, 1H), 8.08 (AA′XX′, 2H, J_{AX} = 9.06, $J_{XX'}$ = 2.62), 7.61 (m, 2H), 7.49 (m, 3H), 7.44 (AA′XX′, 2H, J_{AX} = 8.97, $J_{XX'}$ = 2.44), 7.12 (AA′XX′, 2H, J_{AX} = 8.87, $J_{AA'}$ = 2.50), 6.95 (AA′XX′, 2H, J_{AX} = 8.86, $J_{AA'}$ = 2.42); MS *m/z* 329.1 (M⁺); HRMS calc'd. for $C_{21}H_{15}NO_3$: 329.1052, found 329.1285.

2,5-(4-Methoxyphenyl)-4-phenyl oxazole (30). A solution of bromoketone **26** (87.0 mg, 0.285 mmol) and *p*-methoxybenzamide (43.0 mg, 0.285 mmol) in toluene was heated to reflux for 36 h. Toluene was removed under reduced pressure and resulting residue purified by flash column chromatography (1:4 EtOAc:Hexanes). Recrystallization of desired product from CH_2Cl_2/hexanes afforded oxazole **30** as a colorless solid (52.9 mg, 52%). mp 147–149°C; ¹H NMR (500 MHz, CDCl₃) δ 8.08 (AA′XX′, 2H, J_{AX} = 8.58, $J_{XX'}$ = 2.24), 7.72 (m, 2H), 7.59 (AA′XX′, 2H, J_{AX} = 8.72, $J_{XX'}$ = 2.31), 7.39 (m, 2H), 7.33 (m, 1H), 6.99 (AA′XX′, 2H, J_{AX} = 8.63, $J_{AA'}$ = 2.26), 6.92 (AA′XX′, 2H, J_{AX} = 8.68, $J_{AA'}$ = 2.67), 3.88 (s, 3H), 3.85 (s, 3H); ¹³C NMR (100 MHz, CDCl₃) δ 161.2, 159.9, 159.7, 145.1, 135.3, 132.9, 128.6 (2), 128.1 (2), 128.0 (2), 127.96 (2), 127.9, 121.7, 120.3, 114.2 (2), 114.1 (2), 55.4, 55.3; MS *m/z* 357.2 (M⁺).

2,5-(4-Hydroxyphenyl)-4-phenyl oxazole (31). Oxazole **30** (22.0 mg, 0.062 mmol) was demethylated according to the general BF_3•SMe_2 procedure above to give deprotected oxazole **31** as an off-white powder (18.1 mg, 89%). ¹H NMR (500 MHz, Acetone-*d₆*) δ 8.93 (br s, 1H), 8.77 (br s, 1H), 7.99 (AA′XX′, 2H, J_{AX} = 8.83, $J_{XX'}$ = 2.41), 7.72 (m, 2H), 7.53 (AA′XX′, 2H, J_{AX} = 8.77, $J_{XX'}$ = 2.46), 7.40 (m, 2H), 7.34 (tt, 1H, *J* = 7.36, 1.33), 6.99 (AA′XX′, 2H, J_{AX} = 8.70, $J_{AA'}$ = 2.40), 6.92 (AA′XX′, 2H, J_{AX} = 8.83, $J_{AA'}$ = 2.46); MS *m/z* 329.1 (M⁺); HRMS calc'd for $C_{21}H_{15}NO_3$: 329.1052, found 329.1055.

General procedure for pyrazole synthesis. A suspension of diketone (1 equiv) and appropriate hydrazine hydrochloride (3–5 equiv) in a 3:1 mixture DMF:THF was heated to reflux for 16–24 h with reaction progress being monitored by TLC for disappearance of starting material. The reaction mixtures was cooled to room temperature and poured into iced sat. LiCl solution (10 ml) and EtOAc (10 ml). The layers were separated and the organic layer was washed with brine (10 ml), dried over $MgSO_4$, filtered and concentrated. Purification using flash column chromatography (EtOAc/hexanes systems) afforded the pyrazoles.

3,5-di(4-methoxyphenyl)-1H-pyrazole (34a). Diketone **33** (91 mg, 0.32 mmol) and hydrazine (0.1 ml, 3.2 mmol) were reacted as outlined in general pyrazole procedure to afford **34a** [45] as an off-white solid (32.6 mg, 38%). mp 172–175°C (lit [45] mp 174°C); ¹H NMR (400 MHz, CDCl₃) δ 7.73 (AA′XX′, 4H, J_{AX} = 8.73, J_{AA} = 2.42), 6.97 (AA′XX′, 4H, J_{AX} = 8.73, J_{AA} = 2.42), 6.80 (s, 1H), 3.72 (s, 6H); ¹³C NMR (100 MHz, CDCl3) δ 159.9, 148.3, 126.8, 123.0, 112.9, 98.6, 54.5; MS (FAB) *m/z* (relative intensity, %) 281 (MH⁺, 100).

1-Phenyl-3,5-di(4-methoxyphenyl)-pyrazole (34b). Diketone **33** (100 mg, 0.35 mmol) and phenyl hydrazine hydrochloride (500 mg, 3.5 mmol) were reacted as outlined in general pyrazole procedure above to afford **34b** [46] (30 mg, 25%). mp 159–161°C (lit [46] mp 163°C); ¹H NMR (400 MHz, CDCl₃) δ 7.82 (AA′XX′, 2H, J_{AX} = 8.96, J_{AA} = 2.44), 7.24–7.20 (m, 5H), 7.20 (AA′XX′, 2H, J_{AX} = 8.79, J_{AA} = 2.46), 6.99 (AA′XX′, 2H, J_{AX} = 8.79, J_{AA} = 2.46), 6.84 (AA′XX′, 2H, J_{AX} = 8.96, J_{AA} = 2.44), 6.70 (s, 1H), 3.84 (s, 3H), 3.80 (s, 3H); ¹³C NMR (100 MHz, CDCl₃) δ 159.4, 151.5, 144.1, 140.0, 129.9, 128.8, 127.2, 126.9, 125.5, 125.2, 122.9, 113.9, 113.8, 104.1, 55.2, 55.1; MS (EI, 70 eV) *m/z* (relative intensity, %) 356 (M⁺, 100), 341 (19), 135 (89); HRMS calc'd for $C_{23}H_{20}N_2O_2$: 356.15241, found: 356.152478.

3,5-Di(4-hydroxyphenyl)-1H-pyrazole (35a). Pyrazole **34a** (20 mg, 0.07 mmol) was demethylated with BBr_3 according to the general procedure to afford **35a** [47] as an off-white solid (11 mg, 63%). ¹H NMR (400 MHz, Acetone-*d₆*) δ 8.58 (br s, 2H), 7.75 (AA′XX′, 4H, J_{AX} = 8.95, J_{AA} = 2.46), 6.93 (AA′XX′, 4H, J_{AX} = 8.95, J_{AA} = 2.46), 6.83 (s, 1H); ¹³C NMR (100 MHz, Acetone-*d₆*) δ 157.1, 148.3, 126.5, 123.0, 115.3, 97.5; MS (CI, CH_4) *m/z* (relative intensity, %) 253.1 (MH⁺, 100), 237(10), 161 (5), 123 (15).

1-Phenyl-3,5-di(4-hydroxyphenyl)-pyrazole (35b). Pyrazole **34b** (20 mg, 0.06 mmol) was demethylated with BBr_3 according to the general procedure to afford **34b** [47] as an off-white solid (11.5 mg, 58%). ¹H NMR (400 MHz, CDCl₃) δ 8.64 (s, 1H), 8.45 (s, 1H) 7.79 (AA′XX′, 4H, J_{AX} = 8.78, J_{AA} = 2.38), 7.36 (m, 5H), 7.14 (AA′XX′, 4H, J_{AX} = 8.60, J_{AA} = 2.47), 6.90 (AA′XX′, 2H, J_{AX} = 8.78, J_{AA} = 2.38), 6.81 (AA′XX′, 2H, J_{AX} = 8.78, J_{AA} = 2.47), 6.80 (s, 1H); ¹³C NMR (100 MHz, CDCl₃) δ 157.5, 157.3, 151.3, 144.1, 140.6, 129.9, 128.6, 126.8, 126.7, 124.9, 122.2, 122.1, 115.2, 115.1, 103.7; MS (EI, 70 eV) *m/z* (relative intensity, %) 362.1 (M⁺, 85), 328.1 (100).

4-Ethyl-3,5-di(4-methoxyphenyl)-1H-pyrazole (37a). Diketone **36** (100 mg, 0.32 mmol) and hydrazine (0.12 ml, 3.2 mmol) were reacted as outlined in the general pyrazole procedure above to afford **37a** as a while solid (69 mg, 70%). ¹H NMR (400 MHz, CDCl₃) δ 7.50 (AA′XX′, 4H, J_{AX} = 8.84, J_{AA} = 2.48), 6.94 (AA′XX′, 4H, J_{AX} = 8.90, J_{AA} = 2.50), 3.85 (s, 3H), 2.71 (q, 2H, *J* = 7.38), 1.07 (t, 3H, *J* = 7.44); ¹³C NMR (100 MHz, CDCl₃) δ 159.4, 129.0, 127.4, 124.1, 116.8, 113.9, 55.1, 16.6, 15.3; MS (EI, 70 eV) *m/z* (relative intensity, %) 308.1 (M⁺, 100), 293.1 (73), 160.1 (7), 134 (8).

1-Phenyl-4-ethyl-3,5-di(4-methoxyphenyl)-pyrazole (37b). Diketone **36** (100 mg, 0.35 mmol) and phenyl hydrazine hydrochloride (140 mg, 0.96 mmol) were reacted as outlined in the general pyrazole procedure above to afford 37b as an orange solid (109 mg, 87%). ¹H NMR (400 MHz, CDCl₃) δ 7.72 (AA′XX′, 2H, J_{AX} = 9.03, J_{AA} = 2.44), 7.24 (m, 3H), 7.20 (m, 2H), 7.17 (AA′XX′, 2H, J_{AX} = 8.79, J_{AA} = 2.44), 6.99 (AA′XX′, 2H, J_{AX} = 8.79, J_{AA} = 2.56), 6.90 (AA′XX′, 2H, J_{AX} = 8.79, J_{AA} = 2.44), 3.86 (s, 3H), 3.83 (s, 3H), 2.63 (q, 2H, *J* = 7.57), 1.04 (t, 3H, *J* = 7.57); ¹³C NMR (100 MHz, CDCl₃) δ 159.6, 159.4, 150.8, 141.2, 140.5, 131.5, 129.3, 128.8, 127.0, 126.7, 124.8, 123.5, 120.7, 114.2, 114.1, 55.5, 55.4, 17.3, 15.8; MS (EI, 70 eV) *m/z* (relative intensity, %) 356 (M⁺, 100), 341 (100), 328 (15), 196 (25), 77 (40); HRMS calc'd for $C_{25}H_{24}N_2O_2$: 384.183582, found: 384.183778.

4-Ethyl-3,5-di(4-hydroxyphenyl)-1H-pyrazole (38a). Pyrazole **37a** (69 mg, 0.22 mmol) was demethylated according to the general BBr_3 procedure to afford **38a** as a white solid (35 mg, 57%). ¹H NMR (400 MHz, Acetone-*d₆*) δ 7.49 (AA′XX′, 4H, J_{AX} = 8.85, J_{AA} = 2.46), 6.93 (AA′XX′, 4H, J_{AX} = 8.64, J_{AA} = 2.40), 2.73 (q, 2H, *J* = 7.39), 1.07 (t, 3H, *J* = 7.47); ¹³C NMR (100 MHz, Acetone-*d₆*) δ 156.9, 128.8, 124.3, 122.2, 115.4, 115.2, 16.5, 14.9; MS (CI, CH_4) *m/z* (relative intensity, %) 282.1 (M+H⁺, 100), 263.1 (10), 187.1 (20).

1-Phenyl-4-ethyl-3,5-di(4-hydroxyphenyl)-pyrazole (38b). Pyrazole **37b** (100 mg, 0.26 mmol) was demethylated according to the general BBr_3 procedure to afford **38b** as a white solid (50 mg, 54%). ¹H NMR

(400 MHz, MeOH-d_4) δ 7.51 (AA'XX', 4H, $J_{AX} = 8.67$, $J_{AA} = 2.47$), 7.24–7.42 (m, 5H), 7.05 (AA'XX', 4H, $J_{AX} = 8.81$, $J_{AA} = 2.40$), 6.88 (AA'XX', 2H, $J_{AX} = 8.67$, $J_{AA} = 2.46$), 6.78 (AA'XX', 2H, $J_{AX} = 8.81$, $J_{AA} = 2.40$), 2.60 (q, 2H, $J = 7.53$), 0.98 (t, 3H, $J = 7.39$); MS (EI, 70 eV) m/z (relative intensity, %) 356.1 (M$^+$, 100), 341.1 (100), 328.1 (15), 196.1 (25), 77 (40); HRMS calc'd for $C_{23}H_{21}N_2O_2$: 357.161155, found: 357.160303.

3,5-Di(4-methoxyphenyl)isoxazole (40). To a solution of oxime **39** (1.0 g, 6 mmol) in THF (20 mL) at 0°C was added nBuLi (9.11 ml, 13.3 mmol) as a solution in hexanes. The clear solution was stirred for 30 min at 0°C then methyl 4-methoxybenzoate (498 mg, 3 mmol) was added as a solution in THF (5 ml) over 5 min. The reaction mixture was stirred at 0°C for 30 min, then warmed to room temperature. 5 N HCl (10 ml) was added and the biphasic reaction mixture was brought to reflux overnight (12 h). Upon cooling to 0°C, isoxazole **40** precipitated [33] and was collected via filtration (450 mg, 27%). mp 174–177°C (lit [33] mp 176–177°C); ^{1}H NMR (400 MHz, Acetone-d_6) δ 7.66 (AA'XX', 2H, $J_{AX} = 8.88$, $J_{AA} = 2.44$), 7.63 (AA'XX', 2H, $J_{AX} = 9.1$, $J_{AA} = 2.15$), 6.86 (AA'XX', 2H, $J_{AX} = 8.88$, $J_{AA} = 2.44$), 6.85 (AA'XX', 2H, $J_{AX} = 9.1$, $J_{AA} = 2.44$), 6.57 (s, 1H), 3.73 (s, 3H), 3.72 (s, 3H); ^{13}C NMR (100 MHz, Acetone-d_6) δ 169.8, 162.3, 160.8, 160.7, 127.9, 127.1, 121.5, 120.0, 114.1, 114.0, 95.7, 55.1, 55.0; MS (EI, 70 eV) m/z (relative intensity, %) 281.1 (M$^+$, 5), 150.1 (20), 135.1 (100).

3,5-Di(4-hydroxyphenyl)isoxazole (41). Isoxazole **40** (300 g, 1.1 mmol) was demethylated according to the general BBr$_3$ procedure to afford **41** [34] as a white solid (152 mg, 56%). mp 267–269°C (lit [34] mp 255°C); ^{1}H NMR (400 MHz, Acetone-d_6) δ 10.07 (s, 1H), 9.91 (s, 1H), 7.90 (d, 4H, $J = 8.79$), 7.21 (s, 1H), 6.88 (4H, t, $J = 9.38$); ^{13}C NMR (100 MHz, MeOH-d_4) δ 170.3, 162.8, 159.1, 127.7, 126.9, 119.9, 118.7, 116.3, 115.1, 95.3, 95.0; MS (EI, 70 eV) m/z (relative intensity, %) 253.1 (M$^+$, 60), 133.1 (25), 121.1 (100), 93.0 (20), 77.0 (10), 65.0 (30).

Supplementary material available
Experimental detail regarding the preparation of all intermediates discussed in the synthesis of the above heterocycles is available with the online version of this paper.

References
1. Grese, T.A., *et al.*, & Dodge, J.A. (1997). Molecular determinants of tissue selectivity in estrogen receptor modulators. *Proc. Natl Acad. Sci. USA* **94**, 14105-14110.
2. Kuiper, G.G.J.M., Enmark, E., Pelto-Huikko, M., Nilsson, S. & Gustafsson, J.Å. (1996). Cloning of a novel receptor expressed in rat prostate and ovary. *Proc. Natl Acad. Sci. USA* **93**, 5925-5930.
3. Mosselman, S., Polman, J. & Dijkema, R. (1996). ERb: Identification and charaterization of a novel human estrogen receptor. *FEBS Lett.* **392**, 49-53.
4. Katzenellenbogen, J.A. & Katzenellenbogen, B.S. (1996). Nuclear hormone receptors: ligand-activated regulators of transcription and diverse cell responses. *Chem. Biol.* **3**, 529-536.
5. Horwitz, K.B., *et al.*, & Tung, L. (1996). Nuclear receptor coactivators and corepressors. *Mol. Endocrinol.* **10**, 1167-1177.
6. Glass, C.K., Rose, D.W. & Rosenfeld, M.G. (1997). Nuclear receptor coactivators. *Curr. Opin. Cell. Biol.* **9**, 222-232.
7. Katzenellenbogen, J.A., O'Malley, B.W. & Katzenellenbogen, B.S. (1996). Tripartite steroid hormone receptor pharmacology: interaction with multiple effector sites as a basis for the cell- and promoter-specific action of these hormones. *Mol. Endocrinol.* **10**, 119-131.
8. Magarian, R.A., Overaacre, L.B. & Singh, S. (1994). The medicinal chemistry of nonsteroidal antiestrogens: a review. *Curr. Med. Chem.* **1**, 61-104.
9. Grundy, J. (1957). Artificial estrogens. *Chem. Rev.* **57**, 281-416.
10. Solmssen, U.V. (1945). Synthetic estrogens and the relation between their structure and their activity. *Chem. Rev.* **37**, 481-598.
11. Grese, T.A., *et al.*, & Bryant, H.U. (1998). Synthesis and pharmacology of conformationally restricted raloxifene analogues: highly potent selective estrogen receptor modulators. *J. Med. Chem.* **41**, 1272-1283.
12. Plakowitz, A.D., *et al.*, & Bryant, H.U. (1997). Discovery and synthesis of [6-Hydroxy-3-[4-[2-(1-piperidinyl)ethoxy]phenoxy]-2-(hydroxyphenyl)]benzo[b]thiophene: a novel, highly potent, selective estrogen receptor modulator. *J. Med. Chem.* **40**, 1407-1416.
13. Brown, D.S. & Armstrong, R.W. (1996). Synthesis of tetra-substituted ethylenes on solid support via resin capture. *J. Am. Chem. Soc.* **118**, 6331-6332.
14. Williard, R., *et al.*, & Scanlan, T.S. (1995). Screening and characterization of estrogenic activity from hydroxystilbene library. *Curr. Biol.* **2**, 45-51.
15. Sarshar, S., Siev, D. & Mjalli, A.M.M. (1996). Imidazole libraries on solid support. *Tetrahedron Lett.* **37**, 835-838.
16. Bredereck, H., Gompper, R. & Hayer, D. (1959). Imidazole aus α-diketonen. *Chem. Ber.* **92**, 338-343.
17. Lombardino, J.G. & Weisman, E.H. (1974). Preparation and antiinflammatory activity of some nonacidic trisubstituted imidazoles. *J. Med. Chem.* **17**, 1182-1188.
18. Schubert, V.H., Giesemann, G., Steffen, P. & Bleichert, J. (1962). p-Aryl- und p-Alkoxyphenyl-imidazole. *J. Prakt. Chem.* **18**, 192-202.
19. Hayes, J.F., Mitchell, M.B. & Wicks, C. (1994). A novel synthesis of 2,4,5-triarylimidazoles. *Heterocycles* **38**, 575-585.
20. Gardner, P.D. (1956). Organic peracid oxidation of some enol esters involving R\rearrangement. *J. Am. Chem. Soc.* **78**, 3421-3424.
21. Jenkins, S.S. (1934). The grignard reaction in the synthesis of ketones. IV. A new method of preparing isomeric unsymmetrical benzoins. *J. Am. Chem. Soc.* **56**, 682-684.
22. Patonay, T. & Hoffman, R.V. (1995). Base-promoted reactions of α-azido ketones with aldehydes and ketones: a novel entry to α-azido-hydroxy ketones and 2,5-dihydro-5-hydroxyoxazoles. *J. Org. Chem.* **60**, 2368-2377.
23. Taylor, E.C. & Zoltewicz, J.A. (1960). A new synthesis of aliphatic and aromatic thioamides from nitriles. *J. Am. Chem. Soc.* **82**, 2656-2657.
24. Dolling, K., Zaschke, H. & Schubert, H. (1979). Kristallin-flussige Thiazole. [Liquid-crystalline thiazoles.] *J. Prakt. Chem.* **321**, 643-654.
25. Katrizky, A.R., Boulton, A.J. & Short, D.J. (1960). Interaction at a distance in conjugated systems. Part III. Effect of aryl and heteroaryl groups on the infrared intensities of C=C and C C stretching bands. *J. Chem. Soc.* 1519-1523.
26. Cowper, R.M. & Stevens, T.S. (1940). Mechanism of the reaction between arylamines and benzoins. *J. Chem. Soc.* 347-349.
27. Strzybny, P.P.E., van ES, T. & Backeberg, O.G. (1969). Reaction of α-acyloxyketones with ammonium acetate. *J. South African Chem. Inst.* **22**, 158-164.
28. Marzinzik, A.L. & Felder, E.R. (1996). Solid support synthesis of highly functionalized pyrazoles and isoxazoles; scaffolds for molecular diversity. *Tetrahedron Lett.* **37**, 1003-1006.
29. Reitz, D.B., Beak, P., Farney, R.F. & Helmick, L.S. (1978). Dipole-stabilized carbanions from thioesters. Evidence for stabilization by the carbonyl group. *J. Am. Chem. Soc.* **100**, 5428-5436.
30. Tewari, S.C. & Rastogi, S.N. (1979). Studies in antifertility agents: Part XXII: 1,2-diethyl-1,3-bis-(p-hydroxyphenyl)-1-propene. *Ind. J. Chem.* **18B**, 62-64.
31. Clark, J.H. & Miller, J.M. (1977). Hydrogen bonding in organic synthesis. Part 6. C-Alkylation of β-dicarbonyl compounds using tetralkylammonium fluorides. *J. Chem. Soc., Perkin I*, 1743-1745.
32. Perkins, M., Beam, C.F., Dyer, M.C.D. & Hauser, C.R. (1988). 3-(4-Chlorophenyl)-5-(4-methoxyphenyl)isoxazole. *Org. Syn. Coll. Vol. VI*, 278-281.
33. Ichinose, N., Mizuno, K., Tami, T. & Otsuji, Y. (1988). A novel NO insertion into cyclopropane ring by use of NOBF$_4$. Formation of 2-isoxazolines. *Chem. Lett.*, 233-236.
34. Murthy, A.K., Rao, K.S.R.K.M. & Rao, N.V.S. (1968). Isoxazolylphenols and their absorption spectra. *Aus. J. Chem.* **21**, 2315-2317.
35. Katzenellenbogen, J.A., Myers, H.N., Johnson, H.J., Jr, Kempton, R.J. & Carlson, K.E. (1977). Estrogen photoaffinity labels. 1. Chemical and radiochemical synthesis of hexestrol diazoketone and azide derivatives; photochemical studies in solution. *Biochemistry* **16**, 1964-1970.

36. Anstead, G.M., Carlson, K.E. & Katzenellenbogen, J.A. (1997). The estradiol pharmacophore: ligand structure-estrogen receptor binding affinity relationships and a model for the receptor binding site. *Steroids* **62**, 268-303.

37. von Angerer, E., Prekajac, J. & Strohmeier, J. (1984). 2-Phenylindoles. Relationship between structure, estrogen receptor affinity, and mammary tumor inhibiting activity in the rat. *J. Med. Chem.* **27**, 1439-1447.

38. Hwang, K.J., O'Neil, J.P. & Katzenellenbogen, J.A. (1992). 5,6,11,12-Tetrahydrochrysenes: Synthesis of rigid stilbene systems designed to be fluorescent ligands for the estrogen receptor. *J. Org. Chem.* **57**, 1262-1271.

39. Joule, J.A., Mills, K. & Smith, G.F.J. (1995). *Heterocyclic Chemistry.* Third ed. p 516, Chapman and Hall, New York.

40. von Angerer, E. & Erber, S. (1992). 3-Alkyl-2-phenylbenzo[b]thiophenes: nonsteroidal estrogen antagonists with mammary tumor inhibiting activity. *J. Steroid Biochem. Mol. Biol.* **41**, 557-562.

41. Grese, T.A., *et al.*, & Sata, M. (1996). Benzopyran selective estrogen receptor modulators (SERMS): Pharmacological effects and structural correlation with raloxifene. *Bioorg. Med. Chem. Lett.* **6**, 903-908.

42. Brzozowski, A.M., *et al.* & Carlquist, M. (1997). Molecular basis of agonism and antagonism in the oestrogen receptor. *Nature* **389**, 753-758.

43. Sun, J., *et al.*, & Katzenellenbogen, B.S. (1999). Novel ligands that function as selective estrogens or antiestrogens for estrogen receptor-α or estrogen receptor-β. *Endocrinology,* **140**, 800-804.

44. Katzenellenbogen, J.A., Johnson, H.J. & Myers, H.N. (1973). Photoaffinity labels for estrogen binding proteins of rat uterus. *Biochemistry* **12**, 4085-4092.

45. van Steenis, J. (1946). The nitration of dianisoylmethane and p-methoxydesoxybenzoin. *Recl. Trav. Chim. Pays-Bas* **66**, 29-46.

46. Ando, W., Sato, R., Yamashita, M., Akasaka, T. & Miyazaki, H. (1983). Quenching of singlet oxygen by 1,3,5-triaryl-2-pyraazolines. *J. Org. Chem.* **48**, 542-546.

47. Hergenrother, P.M. (1991). New developments in thermally stable polymers. *Rec. Travl. Chim. Pays-Bas.* **110**, 481-491.
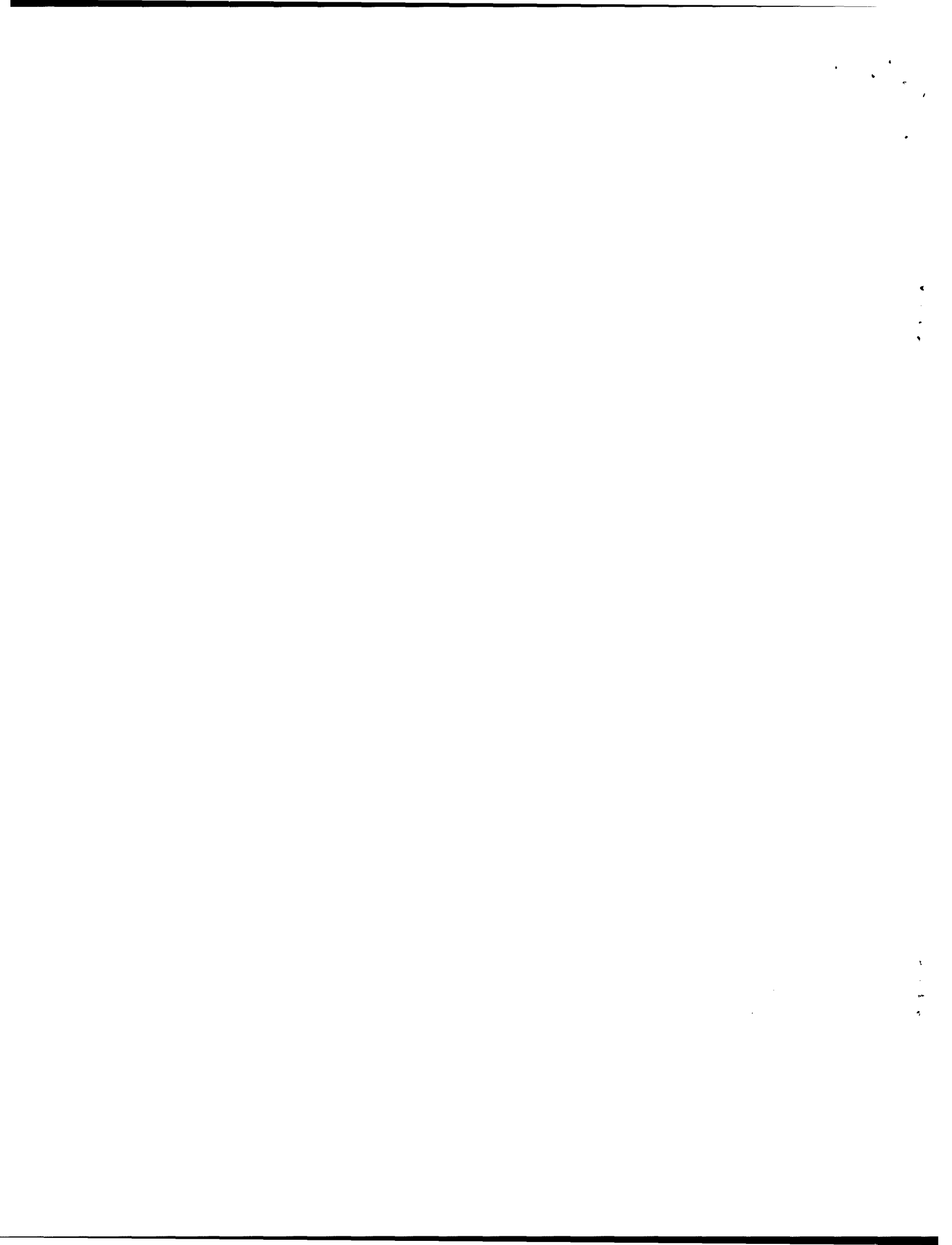
Acyclic Amides as Estrogen Receptor Ligands: Synthesis, Binding, Activity and Receptor Interaction

Shaun R. Stauffer,[a] Jun Sun,[b] Benita S. Katzenellenbogen [b,c]
and John A. Katzenellenbogen [a,*]

[a]*Department of Chemistry, University of Illinois, 461 Roger Adams Laboratory, Box 37-5, 600 S. Mathews Avenue, Urbana, IL 61801, USA*

[b]*Department of Physiology, University of Illinois, 407 S. Goodwin Avenue, Urbana, IL 61801, USA*

[c]*Department of Cell and Structural Biology, University of Illinois, 407 S. Goodwin Avenue, Urbana, IL 61801, USA*

Abstract—We have prepared a series of bisphenolic amides that mimic bibenzyl and homobibenzyl motifs commonly found as substructures in ligands for the estrogen receptor (ER). Representative members were prepared from three classes: N-phenyl benzamides, N-phenyl acetamides, and N-benzyl benzamides; in some cases the corresponding thiocarboxamides and sulfonamides were also prepared. Of these three classes, the N-phenyl benzamides had the highest affinity for ER, the N-phenyl acetamides had lower, and the N-benzyl benzamides were prone to fragmentation via a quinone methide intermediate. In the N-phenyl benzamide series, the highest affinity analogues had bulky N-substituents; a CF_3 group, in particular, conferred high affinity. The thiocarboxamides bound better than the corresponding carboxamides and these bound better than the corresponding sulfonamides. Binding affinity comparisons suggest that the p-hydroxy group on the benzoate ring, which contributes most to the binding, is playing the role of the phenolic hydroxyl of estradiol. Computational studies and NMR and X-ray crystallographic analysis indicate that the two anilide systems studied have a strong preference for the s-cis or exo amide conformation, which places the two aromatic rings in a syn orientation. We used this structural template, together with the X-ray structure of the ER ligand binding domain, to elaborate an additional hydrogen bonding site on a benzamide system that elevated receptor binding further. When assayed on the individual ER subtypes, $ER\alpha$ and $ER\beta$, these compounds show modest binding affinity preference for $ER\alpha$. In a reporter gene transfection assay of transcriptional activity, the amides generally have full to nearly full agonist character on $ER\alpha$, but have moderate to full antagonist character on $ER\beta$. One high affinity carboxamide is 500-fold more potent as an agonist on $ER\alpha$ than on $ER\beta$. This work illustrates that ER ligands having simple amide core structures can be readily prepared, but that high affinity binding requires an appropriate distribution of bulk, polarity, and functionality. The strong conformational preference of the core anilide function in all of these ligands defines a rather rigid geometry for further structural and functional expansion of these series. © 2000 Elsevier Science Ltd. All rights reserved.

Introduction

Recent advances in nuclear hormone receptor pharmacology and mechanism of action have redefined the classification of estrogen receptor (ER) ligands.[1] The selective estrogen receptor modulator class, or SERMs, are considered to be very important because of the potential of SERMs for maintaining bone mineral density and cardiovascular health, and for treating and preventing breast cancer and other hormone-dependent disorders, without adverse stimulation of the uterus and breast.[2] SERMs comprise several structurally diverse classes, including the triarylethylenes, triarylnaphthalenes, benzo[b]furans, benzopyrans, and various other tetracyclic manifestations of these core structures.[3] Collectively, SERMs display a wide range of tissue-selective agonist and antagonist activities, but major efforts continue to be directed toward optimizing ER ligand structure in order to obtain desired tissue-specific properties with minimal side-effects, which is an important concern in maintaining efficacy and patient compliance.[4]

In connection with our interests in novel templates for ER ligands, especially ones that might be suitable for

*Corresponding author. Tel.: +1-217-333-6310; fax: +1-217-333-7325; e-mail: jkatzene@uiuc.edu

combinatorial development,[5] we wondered whether acyclic tertiary amides might be developed as mimics of common structural motifs found at the core of many ER ligands and thus support a combinatorial approach to SERM discovery and optimization. In this report, we describe the design and synthesis of three types of amide-core ER ligands, and we investigate their molecular structure, their structure binding–affinity relationships, and their activity in ERα and ERβ transactivation assays. A number of interesting trends and high affinity amides were discovered during this investigation. One high affinity amide in particular (**16g**) was found to be an ERα-potency selective agonist.

Results and Discussion

Rationale and design

To the best of our knowledge, only two examples of ER ligands containing, either partially or exclusively, an amide core structure are known in the public literature. Hartmann and co-workers studied a small series of bis-phenolic carboxamides[6,7] containing an invariant N-(1,1,1-trifluoro-2-propyl) substituent (e.g., **1**) and found them to be anti-estrogens with weak to moderate potency. An early example of an N-ethyl benzene sulfonamide (**2**)[8] was also reported and shown to be weakly estrogenic in vivo. Neglecting amide bond stereoisomers for the moment, these ligands represent potential mimics (**1**) for either the *anti-* or *syn-*bibenzyl motifs **A** and **B**, respectively (Fig. 1, right), that are found in many common ER ligands (Fig. 1, left). In addition to the bibenzyl structural template of these leads, we envisioned two homologues (**II** and **III**, Fig. 2, right) which mimic the *homo-*bibenzyl motif **C** (Fig. 2, **II**–**III**), a structural element that is also well represented in high affinity ligands for the ER (Fig. 2, left).
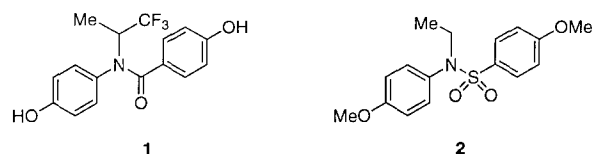
From this analysis, model *para*-substituted bis-phenolic carboxamides, sulfonamides and thioamides containing N-alkyl and trifluoroalkyl substituents (R and R') were considered as potential templates for combinatorial development (Fig. 3). Preparation for many of these compounds is straightforward and thus not unreasonable for adaptation to combinatorial library synthesis.

Chemical syntheses

N-Phenyl benzamides and benzene sulfonamides. To synthesize simple N-alkyl amide analogues in an expeditious manner, we used catalytic phase transfer conditions (Scheme 1). Thus, N-alkylation of the known secondary benzene sulfonamide **3**[8] proceeded under mild conditions using n-Bu$_4$NSO$_4$H, NaOH, and excess alkyl halide in CH$_2$Cl$_2$/H$_2$O.[9] The target N-alkylated sulfonamides **5a–c** were then obtained after deprotection. The less acidic carboxamide **6** was alkylated using a solid–liquid two-phase system, consisting of powdered NaOH and cat. n-Bu$_4$NBr in refluxing benzene, to afford the tertiary amides **9a–e** in good yield.[9,10] Carboxamides **9f** and **9g** were conveniently prepared from the secondary anilines **7** and **8**. Aniline **7** was prepared via reductive alkylation of the corresponding aldimine using a modified literature procedure.[11] Aniline **8** was obtained by reductive amination, using NaBH(OAc)$_3$, *p*-anisidine, and 3-methyl-2-butanone. Thioamides were prepared in relatively good yield by treating the carboxamide (**9a–g**) with Lawesson's reagent.[12] Deprotection with BBr$_3$ or

Structures **1** and **2**

Estrogen Receptor Ligand	Structural Motif	Combinatorial Analog (Class)
Hexestrol	Motif A. *anti*-Bibenzyl	Benzamide (I)
EM-652	Motif B.–*syn*-Bibenzyl	(or SO$_2$ or CS in place of CO)
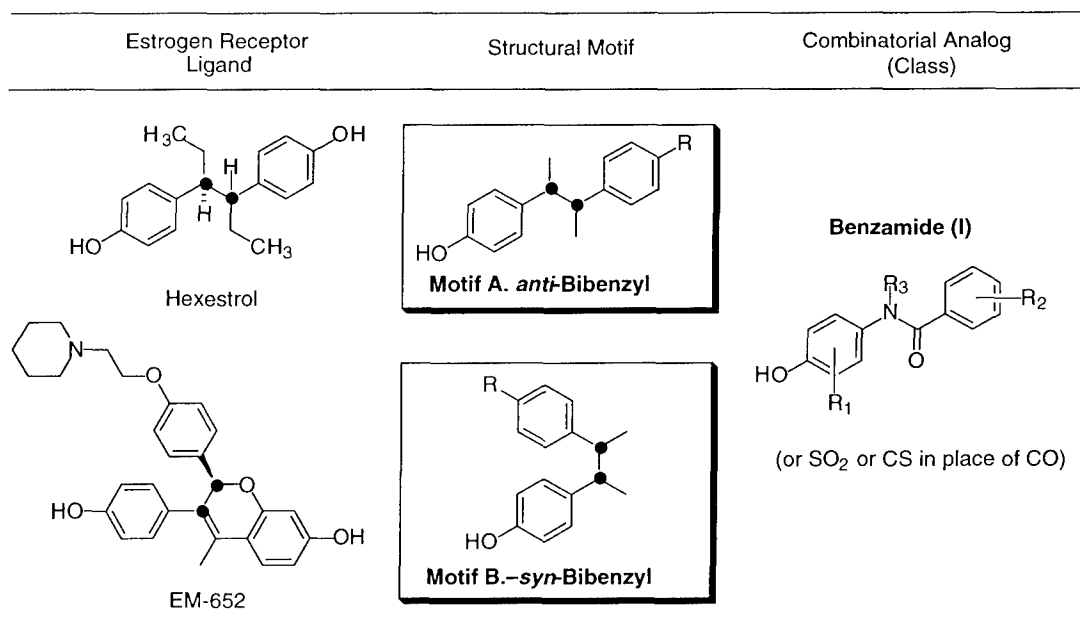
Figure 1. *Syn* and *anti*-bibenzyl motifs and proposed acyclic amide analogues.

Estrogen Receptor Ligand	Structural Motif	Combinatorial Analog (Class)

Benzyl benzamide (II)

(or SO₂ or CS in place of CO)

Phenyl acetamide (III)

(or SO₂ or CS in place of CO)

Motif C. Homo-bibenzyl

Benzestrol

Raloxifene

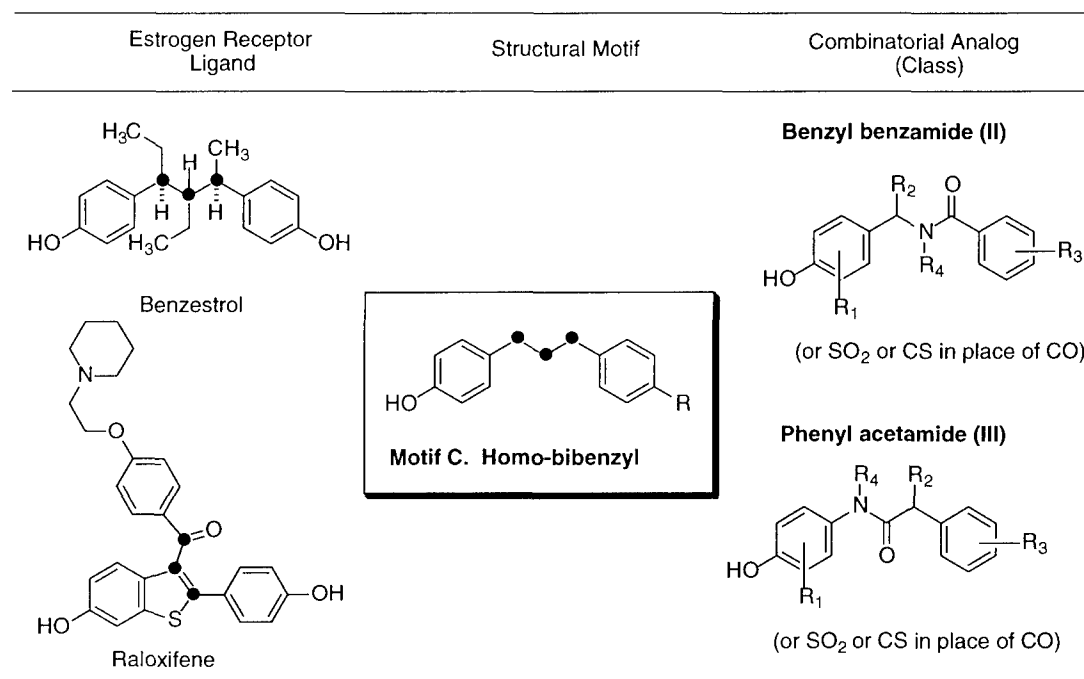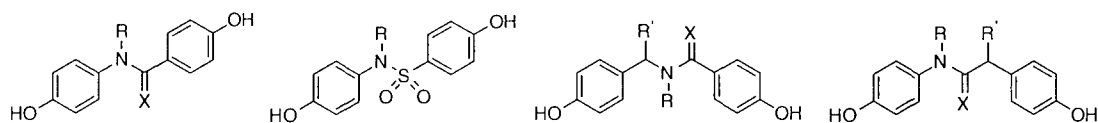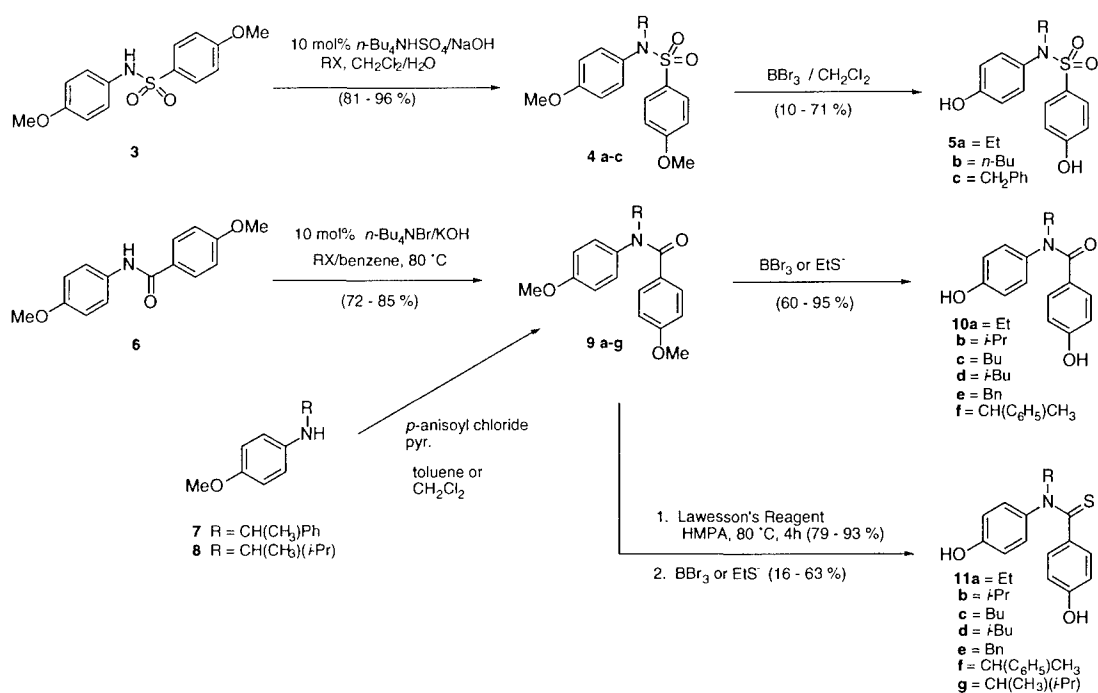**Figure 2.** *Homo*-bibenzyl motif and proposed acylic amide analogues.

Figure 3. Potential amide ER ligand scaffolds for combinatorial chemistry (X = O, S).
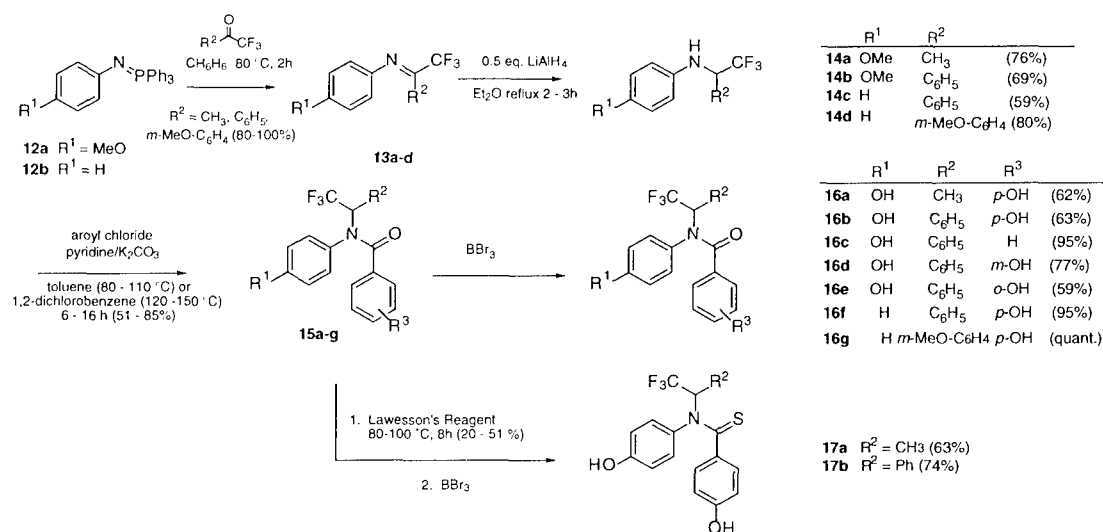

Scheme 1. Synthesis of *N*-phenyl benzamides.

ethanethiolate afforded the target benzamides **10a–f** and thiobenzamides **11a–g**.
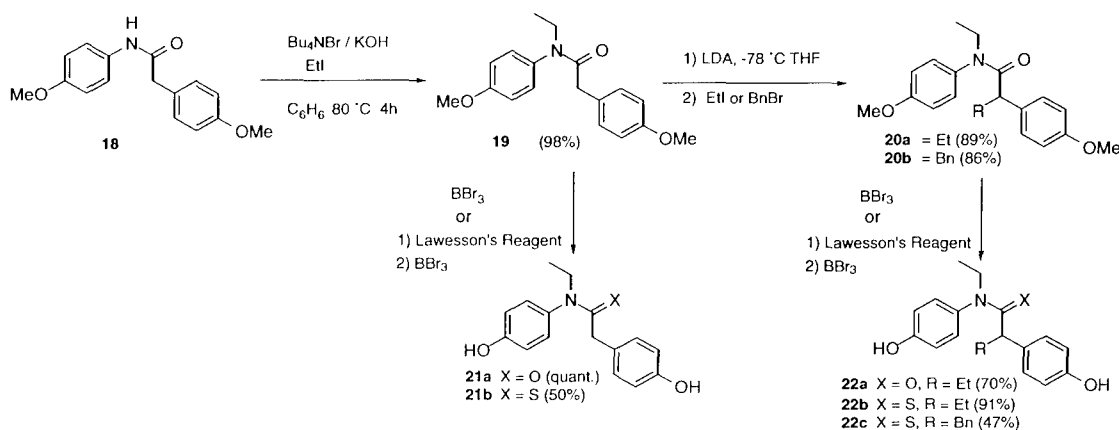
CF₃-containing N-phenyl benzamides. To further explore the effect that a trifluoromethyl group would have on receptor binding affinity, we prepared several carboxamide and thioamide analogues related to the weak antiestrogen (**1**) reported by Hartmann and co-workers.[6] The synthetic route to CF₃-amide analogues, depicted in Scheme 2, was adapted from that reported by Hartmann and required introduction of the CF₃-alkyl substituent at the aniline stage in two steps starting from the corresponding iminophosphoranes. The starting trifluoromethylketones were commercially available, with the exception of 2,2,2-trifluoro-1-(3-methoxyphenyl)ethanone, which was prepared from 3-bromoanisole according to the procedures described by Hatanaka et al. and references therein.[13] Ylides **12a** and **12b** were readily obtained by treatment of the corresponding azides with Ph₃P.[14,15] Subsequent Staudinger reaction to afford the CF₃-substituted imines **13a–d**, followed by LAH reduction, furnished the desired secondary anilines **14a–d** in good overall yield.

Amidation in warm toluene proceeded satisfactorily to provide carboxamides **15a–e**; however, unactivated anilines **14c** and **14d** required 1,2-dichlorobenzene as solvent and higher temperatures to afford benzamides **15f** and **15g** in satisfactory yields. Subsequent deprotection using BBr₃ afforded the desired phenols **16a–g** as before. Thionation of the protected, CF₃-substituted carboxamides proceeded in significantly lower yield (20–51%) than did those with simple N-alkyl substitution (>79%). Alternative thionation conditions, such as P₂S₅ and POCl₃/(TMS)₂S, did not give improved yields. Nevertheless, the two thioamides **17a** and **17b** could be obtained after deprotection with BBr₃.

N-Phenyl acetamides and N-benzyl benzamides. Acetamides were attractive because they offer an additional site for structural diversity that is not available in benzamides (Scheme 3). N-Ethylation of amide **18** using PTC conditions as before afforded **19** in excellent yield. Subsequent α-alkylation using LDA at −78 °C then afforded the disubstituted carboxamides **20a–b** in high yield. Thionation and/or deprotection as before furnished

	R¹	R²	
14a	OMe	CH₃	(76%)
14b	OMe	C₆H₅	(69%)
14c	H	C₆H₅	(59%)
14d	H	m-MeO-C₆H₄	(80%)

	R¹	R²	R³	
16a	OH	CH₃	p-OH	(62%)
16b	OH	C₆H₅	p-OH	(63%)
16c	OH	C₆H₅	H	(95%)
16d	OH	C₆H₅	m-OH	(77%)
16e	OH	C₆H₅	o-OH	(59%)
16f	H	C₆H₅	p-OH	(95%)
16g	H	m-MeO-C₆H₄	p-OH	(quant.)

17a R² = CH₃ (63%)
17b R² = Ph (74%)

Scheme 2. Synthesis of CF₃-containing N-phenyl benzamides.

Scheme 3. Synthesis of N-phenyl-acetamides.

the desired bis-phenolic amides **21a–b** and **22a–c** without complication.

The *N*-benzyl-*N*-alkylbenzamides **24** (Scheme 4), which are essentially amide isomers of the acetamide class, and related benzenesulfonamides (not shown), were also investigated. These *N*-benzyl amides, protected as methyl ethers, could be prepared by routes that are analogous to those used in Schemes 1–3. However, these systems proved to be unstable to various deprotection conditions: BBr₃, ethanethiolate, HBr/AcOH and TMSI all led to decomposition. The only isolatable products were the corresponding secondary amides, presumed to result from an elimination of the 4-hydroxy-*N*-benzyl substituent via a quinone-methide intermediate (Scheme 4). Due to their propensity for elimination, additional efforts were not made to prepare members of the *N*-benzyl benzamide class.

CF₃-containing *N*-phenyl acetamides. Incorporation of the CF₃-group was also explored in the acetamide series, and the synthesis of α-substituted acetamides containing an *N*-(1,1,1-trifluoro-2-propyl) substituent is shown in Scheme 5. Thus, the *N*-(1,1,1-trifluoro-2-propyl) substituted aniline **12a** was treated with 4-methoxyphenylacetyl chloride to afford carboxamide **25**. α-Alkylation as before using LDA at −78 °C and MeI proceeded in excellent yield to give **26** as a ~1:1 mixture of diastereomers as indicated by ¹H NMR and HPLC analysis. Demethylation then afforded the di-substituted phenylacetamide **27** in good yield. Unfortunately,

attempts to thionate **26** with Lawesson's reagent failed; however, treatment of the unsubstituted phenylacetamide **25** with Lawesson's reagent did give thioamide **28**, in albeit low yield. Repeated attempts using other reagents (P₂S₅ and POC₁₃/(TMS)₂S) or higher temperatures failed to provide thioamide **26** or to improve the yield of **28**. Increased steric hindrance about the C=O bond is thought to be responsible for the lack of reactivity of the CF₃-substituted *N*-phenyl acetamides towards O–S replacement, as lower yields for thionation were also observed for the CF₃-containing benzamides (Scheme 2).

Molecular conformation

As was noted in Figure 1, bibenzyl motifs in ER ligands are well represented as both *syn* and *anti* conformations. Since *N*-aryl-benzamides share a similar bibenzyl-like two-atom connection between two aromatic rings, we were interested in their conformational preference to establish which structural motif they might be mimicking. From early ¹H NMR studies of *N*-substituted anilides, there is known to be a surprisingly strong preference for the *exo*-isomer (*N*-phenyl group *trans* to carbonyl oxygen).[16] Even simple *N*-methyl and *N*-ethylformanilides, where steric considerations would place the bulkier alkyl group next to the formyl hydrogen in an *endo* preference, have a 95% *exo* preference in solution.[17] This so-called '*exo*-rule' is quite general, and it has been stated that for *N*-substituted anilides other than formyl, the *exo*-isomer dominates to the exclusion
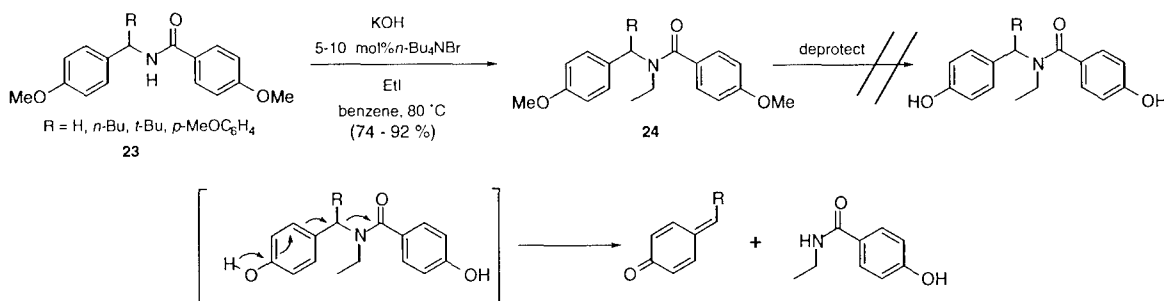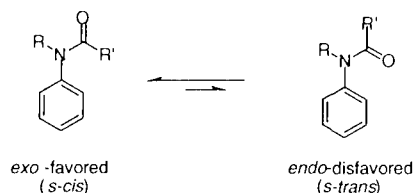

Scheme 4. Attempted synthesis of *N*-benzyl-benzamides.
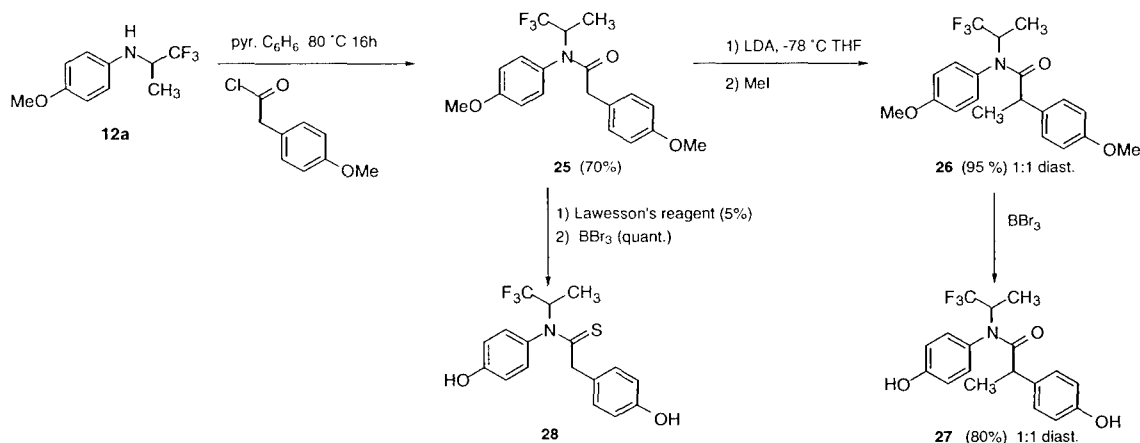
Scheme 5. Synthesis of CF₃-containing *N*-alkyl-phenylacetamides.

of the *endo*-isomer.[16] The *endo*-isomer is detectable only when large *ortho* substituents are present on the *N*-phenyl ring or when R'=H.

exo -favored   endo-disfavored
(s-cis)   (s-trans)

Molecular modeling studies on both carboxamide **16a** and thiocarboxamide **17a** that we have performed using molecular mechanics (MM2) were in agreement with the reported NMR observations, and indicated the *exo* or *s-cis* conformer as being energetically more favorable (Fig. 4). In the case of carboxamide **16a**, a substantial ΔH of 5.3 kcal/mol between the global minimum energy *cis* and *trans* isomers was found, the major energetic difference being due to additional electrostatic contributions in the *s-trans* conformation. Thiocarboxamide **17a** has a smaller ΔH of 0.9 kcal/mol between the global minimum energy *cis* and *trans* isomers (not shown). This result is in accord with destabilization of the *s-cis* (*exo*) thioamide conformer relative to the *s-trans* (*endo*) conformer because of additional steric repulsions between sulfur and the *N*-alkyl substituent that arise from the larger covalent radii of sulfur versus oxygen (1.4 Å for sulfur, 0.74 Å for oxygen) and its longer bond length (C=S 1.64 Å; C=O 1.24 Å).

Direct structural studies of *N*-substituted thioanilides, let alone hindered systems containing a CF$_3$-substituent, have not been reported, as far as we have found. For this reason and because of the relatively small energy difference found from molecular modeling for **17a**, we obtained an X-ray crystallographic structure of the methyl ether derivative of **17a** to firmly establish its preferred stereochemistry about the amide bond. In

addition, for comparison, a crystallographic structure was determined on the less hindered *N*-(*i*-propyl)-carboxamide **10b**. ORTEP representations of these molecules are shown in Figure 5.

As can be seen in Figure 5, both the *i*-propyl carboxamide and CF$_3$-substituted thioamide were found to crystallize in the lower energy *s-cis* conformation. Prominent torsion angles are indicated in Table 1. Comparison of the amide torsional bonds (torsion A) reveals greater deviation of the *N*-aryl ring from the amide plane in thiocarboxamide **17a** compared to **10b** (18° versus 9.7°), consistent with the greater steric hindrance anticipated in the amide plane of the thioamide system. The greater distortion in the thioamide bond planarity is also evident from its improper torsion (torsion E) and its *N*-alkyl torsion **B**. Both structures also show a twisting of the phenyl rings out of the amide plane (**C** and **D**), with the thioamide being more planar. This difference appears in part to be due to additional nearby nonbonding interactions with the CF$_3$-group in thioamide **17a**.

Solution VT ^{1}H NMR experiments (Fig. 6) were also conducted, and the results were found to be consistent with a single amide conformer. Shown in Figure 6 is the ^{1}H NMR spectrum of the aromatic region for thioamide **17a** at −60, +23, and +55 °C in MeOD. The spectra at −60 °C and room temperature are very similar. Interestingly, there is a slow rotation about the N–C bond of the *N*-phenyl group, which results in distinct signals for the *ortho* and *meta* ring protons of the *N*-phenyl ring. Assignments are based on COSY cross couplings. Upon heating to +55 °C, no new signals are observed for either the CH$_3$ group (not shown), which remains a doublet at all three temperatures, or the aroyl protons. However, the *ortho* and *meta* signals of the *N*-phenyl ring coalesce. This type of slow N–C rotation is well known in *N*-phenyl carboxamides and is analogous to hindered bi-phenyl rotations.[16] The lack of

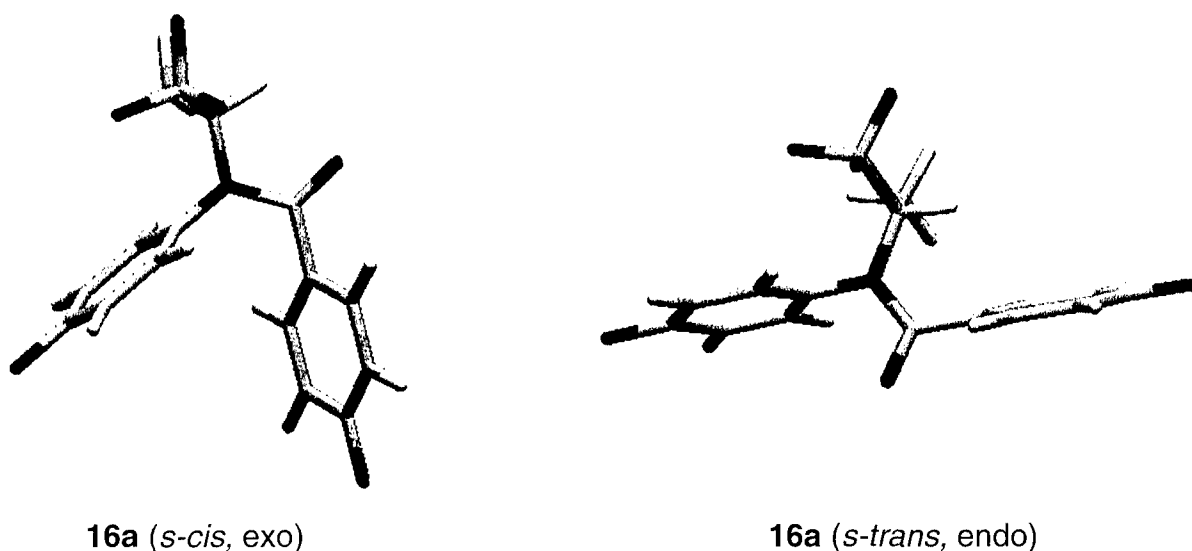**16a** (*s-cis*, exo)   **16a** (*s-trans*, endo)

Figure 4. Capped-stick models of lowest energy *c-cis* and *s-trans* conformers of caboxamide **16a**. This *s-cis* conformer (left) has lower energy (ΔH = 5.3 kcal/mol).
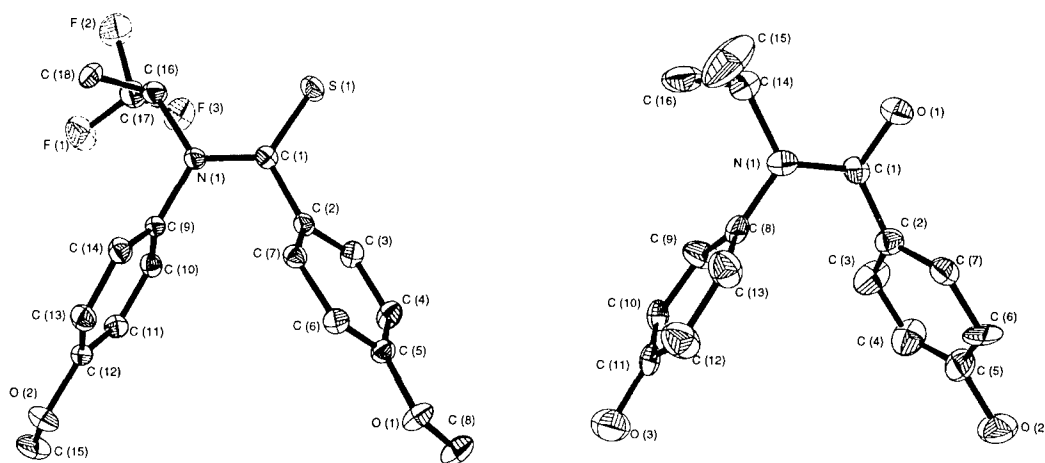
Figure 5. Molecular structures for thiocarboxamide **17a** (left) and carboxamide **10b** (right) (ORTEP; ellipsoids drawn at the 35% probability level).

Table 1. Prominent torsion angles found in carboxamide **10b** and thiocarboxamide **17a**

Torsion	Compound **17a** thioamide 1–4 atoms	Angle	Compound **10b** carboxamide 1–4 atoms	Angle
A	C(2)–C(9)	18°	C(2)–C(8)	9.7°
B	C(16)–S(1)	7.8°	C(14)–O(1)	3.2°
C	C(1)–C(10)	76°	C(1)–C(9)	80°
D	C(3)–N(1)	50°	C(3)–N(1)	62°
E	N-improper torsion	5.4°	N-improper torsion	4.6°

additional signals indicates that there is a single amide conformer in solution, which we presume, on the basis of the computational and X-ray structures, to be the *s-cis*. Furthermore, for thioamides, it is worthy to note that the barrier for *cis–trans* inter-conversion is generally 2–5 kcal greater than it is for the analogous carboxamides. The traditional 'resonance model' used to rationalize the origin of the higher *cis–trans* barriers in thioamides has recently been challenged[18] and is currently under debate.[19–22] Nevertheless, from these studies we believe that it is reasonable to conclude that sterically hindered N-aryl *thio*benzamides also have a strongly preferred *s-cis* conformation, similar to N-substituted *oxo*anilides. Therefore, these systems can be considered as mimics of the *syn*-bibenzyl substructural motif.

Receptor binding affinities and structure–binding affinity relationships

Binding affinities for the estrogen receptor and octanol–water partition coefficients (Log $P^{o/w}$) determinations of the benzamides we have prepared are shown in Table 2 and are organized according to the substituent on the amide nitrogen (either N-alkyl/aryl or N-CF$_3$ containing alkyl/aryl). Binding affinities and Log $P^{o/w}$ determinations for phenylacetamides are presented in Table 3. Binding affinities were obtained from a competitive radiometric binding assay, using [^{3}H]estradiol as tracer and lamb uterine cytosol as a source of ER, and they are expressed as relative binding affinities (RBA), with estradiol having an affinity of 100%. Additional binding
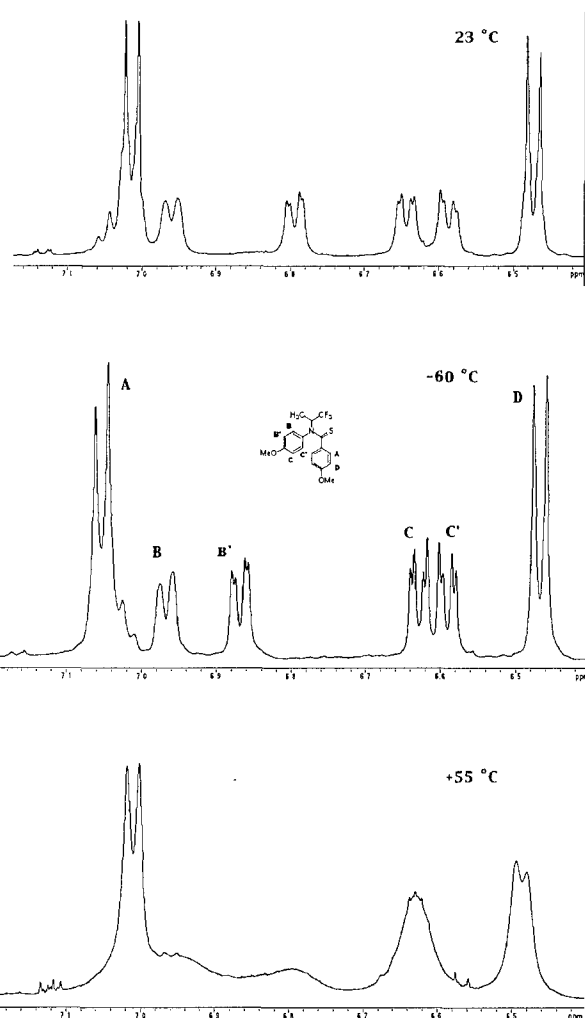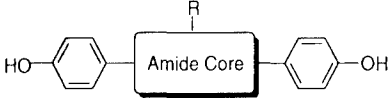

Figure 6. VT-^{1}H NMR for **17a**, aromatic region.

assays of select compounds for receptor subtypes ERα and ERβ, as well as ERα and ERβ transcriptional activation profiles in human endometrial cancer (HEC-1) cells using an estrogen-responsive reporter gene construct, are also shown in Table 4. Log $P^{o/w}$ determinations were obtained according to the method of Minick,

Table 2. Estrogen receptor relative binding affinity RBA (estradiol = 100) and log octanol–water partition coefficient (log $P^{o/w}$) data for *N*-phenyl-benzamides

Compound	Core structure	R group	RBA[a]	Log $P^{o/w}$
5a	-CSO$_2$R-	Et	0.23	2.76
5b		*n*-Bu	0.13	3.66
5c		Bn	0.053	4.62
10a	-CONR-	Et	0.062	2.40
10b		*i*-Pr	0.009	2.31
10c		*n*-Bu	0.042	—
10d		*i*-Bu	0.020	3.15
10e		CH$_2$Ph	0.089	—
10f		CH(C$_6$H$_5$)CH$_3$	0.45	3.96
11a	-CSNR-	Et	0.62	2.80
11b		*i*-Pr	0.83	2.97
11c		*n*-Bu	1.3	3.99
11d		*i*-Bu	1.5	
11e		CH$_2$Ph	0.15	—
11f		CH(C$_6$H$_5$)CH$_3$	2.5	3.98
11g		CH(CH$_3$)(*i*-Pr)	4.6	4.31

[a]Relative binding affinities are the average of duplicate determinations (CV 0.3), measured in lamb uterine cytosol. For estradiol, RBA = 100. For details, see Experimental.

Table 3. Estrogen receptor relative binding affinity RBA (estradiol = 100) and log octanol–water partition coefficient (log $P^{o/w}$) data for *N*-CF$_3$-substituted benzamides

Compound	X	R^1	R^2	R^3	RBA[a]	Log $P^{o/w}$
16a	O	HO	CH$_3$	*p*-HO	0.49	3.29
16b	O	HO	C$_6$H$_5$	*p*-HO	9.0	4.51
16c	O	HO	C$_6$H$_5$	H	0.063	4.46
16d	O	HO	C$_6$H$_5$	*m*-HO	0.45	—
16e	O	HO	C$_6$H$_5$	*o*-HO	0.068	—
16f	O	H	C$_6$H$_5$	*p*-HO	8.9	4.97
16g	O	H	*m*-HOC$_6$H$_4$	*p*-HO	15	4.63
17a	S	HO	CH$_3$	*p*-HO	7.5	3.99
17b	S	HO	C$_6$H$_5$	*p*-HO	14	5.40

[a]Relative binding affinities are the average of duplicate determinations (CV 0.3), measured in lamb uterine cytosol. For estradiol, RBA = 100. For details, see Experimental.

using a standardized Chromegabond MC8 reverse phase HPLC system.[23]

Binding affinity of *N*-phenyl benzamides. The receptor binding affinities for *N*-phenyl benzamides are shown in Table 2. The sulfonamides and carboxamides all have rather low affinity, the highest being carboxamide **10f**. Within the carboxamide series (**10a–f**), it is interesting to compare the effect of branching near the amide core. For example, the ethyl (**10a**) and benzyl (**10e**) compounds have similarly low affinities, and likewise the branched *i*-propyl amide **10b** has very low affinity. However, amide **10f**, which contains both an α-phenyl and methyl substituent, shows a significant, 5- to 7-fold increase in affinity compared to either monosubstituted amide **10a** or **10e**. Overall, the analogous *N*-alkyl

Table 4. Estrogen receptor relative binding affinity RBA (estradiol = 100) and log octanol–water partition coefficient (log $P^{o/w}$) data for *N*-phenyl phenylacetamides

Compound	X	R^1	R^2	RBA[a]	Log $P^{o/w}$
21a	O	CH$_2$CH$_3$	H	0.006	2.68
22a	O	CH$_2$CH$_3$	CH$_2$CH$_3$	0.004	3.52
27	O	CH(CH$_3$)(CF$_3$)	CH$_3$	0.010	—
28	S	CH(CH$_3$)(CF$_3$)	H	0.66	—
21b	S	CH$_2$CH$_3$	H	0.20	3.40
22b	S	CH$_2$CH$_3$	CH$_2$CH$_3$	0.089	4.27
22c	S	CH$_2$CH$_3$	CH$_2$Ph	0.34	—

[a]Relative binding affinities are the average of duplicate determinations (CV 0.3), measured in lamb uterine cytosol. For estradiol, RBA = 100. For details, see Experimental.

thioamides (**11a–g**) bind with affinity 2- to 90-fold greater than their carboxamide counterparts, which is presumably due to their greater hydrophobic character, although there are not great differences in the Log $P^{o/w}$ values, where comparisons can be made. A related trend is also observed in other non-steroidal ligands containing heteroatoms, such as benzo[b]furans and benzo[b]thiophenes, with benzo[b]thiophenes displaying higher affinity than benzo[b]furans.[24,25]

The beneficial effect of placing more sterically encumbered groups near the amide core on receptor affinity is also evident in the thioamide series, because the same relative affinity increases which occurred for carboxamides (**10a** < **10e** < **10f**) are also reflected in the thioamides (**11e** < **11a** < **11f**). Replacement of the phenyl substituent in **11f** with an *i*-propyl group to afford thioamide **11g** results in even greater crowding near the amide plane, enhancing the relative affinity to 4.6%, the highest observed for any simple *N*-phenyl benzamide.

Binding affinity of CF$_3$-containing *N*-phenyl benzamides. The RBA data for the CF$_3$-containing benzamides are presented in Table 3. Immediately apparent is the relatively high binding affinity for thioamide **17b** and carboxamide **16g**, and to a lesser extent amides **16b**, **16f** and **17a**. Compound **16a**, reported by Hartmann and co-workers, is included for comparison.[6] In general, all the CF$_3$-substituted benzamides show affinity enhancements relative to their non-fluorinated amide counterparts (Table 2).

Shown in Figure 7 are four direct comparisons of RBA and Log $P^{o/w}$ data for benzamides from Tables 2 and 3. These four pairs of compounds clearly show the relationship between core structure (O and S substitution) and peripheral group presentation (methyl to phenyl, and methyl to trifluoromethyl) and how these components alter ER affinity.

Comparison of the relative RBAs for these four pairs of amides, starting from the *i*-propyl pair (upper left) to the CF$_3$-containing phenethyl pair (lower right), shows a diminishing effect of sulfur–oxygen replacement as binding affinity increases and as larger substituents are added near the amide core. The sulfur–oxygen
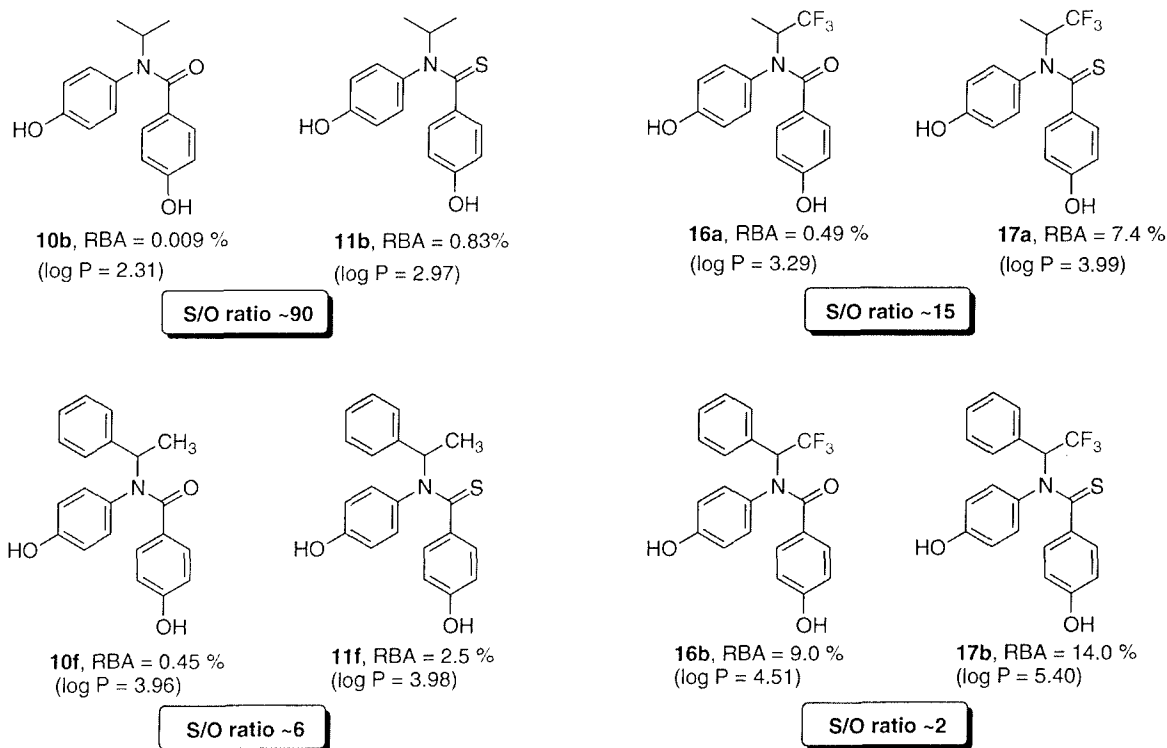
10b, RBA = 0.009 %
(log P = 2.31)

11b, RBA = 0.83%
(log P = 2.97)

S/O ratio ~90

16a, RBA = 0.49 %
(log P = 3.29)

17a, RBA = 7.4 %
(log P = 3.99)

S/O ratio ~15

10f, RBA = 0.45 %
(log P = 3.96)

11f, RBA = 2.5 %
(log P = 3.98)

S/O ratio ~6

16b, RBA = 9.0 %
(log P = 4.51)

17b, RBA = 14.0 %
(log P = 5.40)

S/O ratio ~2

Figure 7. Comparison of the relative binding affinities of the principal carboxamides and thiocarboxamides.

enhancement is greatest in the parent *i*-propyl system (**10b** versus **11b**), where the overall affinity is lowest, and is least when the substituents are phenyl and trifluoro-methyl (**16b** versus **17b**), where the overall affinity is highest. In addition, there is a general increase in binding affinity with increasing lipophilicity. The observed parallel affinity–lipophilicity increase within the series is not too surprising in light of what is known about the hydrophobic character of the ER ligand binding pocket.[26]

CF₃ effect: lipophilic, steric or electrostatic effects? The effect of adding a CF_3 group in place of methyl on the RBA may be the result of several factors, including lipophilic, steric and/or electrostatic effects. In terms of steric effects, a recent review by O'Hagan and Rzepa[27] cites several studies which place an upper size limit of a CF_3-group being close to that of *i*-propyl. The greatest increases in RBA for CH_3 to CF_3 substitution are found in the carboxamide class (20- to 50-fold, versus 5- to 8-fold for thioamide), with the highest being the *i*-propyl compounds (Fig. 7, **16a** versus **10b**). In order to test whether or not RBA increases associated with CF_3-replacement are the result of its steric or its electronic property, the branched $CH(CH_3)(i\text{-Pr})$ thioamide **11g** was prepared to compare with the CF_3 analogue **17a**. Based on the above-mentioned studies, if steric effects alone operate, compound **11g** would be expected to have an RBA close to that of the CF_3-substituted thioamide **17a** (7.5%). The observed RBA, however, for compound **11g** was only 4.6%. This indicates that an additional effect may be contributing to the binding energy, either lipophilic or electrostatic. The fact that

the Log $P^{o/w}$ values for **11g** and **17a** are quite similar, with **11g** being somewhat higher, suggests that the difference in binding affinity is probably not due to a lipophilic component. Thus, based on this data it would seem that the additional component has, in addition to its steric effect, an electronic effect as well.

Optimization of binding orientation and hydroxylation pattern. For unsymmetrical non-steroidal ER ligands, a common approach to determining which phenol is imitating the crucial A-ring phenol of estradiol is to prepare and test the corresponding mono-phenolic derivatives.[28] The highest affinity mono-phenolic analogue is then presumed to be the A-ring mimic, because the hydroxyl substituent at this position is known to be very important in binding to the ER. Many non-steroidal ER ligands benefit from a second hydroxyl hydrogen bonding partner and appear to do so in an *anti*-bibenzyl motif, which places the hydroxyl oxygen–oxygen interatomic distances approx. 10–12 Å. Thus, it was apparent to us that the rigid *s-cis* benzamide conformation (*syn*-bibenzyl motif) in our amides was likely not benefiting from a second hydrogen bonding interaction, because its hydroxyl oxygen–oxygen interatomic distance was only 7.4 Å. The importance for this second hydrogen bond is evident in the recent non-steroidal diethylstilbestrol and raloxifene ERα LBD crystal structures.[26,29] Both of these complexes have an expected A-ring phenol mimic and a second phenol imitating the D-ring 17β-hydroxyl group of estradiol. In both cases, the second phenol uses the same hydrogen bond interaction with His₅₂₄ as does the 17β-hydroxyl group of estradiol.

To obtain an optimal hydroxylation pattern and discern which ring phenol was imitating the A-ring phenol of estradiol, we prepared benzamides **16c–g**. The results of these studies (Table 3) clearly show a pattern indicative of a preferred A-ring phenol mimic. For example, removal of the 4-hydroxyl phenol on the benzamide ring and retention of the 4-hydroxyl of the *N*-phenyl in compound **16c** lead to a nearly complete loss in binding affinity compared to the parent di-hydroxy compound **16b** (RBA = 0.063% versus 9.0%). In contrast, removal of *N*-phenyl hydroxyl and retention of the benzamide 4-hydroxyl result in an analogue **16f**, which retains a binding affinity equivalent to that of the parent compound. These findings clearly implicate the benzoyl ring phenol as the A-ring mimic of estradiol. In addition, as might be expected, positioning the hydroxyls elsewhere on the benzoyl ring is not well tolerated, as both the *ortho*- and *meta*-hydroxy analogues **16d** and **16e** have little or no affinity for the receptor.

Having discerned which phenol in the benzamide system was important for binding, we wished to explore alternative positions for a second hydroxyl group in order to benefit from the second hydrogen bonding interaction which is found in the raloxifene and DES ER binding pockets. Depicted in Figure 8 is a schematic representation of the predicted binding mode and phenol interactions for benzamide **16f** in the binding pocket of ER. This rudimentary model was derived from the interactions that were described to be present in the estradiol (E$_2$) X-ray crystal structure in the ERα LBD, the coordinates of which, at the time of our consideration, were not released.[26] Based on this view, we proposed that a hydroxyl substituent on the phenethyl ring might be positioned in the binding subpocket near His$_{524}$.

The choice of positioning the second OH at the *meta* position on the phenethyl substituent seemed somewhat obvious, since modeling showed that alternative OH substitution on the *N*-phenyl ring fails to provide O·O interatomic distances much greater than in the *para*-substituted system **16b**. Furthermore, the binding mode depicted in Figure 8 actually places the *N*-phenyl group more closely in the 11β subpocket of the ligand binding site, rather than the D-ring subpocket. In choosing the ring-substitution for the hydroxyl on the phenethyl ring, we considered both the *para* and *meta* isomers. However, in light of the problems encountered with quinone methide elimination in the *N*-benzyl benzamide series bearing a *para*-methoxy protecting group, we opted not to prepare the *para*-hydroxy analogue of **16f**, since the electron withdrawing CF$_3$ group would presumably exacerbate quinone methide elimination.

With the recent release of the E$_2$ ERα LBD crystal structure coordinates, we performed molecular docking studies of the proposed *meta*-hydroxybenzamide (**16g**) using TRIPOS' Flexidock routine (see Experimental), to see whether or not the proposed binding mode in Figure 8 was reasonable and whether a *meta*-hydroxy derivative could participate in a hydrogen bonding interaction with His$_{524}$.

The final docked and minimized model, using the *S*-enantiomer of **16g**, is depicted in crossed-stereo in Figure 9. The *R*-enantiomer (not shown) was also modeled in the same manner but resulted in a higher energy complex. The final *S*-enantiomer model converged to an RMS of < 0.05 kcal/mol·Å with a reasonably favorable binding energy. In this conformation, the benzoyl phenol is comfortably accommodated in the A-ring pocket, and the *N*-phenyl group projects into what
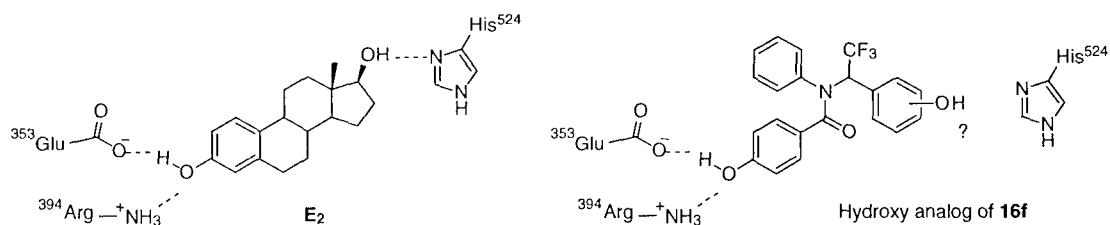

Figure 8. Putative binding mode for *N*-phenyl benzamide template with A-ring mimic interactions and a proposed site for second HO-group.
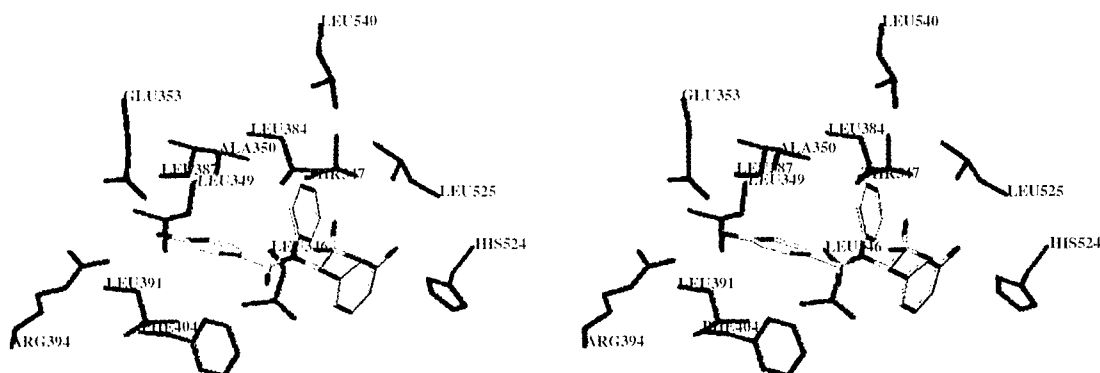

Figure 9. Crossed-stereo view of **16g** docked and minimized in ERα LBD binding pocket showing select residues within 3 Å of the benzamide.
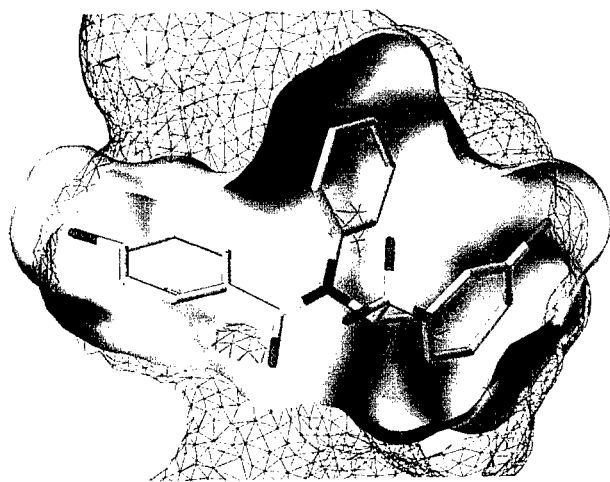
Figure 10. Depiction of solvent accessible surfaces for **16g** in ERα binding pocket.

would resemble the 11β pocket of the ERα-E_2 structure. Interestingly, the amide bond occupies a region of the binding pocket similar to that of the isosteric ethylene unit of DES in the recently solved ERα-DES crystal structure.[29]

Using the above model, we generated Connolly solvent accessible surfaces for the ligand and binding pocket to visualize close contacts (Fig. 10). This view reveals mostly favorable interactions within acceptable van der Waals radii. The ligand itself has a volume of 296 Å^3, which is 51 Å^3 greater than E_2, but is well under the total volume of 450 Å^3 for the binding pocket as reported in the ERα-E_2 crystal structure.[26]

We were grateful to find that the bis-(phenolic) benzamide **16g** had an RBA of 15%, the highest of any carboxamide ER ligand. This value represents a 1.6-fold increase over the affinity of the corresponding monophenolic benzamide **16f** and is close to what one might expect: in E_2 and other non-steroidal ER ligand systems, removal of the 17β hydroxyl, as in E_2, or the second

D-ring hydroxyl mimic, as in raloxifene, result in a 0.6 kcal/mol reduction in binding energy, which corresponds to a 3-fold drop in affinity.[30] The fact that the addition of the second hydroxyl does not give a full 3-fold increase may be due to a somewhat unfavorable hydrogen bond trajectory in the binding pocket. From our model, the distance between the *m*-hydroxyl substituent and His$_{524}$ (3.69 Å) is sufficiently close for some hydrogen bonding interaction, but is not ideal either in terms of distance or geometry. A second more likely explanation may have to do with stereochemical issues: This compound (**16g**) was tested as a racemate, so only one enantiomer is likely to be able to benefit from the second hydrogen bonding interaction. The ERα and ERβ RBAs and the transcriptional activation profile for *rac*-**16g** in HEC-1 cells are discussed below.

N-Phenyl acetamides as ER ligands. The RBA and Log $P^{o/w}$ data for N-alkyl- and CF$_3$-containing acetamides are shown in Table 4. Disappointingly, none of these compounds were found to show appreciable affinity for the ER. Several direct comparisons can be made to other series in this investigation, which suggest that acetamides may not provide viable scaffolds for further combinatorial consideration, despite their potential to support greater structural diversity than the benzamides. Even the CF$_3$-containing acetamide **27** and thioacetamide **28** have affinities less that 1%, which are 50- and 11-fold lower, respectively, than their benzamide counterparts **16a** and **17a**.

One possible explanation for the low affinity in the acetamide class may lie in their conformation. Monte Carlo conformational studies of compound **27** and the unsubstituted analogue **27b**, using molecular mechanics methods, show a distinct preference for a *syn* conformation, as shown in Figure 11. The *syn*-conformer for **27** is predicted to be 5 kcal/mol lower in energy than the *anti*-conformer; even without the α-methyl substituent, which eliminates possible alkyl-N-phenyl steric repulsions, the *syn*-conformer is predicted to be favored by 2.5 kcal/mol (not shown). It is also noted that the barrier to rotation about the acetyl bond was estimated
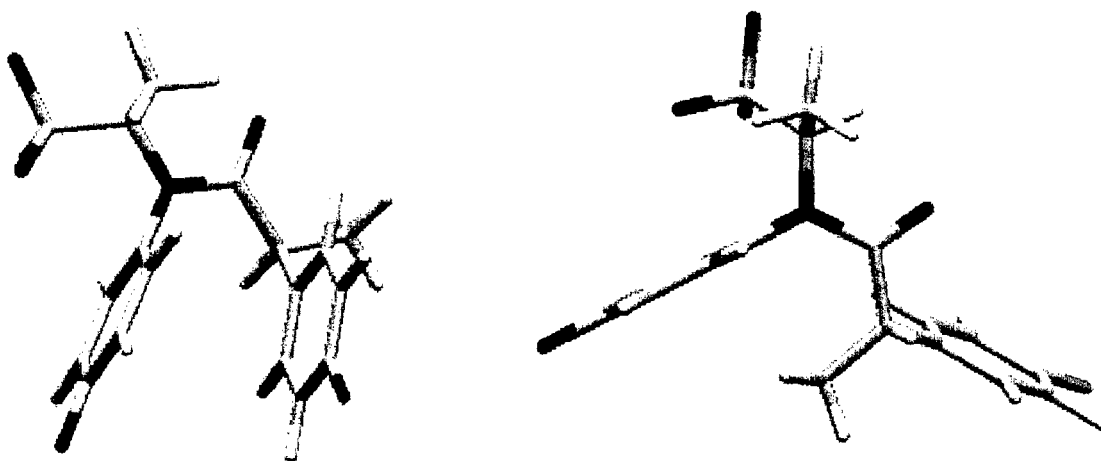

Figure 11. Conformational analysis of N-penyl-penylacetamide **27**.

to be between 4 and 5 kcal/mol for **27**, based on MM2 dihedral drive calculations.

As in the benzamides, in the acetyl conformations of **27** the *exo*-rule is upheld; this places the *N*-phenyl group *exo* with respect to the amide C=O, making the amide configuration *s-cis*. This *exo*-effect may also be operative for the α-phenyl substituent as well, since it also prefers to be essentially *exo* to the amide C=O rather than *endo*. Since the hydroxyl O·O interatomic distances for many estrogens requires a minimum of approximately 10.5 Å, the *syn*-conformation is excluded as a structure that is likely to fit in the ER binding pocket. Based on these studies and the RBA data available at this time, further investigations of the acetamide series did not appear to be warranted.

ERα/ERβ binding affinity, transcriptional activity and enantioselectivity

Shown in Table 5 are the RBA values of select benzamides for purified ERα and ERβ, along with their transcriptional activity in HEC-1 cells using an estrogen-responsive reporter gene construct ((ERE)₃-pS2-CAT) with expression vectors for either ERα or ERβ and benzamide at 10⁻⁶ M. It is apparent that binding affinities show selectivity for ERα, mostly in the range of 2- to 8-fold; compound **16g** has the highest selectivity for ERα of 21-fold (27% versus 1.3%). The enantiomers of **17b**, which were separated using chiral HPLC (ChiralPak AD column), also showed interesting RBA differences between the two receptor subtypes. For example, enantiomer *ent*₂-**17b** was found to have greater selectivity for ERα than enantiomer *ent*₁-**17b** by more than 5-fold, indicating that the individual binding pockets for ERα and ERβ are uniquely sensitive to subtle changes in ligand shape.

In the transcription assays,[31] agonism is measured with 1 μM of compound alone and is expressed as the percent of transcriptional activity with 1 nM E₂ (high values indicate agonist activity); antagonism is measured with 1 μM compound together with 1 nM E₂ (low values indicate antagonist activity). All of the benzamides tested were full or nearly full agonists through ERα,
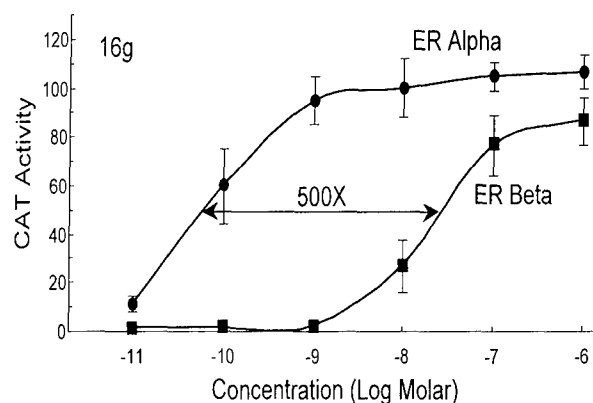

Figure 12. Transcription activation by ERα and ERβ in response to benzamide **16g**. Human endometrial cancer (HEC-1) cells were transfected with expression vectors for ERα or ERβ and an (ERE)₃-pS2-CAT reporter gene and were treated with the indicated concentrations of benzamide **16g** for 24 h. CAT activity was normalized for β-galactosidase activity from an internal control plasmid. Values are the mean ±SD for three or more separate experiments, and are expressed as a percent of the ERα or ERβ response with 1 nM E₂.

whereas some were effective partial antagonists through ERβ. Compound **16g** was a full agonist on ERα and ERβ.

Because of the high activity of amide **16g** at 10⁻⁶ M on both ERα and ERβ, a full dose–response curve was determined to see whether any potency selectivity existed for either ERα or ERβ. As shown in Figure 12, benzamide **16g** behaves as an ERα potency selective agonist, displaying a 500-fold higher potency for activation of ERα over ERβ. It is of note that this high potency selectivity for ERα is greater than the 21-fold ERα affinity selectivity of this compound (cf. Table 5).

Conclusions

Through an analysis of potent non-steroidal estrogens, we have identified common substructural bibenzyl and homobibenzyl motifs in the structure of ER ligands. Based on this simple pharmacophore model, we have

Table 5. Benzamide ERα and ERβ binding affinities and transciptional activity

Compound	RBA (%) (uterine)	RBA (%)[a]			Agonism[b] % CAT Act.		Antagonism[b] % CAT Act. + E₂	
		ERα	ERβ	α/β ratio	ERα	ERβ	ERα	ERβ
11g	4.6	14	2.4	5.8	65	20	90	40
17a	7.5	23	15	1.5	60	20	65	45
16b	9.0	17	2.7	6.3	75	15	90	35
rac-**17b**	14	25	8.9	2.8	80	30	83	35
*ent*₁-**17b**	10	18	11	1.6	85	30	80	48
*ent*₂-**17b**	22	40	4.8	8.3	80	10	90	40
16g	15	27	1.3	21	99	99	100	97

[a]Relative binding affinities are the average of duplicate determinations (CV 0.3), determined with purifed RDα and ERβ preparations. For estradiol, RBA = 100. For details, see Experimental.
[b]HEC-1 cells were transfected with either REα or ERβ expression vectors and an (ERE)₃-pS2-CAT reporter gene. CAT activity was normalized for β-galactosidase activity from an internal control plasmid and is expressed as a percent of the ERα or ERβ response with 1 nM E₂. Benzamides were tested at 10⁻⁶ M concentration to test for agonism and at 10⁻⁶ M with 10⁻⁹ M E₂ to test for antagonism. These assays are generally reproductive with a CV of 30% relative.

made a substantial exploration of the amide functionality as a core replacement that might support compound libraries for developing novel SERMs. Using this approach, we prepared and tested representative examples of bis-phenolic amides which displayed both simple *N*-alkyl substituents and CF$_3$-containing *N*-alkyl substituents. Of the two classes examined, benzamides and acetamides, the benzamides displayed the highest affinity, in particular the CF$_3$-containing benzamides. The recent X-ray crystal structure of E$_2$ bound to ERα and structure–binding affinity relationships have allowed us to design a bis-phenolic benzamide **16g**, which has the highest affinity for any carboxamide ligand for the ER. This compound is also an ERα potency-selective agonist in cell-based assay of ER-mediated transcriptional activity. This work illustrates that ER ligands based on simple amide core structures can be readily prepared. High affinity ER binding, however, requires an appropriate distribution of bulk and functionality. The strong conformational preference of the basic anilide function in all of these ligands defines the scope of further structural and functional expansion of these series.

Experimental

General

Melting points were determined on a Thomas-Hoover UniMelt capillary apparatus and are uncorrected. All reagents and solvents were obtained from Aldrich, Fisher or Mallinckrodt. Tetrahydrofuran was distilled from sodium/benzophenone. Dimethylformamide was vacuum-distilled prior to use, and stored over 4 Å molecular sieves. *n*-Butyllithium was titrated with *N*-pivaloyl-*o*-toluidine. All reactions were performed under a dry N$_2$ atmosphere unless otherwise specified. Reaction progress was monitored by analytical thin-layer chromatography using GF silica plates purchased from Analtech. Visualization was achieved by short-wave UV light (254 nm) or potassium permanganate. Radial preparative-layer chromatography was performed on a Chromatotron instrument (Harrison Research, Inc., Palo Alto, CA) using EM Science silica gel Kieselgel 60 PF$_{254}$ as adsorbent. Flash column chromatography was performed using Woelm 32–63 μm silica gel packing.

Logarithms of octanol–water partition coefficients (Log $P^{o/w}$) were determined using a standardized reverse phase HPLC Chromegabond MC 8 column.[23] HPLC separation of the enantiomers for **17b** was performed on an analytical ChiralPak AD (4.6×25 cm) column from Chiral Technologies using 10% *i*-propanol/hexane as solvent. ^{1}H and ^{13}C NMR spectra were recorded on either a General Electric QE-300 (300 MHz), Varian Unity 400 or 500 MHz spectrometers using CDCl$_3$, MeOD or (CD$_3$)$_2$SO as solvent. Chemical shifts were reported as parts per million downfield from an internal tetramethylsilane standard ($\delta = 0.0$ for ^{1}H) or from solvent references. NMR coupling constants are reported in Hertz. ^{13}C NMR were determined using either the Attached Proton Test (APT) experiment or standard ^{13}C pulse sequence parameters. Low resolution and high resolution electron impact mass spectra were obtained on Finnigan MAT CH-5 or 70-VSE spectrometers. Elemental analyses were performed by the Microanalytical Service Laboratory of the University of Illinois.

Unless otherwise stated, a standard procedure for product isolation was used; this involved quenching by addition of water or an aqueous solution, exhaustive extraction with an organic solvent, washing the extracts, drying over Na$_2$SO$_4$, and solvent evaporation under reduced pressure. Quenching media, extraction solvents, and aqueous washes used are noted parenthetically after the phrase 'product isolation'.

Biological procedures

Relative binding affinity assay. Ligand binding affinities (RBAs) using lamb uterine cytosol as a receptor source were determined by a competitive radiometric binding assay using 10 nM [^{3}H]estradiol as tracer and dextran-coated charcoal as an adsorbent for free ligand.[32] Purified ERα and ERβ binding affinities were determined using a competitive radiometric binding assay using 10 nM [^{3}H]estradiol as tracer, commercially available ERα and ERβ preparations (PanVera Inc., Madison, WI), and hydroxylapatite (HAP) to adsorb bound receptor–ligand complex.[33] HAP was prepared following the recommendations of Williams and Gorski.[34] All incubations were done at 0 °C for 18–24 h. Binding affinities are expressed relative to estradiol on a percent scale (i.e. for estradiol, RBA = 100%). All essays were run in separate, duplicate experiments which were reproducible with a coefficient of variation of less than 30% relative.

Transcriptional activation assay. Human endometrial cancer (HEC-1) cells were maintained in culture and transfected as described previously.[31] Transfection of HEC-1 cells in 60 mm dishes used 0.4 mL of a calcium phosphate precipitate containing 2.5 μg of pCMVβGal as internal control, 2 μg of the reporter gene plasmid, 100 ng of the ER expression vector, and carrier DNA to a total of 5 μg DNA. CAT activity, normalized for the internal control β-galactosidase activity, was assayed as previously described.[31]

Molecular modeling

Small molecule modeling. Dihedral drive and Monte Carlo conformational searches for *N*-phenyl benzamides **16a** and **17a** and *N*-phenyl acetamide **27** were conducted using the MM2 force field as implemented in Macromodel v.5.5 with CHCl$_3$ as a solvent model. All generated conformers from Monte Carlo searches underwent full matrix assisted minimization using the PRCG function with a convergence criteria of 0.001 kcal/mol. Dihedral drives were conducted in 5° steps with a convergence criteria of 0.05 kcal/mol using 1000 minimization steps. Analysis of the energy versus torsion angle provided the estimated rotational barrier.

Receptor docking studies. The starting conformation used for docking studies for **16g** was obtained from a

random conformational search using the TRIPOS' force field (MAXIMIN) as implemented in the program SYBYL, version 6.5.2 (Tripos Inc., St. Louis, MO). The *cis* global minima obtained for benzamide **16g** was then overlaid with E_2 in the E_2-ERα LBD crystal structure[26] using a least squares multifitting of five atoms: atoms C(3), C(10), C(9), C(11), and C(12) of E_2 were fitted with the 1 and 4 carbons of the benzamide phenyl ring, the C=O carbon, the nitrogen and the C(2) carbon of the phenethyl group, respectively. The pre-positioned benzamide was then optimally docked in the ERα binding pocket using TRIPOS' Flexidock. Both hydrogen-bond donors and acceptors within the pocket surrounding the ligand (Glu$_{353}$, Arg$_{394}$ and His$_{524}$) and the ligand itself, in addition to select torsional bonds were defined. The best docked receptor ligand complex from Flexidock then underwent a three-step minimization: first non-ring torsional bonds of the ligand were minimized in the context of the receptor using the torsmin command, followed by minimization of the side-chain residues within 8 Å of the ligand while holding the backbone and residues Glu$_{353}$ and Arg$_{394}$ fixed. A final third minimization of both the ligand and receptor was conducted using the anneal function (hot radius 8 Å, interesting radius 16 Å) while holding residues Glu$_{353}$ and Arg$_{394}$ fixed to afford the final model. Minimizations were done using the TRIPOS' Forcefield (MAXI-MIN) with the Powell gradient method and default settings (final RMS < 0.05 kcal/mol·Å).

X-Ray crystallography

Cystallography details for 17a and 10b. Crystals of **17a** were obtained by slow evaporation from ether at 0 °C. Crystals were mounted on glass fibers with Para-tone-N oil (Exxon) and immediately cooled to −75 °C in a cold nitrogen gas stream on the diffractometer. Standard peak search and indexing procedures gave rough cell dimensions, and least squares refinement using 5344 reflections yielded the cell dimensions as given in Table 6.

Data were collected with an area detector by using the measurement parameters listed in Table 6. No systematic absences are noted for the P-1 space group. The measured intensities were reduced to structure factor amplitudes and their esds by correction for background, scan speed, and Lorentz and polarization effects. While corrections for crystal decay were unnecessary (the data were corrected for crystal decay), a Ψ-scan absorption correction was applied, the maximum and minimum transmission factors being 0.991 and 0.876. Systematically absent reflections were deleted and symmetry equivalent reflections were averaged to yield the set of unique data. All 5344 data were used in the least squares refinement.

The structure was solved using direct methods (SHELXTL). The correct positions for the C, N, O, S, and F atoms were deduced from an E-map. Subsequent least-squares refinement and difference Fourier calculations revealed the positions of the remaining non-hydrogen atoms. The quantity minimized by the least-squares program was $\Sigma w(F_0^2-F_c^2)^2$, where $w = \{[\sigma(F_0^2)]^2 + (0.883P)^2\}^{-1}$ and $P = (F_0^2 + 2F_c^2)/3$. The analytical approximations to the scattering factors were used, and all structure factors were corrected for both real and imaginary components of anomalous dispersion. In the final cycle of least squares, independent anisotropic displacement factors were refined for the non-hydrogen atoms and the aromatic, methyl, and methine hydrogen atoms were fixed in 'idealized' positions with C–H=0.95 Å for the aromatic hydrogens, C–H=0.98 Å for the methyl hydrogens, and C–H=1.00 Å for the methine hydrogen. Successful convergence was indicated by the maximum shift/error of 0.001 for the last cycle. Final refinement parameters are given in Table 6. The largest peak in the final Fourier difference map (0.795 eÅ^{-3}) was located 1.64 Å from C(18). A final analysis of variance between observed and calculated structure factors showed no apparent errors.

Single crystals of **10b** were grown from MeOH by slow evaporation at 23 °C in a partially sealed scintillation

Table 6. Crystal data and structure refinement for thiocarboxamide **17a** and carboxamide **10b**

Complex	17a	10b
Empirical formula	$C_{18}H_{18}F_3NO_2S$	$C_{16}H_{17}NO_3$
fw	369.39	271.31
Temperature	198(2) K	198(2) K
Wavelength	0.71073 Å	1.54178 Å
Cryst syst	triclinic	monoclinic
Space group	P-1	$P2_1/n$
Unit cell dimensions	$a = 9.5099(7)$ Å	$a = 18.248(4)$ Å
	$b = 10.5351(8)$ Å	$b = 9.054(2)$ Å
	$c = 11.1127(8)$ Å	$c = 18.248(4)$ Å
Volume	868.07(11) Å^3	2916.4(10) Å^3
Z	2	8
Density, calcd	1.413 Mg/m^3	1.236 Mg/m^3
Abs coeff	0.228 mm^{-1}	0.695 mm^{-1}
No. of indep refins	5344 [R(int) = 0.0293]	4796 (R(int) = 0.0556)
Refinement method	full matrix least-squares on F^2	full matrix least-squares on F^2
No. of data/restraints/params	3727/0/226	2727/0/362
Goodness-of-fit (GooF) on F^2	0.949	1.062
Final R indices ($I > 2\sigma(I)$)	R1 = 0.0502, wR2 = 0.1393	R1 = 0.0624, wR2 = 0.1662
R indices (all data)	R1 = 0.0892, wR2 = 0.1533	R1 = 0.0767, wR2 = 0.1881

vial. Crystals were mounted on glass fibers with Paratone-N oil (Exxon) and immediately cooled to −75 °C in a cold nitrogen gas stream on the diffractometer. Standard peak search and indexing procedures gave rough cell dimensions. Initial inspection of the data suggested a C-centered orthorhombic cell, but no successful solution could be found in any orthorhombic space group. Eventually, a successful solution was found in a primitive monoclinic cell of half the volume in the space group $P2_1/n$. The refinement stalled at $wR_2 = 0.63$, despite having located all atoms and refining the non-hydrogen atoms anisotropically. The unusual equality in the lengths of the a and c axes, combined with the observation that $F_{obs} \gg F_{calc}$ for all the reflections in the 'most disagreeable reflections' list, suggested that the crystal was twinned. A twin law involving mirror reflection through the (101) plane was assumed, and a refinable parameter describing the relative volume fractions of the two twin individuals was added to the model. The intensities were calculated from the relation $F_{TOT}^2 = f F_{hkl}^2 + (1-f) F_{h'k'l'}^2$, where f is the volume fraction of twin individual one and F_{hkl}^2 and $F_{h'k'l'}^2$ are the contributions from the two twins (the twin law specifies that h'k'l' = lkh). The scale factor refined to 0.500(3), and the wR_2 factor dropped to an acceptible value of 0.185.

In the final cycle of least squares, independent anisotropic displacement factors were refined for the non-hydrogen atoms and the aromatic, methyl, and methine hydrogen atoms were fixed in 'idealized' positions with C–H=0.95 Å for the aromatic hydrogens, C–H=0.98 Å for the methyl hydrogens, and C–H=1.00 Å for the methine hydrogen. Successful convergence was indicated by the maximum shift/error of 0.001 for the last cycle. Final refinement parameters are given in Table 6. The largest peak in the final Fourier difference map (0.795 cÅ^{-3}) was located 1.64 Å from C(18). A final analysis of variance between observed and calculated structure factors showed no apparent errors.

Chemical syntheses

4-Methoxyphenyl-4-methoxybenzene sulfonamide (3).[8] To a mixture of 4-methoxybenzenesulfonylchloride (1.0 equiv) and pyridine (1.1 equiv) in CH$_2$Cl$_2$ (0.5 M) at 0 °C was added dropwise to a solution of p-anisidine (1.5–5.0 equiv) in CH$_2$Cl$_2$ (1.5 M) over 30 min. The reaction mixture was warmed to rt and stirred until completion of reaction as indicated by TLC. Product isolation (H$_2$O, 2 N HCl) and recrystallized from EtOH afforded product as light red crystals (91%): mp 91–92.5 °C, mp[8] 93 °C.

General procedure for phase transfer N-alkylation of sulfonamides.[9] To a CH$_2$Cl$_2$ (0.06 M) solution of sulfonamide (1.0 equiv) was added an equal volume solution of NaOH (5 equiv) and (n-Bu)$_4$NSO$_4$H (0.1 equiv) in H$_2$O. Alkylhalide (2.0 equiv) was then added directly to the bi-phasic solution and stirred at rt. After 12 h the layers were separated. Product isolation (Na$_2$CO$_3$, brine) followed by flash chromatography afforded the pure N-alkyl benzene sulfonamide.

N-(4-Methoxyphenyl)-N-(ethyl)-4-methoxybenzene sulfonamide (4a).[8] Purification by flash chromatography (20% EtOAc:hexane) afforded off-white powder (86%): mp 95–7 °C, mp[8] 100–104 °C; ^{1}H NMR (CDCl$_3$) δ 1.06 (t, 3H, $J = 7.1$ Hz), 3.52 (q, 2H, $J = 7.0$ Hz), 3.81 (s, 3H), 3.84 (s, 3H), 6.82 (d, 2H, $J = 8.8$ Hz), 6.94 (d, 2H, $J = 8.0$ Hz), 6.96 (d, 2H, $J = 8.0$ Hz), 7.54 (d, 2H, $J = 8.8$ Hz).

N-(4-Methoxyphenyl)-N-(butyl)-4-methoxybenzene sulfonamide (4b). Purification by flash chromatography (20% EtOAc:hexane) afforded transparent oil (81%): ^{1}H NMR (CDCl$_3$) δ 0.85 (t, 3H, $J = 7.2$ Hz), 1.34 (m, 4H), 3.46 (t, 2H, $J = 6.8$ Hz), 3.80 (s, 3H), 3.86 (s, 3H), 6.81 (d, 2H, $J = 9.0$ Hz), 6.92 (app t, 4H, $J = 9.1$ Hz), 7.51 (d, 2H, $J = 9.0$ Hz); MS (EI, 70 eV) m/z 349 (M$^+$); HRMS calcd for (C$_{18}$H$_{23}$NO$_4$S, 349.1347, found 349.1348).

N-(4-Methoxyphenyl)-N-(benzyl)-4-methoxybenzene sulfonamide (4c). Recrystallization from 20% EtOAc/hexane afforded flocculent white crystals (93%): mp 141–142 °C; ^{1}H NMR (CDCl$_3$) δ 3.72 (s, 3H), 3.87 (s, 3H), 4.67 (s, 2H), 6.89 (d, 2H, $J = 11$ Hz), 6.86 (d, 2H, $J = 11.5$ Hz), 6.94 (d, 2H, $J = 11$ Hz), 7.21 (m, 5H), 7.59 (d, 2H, $J = 11$ Hz); ^{13}C NMR (CDCl$_3$) δ 55.1, 55.4, 55.8, 114.2, 127.7, 128.5, 128.7, 129.9, 130.4, 130.4, 131.7, 136.3, 158.9, 163.0; HRMS calcd for C$_{21}$H$_{21}$NSO$_4$, 383.1191, found 383.118.

General demethylating procedure using BBr$_3$. To a solution of methyl ether compound in CH$_2$Cl$_2$ at −78 °C was added a 1.0 M BBr$_3$ in CH$_2$Cl$_2$ (3 equiv) dropwise over 15 mm. The reaction was allowed to reach rt and stir overnight or until disappearance of starting material as indicated by TLC. The mixture was then cooled to 0 °C. Product isolation (H$_2$O, Et$_2$O, brine) and purification via radial or flash chromatography or recrystallization from an appropriate solvent afforded the desired phenolic compounds.

General demethylating procedure using EtSH. To a stirred DMF solution of NaH (6.2 equiv of a 60% w/w dispersion) at 0 °C was added dropwise 6.0 equiv of EtSH. After 30 min the mixture was warmed to rt and a solution of the methyl ether protected compound in 5 mL DMF was added dropwise. The reaction mixture was heated to reflux for 4 h; then cooled in an ice-bath and acidified with 2 N HCl. Remaining product isolation (EtOAc, brine) and purification afforded the phenolic compounds.

N-(4-Hydroxyphenyl)-N-(ethyl)-4-hydroxybenzene sulfonamide (5a). Deprotected according to BBr$_3$ procedure. SiO$_2$ plug (30% EtOAc/hexane) to afford off-white crystals (62%): ^{1}H NMR ((CD$_3$)$_2$SO) δ 0.98 (t, 3H, $J = 7.2$ Hz), 3.43 (q, 2H, $J = 6.8$ Hz), 6.67 (d, 2H, $J = 8.7$ Hz), 6.76 (d, 2H, $J = 8.4$ Hz), 6.86 (d, 2H, $J = 8.5$ Hz), 7.34 (d, 2H, $J = 8.7$ Hz); ^{13}C NMR ((CD$_3$)$_2$SO) δ 14.1 (CH$_3$), 45.2 (CH$_2$), 115.7 (ArCH), 115.8 (ArCH), 122.6 (ArC), 128.1 (ArC), 129.9 (ArCH), 130.1 (ArCH), 157.1 (ArC), 161.6 (ArC); MS (EI, 70 eV) m/z 293 (M$^+$); HRMS calcd for C$_{14}$H$_{15}$NSO$_4$, 293.0721, found 293.0722.

N-(4-Hydroxyphenyl)-N-(butyl)-4-hydroxybenzene sulfonamide (5b). Deprotected according to BBr₃ procedure to afford tan crystals, recrystallized from EtOAc/hexane (71%): mp 137–138 °C; ¹H NMR (CDCl₃) δ 0.86 (t, 3H, $J = 7.0$ Hz), 1.35 (m, 4H), 3.48 (t, 2H, $J = 7.0$ Hz), 6.42 (d, 2H, $J = 8.8$ Hz), 6.87 (app t, 4H, $J = 8.9$ Hz), 7.47 (d, 2H, $J = 9.0$ Hz) ¹³C NMR (CD₃)₂SO) δ 13.8 (CH₃), 19.2 (CH₂), 29.9 (CH₂), 49.7 (CH₂), 115.6 (ArCH), 115.7 (ArCH), 122.6 (ArCH), 128.0 (ArC), 129.9 (ArCH), 130.0 (ArC), 157.0 (ArC), 161.6 (ArC); MS (EI, 70 eV) m/z 321 (M⁺); HRMS calcd for C₁₆H₁₉NSO₄, 321.1034, found 321.1035. Anal. (C₁₆H₁₉N·0.3 H₂O): C, 58.81; H, 6.05; N, 4.29. Found: C, 58.60; H, 6.03; N, 4.13.

N-(4-Hydroxyphenyl)-N-(benzyl)-4-hydroxybenzene sulfonamide (5c). Deprotected according to BBr₃ procedure to afford title compound after purification by radial chromatography (10%): ¹H NMR (CDCl₃) δ 4.65 (s, 2H), 6.66 (d, 2H, $J = 8.5$ Hz), 6.80 (d, 2H, $J = 8.5$ Hz), 6.96 (d, 2H, 8.8), 7.21 (br s, 5H), 7.59 (d, 2H, $J = 8.9$ Hz); MS (EI, 70 eV) m/z 355 (M⁺); HRMS calcd for C₁₉H₁₇NSO₄, 355.0878, found 355.0881.

N-(4-Methoxyphenyl)-4-methoxybenzamide (6).[35] A CH₂Cl₂ solution of p-anisidine (1.3 equiv) was added dropwise to a stirring CH₂Cl₂ solution (2–5 mL) of pyridine (1.1 equiv) and p-anisoyl chloride (1.0 equiv) at 0 °C. Upon complete addition of amine (30 mm) mixture was allowed to reach rt, then re-cooled and vacuum filter to afford the crude carboxamide. Recrystallization from EtOH/benzene afforded the pure carboxamide as off-white crystals (72%): mp 199–200.5 °C, mp[32] 202–203 °C.

N-(1-Phenethyl)-4-methoxyaniline (7).[7] To a 0 °C EtOH solution containing p-anisidine (1.0 equiv) and catalytic p-toluene sulfonic acid·H₂O (0.05 equiv) was added freshly distilled benzaldehyde dropwise. The mixture was allowed to reach rt and complete imine formation occurred within 0.5 h. The crude mixture was concentrated in vacuo, and product isolation followed (EtOAc, brine) to afford a dark brown powder. ¹H NMR confirmed imine which was directly used in the next step without further purification. *CH₃ addition*: Crude imine was dissolved in toluene and cooled to −78 °C. To this was added MeLi (1.0 M toluene solution, 3 equiv) dropwise over 15 mm. After 60 min at −78 °C, the crude mixture was warmed to rt and stirred for an additional 2 h. The reaction was then cooled in an ice-bath and quenched with cold MeOH followed by addition of satd NH₄Cl until neutral pH. Concentration in vacuo followed by remaining workup (EtOAc, H₂O, brine) afforded amine as a red oil. Kügelrohr distillation provided pure product, which crystallized on standing as a red orange powder (75%): ¹H NMR (CDCl₃) δ 1.50 (d, 3H, $J = 7.0$ Hz), 3.69 (s, 3H), 4.41 (q, 1H, $J = 7.0$ Hz), 6.47 (AA'BB', 2H, $J = 9.0$, 3.0 Hz), 6.69 (AA'BB', 2H, $J = 9.0$, 3.5 Hz), 7.29 (m, 5H); ¹³C NMR (CDCl₃) δ 25.4 (CH₃), 54.5 (CH), 55.9 (CH₃), 114.7 (ArCH), 114.9 (ArCH), 126.1 (ArCH), 127.0 (ArCH), 128.8 (ArCH), 141.7 (ArC), 145.7 (ArC), 152.1 (ArC); MS (EI, 70 eV) m/z 227 (M⁺); anal. (C₁₅H₁₇NO): C,

79.26; H, 7.54; N, 6.16. Found: C, 79.31; H, 7.54; N, 6.27.

N-[2-(3-Methyl)butane]-4-methoxyaniline (8). To a THF solution at 0 °C containing p-anisidine (1 equiv), 3-methyl-2-butanone (1.0 equiv), and acetic acid (1.0 equiv) was added solid NaHB(OAc)₃. The mixture was allowed to reach rt and stirred for 15 h. The mixture was re-cooled to 0 °C; careful workup (H₂O, EtOAc, NaHCO₃, brine, MgSO₄) and concentration in vacuo afforded crude amine. Kügelrohr distillation provided pure product as light yellow oil (71%): bp 100 °C (0.3 mm); ¹H NMR (CDCl₃) δ 0.93 (d, 3H, $J = 6.5$ Hz), 1.00 (d, 3H, $J = 6.5$ Hz), 1.10 (d, 3H, $J = 6.0$ Hz), 1.86 (m, 1H, $J = 6.5$ Hz), 3.23 (br s, 1H, ArNH), 3.28 (dq, 1H, $J = 7.0$, 6.0 Hz), 3.77 (s, 3H), 6.58 (d, 2H, $J = 7.0$ Hz), 6.80 (d, 2H, $J = 7.0$ Hz); ¹³C NMR (CDCl₃) δ 16.5 (CH₃), 17.3 (CH₃), 19.3 (CH₃), 32.1 (CH), 54.5 (CH), 55.8 (CH₃), 114.6 (ArCH), 114.9 (ArCH), 142.1 (ArC), 151.7 (ArC); MS (EI, 70 eV) m/z 193 (M⁺); anal. (C₁₂H₁₉NO): C, 74.57; H, 9.91; N, 7.25. Found: C, 74.46; H, 9.76; N, 7.32.

General procedure for phase transfer N-alkylation of carboxamides.[9,10] Alkylhalide (3 equiv) in benzene was added dropwise to a stirring mixture of carboxamide (1 equiv), finely powdered potassium hydroxide (2 equiv), and n-tetrabutylammonium bromide (0.05 equiv) in benzene (0.2 M) at rt. Reaction mixture was heated to 80 °C and maintained at this temperature until disappearance of starting material was observed by TLC (1–3 h). The reaction mixture was then cooled to rt and the salts removed by filtration. Product isolation (H₂O, brine), followed by flash chromatography (10–25% EtOAc/hexane) afforded product, usually as an oil.

General amidation procedures for anilines 7–8 and CF₃-containing anilines 14a–d. A 0.18 M benzene or toluene solution containing 1 equiv of aniline (14a, 14b, 7–8) in addition to 3 equiv of dry powdered K₂CO₃ and 1 equiv of pyridine was treated with 1.5 equiv of the corresponding acid chloride and heated between 80 and 110 °C. The reaction was monitored by TLC and the reaction cooled to rt upon completion. The crude mixture was filtered, concentrated in vacuo and taken up in Et₂O. Product isolation (H₂O, brine) and chromatographic purification afforded the protected carboxamide (15a–e and 9f and 9g).

Benzamides **15f** and **15g** were prepared from anilines **14c** and **14d** and the corresponding acid chloride (1.5 equiv) using 1,2-dichlorobenzene as solvent, 3 equiv of dry powdered K₂CO₃ and heated to 120–150 °C for 16 h or until disappearance of starting aniline. Reaction mixture was cooled to rt and eluted over silica with hexane to remove 1,2-dichlorobenzene. Gradient chromatography with 10, 20, and 30% EtOAc/hexane afforded the pure carboxamides **15f** and **15g** upon concentration.

N-(4-Methoxyphenyl)-N-(ethyl)-4-methoxybenzamide (9a). Yellow oil (72%): ¹H NMR (CDCl₃) δ 1.12 (t, 3H, $J = 7.2$ Hz, CH₃), 3.62 (s, 3H, OCH₃), 3.65 (s, 3H, OCH₃), 3.84 (q, 2H, $J = 7.0$ Hz, CH₂), 6.57 (d, 2H,

$J = 8.9$ Hz, ArH *ortho* OCH_3, *meta* RNCO). 6.68 (d, 2H, $J = 8.9$ Hz, ArH *ortho* OCH_3, *meta* CONR), 6.87 (d, 2H, $J = 8.9$ Hz, ArH *ortho* RNCO), 7.20 (d, 2H, $J = 8.7$ Hz, ArH *ortho* CONR); ^{13}C NMR (CDCl$_3$) δ 12.7 (CH$_3$), 45.5 (CH$_2$), 55.0 (OCH$_3$), 55.2 (OCH$_3$), 112.8 (ArCH), 114.2 (ArCH), 128.4 (ArC), 128.9 (ArCH), 130.7 (ArCH), 136.3 (ArC), 157.8 (ArC), 160.2 (ArC), 169.6 (C=O); MS (EI, 70 eV) *m/z* 285 (M$^+$); HRMS calcd for C$_{17}$H$_{19}$NO$_3$, 285.1365, found 285.1364.

N-(4-Methoxyphenyl)-N-(2-propyl)-4-methoxybenzamide (9b). Amber oil (43%): ^{1}H NMR (CDCl$_3$) δ 1.16 (d, 6H, $J = 6.5$ Hz), 3.72 (s, 3H), 3.75 (s, 3H), 5.09 (br s, 1H), 6.63 (d, 2H, $J = 8.5$ Hz), 6.74 (d, 2H, $J = 9.0$ Hz), 6.93 (d, 2H, $J = 8.5$ Hz), 7.21 (d, 2H, $J = 8.5$ Hz); ^{13}C NMR (CDCl$_3$) δ 21.2 (CH$_3$), 55.3 (CH$_3$), 55.5 (CH$_3$), 113.0 (ArCH), 113.9 (ArCH), 129.1 (ArC), 130.4 (ArCH), 131.8 (ArCH), 132.5 (ArC), 158.6 (ArC), 160.1 (ArC), 170.5 (C=O); MS (EI, 70 eV) *m/z* 299 (M$^+$); HRMS calcd for C$_{18}$H$_{21}$NO$_3$ 299.1521, found 299.1521.

N-(4-Methoxyphenyl)-N-(butyl)-4-methoxybenzamide (9c). Yellow oil (81%): ^{1}H NMR (CDCl$_3$) δ 0.84 (t, 3H, $J = 7.3$ Hz, CH$_3$), 1.29 (sext, 2H, $J = 7.0$ Hz, CH$_3$CH$_2$), 1.53 (quint, 2H, $J = 7.8$ Hz, CH$_2$CH$_2$CH$_2$), 3.62 (s, 3H, OCH$_3$ *ortho* RNCO), 3.66 (s, 3H, OCH$_3$ *ortho* CONR), 3.78 (t, 2H, $J = 7.7$ Hz, CH$_2$CH$_2$N), 6.58 (d, 2H, $J = 8.8$ Hz, ArH *ortho* OCH$_3$, *meta* RNCO), 6.68 (d, 2H, $J = 8.9$ Hz, ArH *ortho* OCH$_3$, and *meta* CONR), 6.88 (d, 2H, $J = 8.9$ Hz, ArH *ortho* RNCO), 7.19 (d, 2H, $J = 8.9$ Hz, ArH *ortho* CONR); ^{13}C NMR (CDCl$_3$) δ 13.7 (CH$_3$), 20.0 (CH$_2$), 29.5 (CH$_2$), 50.3 (CH$_2$), 54.9 (OCH$_3$), 55.1 (OCH$_3$), 112.7 (ArCH), 114.1 (ArCH), 128.4 (ArC), 128.6 (ArCH), 130.5 (ArCH), 136.5 (ArC), 157.6 (ArC), 160.0 (ArC), 169.6 (ArC); MS (EI, 70 eV) *m/z* 313 (M$^+$); HRMS calcd for C$_{19}$H$_{23}$NO$_3$, 313.7794, found 313.7879.

N-(4-Methoxyphenyl)-N-(benzyl)-4-methoxybenzamide (9e). White flakes (82%): mp 104–106 °C; ^{1}H NMR (CDCl$_3$) δ 3.72 (s, 3H, OCH$_3$ *para* RNCO), 3.74 (s, 3H, OCH$_3$ *para* CONR), 5.09 (s, 2H, CH$_2$Ph), 6.68 (d, 2H, $J = 9.2$ Hz, ArH *ortho* OCH$_3$, and *meta* RNCO), 7.31 (m, 9H, Ph and ArH); ^{13}C NMR (CDCl$_3$) δ 54.3 (PhCH$_2$), 55.3 (OCH$_3$), 55.5 (OCH$_3$), 113.1 (ArCH), 114.3 (ArCH), 127.4 (ArCH), 128.6 (ArCH), 128.3 (ArC), 128.7 (ArCH), 128.9 (ArCH), 131.1 (ArCH), 137.0 (ArC), 138.0 (ArC), 158.0 (ArC), 160.6 (ArC), 170.2 (ArC); MS (EI, 70 eV) *m/z* 347 (M$^+$); HRMS calcd for C$_{22}$H$_{21}$NO$_3$, 347.1521, found 347.1522.

N-(4-Methoxyphenyl)-N-(1-phenethyl)-4-methoxybenzamide (9f). Prepared according to general procedure above using aniline 7 and *p*-anisoyl chloride. Purification by flash chromatography (2% (CH$_3$)$_2$CO/CH$_2$Cl$_2$) afforded product as clear oil (70%): ^{1}H NMR (CDCl$_3$) δ 1.48 (d, 3H, $J = 6.8$ Hz), 3.67 (s, 3H), 3.69 (s, 3H), 6.38 (br q, 1H, $J = 6.8$ Hz), 6.56 (br d overlapping br s, 4H), 6.62 (d, 2H, $J = 8.8$ Hz), 7.23 (d, 2H, $J = 8.5$ Hz), 7.29 (m, 5H); ^{13}C NMR (CDCl$_3$) δ 16.9 (CH$_3$), 53.3 (CH), 55.2 (CH$_3$), 55.3 (CH$_3$), 112.9 (ArCH), 113.6 (ArCH), 127.5 (ArCH), 128.2 (ArCH), 128.3 (ArCH), 129.2 (ArC), 130.6 (ArCH), 131.5 (ArCH), 132.7 (ArC), 141.7

(ArC), 158.3 (ArC), 160.2 (ArC), 170.6 (C=O); MS (EI, 70 eV) *m/z* 361 (M$^+$).

N-(4-Methoxyphenyl)-N-(1-methyl-2-methyl-1-propyl)-4-methoxybenzamide (9g). Prepared according to general procedure above using aniline 8 and *p*-anisoyl chloride. Purification by flash chromatography (25% EtOAc/hexane) afforded product as light yellow oil (90%): ^{1}H NMR (CDCl$_3$) δ 0.93 (d, 6H, $J = 6.7$ Hz), 1.90 (sept, 1H, $J = 7.0$ Hz), 3.69 (s, 3H), 3.71 (s, 3H), 3.73 (d, 2H, $J = 7.0$ Hz), 6.62 (d, 2H, $J = 8.5$ Hz), 6.71 (d, 2H, $J = 9.0$ Hz), 6.93 (d, 2H, $J = 8.6$ Hz), 7.20 (d, 2H, $J = 8.9$ Hz); ^{13}C NMR (CDCl$_3$) δ 20.3 (CH$_3$), 27.0 (CH), 55.2 (CH$_3$), 55.4 (CH$_3$), 57.2 (CH$_2$), 113.0 (ArCH), 114.3 (ArCH), 128.7 (ArCH), 129.0 (ArC), 130.7 (ArCH), 137.1 (ArC), 157.8 (ArC), 160.3 (ArC), 170.3 (C=O); MS (EI, 70 eV) *m/z* 313 (M$^+$).

N-(4-Hydroxyphenyl)-N-(ethyl)-4-hydroxybenzamide (10a). Deprotected according to BBr$_3$ procedure to afford off-white powder, recrystallized from MeOH (70%): mp 208–209 °C; ^{1}H NMR ((CD$_3$)$_2$SO) δ 1.03 (t, 3H, $J = 6.9$ Hz, CH$_3$), 3.72 (q, 2H, $J = 7.1$ Hz, CH$_2$), 6.52 (d, 2H, $J = 8.6$ Hz, ArH *meta* RNCO), 6.62 (d, 2H, $J = 8.5$ Hz, ArH *meta* CONR), 6.86 (d, 2H, $J = 8.6$ Hz, *ortho* RNCO), 7.06 (d, 2H, $J = 8.5$ Hz, *ortho* CONR), 9.48 (s, 1H, OH), 9.71 (s, 1H, OH); ^{13}C NMR ((CD$_3$)$_2$SO) δ 12.6 (CH$_3$), 39.1 (CH$_2$), 114.3 (ArCH), 115.7 (ArCH), 127.1 (ArC), 129.1 (ArC), 130.5 (ArCH), 134.7 (ArC), 155.7 (ArC), 158.3 (ArC), 168.9 (ArC); MS (EI, 70 eV) *m/z* 257 (M$^+$); HRMS calcd for C$_{15}$H$_{15}$NO$_3$, 257.1052, found 257.1051.

N-(4-Hydroxyphenyl)-N-(2-propyl)-4-hydroxybenzamide (10b). Deprotected according to BBr$_3$ procedure to afford powder, recrystallized from MeOH (77%): mp 210–212 °C; ^{1}H NMR (MeOD) δ 1.15 (d, 6H, $J = 6.8$ Hz), 4.94 (br s, 1H), 6.56 (br s, 2H), 6.67 (d, 2H, $J = 8.4$ Hz), 6.88; MS (EI, 70 eV) 271 (M$^+$); anal. (C$_{16}$H$_{17}$NO$_3$·0.1 H$_2$O): C, 70.36; H, 6.36; N, 5.13. Found: C, 70.35; H, 6.37; N, 4.90.

N-(4-Hydroxyphenyl)-N-(butyl)-4-hydroxybenzamide (10c). Deprotected according to BBr$_3$ procedure and purified by flash chromatography (25% EtOAc/hexane) to afford off-white crystals (95%): mp 174–175 °C; ^{1}H NMR ((CD$_3$)$_2$SO) δ 0.84 (s, 3H), 1.25 (sext, 2H, $J = 7.6$ Hz), 1.43 (quint, 2H, $J = 7.6$ Hz), 3.69 (t, 2H, $J = 7.5$ Hz), 6.51 (d, 2H, $J = 8.6$ Hz), 6.61 (d, 2H, $J = 8.7$ Hz), 6.85 (d, 2H, $J = 8.7$ Hz), 7.03 (d, 2H, $J = 8.5$ Hz); ^{13}C NMR ((CD$_3$)$_2$SO) δ 14.1 (CH$_3$), 19.9 (CH$_2$), 40.2 (CH$_2$), 114.5 (ArCH), 115.9 (ArCH), 127.4 (ArC), 129.2 (ArCH), 130.6 (ArCH), 135.1 (ArC), 155.8 (ArC), 158.4 (ArC); MS (EI, 70 eV) *m/z* 285 (M$^+$); HRMS (EI) calcd for C$_{17}$H$_{19}$NO$_3$, 285.1365, found 285.1368; anal. (C$_{17}$H$_{19}$NO$_3$·0.5 H$_2$O): C, 69.37; H, 6.85; N, 4.76. Found: C, 69.30; H, 6.65; N, 4.57.

N-(4-Hydroxyphenyl)-N-(2-methyl-1-propyl)-4-hydroxybenzamide (10d). Deprotected according to BBr$_3$ procedure and purified by flash chromatography (25% EtOAc/hexane) to afford white foam (quant): mp 166 °C dec.; ^{1}H NMR ((CD$_3$)$_2$SO) δ 0.93 (d, 6H, $J = 6.5$ Hz),

1.82 (m, 1H, $J = 6.5$ Hz), 3.66 (d, 2H, $J = 7.5$ Hz), 6.59 (d, 2H, $J = 8.5$ Hz), 6.68 (d, 2H, $J = 9$ Hz), 6.94 (d, 2H, $J = 8.5$ Hz), 7.10 (d, 2H, $J = 8.5$ Hz); MS (EI, 70 eV) m/z 285 (M$^+$); anal. (C$_{17}$H$_{19}$NO$_3$·1.0 H$_2$O): C, 67.31; H, 6.98; N, 4.62. Found: C, 67.45; H, 6.74; N, 4.41.

N-(4-Hydroxyphenyl)-N-(benzyl)-4-hydroxybenzamide (10e).

Deprotected according to EtSH procedure and purified by flash chromatography (25% EtOAc/hexane), which upon solvent concentration and recrystallization from CHCl$_3$ afforded title compound as off-white flakes (60%): mp 103–105 °C; ^{1}H NMR ((CD$_3$)$_2$SO) δ 4.95 (s, 2H, CH$_2$), 6.53 (d, 2H, $J = 6.3$ Hz, ArH meta RNCO), 6.56 (d, 2H, $J = 6.2$ Hz, ArH ortho RNCO), 6.77 (d, 2H, $J = 8.7$ Hz, ArH meta CONR), 7.13 (d, 2H, $J = 8.7$ Hz, AsH ortho CONR), 7.25 (m, 5H, Ph), 9.67 (broad s, 2H, OH); ^{13}C NMR ((CD$_3$)$_2$SO) δ 53.1 (CH$_2$), 114.2 (ArCH), 115.5 (ArCH), 122.3 (ArC), 126.6 (ArC), 126.9 (ArCH), 127.9 (ArCH), 128.3 (ArCH), 128.7 (ArCH), 130.6 (ArCH), 134.9 (ArC), 137.9 (ArC), 155.5 (ArC), 158.5 (ArC), 169.4 (ArC); MS (EI, 70 eV) m/z 319 (M$^+$); HRMS (EI) calcd for C$_{20}$H$_{17}$N0$_3$, 319.1208, found 319.1206; anal. (C$_{20}$H$_{17}$NO$_3$·2.5 H$_2$O): C, 65.92; H, 6.09; N, 3.84. Found: C, 65.58; H, 5.81; N, 3.53.

N-4-Hydroxyphenyl-N-(1-phenethyl)-4-hydroxybenzamide (10f).

Deprotected according to BBr$_3$ procedure recrystallized from MeOH/CH$_2$Cl$_2$ to afford white powder (95%): mp 204–206 °C; ^{1}H NMR (MeOD) δ 1.50 (d, 3H, $J = 6.8$ Hz), 4.95 (s, under MeOH), 6.24 (br s, 2H), 6.49 (br s, 2H), 6.54 (br s, 2H), 6.54 (d, 2H, $J = 8$ Hz), 7.10 (d, 2H, $J = 8$ Hz), 7.28 (m, 5H); ^{13}C NMR (MeOD) δ 17.4 (CH$_3$), 49.0 (CH), 115.3 (ArCH), 115.9 (ArCH), 124.9 (ArCH), 128.6 (ArCH), 128.9 (ArC), 129.1 (ArCH), 129.3 (ArCH), 131.4 (ArCH), 132.4 (ArC), 132.7 (ArCH), 142.5 (ArC), 157.9 (ArC), 159.8 (C=O); MS (EI, 70 eV) m/z 333 (M$^+$); HRMS (EI) calcd for C$_{21}$H$_{19}$NO$_3$, 333.1365, found 333.1360; anal. (C$_{21}$H$_{19}$NO$_3$): C, 75.66; H, 5.74; N, 4.20. Found: C, 75.51; H, 5.80; N, 4.21.

General thionation procedure[12]

The carboxamide (1.01 mmol) and Lawesson's reagent (0.51 mmol) in 3 mL of HMPA were heated to 80–100 °C until the carboxamide had been consumed. After disappearance of carboxamide, the reaction mixture was allowed to cool to rt and then poured onto 5 mL of water. Product was extracted repeatedly with Et$_2$O, dried over Na$_2$SO$_4$, rotary evaporated in vacuo and purified via flash chromatography. The protected thioamides were then directly used in the deprotection step with minimal purification.

N-(4-Hydroxyphenyl)-N-(ethyl)-4-hydroxythiobenzamide (11a).

Deprotected according to BBr$_3$ procedure and purified by flash chromatography (25% EtOAc/hexane) to afford yellow foam (63%): ^{1}H NMR ((CD$_3$)$_2$SO) δ 1.16 (t, 3H, $J = 6.8$ Hz, CH$_3$), 4.34 (q, 2H, $J = 6.8$ Hz, CH$_2$), 6.44 (d, 2h, $J = 8.4$ Hz, ArH meta RNCS), 6.59 (d, 2H, $J = 8.9$ Hz, ArH meta CSNR), 6.87 (d, 2H, $J = 8.7$ Hz, ArH ortho RNCS), 6.99 (d, 2H, $J = 8.6$ Hz, ArH ortho CSNR); ^{13}C NMR ((CD$_3$)$_2$SO) δ 11.1 (CH$_3$), 52.1 (CH$_2$), 114.1 (ArH), 115.6 (ArH), 115.7 (ArH), 122.6 (ArH),

128.5 (ArH), 129.8 (ArH), 135.3 (ArC), 136.4 (ArC), 156.3 (ArC), 157.6 (ArC), 201.0 (CS); MS (EI, 70 eV) m/z 273 (M$^+$); HRMS (EI) calcd for C$_{15}$H$_{15}$NSO$_2$, 273.0824, found 273.0824; anal. (C$_{15}$H$_5$NSO$_2$·0.3 H$_2$O): C, 64.63; H, 5.64; N, 5.02. Found: C, 64.51; H, 5.93; N, 4.64.

N-(4-Hydroxyphenyl)-N-(i-propyl)-4-hydroxythiobenz-amide (11b).

Deprotected according to BBr$_3$ procedure and purified by flash chromatography (25% EtOAc/hexane) to afford yellow foam (98%): ^{1}H NMR (MeOD, i-propyl rotamers 1:4:1 ratio) δ 1.15 (d, 1H, $J = 6.5$ Hz), 1.20 (d, 4H, $J = 6.5$ Hz), 1.27 (d, 1H, $J = 6.5$ Hz), 6.00 (sept, 1H, $J = 6.5$ Hz), 6.46 (d, 2H, $J = 8.5$ Hz), 6.61 (d, 2H, $J = 9$ Hz), 6.81 (d, 2H, $J = 8.5$ Hz), 6.96 (d, 2H, $J = 8.5$ Hz) additional minor ArCH resonances not listed; ^{13}C NMR (MeOD) δ 20.6 (CH$_3$), 21.9 (CH$_3$ minor), 54.8 (CH), 114.8 (ArCH), 115.9 (ArCH), 130.1 (ArCH), 131.7 (ArCH), 133.4 (ArC), 137.8 (ArC), 157.9 (ArC), 158.0 (ArC), 204.4 (C=S); MS (EI, 70 eV) m/z 287 (M$^+$); HRMS, C$_{16}$H$_{17}$NSO$_2$, 287.0980; found, 287.0971.

N-(4-Hydroxyphenyl)-N-(n-butyl)-4-hydroxythiobenzamide (11c).

Deprotected according to BBr$_3$ procedure and purified by radial chromatography (5% MeOH/CH$_2$Cl$_2$) to afford yellow oil (10%): ^{1}H NMR ((CD$_3$)$_2$SO) δ 0.84 (s, 3H, $J = 7.5$ Hz, CH$_3$), 1.27 (sext, 2H, $J = 6.8$ Hz, CH$_3$CH$_2$), 1.61 (quint, 2H, $J = 8.0$ Hz, CH$_2$CH$_2$), 4.30 (t, 2H, $J = 7.7$ Hz, CH$_2$NCS), 6.43 (d, 2H, $J = 8.5$ Hz, ArH meta RNCS), 6.58 (d, 2H, $J = 8.2$ Hz, ArH meta CSNR), 6.87 (d, 2H, $J = 8.2$ Hz, ArH ortho RNCS), 6.97 (d, 2H, $J = 8.5$ Hz, ArH ortho CSNR); ^{13}C NMR ((CD$_3$)$_2$SO) δ 14.2 (CH$_3$), 19.7 (CH$_2$), 27.9 (CH$_2$), 56.8 (CH$_2$), 114.1 (ArCH), 115.9 (ArCH), 128.5 (ArCH), 129.9 (ArCH), 135.2 (ArC), 136.8 (ArC), 156.2 (ArC), 157.7 (ArC), 201.0 (C=S); MS (EI, 70 eV), m/z 301 (M$^+$); HRMS calcd for C$_{17}$H$_{19}$NO$_2$S, 301.1136; found 301.1133.

N-(4-Hydroxyphenyl)-N-(i-butyl)-4-hydroxythiobenzamide (11d).

Deprotected according to BBr$_3$ procedure and purified by flash chromatography (35% EtOAc/hexane) to afford yellow foam (86%): ^{1}H NMR (CDCl$_3$) δ 0.98 (d, 6H, $J = 6.8$ Hz), 2.16 (m, 1H, $J = 6.8$ Hz), 4.34 (d, 2H, $J = 7.6$ Hz), 6.41 (d, 2H, $J = 8.8$ Hz), 6.60 (d, 2H, $J = 8.8$ Hz), 6.79 (d, 2H, $J = 8.8$ Hz), 6.96 (d, 2H, $J = 8.8$ Hz); ^{13}C NMR (CDCl$_3$) δ 20.3, 26.9, 27.2, 50.8, 63.9, 114.5, 116.1, 127.9, 129.5, 136.4, 137.7, 155.4, 156.5, 203.0; MS (EI, 70 eV) m/z 301 (M$^+$); HRMS calcd for C$_{17}$H$_{19}$NO$_2$S, 301.1136; found, 301.1144.

N-(4-Hydroxyphenyl)-N-(benzyl)-4-hydroxythiobenzamide (11e).

Deprotected according to EtSH procedure and purified by flash chromatography (35% EtOAc/hexane) to afford yellow foam (16%): ^{1}H NMR ((CDCl$_3$)) δ 5.76 (s, 2H, CH$_2$), 6.59 (d, 2H, $J = 8.4$ Hz, ArH meta RNCS), 6.61 (d, 2H, $J = 8.3$ Hz, ArH meta CSNR), 6.77 (d, 2H, $J = 8.8$ Hz, ArH ortho RNCS), 7.27 (m, 5H, Ph), 7.38 (d, 2H, $J = 6.4$ Hz, ArH ortho CSNR); MS (EI, 70 eV) m/z 335 (M$^+$); HRMS calcd for C$_{20}$H$_{17}$NO$_2$S, 335.0980; found, 335.0984.

N-(4-hydroxyphenyl)-N-(1-phenethyl)-4-hydroxythiobenz-amide (11f).

Deprotected according to BBr$_3$ procedure

and recrystallized from CHCl$_3$ to afford light yellow powder (quant): mp 174–175 °C; ^{1}H NMR (CDCl$_3$) δ 1.55 (d, 3H, $J=7.2$ Hz); 5.89 (br s, 1H); 6.27 (br s, 1H) 6.44 (d, 2H, $J=8.8$ Hz), 6.5 (br s, 1H), 6.71 (br s, 1H), 6.96 (d, 2H, $J=8.8$ Hz), 7.32 (m, 5H), 7.52 (q, 1H, $J=6.8$ Hz); MS (EI, 70 eV) m/z 349 (M$^+$); anal. (C$_{21}$H$_{19}$NO$_2$S·0.4 H$_2$O): C, 70.72; H, 5.60; N, 3.93. Found: C, 70.88; H, 5.42; N, 3.98.

N-(4-Hydroxyphenyl)-N-[2-(3-methyl)-butyl]-4-hydroxy-thiobenzamide (11g). Deprotected according to BBr$_3$ procedure and purified by flash chromatography (25% EtOAc/hexane) to afford foam (37%, two steps from carboxamide): ^{1}H NMR (CDCl$_3$) δ (major methyl rotamer) 0.95 (d, 3H, $J=6.6$ Hz), 1.14 (d, 3H, $J=6.9$ Hz), 1.21 (d, 3H, $J=6.3$ Hz), 1.82 (br m, 1H), 5.82 (quin, 1H, $J=7.4$ Hz), 6.30 (d, 2H, $J=8.5$ Hz), 6.60 (br m, 4H), 6.83 (d, 2H, $J=8.5$ Hz); ^{13}C NMR (CDCl$_3$) δ 17.1 (CH$_3$), 19.8 (CH$_3$), 20.9 (CH), 32.5 (CH), 114.7 (ArCH), 115.6 (ArCH), 128.8 (ArCH), 129.5 (ArCH), 133.2 (ArC), 137.2 (ArC), 155.2 (ArC), 155.3 (ArC), 204.4 (C=S); MS (EI, 70 eV) m/z 315 (M$^+$); anal. (C$_{18}$H$_{21}$NO$_2$S·0.8 H$_2$O): C, 65.54; H, 6.91; N, 4.35. Found: C, 65.15; H, 6.67; N, 3.91.

Triphenylphosphine-4-methoxyphenylimine (12a).[36] *p*-Anisidine was diazotized in 50% H$_2$SO$_4$ and then added to a NaN$_3$–sodium acetate buffered solution.[15] The azide was extracted with diethyl ether and the phenolic side-product removed by Na$_2$CO$_3$ wash. Concentration in vacuo afforded the crude azide which was directly used in the next step. *Ylide formation*: to an etheral solution of azide was added an equimolar solution of PPh$_3$ at rt. After the solution was heated under reflux for 2 h and N$_2$ evolution ceased, the solvent was concentrated and resulting Ph$_3$P=O oxide removed. The crude imine was passed over SiO$_2$ plug (ether) to remove additional oxide. Final concentration and tituration with hexanes afforded pure imine as orange crystals (53% from *p*-anisidine): mp 116–117.5 °C; mp[33] 119–120 °C.

Triphenylphosphine-phenylimine (12b).[14,37] A cold aqueous solution of NaNO$_2$ (1.2 equiv) was added dropwise to a solution of aniline in 10% HCl at 0–5 °C with vigorous stirring. The mixture was kept below 5 °C for 30 min, and then a solution of NaN$_3$ in water was added dropwise while the temperature was kept below 5 °C. After 1 h the reaction was warmed to rt and extracted with diethyl ether. The extracts were dried over Na$_2$SO$_4$ and concentrated to afford the crude azide[14] as an oil, which was directly used in the next step without additional purification. *Ylide formation*: same as described for 12a to afford light yellow crystals upon solvent concentration (64% from aniline): mp 128–130 °C (mp[34] 131–132 °C).

N-(1,1,1-Trifluoro-2-propylidene)-4-methoxyaniline (13a).[6] Ylide 12a and trifluoroacetone were heated to reflux in C$_6$H$_6$ for 12 h. The reaction was cooled to rt and concentrated in vacuo. The residue was triturated with Et$_2$O to remove Ph$_3$PO and the resulting filtrate concentrated followed by Kügelrohr distillation under

reduced pressure to afford product as light yellow oil (92%): bp 66 °C (0.1 mm); ^{1}H NMR (CDCl$_3$) δ 2.06 (s, 3H), 3.81 (s, 3H), 6.79, 6.92 (AA'BB', 4H, $J=8.8$, 4.0 Hz); ^{13}C NMR δ 14.6 (CH$_3$), 55.6 (CH$_3$), 114.5 (ArCH), 120.5 (q, CF$_3$, $J=273$ Hz), 121.1 (ArCH), 121.5 (ArCH), 140.5 (ArC), 157.1 (q, CCF$_3$, $J=33$ Hz), 157.6 (ArC); MS (EI, 70 eV) m/z 217 (M$^+$); anal. (C$_{10}$H$_{10}$NF$_3$O): C, 55.30; H, 4.64; N, 6.45. Found: C, 55.59; H, 4.99; N, 6.64.

N-(1,1,1-Trifluoro-2-propyl)-4-methoxyaniline (14a).[6] To a Et$_2$O solution of LiAlH$_4$ (0.5 equiv) at 0 °C was added a Et$_2$O solution of propylidene 13a dropwise over 30 min. Upon complete addition the mixture was refluxed for 2 h. The mixture was then cooled to 0 °C and quenched using a 1:1:3 work up (H$_2$O:3M NaOH:H$_2$O). The resulting mixture was decanted into a separatory funnel, the aqueous layer separated and ether layer washed with brine, dried over MgSO$_4$ and concentrated. Purification by Kügelrohr distillation provided pure amine as light red oil (64%): bp 80 °C (0.2 mm); ^{1}H NMR (CDCl$_3$) δ 1.34 (d, 3H, $J=7.0$ Hz), 3.32 (br s, 1H), 3.72 (s, 3H), 3.87 (m, 1H), 6.61 (AA'BB', 2H, $J=8.8$, 4.0 Hz), 6.77 (AA'BB', 2H, $J=8.8$, 3.5 Hz); ^{13}C NMR (CDCl$_3$) δ 15.2 (CH$_3$), 52.7 (q, CHCF$_3$, $J=30$ Hz), 55.8 (CH$_3$), 115.1 (ArCH), 115.4 (ArCH), 126.5 (q, CF$_3$, $J=280$ Hz), 140.2 (ArC), 153.2 (ArC); MS (EI, 70 eV) m/z 219 (M$^+$).

N-(1,1,1-Trifluoro-2-phenethyl)-4-methoxyaniline (14b). Prepared according to procedures outlined above from ylide 12a and trifluoroacetophenone. The imine was isolated then used directly in reduction step to afford the title compound as a light yellow oil upon distillation (69%): bp 110 °C (0.1 mm); ^{1}H NMR (CDCl$_3$) δ 3.72 (s, 3H), 4.10 (br s, 1H), 4.81 (q, 1H, $J=7.0$ Hz), 6.61 (AA'BB', 2H, $J=8.8$, 4.0 Hz), 6.75 (AA'BB', 2H, $J=8.8$, 3.5 Hz), 7.40 (m, 5H); ^{13}C NMR (CDCl$_3$) δ 55.8 (CH$_3$), 62.0 (CHCF$_3$, q, $J=30$ Hz), 115.0 (ArCH), 115.9 (ArCH), 125.5 (q, CF$_3$, $J=280$ Hz), 128.2 (ArCH), 129.1 (ArCH), 129.3 (ArCH), 134.5 (ArC), 139.7 (ArC), 153.5 (ArC); MS (EI, 70 eV) m/z 281 (M$^+$); anal. (C$_{15}$H$_{14}$NF$_3$O): C, 64.05; H, 5.02; N, 4.98. Found: C, 63.90; H, 4.84; N, 5.05.

N-(1,1,1-Trifluoro-2-phenethyl)-aniline (14c). Prepared according to procedures outlined above using ylide 12b and trifluoroacetophenone. The imine was isolated then used directly in reduction to afford the title compound as a clear oil upon distillation (59%): bp 100 °C (0.5 mm); ^{1}H NMR (CDCl$_3$) δ 4.36 (d, 1H, $J=6.5$ Hz, NH), 4.96 (quint, 1H, $J=7.0$ Hz), 6.68 (d, 2H, $J=8.0$ Hz), 6.82 (t, 1H, $J=7.0$ Hz), 7.20 (d, 2H, $J=7.0$ Hz), 7.42 (m, 3H), 7.50 (d, 2H, $J=6.5$ Hz); ^{13}C NMR (CDCl$_3$) δ 60.7 (q, CHCF$_3$, $J=29$ Hz), 114.1 (ArCH), 119.5 (ArCH), 122.5 (q, CF$_3$, $J=278$ Hz), 128.1 (ArCH), 129.2 (ArCH), 129.4 (ArCH), 129.6 (ArCH), 134.3 (ArC), 145.8 (ArC); MS (EI, 70 eV) m/z 251 (M$^+$); anal. (C$_{14}$H$_{12}$F$_3$N): C, 66.93; H, 4.81; N, 5.57. Found: C, 66.79; H, 4.80; N, 5.54.

N-[1,1,1-Trifluoro-2-(3-methoxy)-phenethyl]-aniline (14d). *2,2,2-Trifluoro-1-(3-methoxyphenyl)-ethanone precursor).*[13]

Mg turnings (1.25 g, 50 mmol), 3-methoxyphenyl bromide (9.35 g, 50 mmol), and anhydrous THF (50 mL) were gingerly heated until a vigorous reaction took place. When all the Mg turnings were dissolved the reaction mixture was cooled to 0 °C. A solution of *N*-trifluoroacetylpiperidine[35] (7.52 g, 45 mmol) in anhydrous THF (10 mL) was added to the Grignard reagent dropwise over 0.5 h with stirring at 0 °C. Upon complete addition, ice-bath was removed and the mixture stirred for 2 h. The reaction was quenched by the addition of satd aq NH_4Cl (5 mL), and the precipitates removed by filtration. The filtrate was dried over $MgSO_4$, evaporated in vacuo, and the crude ketone distilled to give 6.6 g (72%) of a colorless liquid: bp 50 °C (0.5 mm) (bp[9] 84–85 °C (12 mm).

The above prepared 2,2,2-trifluoro-1-(3-methoxyphenyl)-ethanone was then reacted with ylide **12a** as described previously. Imine isolation and LAH reduction afforded the title compound as a light green oil upon distillation (80%): bp 125 °C (0.8 mm); ^{1}H NMR (CDCl$_3$) δ 3.79 (s, 3H), 4.31 (br s, 1H), 4.87 (q, 1H, $J = 7.2$ Hz), 6.63 (d, 2H, $J = 7.6$ Hz), 6.76 (td, 1H, $J = 7.6, 0.8$ Hz), 6.89 (dd, 1H, $J = 8.5, 2.4$ Hz), 6.99 (br s, 1H), 7.03 (d, 1H, $J = 7.6$ Hz), 7.15 (m, 2H), 7.28 (t, 1H, $J = 8.0$ Hz); ^{13}C NMR (CDCl$_3$) δ 55.1 (CH$_3$), 60.3 (q, CHCF$_3$, $J = 30$ Hz), 113.8 (ArCH), 114.1 (ArCH), 119.1 (ArCH), 120.1 (ArCH), 124.9 (q, CF$_3$, $J = 281$ Hz), 128.7 (ArCH), 129.2 (ArCH), 129.8 (ArCH), 135.5 (ArC), 145.4 (ArC), 159.8 (ArC); MS (EI, 70 eV) *m/z* 281 (M$^+$); anal. (C$_{15}$H$_{14}$F$_3$NO): C, 64.05; H, 5.02; N, 4.98. Found: C, 64.15; H, 4.99; N, 4.84.

N-(4-Methoxyphenyl)-N-(1,1,1-trifluoro-2-propyl)-4-methoxybenzamide (15a).[6] Prepared according to general procedure for CF$_3$-containing anilines and purified by flash chromatography (25% EtOAc/hexane) to afford product as white powder (68%): mp 85–86 °C; ^{1}H NMR (CDCl$_3$) δ 1.21 (d, 3H, $J = 7.0$ Hz), 3.69 (s, 3H), 3.73 (s, 3H), 5.79 (sept, 1H, $J = 6.5$ Hz), 6.62 (d, 2H, $J = 8.5$ Hz), 6.75 (br s, 2H), 7.12 (br s, 2H), 7.22 (d, 2H, $J = 8.5$ Hz); ^{13}C NMR (CDCl$_3$) δ 12.5 (CH$_3$), 55.2 (CH$_3$), 55.4 (CH$_3$), 113.1 (ArCH), 114.1 (ArCH), 125.2 (q, CF$_3$, $J = 282$ Hz), 128.0 (ArC), 130.6 (ArCH), 131.7 (ArC), 159.0 (ArC), 160.6 (ArC), 171.6 (C=O); MS (EI, 70 eV) *m/z* 353 (M$^+$).

N-(4-Methoxyphenyl)-N-(1,1,1-trifluoro-2-phenethyl)-4-methoxybenzamide (15b). Prepared according to general procedure for CF$_3$-containing anilines and purified by flash chromatography (25% EtOAc/hexane) to afford product as transparent oil (77%): ^{1}H NMR (CDCl$_3$) δ 3.68 (s, 3H), 3.69 (s, 3H), 6.05 (br s, 1H), 6.42 (br s, 1H), 6.61 (d overlapping br s, 3H, $J = 8.5$ Hz) 7.04 (br q, 1H, $J_{HF} = 6.5$ Hz), 7.25 (m, 8H); ^{13}C NMR (CDCl$_3$) δ 55.1 (CH$_3$), 55.2 (CH$_3$), 58.8 (ArCHCF$_3$), 113.0 (ArCH), 113.6 (ArCH), 125.1 (q, CF$_3$, $J = 281$ Hz), 127.5 (ArC), 128.5 (ArCH), 129.0 (ArCH), 130.0 (ArCH), 130.7 (ArCH), 131.9 (ArC), 132.0 (ArCH), 132.9 (ArCH), 158.8 (ArC), 160.5 (ArC), 171.4 (C=O); MS (EI, 70 eV) *m/z* 415 (M$^+$); HRMS calcd for C$_{23}$H$_{20}$F$_3$NO$_3$, 415.1395. Found, 415.1387.

N-(4-Methoxyphenyl)-N-(1,1,1-trifluoro-2-phenethyl)-benzamide (15c). Prepared according to general procedure for CF$_3$-containing anilines and purified by flash chromatography (10% EtOAc/hexane) to afford product as light yellow oil (73%): bp 125 °C (0.3 mm); ^{1}H NMR (CDCl$_3$) δ 3.61 (s, 3H), 6.01 (br s, 1H), 6.52 (2 overlapping br s, 3H), 7.12 (m, 4H), 7.26 (m, 6H); ^{13}C NMR (CDCl$_3$) δ 55.4 (CH$_3$), 58.1 (CHCF$_3$), 113.6 (ArCH), 125.1 (q, CF$_3$, $J = 282$ Hz), 127.9 (ArCH), 128.7 (ArCH), 129.2 (ArCH), 129.6 (ArCH), 130.2 (ArCH), 131.4 (ArC), 131.9 (ArC), 132.4 (ArCH), 135.7 (ArC), 159 (ArC), 172.1 (C=O); MS (EI, 70 eV) *m/z* 385 (M$^+$); anal. (C$_{22}$H$_{18}$F$_3$NO$_2$): C, 68.57; H, 4.71; N, 3.68. Found: C, 68.22; H, 5.03; N, 3.68.

N-(4-Methoxyphenyl)-N-(1,1,1-trifluoro-2-phenethyl)-3-methoxybenzamide (15d). Prepared according to general procedure for CF$_3$-containing anilines and purified by flash chromatography (10% EtOAc/hexane) to afford product as transparent oil (79%): ^{1}H NMR (CDCl$_3$) δ 3.66 (2-s, 3H, ~1.2/1 ratio benzoyl rotamers), 3.88 (s, 3H), 6.78 (br d, 1H, $J = 8.5$ Hz), 6.8 (br s, 1H), 7.03 (q, 1H, $J = 6.5$ Hz, CHCF$_3$), 7.25 (m, 5H), 7.65 (dd, 1H, $J = 8.5, 2.3$ Hz), 7.75 (app dt, 1H, $J = 7.6, 0.8$ Hz); MS (EI, 70 eV) *m/z* 415 (M$^+$).

N-(4-Methoxyphenyl)-N-(1,1,1-trifluoro-2-phenethyl)-2-methoxybenzamide (15e). Prepared according to general procedure for CF$_3$-containing anilines and purified by flash chromatography (10% EtOAc/hexane) to afford product as transparent oil (36%, 84% corrected for recovered aniline); ^{1}H NMR (CDCl$_3$) δ 3.63 (s, 3H), 3.68 (s, 3H), 6.10 (br s, 1H), 6.43 (br s, 2H), 6.58 (d, 2H, $J = 8.5$ Hz), 6.72 (app t, 2H, $J = 8.5$ Hz), 7.21 (m, 7H); MS (EI, 70 eV) *m/z* 415 (M$^+$).

N-(Phenyl)-N-(1,1,1-trifluoro-2-phenethyl)-4-methoxybenzamide (15f). Prepared according to the general procedure for CF$_3$-containing anilines using 1,2-dichlorobenzene as solvent and purified by flash chromatography (10% EtOAc/hexane) to afford product as a transparent oil (54%): ^{1}H NMR (CDCl$_3$) δ 3.69 (s, 3H), 6.62 (d, 2H, $J = 8.5$ Hz), 7.11 (m, 3H), 7.25 (m, 9H); ^{13}C NMR (CDCl$_3$) δ 55.1 (CH$_3$), 58.5 (CHCF$_3$), 113.0 (ArCH), 125.2 (q, CF$_3$, $J = 282$ Hz), 127.3 (ArC), 127.9 (ArCH), 128.6 (ArCH), 129.0 (ArCH), 129.9 (ArCH), 130.7 (ArCH), 130.9 (ArCH), 131.9 (ArC), 139.5 (ArC), 161.0 (ArC), 171.2 (C=O); MS (EI, 70 eV) *m/z* 385 (M$^+$); anal. (C$_{23}$H$_{20}$NO$_3$F$_3$·1.1 CHCl$_3$): C, 52.95; H, 3.89; N, 2.56. Found: C, 52.84; H, 3.90; N, 2.65.

N-(Phenyl)-N-[1,1,1-trifluoro-2-(3-methoxy)-phenethyl]-4-methoxybenzamide (15g). Prepared according to general procedure for CF$_3$-containing anilines using 1,2-dichlorobenzene as solvent and purified by flash chromatography (10–25% EtOAc/hexane) to afford product as transparent oil (51%): ^{1}H NMR (CDCl$_3$) δ 3.68 (s, 3H), 3.69 (s, 3H), 6.61 (d, 2H, $J = 8.5$ Hz), 6.77 (s, 1H), 6.88 (app td, 2H, $J = 8.5, 3.5$ Hz), 7.10 (m, 5H), 7.18 (app t, $J = 8.0$ Hz), 7.26 (d, 2H, $J = 8.5$ Hz); ^{13}C NMR (CDCl$_3$) δ 55.3 (CH$_3$), 55.4 (CH$_3$), 58.7 (CHCF$_3$), 113.1

(ArCH), 115.0 (ArCH), 115.5 (ArCH), 122.5 (ArCH), 125.4 (q, CF_3, $J = 281$ Hz), 127.5 (ArC), 128.1 (ArCH), 128.7 (ArCH), 129.7 (ArCH), 130.9 (ArCH), 131.1 (ArCH), 133.3 (ArC), 139.7 (ArC), 159.6 (ArC), 160.9 (ArC), 171.4 (C=O); MS (EI, 70 eV) m/z 415 (M$^+$).

N-(4-Hydroxyphenyl)-*N*-(1,1,1-trifluoro-2-propyl)-4-hydroxybenzamide (16a).[6]
Deprotected according to BBr_3 procedure and recrystallized from EtOAc/hexane to afford white powder (62%): mp 203–205 °C (mp[6] 207–207.5 °C); ^{1}H NMR (acetone-d_6) δ 1.24 (d, 3H, $J = 6.5$ Hz), 5.78 (q, 1H, $J = 6.5$ Hz), 6.62 (d, 2H, $J = 8.8$ Hz), 6.78 (br s, 2H), 7.05 (br s, 2H), 7.18 (d, 2H, $J = 8.8$ Hz), 8.61 (s, 1H), 8.70 (s, 1H); ^{13}C NMR (acetone-d_6) δ 12.6 (CH_3), 51.3 (q, CH, $^3J_{H-F} = 30$ Hz), 114.9 (ArCH), 115.0 (ArCH), 116.2 (ArCH), 126.8 (q, CF_3, $^1J_{CF} = 282$ Hz), 128.2 (ArC), 131.4 (ArCH), 131.6 (ArC), 157.7 (ArC), 159.3 (ArC), 171.8 (C=O); MS (EI, 70 eV) m/z 325 (M$^+$); anal. ($C_{16}H_{14}NO_3F_3$): C, 59.08; H 4.34; N, 4.31. Found: C, 59.14; H, 4.37; N, 3.96.

N-(4-Hydroxyphenyl)-*N*-(1,1,1-trifluoro-2-phenethyl)-4-hydroxybenzamide (16b).
Deprotected according to BBr_3 procedure and purified by radial chromatography (25% EtOAc/hexane) to afford product as thick oil (53%): ^{1}H NMR (MeOD) δ 5.91 (br s, 1H) 6.32 (br s, 1H), 6.54 (d, 2H, $J = 8.8$ Hz), 6.62 (br s, 1H), 6.94 (q, 1H, $J_{H-F} = 9.2$ Hz), 7.13 (d, 2H, $J = 8.8$ Hz), 7.23 (m, 6H); ^{13}C NMR (MeOD) δ 60.2 (CH), 113.9 (ArCH), 114.5 (ArCH), 125.0 (q, CF_3, $J = 282$ Hz), 125.8 (ArC), 128.0 (ArCH), 128.7 (ArCH), 129.6 (ArCH) 130.0 (ArCH), 130.2 (ArC), 131.3 (ArC), 131.8 (ArC), 156.9 (ArC), 158.8 (ArC), 172.7 (C=O); MS (EI, 70 eV) m/z 387 (M$^+$); anal. ($C_{21}H_{16}F_3NO_3 \cdot 0.1$ H_2O): C, 64.81; H, 4.20; N, 3.60. Found: C, 64.68; H, 4.30; N, 3.45

N-(4-Hydroxyphenyl)-*N*-(1,1,1-trifluoro-2-phenethyl)-benzamide (16c).
Deprotected according to BBr_3 procedure and recrystallized from EtOAc/hexane to afford white powder (83%): mp 158–159 °C, ^{1}H NMR (CDCl$_3$) δ 5.91 (br s, 1H), 6.30 (br s, 1H), 6.61 (br s, 1H), 6.74 (s, 1H), 6.95 (q, 1H, $J = 8.8$ Hz), 7.24 (m, 9H); MS (EI, 70 eV) m/z 371 (M$^+$); anal. ($C_{21}H_{16}F_3NO_2$): C, 67.92; H, 4.34; N, 3.77. Found: C, 68.05; H, 4.35; N, 3.63.

N-(4-Hydroxyphenyl)-*N*-(1,1,1-trifluoro-2-phenethyl)-3-hydroxybenzamide (16d).
Deprotected according to BBr_3 procedure and recrystallized from EtOAc/hexane to afford off-white powder (77%): mp 163–164 °C; ^{1}H NMR (CDCl$_3$) δ 5.92 (br s, 1H), 6.28 (br s, 1H), 6.64 (m, 2H), 6.96 (m, 3H), 7.31 (m, 7H); MS (EI, 70 eV) m/z 387 (M$^+$); anal. ($C_{21}H_{16}NO_3F_3 \cdot H_2O$): C, 62.52; H, 4.48; N, 3.46. Found: C, 62.52; H, 4.17; N, 3.27.

N-(4-Hydroxyphenyl)-*N*-(1,1,1-trifluoro-2-phenethyl)-2-hydroxybenzamide (16e).
Deprotected according to BBr_3 procedure and recrystallized from EtOAc/hexane to afford off-white powder (59%): mp 191.5–193 °C; ^{1}H NMR (MeOD) δ 6.10 (br s, 2H), 6.59 (app q, 2H, $J = 7.6$, 7.2 Hz), 6.96 (m, 3H), 7.32 (m, 6H); MS (EI, 70 eV) m/z 387 (M$^+$); anal. ($C_{21}H_{16}F_3NO_3 \cdot 0.7$ H_2O): C, 63.06; H, 4.38; N, 3.50. Found: C, 63.04; H, 4.08; N, 3.50.

N-(Phenyl)-*N*-(1,1,1-trifluoro-2-phenethyl)-4-hydroxybenzamide (16f).
Deprotected according to BBr_3 procedure and recrystallized from EtOAc/hexane to afford off-white powder (quant): mp 114–116 °C; ^{1}H NMR (CDCl$_3$) δ 6.48 (d, 2H, $J = 8.4$ Hz), 7.0 (m, 4H) 7.15 (d, 2H, $J = 8.4$ Hz), 7.26 (d, 6H), 7.72 (s, 2H, exchange with D_2O); ^{13}C NMR (MeOD) δ 50.8 (CH), 114.9 (ArCH), 125.0 (q, CF_3, $J_{CF} = 281$ Hz), 126.3 (ArC), 128.2 (ArCH), 128.6 (ArCH), 129.3 (ArCH), 130.0 (ArCH), 130.8 (ArCH), 131.0 (ArCH), 131.6 (ArC), 139.2 (ArC), 158.2 (ArC), 172.6 (C=O); MS (EI, 70 eV) m/z 371 (M$^+$); anal. ($C_{21}H_{16}F_3NO_2 \cdot 0.5$ H_2O): C, 66.31; H, 4.50; N, 3.68. Found: C, 66.19; H, 4.27; N, 3.57.

N-(Phenyl)-*N*-(1,1,1-trifluoro-2-(3-hydroxyphenethyl))-4-hydroxybenzamide (16g).
Deprotected according to BBr_3 procedure and recrystallized from CHCl$_3$ to afford small off-white crystals (95%): mp 163–165 °C; ^{1}H NMR (CDCl$_3$) δ 6.43 (d, 2H, $J = 8.5$ Hz), 6.67 (d, 1H, $J = 8.0$ Hz), 6.82 (dd, 1H, $J = 8.5$, 2 Hz), 6.91 (s, 1H), 7.08 (m, 8H), 7.62 (s, 1H); ^{13}C NMR (CDCl$_3$) 114.9 (ArCH), 116.6 (ArCH), 117.0 (ArCH), 121.2 (ArCH), 124.6 (q, CF_3, $J = 226$ Hz), 126.1 (ArC), 128.3 (ArCH), 128.6 (ArCH), 129.8 (ArCH), 130.6 (ArCH), 132.6 (ArC), 138.8 (ArC), 156.3 (ArC), 157.8 (ArC), 173.0 (C=O); MS (EI, 70 eV) m/z 387 (M$^+$); anal. ($C_{21}H_{16}F_3NO_3$): C, 65.12; H, 4.16; N, 3.62. Found: C, 64.78; H, 4.18; N, 3.38.

N-(4-Hydroxyphenyl)-*N*-(1,1,1-trifluoro-2-propyl)-4-hydroxythiobenzamide (17a).
Deprotected according to BBr_3 procedure and recrystallized from ether to afford yellow powder (93%): ^{1}H NMR (MeOD) δ 1.33 (d, 3H, $J = 7.5$ Hz), 6.47 (d, 2H, $J = 8$ Hz), 6.58 (d, 1H, $J = 6.5$ Hz), 6.64 (d, 1H, $J = 6$ Hz), 6.79 (d, 1H, $J = 8.5$ Hz), 6.96 (d, 1H, $J = 8.0$ Hz), 7.01 (d, 3H, $J = 8.5$ Hz; ArCH *ortho* C=O and CHCF$_3$); MS (EI, 70 eV) m/z 341 (M$^+$); anal. ($C_{16}H_{14}F_3NO_2S \cdot 0.1$ H_2O): C, 56.00; H, 4.17; N, 4.08. Found: C, 55.76; H, 4.13; N, 3.74.

N-(4-Hydroxyphenyl)-*N*-(1,1,1-trifluoro-2-phenethyl)-4-hydroxythiobenzamide (17b).
Deprotected according to BBr_3 procedure and purified by chromatography (5% MeOH/CH$_2$Cl$_2$) to afford title compound as yellow foam (74%): ^{1}H NMR (CDCl$_3$) δ 5.47 (br s, 1H, OH), 5.58 (br s, 1H, OH), 5.86 (d, 1H, $J = 5.5$ Hz, ArH *ortho* to OH on aniline ring), 6.25 (d, 1H, $J = 5.5$ Hz, ArH *ortho* to OH on aniline ring), 6.36 (d, 2H, $J = 8$ Hz, ArH *ortho* to OH on benzamide ring), 6.57 (d, 1H, $J = 6$ Hz, ArH *ortho* to N–C=S), 6.93 (d, 2H, $J = 9$ Hz, ArH *ortho* to C=S), 6.98 (d, 1H, $J = 6$ Hz, ArH *ortho* to N–C=S), 8.39 (q, 1H, $J_{HF} = 9$ Hz); ^{13}C NMR (CDCl$_3$) δ 63.8 (CHCF$_3$), 114.6 (ArCH), 115.0 (ArCH), 115.5 (ArCH), 125.1 (q, $J = 163$ Hz, CF_3), 129.0 (ArCH), 129.3 (ArCH), 129.8 (ArCH), 129.9 (ArCH), 131.4 (ArC), 133.4 (ArC), 136.3 (ArC), 155.3 (ArC), 155.7 (ArC), 208.3 (C=S); MS (EI, 70 eV) m/z 403 (M$^+$); HRMS calcd for $C_{21}H_{16}F_3NO_2S$, 403.0853, found 403.0858; anal. ($C_{21}H_{16}F_3NO_2S \cdot 0.3$ H_2O): C, 61.70; H, 4.09; N, 3.43. Found: C, 61.68; H, 3.92; N, 3.25.

N-(4-Methoxyphenyl)-4-methoxyphenylacetamide (18).
To a 0 °C CH$_2$Cl$_2$ solution of *p*-anisidine (1.3 equiv) and pyridine (1.1 equiv) was added dropwise a CH$_2$Cl$_2$

solution (2 5 mL) of 4-methoxyphenylacetyl chloride (1.0 equiv). Upon complete addition (15 min) mixture was allowed to reach rt. Upon completion of the reaction, the mixture was diluted with CH_2Cl_2 folowed by product isolation (H_2O, $CuSO_4$, brine). Recrystallization from EtOAc/hexane afforded the title carboxamide as small white crystals (82%): mp 127–128 °C; ^1H NMR ($CDCl_3$) δ 3.65 (s, 2H), 3.76 (s, 3H), 3.82 (s, 3H), 6.80 (d, 2H, $J = 9.0$ Hz), 6.92 (d, 2H, $J = 8.5$ Hz), 7.07 (s, 1H), 7.23 (d, 2H, $J = 9.0$ Hz), 7.30 (d, 2H, $J = 8.5$ Hz); ^{13}C NMR ($CDCl_3$) δ 43.7 (CH_2), 55.3 (CH_3), 55.5 (CH_3), 114.1 (ArCH), 114.6 (ArCH), 121.8 (ArCH), 126.5 (ArC), 130.7 (ArCH), 130.8 (ArC), 156.5 (ArC), 159.0 (ArC), 169.7 (C=O); MS (EI, 70 eV) m/z 271 (M$^+$); anal. ($C_{16}H_{17}NO_3$): C, 70.83; H, 6.32; N, 5.16. Found: C, 70.87; H, 6.29; N, 5.29.

N-(4-Methoxyphenyl)-*N*-(ethyl)-4-methoxyphenylacetamide (19).

Prepared according to phase transfer catalysis conditions described above for carboxamides. Purification by either Kügelrohr distillation or flash chromatography (25% EtOAc/hexane) afforded product as red–orange oil (quant): bp 150 °C (0.2 mm); ^1H NMR ($CDCl_3$) δ 1.08 (t, 3H, $J = 7.0$ Hz), 3.33 (s, 2H), 3.70 (q, 2H, $J = 7.1$ Hz), 3.78 (s, 3H), 3.84 (s, 3H), 6.77 (d, 2H, $J = 8.5$ Hz), 6.79 (d, 2H, $J = 8.5$ Hz), 6.97 (d overlapping, 2H, $J = 8.5$ Hz), 6.98 (d overlapping, 2H, $J = 8.5$ Hz); ^{13}C NMR ($CDCl_3$) δ 13.2 (CH_3), 40.5 (CH_2), 44.4 (CH_2), 55.4 (CH_3O), 55.7 (CH_3O), 113.9 (ArCH), 114.8 (ArCH), 127.9 (ArC), 129.9 (ArCH), 130.2 (ArCH), 135.2 (ArC), 158.4 (ArC), 159.2 (ArC), 171.2 (C=O); MS (EI, 70 eV) m/z 299 (M$^+$); anal. ($C_{18}H_{21}NO_3 \cdot 0.1$ $CHCl_3$): C, 69.83; H, 6.83; N, 4.50. Found: C, 69.82; H, 6.98; N, 3.98.

N-(4-Methoxyphenyl)-*N*-(ethyl)-α-ethyl-4-methoxyphenylacetamide (20a).

n-BuLi in hexane (1.56 M, 2.0 equiv) was added dropwise to a −78 °C THF (*i*-propyl)$_2$NH (2.2 equiv) solution, then warmed to 0 °C. After 0.5 h at 0 °C the mixture was re-cooled to −78 °C and a THF solution of acetamide **19** (1.0 equiv) added dropwise. After 20 min EtI (1.3 equiv) was added in one portion and the mixture allowed to reach rt. Product isolation (H_2O, Et_2O, Na_2SO_4) and purification by flash chromatography (25% EtOAc/hexane) as light yellow oil (95%): ^1H NMR ($CDCl_3$) δ 0.78 (t, 3H, $J = 7.5$ Hz, CH_3 α-ethylacetamide), 1.05 (t, 3H, $J = 7.0$ Hz, CH_3 *N*-ethyl), 1.60 (dquint, 1H, $J = 14.0$, 7.0 Hz, α-CH_2), 2.04 (dquint, 1H, $J = 14.0$, 7.0 Hz, α-CH_2), 3.27 (dd, 1H, $J = 8.5$, 7.0 Hz, CH α-benzylic), 3.67 (m, 2H, -NCH_2CH_3), 3.77 (s, 3H), 3.85 (s, 3H), 6.75 (d, 2H, $J = 8.8$ Hz), 6.87 (br s, 4H), 6.98 (d, 2H, $J = 8.8$ Hz); ^{13}C NMR ($CDCl_3$) δ 12.5 (CH_3), 13.1 (CH_3), 28.5 (CH_2), 44.3 (CH_2), 55.2 (CH_3), 55.6 (CH_3), 113.7 (ArCH), 114.5 (ArCH), 129.2 (ArCH), 132.9 (ArC), 135.0 (ArC), 158.4 (ArC), 159.0 (ArC), 173.5 (C=O); MS (EI, 70 eV) m/z 327 (M$^+$); anal. ($C_{20}H_{25}NO_3$): C, 73.37; H, 7.70; N, 4.28. Found: C, 72.84; H, 7.56; N, 3.59.

N-(4-Methoxyphenyl)-*N*-(ethyl)-α-benzyl-4-methoxyphenylacetamide (20b).

Preparation as described in **20a** and purification by flash chromatography (15% EtOAc/hexane) afforded title compound as an oil (86%): ^1H

NMR ($CDCl_3$) δ 0.94 (t, 3H, $J = 7.2$ Hz, NCH_2CH_3), 2.75 (dd, 1H, $J = 12.8$, 4.8 Hz, methine H), 3.43 (m, 2H, NCH_2CH_3), 3.58 (dd, 1H, $J = 10.2$, 5.1 Hz), 3.70 (dd, 1H, $J = 13.3$, 7.1 Hz) 3.76 (s, 3H), 3.79 (s, 3H), 6.15 (br s, 1H), 6.75 (d, 2H, $J = 8.3$ Hz), 6.78 (d, 2H, $J = 6.7$ Hz), 7.09 (m, 4H), 7.24 (m, 3H); ^{13}C NMR ($CDCl_3$) δ 12.8 (CH_3), 41.5 (CH_2), 44.2 (CH_2), 50.3 (CH), 55.2 (OCH_3), 55.4 (OCH_3), 113.7 (ArCH), 114.3 (ArCH), 126.2 (ArCH), 128.2 (ArCH), 129.1 (ArCH), 129.4 (ArCH), 130.0 (ArCH), 132.4 (ArC), 134.6 (ArC), 140.1 (ArC), 158.5 (ArC), 158.9 (ArC), 172.5 (C=O); MS (EI, 70 eV) m/z 389 (M$^+$).

N-(4-Hydroxyphenyl)-*N*-(ethyl)-4-hydroxyphenylacetamide (21a).

Deprotected according to BBr_3 procedure and purified by chromatography (50% EtOAc/hexane) to afford tan foam (quant): mp 75 °C dec.; ^1H NMR ((CD_3)$_2$SO) δ 0.96 (t, 3H, $J = 7.5$ Hz), 3.16 (s, 2H), 3.36 (q, 2H, $J = 7.5$ Hz), 6.59 (d, 2H, $J = 8.5$ Hz), 6.78 (m, 4H), 6.97 (d, 2H, $J = 8.5$ Hz), 9.18 (br s, 1H), 9.62 (br s, 1H); MS (EI, 70 eV) m/z 271 (M$^+$); anal. ($C_{16}H_{17}$ $NO_3 \cdot 0.9$ H_2O): C, 66.84; H, 6.59; N, 4.87. Found: C, 66.95; H, 6.20; N, 4.77.

N-(4-Hydroxyphenyl)-*N*-(ethyl)-4-hydroxyphenylthioacetamide (21b).

Deprotected according to BBr_3 procedure and purified by chromatography (50% EtOAc/hexane) to afford tan powder (84%): mp 156–157 °C; ^1H NMR ((CD_3)$_2$SO) δ 1.08 (t, 3H, $J = 7.0$ Hz), 3.67 (s, 2H), 4.14 (q, 2H, $J = 2$ Hz), 6.54 (d, 2H, $J = 8.5$ Hz), 6.75 (app t, 4H, $J = 8.0$ Hz), 6.87 (d, 2H, $J = 8.5$ Hz), 9.17 (s, OH), 9.78 (s, OH); MS (EI, 70 eV) m/z 287 (M$^+$); HRMS calcd for $C_{16}H_{17}NO_2S$, 287.0980; found, 287.0977; anal. ($C_{16}H_{17}NO_2S \cdot 0.2H_2O$): C, 66.04; H, 6.03; N, 4.81. Found: C, 65.97; H, 6.03; N, 4.78.

N-(4-Hydroxyphenyl)-*N*-(ethyl)-α-ethyl-4-hydroxyphenylacetamide (22a).

Deprotected according to BBr_3 procedure and purified by chromatography (50% EtOAc/hexane) to afford white foam (70%): ^1H NMR ($CDCl_3$) δ 0.76 (t, 3H, $J = 7.5$ Hz), 1.04 (t, 3H, $J = 7.0$ Hz), 1.54 (m, 1H, CH_2 β-amide), 1.94 (m, 1H, CH_2 β-amide), 3.27 (t, 1H, $J = 7.0$ Hz, CH α-amide), 3.62 (m, 2H, -NCH_2CH_3), 6.63 (d, 2H, $J = 8.8$ Hz), 6.79 (d, overlapping br s, 2H, $J = 8.8$ Hz), 7.05 (br s, 4H); ^{13}C NMR ($CDCl_3$) δ 12.5 (CH_3), 13.0 (CH_3), 28.2 (CH_2), 44.8 (CH_2), 50.7 (CH), 116.1 (ArCH), 128.6 (ArCH), 129.3 (ArCH), 131.7 (ArCH), 133.7 (ArC), 155.4 (ArC), 156.8 (ArC), 174.7 (C=O); MS (EI, 70 eV) m/z 299 (M$^+$); HRMS calcd for $C_{18}H_{21}NO_3$, 299.1521, found 299.1520.

N-(4-Hydroxyphenyl)-*N*-(ethyl)-α-ethyl-4-hydroxyphenylthioacetamide (22b).

Deprotected according to BBr_3 procedure and purified by chromatography (25% EtOAc/hexane) to afford yellow residue (95%): ^1H NMR (MeOD) δ 0.73 (t, 3H, $J = 7.3$ Hz), 1.14 (t, 3H, $J = 7.2$ Hz), 1.76 (m, 1H, CH_2 β-amide), 2.17 (m, 1H, CH_2 β-amide), 3.62 (dd, 1H, $J = 7.8$, 7.0 Hz, CH α-amide), 4.16 (m, 1H, CH_2 α-NCO), 4.30 (m, 1H, CH_2 α-NCO), 6.56 (dd, 1H, $J = 8.4$, 2.6 Hz), 6.56 (AA'BB', 2H, $J = 8.7$, 2.3 Hz), 6.75 (dd, 1H, $J = 8.4$, 2.8 Hz), 6.91 (dd, 1H, $J = 8.6$, 2.7 Hz), 6.94 (AA'BB', 2H, $J = 8.5$, 1.9 Hz),

7.0 (dd, 1H, $J = 8.7$, 2.8 Hz); ^{13}C NMR (CDCl$_3$) δ 11.4 (CH$_3$), 12.6 (CH$_3$), 13.9 (CH$_2$), 52.3 (CH$_2$), 56.2 (CH), 115.0 (ArCH), 116.3 (ArCH), 128.5 (ArCH), 129.1 (ArCH), 129.9 (ArCH), 133.5 (ArC), 136.5 (ArC), 154.6 (ArC), 155.9 (ArC), 207.5 (C=S); MS (EI, 70 eV) m/z 315 (M$^+$); HRMS calcd for C$_{18}$H$_{21}$NO$_2$S, 315.1293; found, 315.1301.

N-(4-Hydroxyphenyl)-N-(ethyl)-α-benzyl-4-hydroxyphenylthioacetamide (22c). Deprotected according to BBr$_3$ procedure and purified by chromatography (15% EtOAc/hexane) to afford yellow residue (47%): ^{1}H NMR (MeOD) δ 1.05 (t, 3H, $J = 7.2$ Hz), 2.90 (dd, 1H, $J = 12.9$, 4.9 Hz, PhCH$_2$), 3.66 (dd, 1H, $J = 12.9$, 9.5 Hz, PhCH$_2$), 3.95 (m, 1H, CH$_3$CH$_2$), 4.05 (dd, 1H, $J = 9.3$, 5.2 Hz, PhCH$_2$CH-), 4.30 (m, 1H, CH$_3$CH$_2$), 6.02 (dd, 1H, $J = 8.4$, 2.7 Hz), 6.56 (d, 2H, $J = 8.3$ Hz), 6.66 (overlapping dds, 2H, $J = 9.2$, 3.1 Hz), 6.75 (dd, 1H, $J = 8.8$, 3.0 Hz), 7.00 (d, 2H, $J = 8.7$ Hz), 7.10 (m, 5H); HRMS calcd for C$_{23}$H$_{23}$NSO$_2$, 377.1449; found, 377.1443.

N-(4-Methoxyphenyl)-N-(1,1,1-trifluoro-2-propyl)-4-methoxyphenylacetamide (25). Prepared according to general amidation procedure for CF$_3$-containing anilines; product isolation and purification via flash chromatography (25% EtOAc/hexane) afforded title compound as light yellow oil (40%): ^{1}H NMR (CDCl$_3$) δ 1.16 (d, 3H, $J = 7$ Hz), 3.32 (s, 2H), 3.76 (s, 3H), 3.84 (s, 3H), 5.61 (sept, 1H, $J = 7.6$ Hz), 6.77 (d, 2H, $J = 8.9$ Hz), 6.90 (m, 3H), 6.92 (d, 2H, $J = 8.9$ Hz), 7.06 (m, 1H); ^{13}C NMR (CDCl$_3$) δ 12.5 (CH$_3$), 40.7 (CH$_2$), 50.1 (q, CHCF$_3$, $J = 31$ Hz), 55.3 (CH$_3$O), 55.6 (CH$_3$O), 113.9 (ArCH), 114.3 (ArCH), 114.6 (ArCH), 125.1 (q, CF$_3$, $J = 283$ Hz), 127.0 (ArC), 129.9 (ArC), 130.2 (ArCH), 132.0 (ArCH), 158.6 (ArC), 159.9 (ArC), 172.8 (C=O); HRMS calcd for C$_{19}$H$_{20}$NF$_3$O$_3$, 367.1395, found, 367.1394; anal. (C$_{19}$H$_{20}$NF$_3$O$_3$): C, 62.12; H, 5.49; N, 3.81. Found: C, 61.76; H, 5.58; N, 3.66.

N-(4-Methoxyphenyl)-N-(1,1,1-trifluoro-2-propyl)-α-methyl-4-methoxyphenylacetamide (26). n-BuLi in hexane (1.56 M, 2.0 equiv) was added dropwise to a −78 °C THF (i-propyl)$_2$NH (2.2 equiv) solution, then warmed to 0 °C. After 0.5 h at 0 °C the mixture was re-cooled to −78 °C and a THF solution of N-(1,1,1-trifluoro-2-propyl) substituted acetamide **25** (1.0 equiv) was added dropwise. After 20 min MeI (1.3 equiv) was added in one portion and the mixture allowed to reach rt. Crude product isolation (H$_2$O, Et$_2$O, Na$_2$SO$_4$) afforded an amber oil (83%) which was determined by both ^{1}H NMR and HPLC to be an approx. 1:1 ratio of diastereomers for the expected product: ^{1}H NMR (CDCl$_3$) δ 1.05 (2-ds, 3H, $J = 7.5$ Hz), 1.28 (2-ds, 3H, $J = 7.5$ Hz), 3.42 (overlapping qs, 1H, $J = 7.5$ Hz), 5.58 (m, 1H, CHCF$_3$), 6.44 (2-dds, 1H, $J = 8.8$, 2.8 Hz), 6.68 (dd, 0.5 H, $J = 8.8$, 2.8 Hz), 6.70 (m, 2.5H), 6.81 (m, 2H), 7.01 (2-dds, 1H, $J = 8.4$, 2.3 Hz), 7.20 (2-dds, 1H, $J = 8.4$, 2.3 Hz); HPLC (254 nm) 25% EtOAc/hexane, Micropac SiO$_2$ column: 5.82 min. (46.2%), 7.19 min. (53.7%), sd ±5%.

N-(4-Hydroxyphenyl)-N-(1,1,1-trifluoro-2-propyl)-α-methyl-4-hydroxyphenylacetamide (27). Deprotection using BBr$_3$ procedure and chromatography (35% EtOAc/hexane) afforded title compound as a white powder (95%) with a 1:1 ratio of diastereomers as found by ^{1}H NMR: mp 165–170 °C; ^{1}H NMR (MeOD) δ 1.10 (overlapping ds, 3H, $J = 7.5$ Hz), 1.25 (overlapping ds, 3H, $J = 7.5$ Hz), 3.49 (overlapping qs, 1H, $J = 7.5$ Hz), 5.52 (m, 1H, CHCF$_3$), 6.43 (2-dds, 1H, $J = 8.8$, 2.8 Hz), 6.57 (dd, 0.5H, $J = 8.8$, 2.8 Hz), 6.64 (m, 2.5H), 6.72 (m, 2.5H), 6.86 (app td, 1H, $J = 8.4$, 2.3 Hz), 7.07 (2-dds, 1H, $J = 8.4$, 2.3 Hz); MS (EI, 70 eV) m/z 353 (M$^+$); HRMS calcd for C$_{18}$H$_{18}$NF$_3$O$_3$, 353.1238; found, 353.1235.

N-(4-Hydroxyphenyl)-N-(1,1,1-trifluoro-2-propyl)-4-hydroxyphenylthioacetamide (28). Carboxamide **25** (0.3 mmol, 100 mg) was treated with Lawesson's reagent as outlined in general procedure. Product isolation (H$_2$O, Et$_2$O, Na$_2$SO$_4$) and radial chromatography (20% EtOAc/hexane) afforded 5 mg of protected thiocarboxamide in low yield (5%). Subsequent deprotection using BBr$_3$ procedure afforded the title compound as a light yellow residue upon SiO$_2$ purification (30% EtOAc/hexane, quant): ^{1}H NMR (MeOD) δ 1.24 (d and m, 3H, $J = 7.8$ Hz), 3.85 (ABq, 2H, $J = 13$ Hz), 5.56 (sept, 1H, $J = 7.8$ Hz), 6.72 (m, 4H), 6.85 (m, 4H); HPLC: Whatman C18 column, 90%MeOH:10%H$_2$O R$_t$ = 3.123 > 98% pure at 254 nm.

Acknowledgements

References and Notes

1. Katzenellenbogen, J. A.; O'Malley, B. W.; Katzenellenbogen, B. S. Mol. Endocrinol. **1996**, 10, 119.

2. Grese, T. A.; Dodge, J. A. Curr. Pharm. Des. **1998**, 4, 71.

3. Gao, H.; Katzenellenbogen, J. A.; Garg, R.; Hansch, C. Chem. Rev. **1999**, 99, 723.

4. Palkowitz, A. D.; Glasebrook, A. L.; Thrasher, K. J.; Hauser, K. L.; Short, L. L.; Phillips, D. L.; Muehl, B. S.; Sato, M.; Shetler, P. K.; Cullinan, G. J.; Pelt, T. R.; Bryant, H. U. J. Med. Chem. **1997**, 40, 1407.

5. Fink, B. E.; Mortsensen, D. S.; Stauffer, S. R.; Aron, Z. D.; Katzenellenbogen, J. A. *Chem. Biol.* **1999**, *6*, 205.

6. Hartmann, R. W.; vom Orde, H.-D.; Heindl, A.; Schönenberger, H. *Arch. Pharm.* **1988**, *321*, 497.

7. Hartmann, R. W.; vom Orde, H.-D.; Schönenberger, H. *Arch. Pharm.* **1990**, *323*, 73.

8. Osawa, Y. *Nippon Kagaku Zasshi* **1963**, *84*, 137.

9. Zwierzak, A.; Gajda, T. *Synthetic, Communications* **1981**, 1005.

10. Diéz-Barra, E.; Loupy, A.; Sansoulet, J.; Carrillo, J. *Synthetic Communications* **1992**, *22*, 1661.

11. Tomioka, K.; Inoue, I.; Shindo, M.; Koga, K. *Tetrahedron Lett.* **1991**, *32*, 3095.

12. Scheibye, S.; Pedersen, B. S.; Lawesson, S.-O. *Bull. Soc. Chim. Belg.* **1978**, *87*, 229.

13. Hatanaka, Y.; Hashimoto, M.; Kurihara, H.; Nakayama, H.; Kanaoka, Y. *J. Org. Chem.* **1994**, *59*, 383.

14. Tanno, M.; Sueyoshi, S.; Kamiya, S. *Chem. Pharm. Bull* **1982**, *30*, 3125.

15. Dyall, L. K.; Suffolk, P. M.; Dehaen, W.; L'abbe, G. *J. Chem. Soc. Perkin Trans. 2* **1994**, 2115.

16. Stewart, W. E.; Siddall III, T. H. *Chem. Rev.* **1970**, *70*, 517.

17. Bourn, A. J. R.; Gillies, D. G.; Randall, E. W. *Tetrahedron* **1966**, *22*, 3132.

18. Wiberg, K. B.; Breneman, C. L. *J. Am. Chem. Soc.* **1992**, *117*, 831.

19. Lauvergnat, D.; Hiberty, P. C. *J. Am. Chem. Soc.* **1997**, *119*, 9478.

20. Hadad, C. M.; Rablen, P. R.; Wiberg, K. B. *J. Org. Chem.* **1998**, *63*, 8668.

21. Neugebauer Crawford, S. M.; Taha, A. N.; True. N. S.; LeMaster, C. B. *J. Phys. Chem. A* **1997**, *101*, 4699.

22. Laidig, K. E.; Cameron, L. M. *J. Am. Chem. Soc.* **1996**, *118*, 1737.

23. Minick, D.; Frenz, J.; Patrick, M.; Brent, D. *J. Med. Chem.* **1988**, *31*, 1923.

24. Erber, S.; Ringshandl, R.; von Angerer, E. *Anti-Cancer Drug Des.* **1991**, *6*, 414.

25. von Angerer, E.; Erber, S. *J. Steroid. Biochem. Mol. Biol.* **1992**, *41*, 557.

26. Brzozowski, A. M.; Pike, A. C.; Dauter, Z.; Hubbard, R. E.; Bonn, T.; Engstrom, O.; Öhman, L.; Greene, G. L.; Gustafsson, J.-A.; Carlquist, M. *Nature* **1997**, *389*, 753.

27. O'Hagan, D., Rzepa, H. S. *Chem. Commun.* **1997**, 645.

28. Anstead, G. M.; Wilson, S. R.; Katzenellenbogen, J. A. *J. Med. Chem.* **1989**, *32*, 2163.

29. Shiau, A. K.; Barstad, D.; Loria, P. M.; Cheng, L.; Kushner, P. J.; Agard, D. A.; Greene, G. L. *Cell* **1998**, *95*, 927.

30. Anstead, G. M.; Peterson, C. S.; Katzenellenbogen, J. A. *J. Steroid Biochem.* **1989**, *33*, 877.

31. Sun, J.; Meyers, M. J.; Fink, B. E.; Rajendran, R.; Katzenellenbogen, J. A.; Katzenellenbogen, B. S. *Endocrinology* **1999**, *140*, 800.

32. Katzenellenbogen, J. A.; Johnson, Jr., H. J.; Myers, H. N. *Biochemistry* **1973**, *12*, 4085.

33. Carlson, K. E.; Choi, I.; Gee, A.; Katzenellenbogen, B. S.; Katzenellenbogen, J. A. *Biochemistry* **1997**, *36*, 14897.

34. Williams, D.; Gorski, J. *Biochem.* **1974**, *13*, 5537.

35. Chapman: Fidler *J. Chem. Soc.* **1936**, 448.

36. Johnson, A. W.; Wong, S. C. K. *Can. J. Chem.* **1966**, *44*, 2793.

37. Staudinger, H.; Meyer, J. *Helv. Chim. Acta* **1919**, *2*, 643.

Solid-Phase Synthesis of Tetrasubstituted Pyrazoles, Novel Ligands for the Estrogen Receptor

Shaun R. Stauffer and John A. Katzenellenbogen

Department of Chemistry, University of Illinois,
Urbana, Illinois 61801

JOURNAL OF

combinatorial

CHEMISTRY

Solid-Phase Synthesis of Tetrasubstituted Pyrazoles, Novel Ligands for the Estrogen Receptor

Shaun R. Stauffer and John A. Katzenellenbogen*

Department of Chemistry, University of Illinois, Urbana, Illinois 61801

Received January 11, 2000

Most ligands for the estrogen receptor (ER) are not well suited for synthesis by combinatorial means, because their construction involves a series of carbon—carbon bond forming reactions that are not uniformly high yielding. In previous work directed to overcoming this limitation, we surveyed various phenol-substituted five-membered heterocycles, hoping to find a system that would afford both high ER binding affinity and whose synthesis could be adapted to solid-phase methods (Fink et al. *Chem. Biol.* **1999**, *6*, 206—219.) In this report, we have developed a reliable and efficient solid-phase method to prepare the best of these heterocycles, the tetrasubstituted pyrazoles, and we have used this methodology to produce small, discrete libraries of these novel ER ligands. We used a combination of FT-IR and nanoprobe ^{1}H NMR-MAS to characterize intermediates leading up to the final pyrazole products directly on the bead. We also developed a scavenging resin, which enabled us to obtain products free from inorganic contaminants. We prepared a 12-member test library, and then a 96-member library, and in both cases we determined product purity and ER binding affinity of all of the library members. Several interesting binding affinity patterns have emerged from these studies, and they have provided us with new directions for further exploration, which has led to pyrazoles having high affinity and potency as agonists and antagonists toward the ERα subtype.

Introduction

In recent years, combinatorial chemistry, with its ability to generate a large set of structurally related analogues, has become a bona fide tool for increasing productivity in the functional assessment of compound libraries and the rapid development of structure—activity relationships.[1] Combinatorial techniques for preparing peptide libraries are well established, but methods for the combinatorial synthesis of small-molecule libraries for the development of useful pharmaceuticals remains a formidable challenge. Small molecules are generally not oligomeric, and a diverse range of chemical transformations may be required for their synthesis. Therefore, the development of an appropriate parallel synthesis format is not always straightforward. This limitation is increasingly encountered in the quest for chemical diversity, because the fidelity of a given library member can be compromised when the building block components are not uniformly reactive. Consequently, there has been an active quest to develop the sort of truly general, high yielding transformations necessary to maintain high quality in the preparation of small-molecule libraries.

Novel estrogens having tissue selective action suitable for menopausal hormone replacement or the treatment and prevention of breast cancer are actively being sought by the pharmaceutical industry.[2] These agents, often referred to as selective estrogen receptor modifiers or SERMs, generally consist of a nonsteroidal core structure onto which is
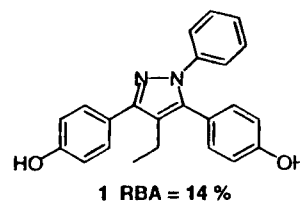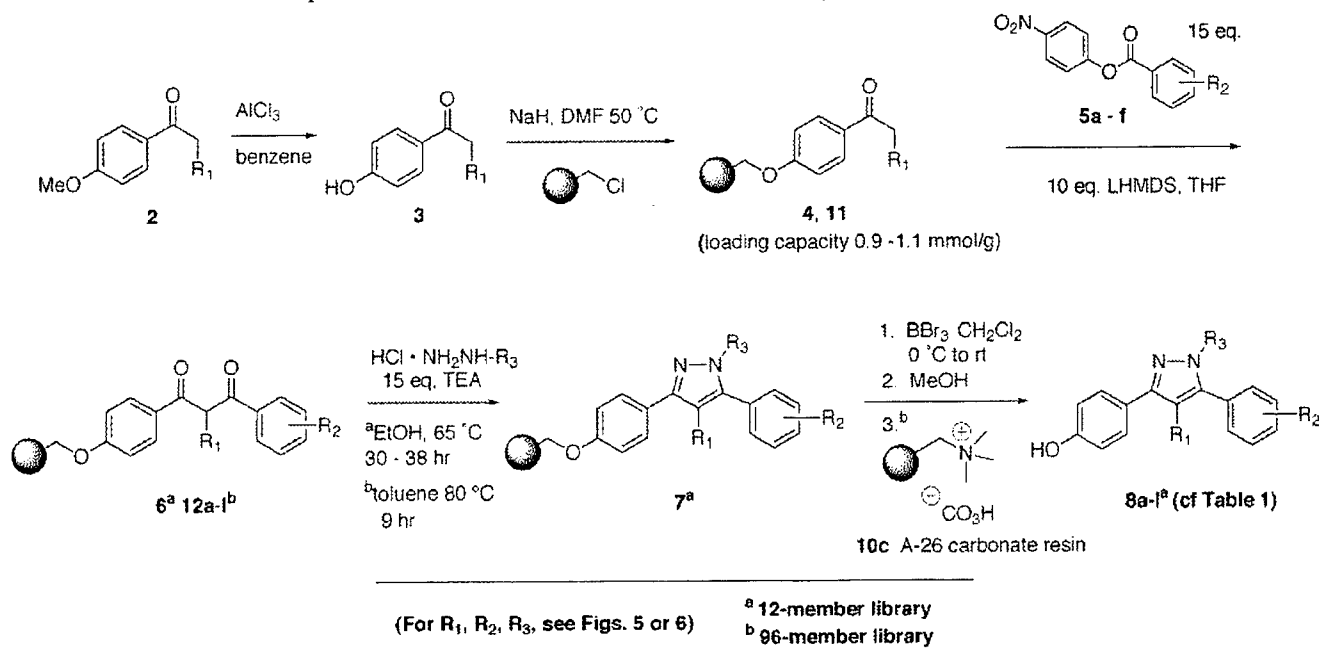

Figure 1. Estrogen receptor-α selective pyrazole discovered from a solution-phase study. RBA is relative binding affinity for the estrogen receptor; for estradiol, RBA = 100%.

appended a basic or polar function.[3] Most ligands for the estrogen receptor (ER), however, are not well suited for synthesis by combinatorial means, because their construction generally involves a series of carbon—carbon bond forming reactions that are not uniformly high yielding, nor necessarily easily adaptable to solid-phase synthesis methods. Two small combinatorial libraries of nonsteroidal ER ligands have been reported,[4,5] but these efforts produced either low affinity ligands or ones of limited structural diversity.

To circumvent these current limitations and to expand the possible combinatorial approaches to ER ligands, we have proposed a novel modular ER pharmacophore consisting of a *variable* core structure, onto which are linked four independent substituents of defined variability. Using this paradigm, we have investigated core structures consisting of five-membered heterocycles, as well as other functionalities.[6] Among the five-membered systems that we have studied to date, we found that 1,3,5-triaryl-4-alkyl-pyrazoles, such as compound **1** (Figure 1), showed high binding affinity for the estrogen receptor, and intriguingly this compound had 100-fold higher potency as an agonist in a cell-based transcription assay through ERα than through ERβ.[7] Com-

Scheme 1. Routes for the Preparation of the 12-Member and the 96-Member Pyrazole Libraries

(For R_1, R_2, R_3, see Figs. 5 or 6)

[a] 12-member library
[b] 96-member library

Results and Discussion

pounds that show high ER subtype selectivity are in great demand as agents to define the biological roles of these subtypes[8] and as potential tissue-selective estrogens for the uses noted above.

Because of these interesting initial findings, we wished to use a combinatorial approach to explore this pyrazole template further, to gain a better understanding of its structure—binding affinity pattern with the ER and to discover additional compounds with ER subtype selectivity. In particular, we hoped that such an expanded study would enable us to determine the preferred binding orientation for these pyrazoles in the ER, an issue that was not settled by our initial investigations.[6] We required this information to guide our future placement of pharmacophore elements in the design of selective antiestrogens (Stauffer, S. R., Huang, Y., Aron, Z., Coletta, C. J., Sun, J., Katzenellenbogen, B. S., Katzenellenbogen, J. A., unpublished).

As we had noted in their original conception,[6] the tetrasubstituted pyrazoles offer an attractive template for the combinatorial development of ligands for the estrogen receptor. Their heterocyclic nucleus provides a core upon which several common substructural motifs found in high affinity ER ligands can adequately be displayed in several possible configurations, and their synthesis involves simple condensation reactions, some of which have already been demonstrated on solid phase, although mostly for trisubstituted pyrazole derivatives.[9-12]

This work describes our efforts in the design and preparation of libraries of tetrasubstituted pyrazoles as ER ligands and our evaluation of the binding affinities of the library members. These studies have led us to a new series of high affinity compounds that display very high ERα agonist selectivity in cell-based transactivation assays, the details of which will be reported elsewhere (Stauffer, S. R., Sun, J., Katzenellenbogen, B. S., Coletta, C. J., Katzenellenbogen, J. A., unpublished).

Library Strategy. It was our intention to prepare discrete analogues (96-member libraries) of our tetrasubstituted pyrazole pharmacophore, noted above, in a parallel split-split format to produce material for ER binding affinity assays. Synthetically, the classical 1,3-dione-hydrazine condensation route (illustrated in Scheme 1) seemed attractive, because it is well precedented and can be accomplished under conditions that are potentially adaptable to solid-phase synthesis.[6] Also, the β-diketone component can be readily generated from a crossed-Claisen condensation reaction.

Using this route, we can introduce molecular diversity in the target pyrazole in either the alkylphenone, the ester, or the hydrazine component. Our choice to introduce the C-4 alkyl group early on within the ketone, rather than by alkylating the β-diketone intermediate, was based on solution feasibility studies; in contrast to the pyrazole synthesis strategy reported by Marzinzik and Felder,[9] we found that alkylation was not general for the preparation of 1,3-diaryl-propane-1,3-diones. Our approach is also attractive because many of the 4'-methoxy-alkylphenone precursors are commercially available or can be produced in one step via Friedel—Crafts acylation reactions.

Linker. We selected the phenol component as the site for attachment of the pyrazole to the polymer support because it is convenient and it is the one functional group that is present in all of the pyrazoles. Merrifield's resin was used as the solid support, so the tethered phenol became attached to the resin as a *p*-substituted benzyl ether.

Our overall linker strategy is advantageous for two reasons: First, we knew from solution studies for tetrasubstituted pyrazoles of this type that a robust linker would be required to withstand the conditions for pyrazole formation (DMF/THF 120 °C).[6] Thus, we expected that the stable benzyl ether link would be more satisfactory than other more labile linkers. Second, we anticipated that the strong acidic
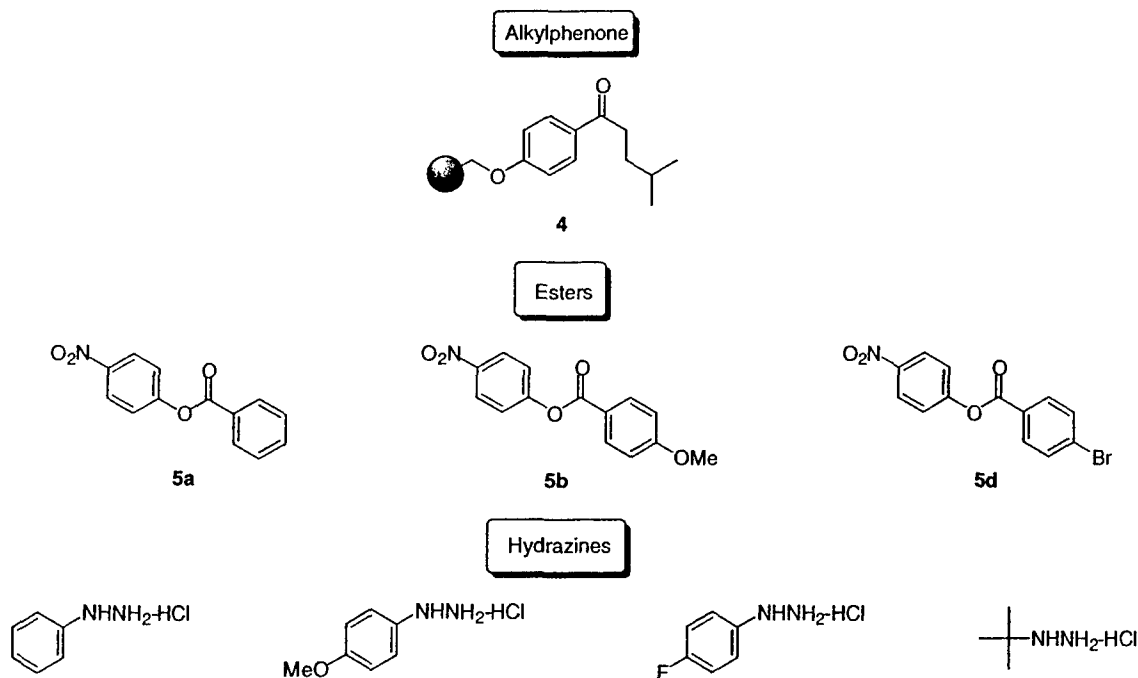
Figure 2. Components for 12-member library.

conditions required for product cleavage from the resin (i.e., BBr₃) could be adjusted to cleave, as well, any methyl ethers protecting other phenolic components. This approach is similar to that reported by Green for the preparation of lavendustin analogues,[13] but different in that our linker is a benzyl ether rather than a benzyl ester.

Method Development. The adaptation of the pyrazole synthesis from solution phase to solid phase required extensive optimization and later modification. Our initial route is shown in Scheme 1, and it was used for the preparation a small 12-member library, which was intended to serve as a standard for later, larger library design. In addition, this smaller library was developed to evaluate the generality of the reaction conditions by using various electronically demanding building blocks (Figure 2). The conditions described below were initially developed using our original lead compound **1** as a model.

Few starting alkylphenones (**2**, Scheme 1) are available commercially, but they were readily prepared via Friedel–Crafts acylation, using anisole and the desired acid chloride. Thus, the protected *p*-methoxy-alkylphenone **2** was obtained and then demethylated using AlCl₃ to afford **3**, which was subsequently loaded onto Merrifield's resin (Novabiochem Inc., 1.39 mmol/g), according to the method of Ellman and co-workers.[14] Formation of the resin-bound ketone **4** was ascertained using standard techniques (FT-IR, null %Cl combustion analysis), and a portion was cleaved with BF₃–SMe₂ to determine the loading capacity based on mass recovery. After minimal workup, the expected ketone was cleanly observed by ¹H NMR and HPLC (purity >99%), and the loading capacity was found to be between 0.9 and 1.1 mmol/g.

Following ketone immobilization, we used a crossed-Claisen condensation reaction to form the requisite β-diketones (**6**). This transformation proceeds satisfactorily using excess lithium hexamethyldisilazide (LHMDS) and activated

p-nitrophenyl esters (**5a,b,d**) in THF. Other bases, such as NaNH₂ or KOt-Bu, were less effective, particularly with higher alkylphenones (e.g., propiophenone and higher). In addition, *p*-nitrophenyl activated esters proved to be most general in providing high yields of the dione. In most cases, the active ester could be present in the reaction vessel during the addition of base. However, esters with electron withdrawing groups, such as compound **5d** (Figure 2), required preformation of the resin-bound enolate prior to the addition of the ester, because of competing nucleophilic addition of the disilamide anion to the activated ester.

We found nanoprobe ¹H NMR-MAS to be an indispensable tool for following β-dione formation on solid-phase and for optimizing reaction conditions. Although FT-IR was useful for monitoring ketone immobilization, we did not find it satisfactory for evaluating the progress of dione formation. We had expected that a shift in the C=O stretch of the alkylphenone at 1675 cm⁻¹ would occur as the dione formed and equilibrated with its intramolecularly hydrogen bonded enol tautomer. We were surprised, however, when the ¹H NMR spectrum of 1,3-bis(4-methoxyphenyl)-2-ethyl-1,3-propanedione showed that these α-substituted β-diketones exist exclusively in the diketo tautomeric form in solution. We presume that this is due to the A-strain present in these substituted molecules, because ¹H NMR analysis shows that the less hindered 1,3-diaryl-1,3-propanediones, which do not bear a 2-alkyl substituent, exist as mixtures of both enol and diketo tautomers. In most cases FT-IR revealed a C=O doublet for the dione. However, the intensity of this signal was often weak and variable, and thus was not a reliable indicator of reaction progress. In contrast, by using ¹H NMR-MAS and nanoprobe technology, we were able to conveniently and quickly ascertain the level of β-diketone formation.

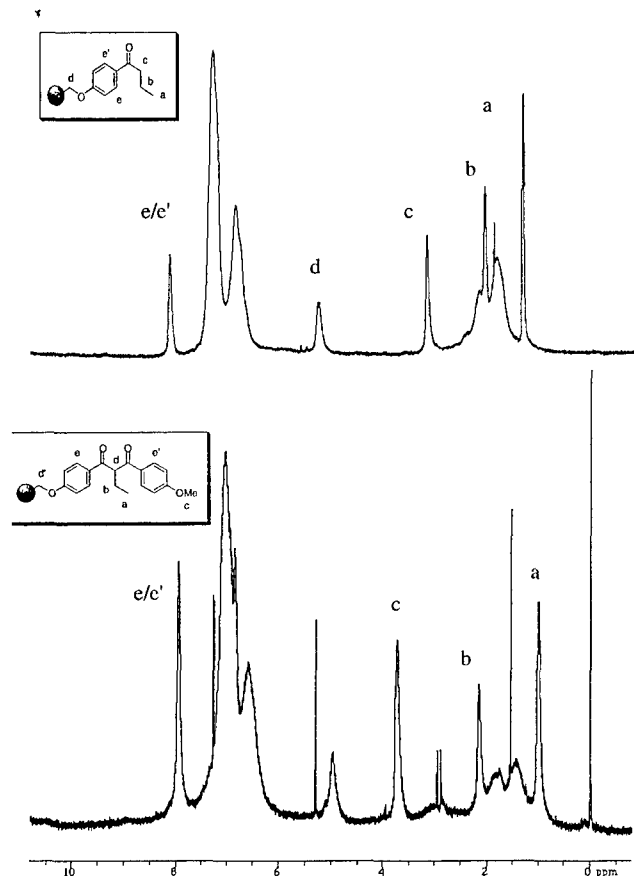Shown in Figure 3 panel A (top) is the spectrum for the starting resin-bound 4-hydroxy-butryophenone, and in panel

Figure 3. Panel A (top): ^{1}H NMR-MAS of polymer-bound butryophenone derivative **11**. Panel B (bottom): ^{1}H NMR-MAS of β-diketone product **12b** after Claisen condensation reaction.

Table 1. HPLC Purity Determination and Estrogen Receptor Binding Affinities (RBA Values) of C(4) *i*-Butyl Pyrazole Library

(8a − l)

compd	R_1	R_2	HPLC purity^a (%)	% RBA^b
8a	H	Ph	80	0.38/0.13^c
8b	H	*p*-OHC$_6$H$_4$	67	9.3/0.86^c
8c	H	*p*-FC$_6$H$_4$	92	0.04
8d	H	*t*-Bu	29	0.47
8e	OH	Ph	62	5.4
8f	OH	*p*-OHC$_6$H$_4$	>99	7.6
8g	OH	*p*-FC$_6$H$_4$	90	4.0
8h	OH	*t*-Bu	23	3.8
8i	Br	Ph	75	0.76/0.01^c
8j	Br	*p*-OHC$_6$H$_4$	>85	3.3
8k	Br	*p*-FC$_6$H$_4$	>80	0.17
8l	Br	*t*-Bu	28	0.90

^{a} RP-HPLC, 80% MeOH:H$_2$O, flow rate of 1.0 mL/min, detection at 254 nm (performed before purification by radial chromatography). ^{b} Relative Binding Affinity (RBA) values determined by a modification of our standard competitive binding assay using only three concentrations of ligand; all compounds tested were at >80% purity. ^{c} Independent assays performed on the two individual regioisomers.

B (bottom) is the spectrum for the expected dione product after Claisen condensation with 4-methoxy-(4′-nitrophenyl)-benzoate. Because we are using a short linker, which holds these molecular segments close to the rigid polystyrene backbone, the line widths for these signals remain fairly large (20 Hz), and as a result, coupling information is unavailable. Despite this limitation, however, we can readily discern diagnostic chemical shift differences between the product and starting material, so that we confidently assess the success or failure of the reaction.

To form the tetrasubstituted pyrazole on solid phase, we first tried conditions that had been successfully used for the solution-phase synthesis (heating the dione and hydrazine hydrochloride salt to 110–120 °C in DMF/THF solutions for up to 16 h), as well as conditions developed my Marzinzik and Felder for solid-phase pyrazole synthesis (DMA as a solvent at 80 °C).[9] Unfortunately, even with extended heating, neither of these methods gave the desired heterocycle. When we used triethylamine (TEA) to neutralize the hydrazine hydrochloride and DMF as solvent, we obtained low yields of the desired product, but purity after cleavage/deprotection was less than 35%. Ultimately, we found that toluene as solvent with the addition of TEA was effective, affording the pyrazole product **1** in >90% purity after cleavage/deprotection. One should note that subsequently we found that these reaction conditions, which involved heating toluene to 80 °C for 9 h, were not compatible with our 96-well reaction plate (Polyfiltronics 96-well Unifilter plate). Nevertheless, at the time we used these conditions to prepare

a 12-member library of pyrazoles and then later modified the pyrazole-forming step to make it compatible with our 96-well reaction plate (see below).

The diones (**6**) needed for this (and the larger library) were prepared in a single batch, using a homemade reaction block capable of holding 16–20 mL sealed conical polypropylene tubes as reaction vessels. The block was rotated in an oven at 40 °C for 4 h, using a modified rotary evaporator motor. After washing the resins and drying them overnight, we verified dione formation by nanoprobe ^{1}H NMR-MAS. Each dione resin was then split into the appropriate number of portions and reacted with the appropriate hydrazine, the cyclization products then being cleaved/deprotected with BBr$_3$. For this smaller 12-member library, the cleaved material was collected, treated to a minimal workup (MeOH, passage through a SiO$_2$ plug), and analyzed for purity by HPLC.

Shown in Table 1 are the HPLC-evaluated purities and the ER binding affinities for the C-(4)-*iso*-butyl pyrazoles (**8a−l**) in the 12-membered library. The HPLC purity values listed were obtained on the pyrazoles after only minimal workup, yet some of these are quite high (>90%). The pyrazoles derived from *tert*-butylhydrazine were of the lowest quality. The major byproduct in those having lower purity was the corresponding β-diketone intermediate, and in some cases small amounts of the starting ketone. Prior to binding affinity determination, all compounds were purified by radial chromatography, so that their purities were at least 80%. The molecular ions of all purified pyrazoles in the C(4) *i*-butyl series were also verified by ES-MS.

The binding affinities of these pyrazoles were determined in a competitive radiometric binding assay (for details see Experimental Section), using [^{3}H]estradiol as tracer and lamb

uterine cytosol as a source of ER, and they are expressed as relative binding affinity values (RBA), with estradiol having an RBA of 100%. In the past, we have found that repeat determinations of binding affinities by this assay have a coefficient of variation of 0.3.

We were concerned that even small amounts of contaminants in the purified pyrazoles might be affecting the RBA determinations. To test this, we examined the effect of dihydroxyphenyl dione **9** on the affinity determination of pyrazole **1**. This dione (**9**) itself binds to the ER only very weakly (RBA = 0.012%), and when it was added to pyrazole **1** at 10, 20, and 30%, we noted no effect on the RBA value obtained for pyrazole **1**. Thus, we believe that the binding affinity values we have determined for all of these pyrazoles (Table 1) are valid.
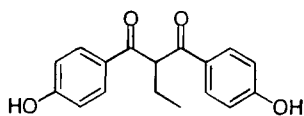
9 RBA = 0.012 %

Overall, the *i*-butyl pyrazoles bind to ER with reasonable affinity (Table 1), and even within this small set of compounds some structure−affinity trends are apparent. Clearly, there is a primary preference for hydroxy substitution at R$_1$, as in most cases, and the pyrazoles in the **8e−h** series bind better than those in the **8a−d** and **8i−l** series. Bromine substitution (series **8i−l**) is unusual for nonsteroidal ligands, but pyrazole **8j** (1.4:1 ratio of regioisomers) has a reasonable affinity of 3.3%. The reasonable affinity of the *tert*-butyl pyrazole **8h** suggests that bulky substituents other than phenyl are tolerated at R$_2$. The highest affinity members of this small pyrazole library, **8b** and **8f**, contain two and three hydroxyl substituents, respectively. The similar but lower affinity diphenolic pyrazole **8e** suggests that two distinct binding orientations may exist for **8e** and **8b**.

In those cases where more than one regioisomer was expected and they could be separated by HPLC, two RBA values are indicated. In three cases where we could do this, one regioisomer showed a higher affinity: In both the monohydroxy pyrazole **8a** and dihydroxy pyrazole **8b**, a 3−10-fold preference was found for one regioisomer, and in the case of pyrazole **8i**, this preference is much greater.

At this point, we could not make a definitive assignment of the structure of these regioisomers, but these results suggest that only one of them is providing an effective mimic of the A-ring of estradiol. In other work, we have carried out independent, regioselective syntheses of single pyrazole regioisomers in a related series, and we have conducted molecular graphics modeling studies of how these isomers might fit into the ligand binding domain of ER (Stauffer, S. R., Huang, Y., Coletta, C. J., Katzenellenbogen, J. A., unpublished). These studies suggest that there are indeed preferred orientations of these regioisomers within the ER binding pocket. However, it appears that the preferred orientation may switch, depending on the substituent display.

Adaptation to a 96-Well Format. To prepare the 96-member library, we used the Polyfiltronics 96-well Unifilter plate. The Unifilter plate contains a single underlying membrane which is designed to hold back most organic solvents, except when a vacuum is applied. Unfortunately, the Polyfiltronics plate did not withstand our conditions for pyrazole formation, using prolonged heating with toluene at 80 °C.

In our search for alternate conditions for pyrazole formation which the Polyfiltronics plate would withstand, we used pyrazole **1** as a model, and we explored a greater number of solvents and solvent mixtures for pyrazole formation (THF, BuCN, HC(OMe)$_3$, CH$_3$NO$_2$, and alcohols) with and without various additives (TiCl$_4$, Na$_2$SO$_4$, and 4 Å molecular sieves), at room temperature and at elevated temperatures. Ultimately, only alcohol solvents proved to be effective in forming the pyrazole product and were compatible with the Unifilter plate.

In this larger library, we also wanted to develop an expedited method for product isolation, whereby we could quench the cleavage/deprotection reagent BBr$_3$ and neutralize the HBr generated without introducing water, thereby avoiding cumbersome liquid−liquid phase extractions. Our approach was to develop a scavenger resin to neutralize the HBr and remove the inorganic contaminants by sequestration. Our initial efforts were based on work by Cardillo and co-workers,[15] involving the use of macroreticular carbonate resin as a reagent in the hydrolysis of alkyl halides.

Resin **10a** (Scheme 2), which is readily prepared from the chloride form of the ion exchange Amberlyst A-26 resin, was effective in quenching the BBr$_3$, but not surprisingly the final product was contaminated with NaBr. However, by modifying the resin to a sodium-free, bicarbonate form, we could still neutralize the HBr, but now with the liberation of only CO$_2$ and H$_2$O. Moreover, the polymer-bound quaternary ammonium groups sequestered any bromide ions from solution. Thus, by treating the crude cleaved/deprotected product with this bicarbonate resin, we could remove all of the inorganic contaminants, leaving the desired pyrazole remaining in solution together with only MeOH (bp 65 °C), B(OMe)$_3$ (bp 58 °C), and a small amount of H$_2$O, so that solvent removal gave the product free from any reagent contamination.

Two methods were used to prepare the bicarbonate form of A-26 resin (Scheme 2). Both resins (**10b** and **10c**) afford the product pyrazole in reasonable purity, but the bicarbonate resin which was prepared using NaHCO$_3$ (**10b**) still contained small amounts of Na ions, risking product contamination with NaBr. The preferred method to prepare Na ion-free resin was first to convert the chloride form of the A-26 resin to the hydroxide form and then generate the bicarbonate resin by bubbling CO$_2$ through an aqueous suspension of the resin. This ensured that there was no Na ion contamination, and this material (**10c**) afforded the pyrazole product with somewhat better purity. Shown in Scheme 1 is the overall optimized solid-phase synthesis route to the 96-member pyrazole library. The notable modifications from the original route used to prepare the 12-member library are the conditions for the pyrazole-forming step and final workup procedure involving the bicarbonate resin **10c**.

The individual components chosen for the 96-member library are shown in Figure 4. The components used to
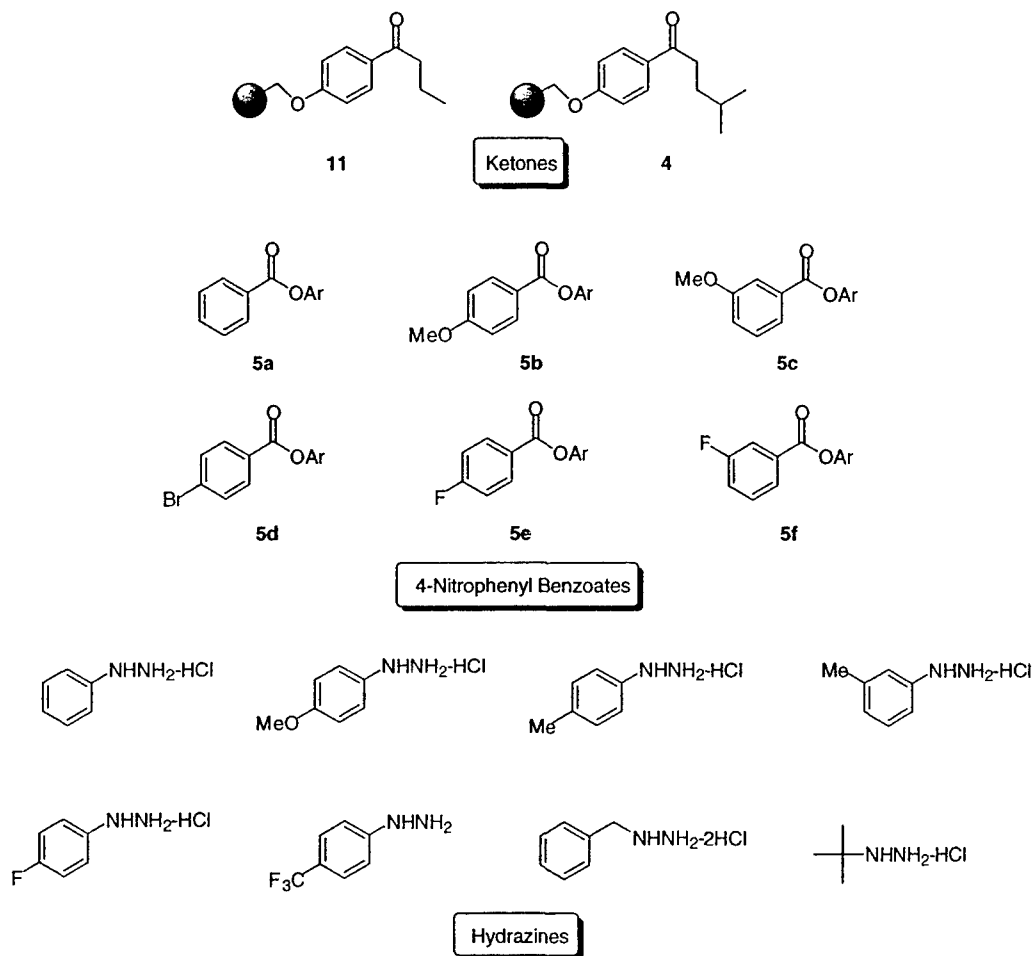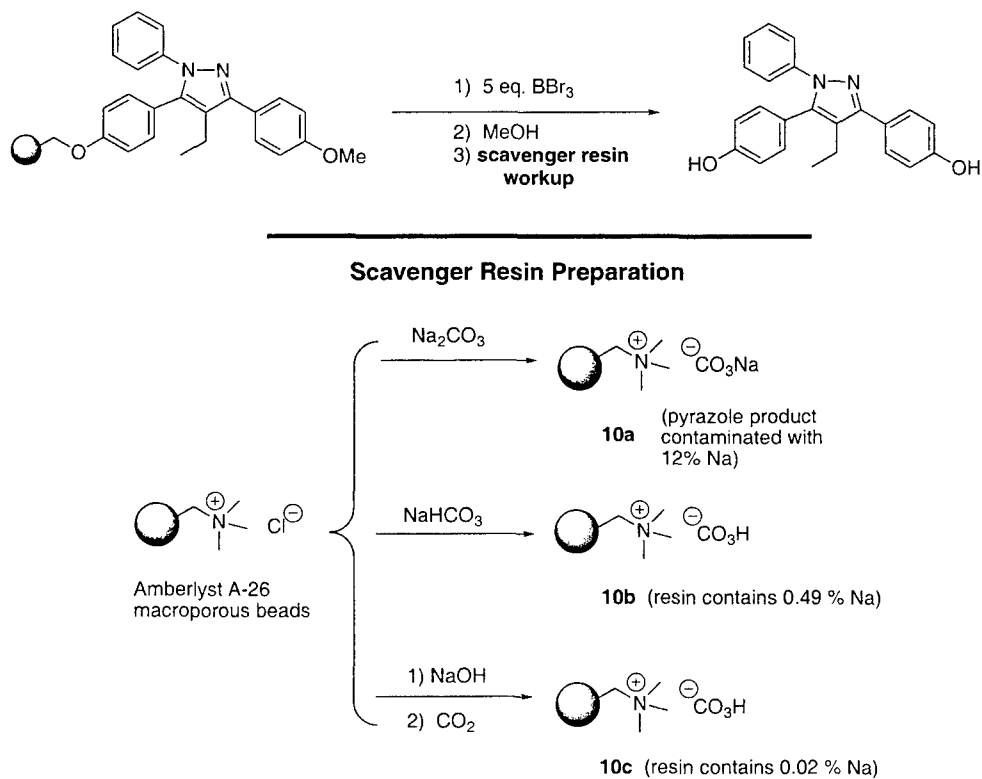
11   Ketones   4

5a   5b   5c

5d   5e   5f

4-Nitrophenyl Benzoates

Hydrazines

Figure 4. Components for 96-member pyrazole library.

Scheme 2. Development and Use of Bicarbonate Resin for HBr Neutralization

1) 5 eq. BBr₃

2) MeOH
3) **scavenger resin**
   workup

Scavenger Resin Preparation

Na₂CO₃

(pyrazole product
10a contaminated with
12% Na)

Amberlyst A-26
macroporous beads

NaHCO₃

10b (resin contains 0.49 % Na)

1) NaOH
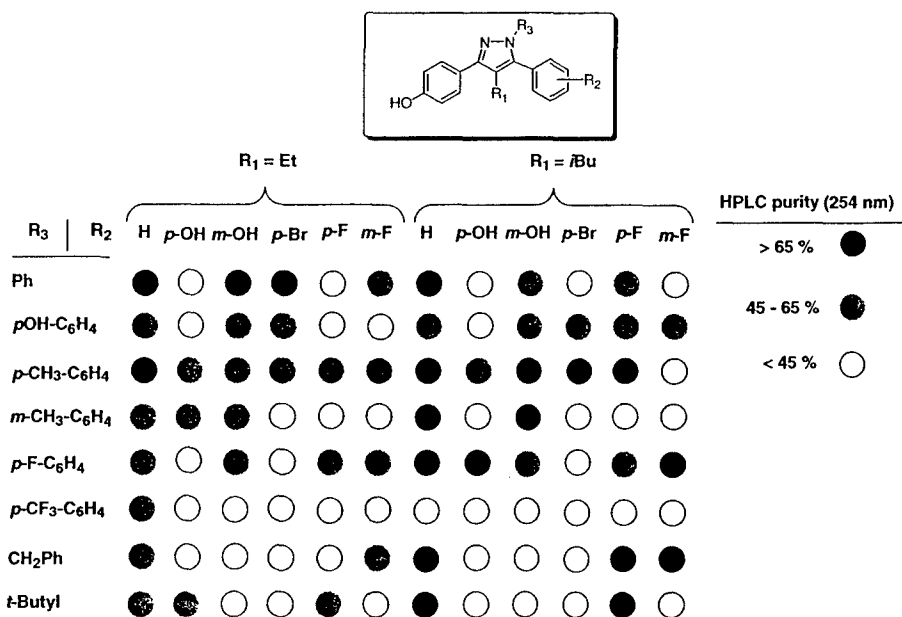
2) CO₂

10c (resin contains 0.02 % Na)

Figure 5. HPLC purities for 96-member ER library.

prepare the *i*-butyl library (Figure 2, Table 1) were again included as standards to measure the success and reproducibility of the synthesis and to verify the RBA assays. The progress of pyrazole formation for suspected "worst-case" combinations, such as CF$_3$-phenyl and *tert*-butyl hydrazines reacting with halogen-substituted diones, was monitored using FT-IR. The disappearance of the C=O signal at 1670 cm^{-1} was a reliable marker for determining the progress of individual reactions. Unfortunately, for several CF$_3$-substituted hydrazines we were unable to drive the reaction to completion, even after subjecting these resins to fresh reagent and heating for an additional 20 h. In any event, cleavage/deprotection with BBr$_3$ followed, and reactions were carefully quenched with MeOH and then incubated with bicarbonate resin **10c** for 1 h at 50−60 °C to ensure complete HBr neutralization and bromide ion sequestration. After being cooled, the pyrazole products were collected and concentrated, then reconstituted in 1 mL McOH and analyzed using a standard, steep gradient elution on a high throughput reverse-phase HPLC column. Because the pyrazoles are uniformly fluorescent, we used fluorescence detection in tandem with UV detection to identify which of the eluted peaks was the pyrazole. This proved to be a robust approach to characterizing product purity. After obtaining the purity for each member, we determined the ER binding affinity in a simplified, three-point assay (see Experimental Section for details).

Purity and ER Binding Affinity Relationships. A summary of the HPLC purities for the final pyrazoles is shown in Figure 5, according to gray scale coded ranges. The average purity for the library was 50% (±15%). This is not an unreasonable level of purity when you consider that this library included components, such as *tert*-butyl hydrazine hydrochloride, which we have found to be less reactive than the aromatic hydrazines. As before, the principal impurities could be identified as the unreacted dione precursors, which we had previously shown did not affect the results of the binding assay (see above). On the basis of product yields,

p-CF$_3$-substituted phenyl hydrazines appear to be even less reactive than *t*-butyl hydrazine hydrochloride, because this group of pyrazoles had the lowest overall purity of the whole library. Where regioisomers were expected within this series (see above), it was difficult to assign the product peaks, even with the help of fluorescence as a marker. In these cases, we assumed the purity to be 30%.

Shown in Figure 6 are the relative binding affinity (RBA) values for the 96-member library, indicated as ranges according to a gray scale coded legend. Several members of the library showed appreciable affinity for the ER. Particularly gratifying was the fact that most members of the 12-member *i*-butyl control library (Table 1) had RBA values which were reproduced quite well in the larger library (i.e., within 30%, relative), with the exception of **8f** (7.6%) vs **B-8** (23%). A repeat assay **8f** showed that its determination in the original 12-member library was low. The binding affinity of 16 additional select members was also re-tested after chromatographic purification (>80%), and the RBA values for these members also agreed quite well with the original determinations on the crude isolated products.

The use of an affinity array chart in Figure 6 permits a rapid, visual assessment of binding affinity patterns. For example, it is readily apparent that, for pyrazoles in both the R$_1$ ethyl and *i*-butyl series (column 2 and 8), those with HO substituents at R$_2$ have, overall, the highest affinity. Within these two series (columns 2 and 8), a number of substituents are tolerated at R$_3$, the best being *p*-HO−C$_6$H$_4$, for which the two highest affinity pyrazoles are represented, pyrazole **B-2** (14%) and **B-8** (23%). For pyrazoles with R$_3$ = *p*-HO−C$_6$H$_4$ (row B), a number of substituents are tolerated to varying degrees; those with fluorine substituents on R$_2$ for both the ethyl and *i*-butyl series bind moderately well (RBA = 1−5%). For members with R$_1$ = *i*-butyl and R$_3$ = *p*-HO−C$_6$H$_4$, even more polar substituents appear to bind well. Particularly noteworthy is the *m*-HO analogue **B-9**, which has a relative binding affinity of 6.8%, and the fluoro derivative **B-11**. By contrast, few other R$_3$ substituents are
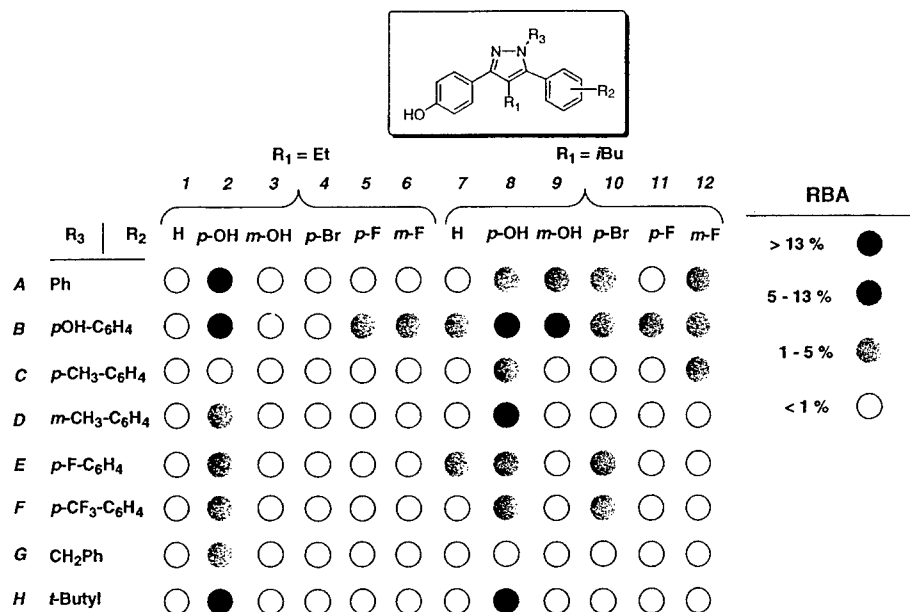
		R₁ = Et						R₁ = iBu						RBA	
		1	2	3	4	5	6	7	8	9	10	11	12		
R₃	R₂	H	p-OH	m-OH	p-Br	p-F	m-F	H	p-OH	m-OH	p-Br	p-F	m-F	> 13 %	●
A	Ph	○	●	○	○	○	○	○	◉	◉	◉	○	◉	5 - 13 %	●
B	pOH-C₆H₄	○	●	○	○	◉	◉	◉	●	●	◉	◉	◉	1 - 5 %	◉
C	p-CH₃-C₆H₄	○	○	○	○	○	○	○	◉	○	○	○	◉	< 1 %	○
D	m-CH₃-C₆H₄	○	◉	○	○	○	○	○	●	○	○	○	○		
E	p-F-C₆H₄	○	◉	○	○	○	○	◉	◉	○	◉	○	○		
F	p-CF₃-C₆H₄	○	◉	○	○	○	○	○	◉	○	◉	○	○		
G	CH₂Ph	○	◉	○	○	○	○	○	○	○	○	○	○		
H	t-Butyl	○	●	○	○	○	○	○	●	○	○	○	○		

Figure 6. ER binding affinity for 96-member pyrazole library. (In unsymmetrical systems, i.e., $R_2 \neq$ p-OH, the average regioisomer ratio was 1.4 to 1.)

well tolerated by the ER, one exception, however, being the *tert*-butyl pyrazoles **H-2** and **H-8**, which each have affinities of 6–7%. As was the case with pyrazole **8j** from the 12-member *i*-butyl library, several pyrazoles with p-bromo substituents at R_2 have reasonable affinity (~2–3%). However, these affinities are much lower when R_1 = ethyl (RBA <1%), than when R_1 = *i*-butyl.

In investigations to be reported elsewhere (Stauffer, S. R., Coletta, C. J., Sun, J., Katzenellenbogen, B. S., Katzenellenbogen, J. A., unpublished), we have made other analogues based on the high affinity 1,3,5-p-hydroxyphenyl-pyrazole template, and we have found a compound with an RBA of 30% that shows very high affinity and potency selectivity for ERα. We have also prepared other pyrazoles that act as ERα potency selective antagonists (Stauffer, S. R., Huang, Y., Aron, Z. D., Coletta, C. J., Sun, J., Katzenellenbogen, B. S., Katzenellenbogen, J. A., upublished).

Conclusions

We have developed a consistent and efficient method to prepare and isolate tetrasubstituted pyrazoles using a solid-phase strategy, and we have used this approach for the production of small, discrete libraries of estrogen receptor (ER) ligands. A combination of FT-IR and nanoprobe ¹H NMR-MAS allowed us to characterize intermediates leading up to the final pyrazole products directly on the bead. We also developed a scavenging resin to afford the cleaved/deprotected products free from inorganic contaminants. Using this approach, we prepared a 12-member test library, and then a more extensive 96-member library, and we determined product purity and ER binding affinity of all the library members. Several interesting binding affinity patterns emerged from these studies, and they have provided us with clear directions for further exploration of these tetrasubstituted pyrazoles, through which we have found a high affinity and high potency agonist with excellent selectivity for ERα and pyrazoles that selectivity *antagonize* ERα.

Experimental Methods

General. Melting points were determined on a capillary apparatus and are uncorrected. All reagents and solvents were obtained from Aldrich, Fisher, or Mallinckrodt. Tetrahydrofuran was freshly distilled from sodium/benzophenone. Dimethylformamide was vacuum distilled prior to use and was stored over 4 Å molecular sieves. Et_3N was stirred with phenylisocyanate, filtered, distilled, and stored over 4 Å molecular sieves. All reactions were performed under a dry N_2 atmosphere unless otherwise specified. Radial preparative-layer chromatography was performed on a Chromatotron instrument (Harrison Research, Inc., Palo Alto, CA) using EM Science silica gel Kieselgel 60 PF_{254} as adsorbent. Flash column chromatography[16] was performed using Woelm 32–63 μm silica gel packing. Resin bound ketone **11** was prepared according to procedure outlined in Scheme 1 from commercially available 4′-methoxybutyrophenone or from anisole and the acid chloride.

¹H and ¹³C NMR spectra were recorded on 400 or 500 MHz spectrometers, using $CDCl_3$ or MeOD as solvent. Chemical shifts were reported as parts per million downfield from an internal tetramethylsilane standard ($\delta = 0.0$ for ¹H) or from solvent references. NMR coupling constants are reported in hertz. ¹³C NMR data were determined using either the Attached Proton Test (APT) experiment or standard ¹³C pulse settings. Low resolution electrospray mass spectrometry was performed using a VG Quattro (quadrupole-hexapole-quadrupole, QHQ) mass spectrometer system (Fisons Instruments, VG Analytical; Manchester, U.K.).

FT-IR Analysis and Nanoprobe ¹H NMR-MAS Spectra. FT-IR analysis was performed on an FTIR spectrometer, and absorption bands are reported in cm⁻¹. Infrared analysis was accomplished by placing approximately 1–2 mg of resin between two NaCl plates, swelling the beads in $CHCl_3$, and immediately recording an FT-IR spectrum. Solid-phase NMR spectra were obtained on a Varian 500 MHz wide-bore spectrometer using a nanoprobe. The polystyrene-bound

dione intermediates **12a**−**l** were characterized using 2 mg or less of resin in a pre-swollen $CDCl_3$ solution (nanotube, approximately 40 μL total volume). The sample was spun about the magic angle (54.7 °C) at 2.3−2.5 kHz, and four scans were collected for each ^1H experiment, using a pulse width of 15 μs and delay time of 4 ms. Tetramethylsilane was used as an internal reference.

Relative Binding Affinity Assay. Ligand binding affinities (RBAs) using lamb uterine cytosol as a receptor source were determined by a competitive radiometric binding assay. This assay is conducted in 96-well microtiter plates in a total volume of 70 μL, using ca. 1 nM of estrogen receptor binding equivalents, 10 nM [^3H]estradiol as tracer, and dextran-coated charcoal as an adsorbent for free ligand.[17] On the basis of interspecies comparison, lamb uterus is thought to contain predominantly estrogen receptor subtype α.[18,19] All incubations were done at 0 °C for 18−24 h. Binding affinities are expressed relative to estradiol (RBA = 100%) and are reproducible with a coefficient of variation of 0.3. RBA determinations for the 96-member library were performed using a three-point assay, at ligand concentrations of 10^{-4}, 10^{-6}, and 10^{-8} M and were corrected for individual purity level.

Chemical Syntheses. 4′-Methoxy-4-methyl-valerylophenone (2). To a stirred solution of $AlCl_3$ (6.4 g, 48 mmol) in 1,2-dichloroethane at 0 °C was added 4-methyl-valeryl chloride (5.3 g, 39.0 mmol) dropwise over approximately 10 min. The resulting solution was warmed to room temperature, stirred for 0.5 h, then re-cooled to 0 °C, and a 1,2-dichloroethane solution of anisole (5.1 mL, 46 mmol in 20 mL) was added dropwise. The reaction was stirred at room temperature for 9 h, then cooled to 0 °C, quenched with H_2O, and extracted with CH_2Cl_2. The organic layer was washed with saturated $NaHCO_3$ and brine, then dried over $MgSO_4$, and concentrated to afford product as a pale yellow oil (6.0 g, 75%): ^1H NMR ($CDCl_3$) δ 0.94 (d, 6H, $J = 6.0$), 1.60 (m, 3H, overlapping methine and β-CH_2), 2.90 (t, 2H, $J = 6.8$), 3.87 (s, 3H), 6.92 (d, 2H, $J = 8.8$), 7.90 (d, 2H, $J = 8.8$); ^{13}C NMR ($CDCl_3$) δ 22.6, 28.5, 33.9, 36.4, 55.2, 113.5, 130.2, 163.6, 198.7; MS (EI, 70 eV) m/z 206.1 (M^+). Anal. ($C_{13}H_{18}O_2$): C, 75.69; H, 8.80. Found: C, 75.63; H, 8.59.

4′-Hydroxy-4-methyl-valerylophenone (3). To a stirred solution of $AlCl_3$ (19.4 g, 145 mmol) in benzene (300 mL) at 0 °C was added a benzene solution (60 mL) of ketone **2** over 20 min. The reaction mixture was then brought to reflux for 2 h. After cooling to room temperature the mixture was poured over 400 mL of water, and then the organic layer washed with saturated $NaHCO_3$ and brine. The organic layer was then dried over $NaSO_4$ and concentrated to afford the phenolic product as a tan solid which was then used directly in the next step to functionalize Merrifield's resin (8.97 g, 96%): ^1H NMR ($CDCl_3$) δ 0.94 (d, 6H, $J = 6.0$) 1.27 (m, 3H, overlapping methine and β-CH_2), 2.90 (t, 2H, $J = 8$), 6.87 (d, 2H, $J = 8.5$), 7.91 (d, 2H, $J = 9.0$).

Alkylphenone Loading onto Merrifield Resin (4, 11). To a solution of the phenolic ketone (28.0 mmol, either **3** or 4′-hydroxy-butyrophenone) in DMF (144 mL) at 0 °C was added NaH as a 60% oil dispersion (1.05 g, 26.4 mmol). The reaction mixture was returned to room temperature;

Merrifield resin (5.74 g, 1.39 mmol/g Novabiochem, Inc.) was added, and the reaction was heated to 55 °C for 22 h. The solution was then cooled to room temperature and quenched by addition of methanol (150 mL). The resin-bound product was then isolated via vacuum filtration and rinsed with methanol/DMF 1:1 (1 × 300 mL), DMF (3 × 350 mL), CH_2Cl_2 (3 × 350 mL), and methanol (3 × 350 mL). The resulting salmon-colored resin was then dried in vacuo for 18 h to afford >6 g of immobilized ketone. FT-IR analysis revealed the C=O stretch at 1670 cm^{-1}, which verified that the resin-bound ketone was produced. In addition, %Cl analysis was performed to verify the absence of halogen, indicating that most of the chloromethyl sites were substituted. Loading capacity, which ranged from 0.9 to 1.1 mmol/g, was determined from the mass recovery of expected product by cleaving a small portion of the ketone resin using BF_3−SMe_2.

General Procedure for Preparation of p-Nitrophenyl Benzoate Esters (5a−f). To a mechanically stirred solution of the substituted benzoic acid (52.6 mmol), p-nitrophenol (22.2 g, 157.8 mmol), and DMAP (3.2 g, 26.3 mmol) in 100 mL CH_2Cl_2 at 0 °C was added diisopropylcarbodiimide (57.9 mmol) dissolved in CH_2Cl_2 (100 mL) dropwise over 10 min. The resulting solution was allowed to stir for 18 h at room temperature. The reaction mixture was filtered, and the filtrate was concentrated under reduced pressure. The crude esters were recrystallized from EtOH or EtOAc to afford the desired ester (55−95%). Products were judged pure by comparison to literature melting points[20] and then used in the next step of the synthesis.

2-Ethyl-1,3-bis-(4-hydroxyphenyl)-propane-1,4-dione (9). The methoxy-protected derivative of **1** (prepared in 95% yield from 4-methoxybutyrophenone and the p-nitrophenylbenzoate ester using LHMDS, under the same conditions used for the solid-phase synthesis; see **12a**−**l**, and purified by flash chromatography (ethyl acetate/hexanes)) was treated with 5 equiv of 1.0 M BBr_3 in CH_2Cl_2 at 0 °C. The mixture was allowed to reach room temperature and stir for 5 h. The reaction was then re-cooled to 0 °C and carefully quenched with water and repeatedly extracted with Et_2O. The combined organic layers were dried over Na_2SO_4, and upon solvent removal the title compound was afforded as a tan foam: ^1H NMR (MeOD) δ 0.99 (t, 3H, $J = 7.5$), 2.01 (q, 2H, $J = 7.5$) 5.32 (t, 1H, $J = 1.5$), 6.81 (AA′BB′, 2H, $J = 7.0$, 3.0), 7.90 (AA′BB′, 2H, $J = 6.5$, 3.0); ^{13}C NMR (MeOD) δ 11.4, 23.0, 56.6, 115.1, 128.0, 130.9, 162.8, 195.9; MS (EI, 70 eV) m/z 284 (M^+). Anal. ($C_{12}H_{16}O_4$): C, 71.28; H, 5.67. Found: C, 70.90; H, 5.57.

Preparation of Bicarbonate Form of Amberlyst A-26 Resin Using NaOH/CO_2 (10c). A medium sintered glass filter containing 15 g of Amberlyst A-26 resin in the chloride form (average capacity ~3.7 mequiv/g) was treated portionwise with 1 L of an aqueous 1.0 M NaOH solution. The resin in the hydroxide form was then dried under aspirator vacuum and suspended in a 150 mL water solution. A flow of CO_2 gas was bubbled into the aqueous solution for approximately 30 min with gentle mixing. The resin was then washed sequentially with MeOH, acetone, and ether,

and then extensively dried in vacuo. Elemental analysis indicated essentially no Na ion contamination (0.02%).

Solid-Phase Conditions Used To Prepare 12-Member Pyrazole Library (8a−l). A THF suspension for each of the six dione resins (50 mg, loading capacity 0.92−0.98 mmol/g, prepared according to procedure below), one of the four appropriate hydrazine hydrochlorides (15 equiv), and triethylamine (15 equiv) in toluene (2 mL) were heated to 80 °C for 9 h in a glass cell culture tube with a Teflon-lined screwed cap. Mixing was achieved using a rotating reaction block via a modified rotary evaporator motor. The reaction mixtures were cooled to room temperature and then isolated via vacuum filtration in coarse sintered glass frits. The product resins were rinsed with methanol/DMF 1:1 (2 × 5 mL), DMF (3 × 5 mL), CH_2Cl_2 (3 × 10 mL), and methanol (2 × 5 mL). The resulting resins were dried in vacuo for 18 h and then pre-swollen in a 2 mL CH_2Cl_2 solution under N_2 at −78 °C, using 10 mL conical vials, each containing a magnetic stir bar. Pyrazole cleavage/deprotection was followed by addition of 1 M BBr_3 (5 equiv, 0.7 mL) in CH_2-Cl_2. The reaction was allowed to warm to room temperature and stir for 6 h and was quenched at 0 °C by the addition of CH_3OH (2 mL). The resins were isolated by vacuum filtration and rinsed twice with 5 mL portions of CH_3OH. The individual filtrates were concentrated in vacuo, dissolved in MeOH, and concentrated once again. This procedure was repeated twice, prior to RP-HPLC analysis. Pyrazoles **8a−l** were then purified to >80% HPLC purity by radial chromatography (10−20% MeOH/CH_2Cl_2) and submitted for ES-MS and RBA analysis. The expected molecular ion pattern by electrospray was observed in all cases: (**8a**) ES-MS calcd for $C_{25}H_{24}N_2$ 368.4, found MH^{2+} 370.1 (individual isomers separately measured); (**8b**) ES-MS calcd for $C_{25}H_{24}N_2O_2$ 384.5, found MH^+ 385.2 (individual isomers separately measured); (**8c**) ES-MS calcd for $C_{25}H_{23}FN_2O$ 386.5, found MH^+ 387.2; (**8d**) ES-MS calcd for $C_{23}H_{28}N_2O$ 348.5, found MH^+ 349.1; (**8e**) ES-MS cacld for $C_{25}H_{24}N_2O_2$ 384.5, found MH^{2+} 386.2; (**8f**) ES-MS calcd for $C_{25}H_{24}N_2O_3$ 400.5, found MH^+ 401.1; (**8g**) ES-MS calcd for $C_{25}H_{23}FN_2O_2$ 402.5, found MH^+ 403.1; (**8h**) ES-MS calcd for $C_{23}H_{28}N_2O_2$ 364.5, found MH^+ 365.2; (**8i**) ES-MS calcd for $C_{25}H_{23}BrN_2O$ 446.1, found MH^+ 447.0 (individual isomers separately measured); (**8j**) ES-MS calcd for $C_{25}H_{23}BrN_2O_2$ 462.1, found MH^+ 463.1; (**8k**) ES-MS calcd for $C_{25}H_{22}BrFN_2O$ 464.1, found MH^+ 465.1; (**8l**) ES-MS calcd for $C_{23}H_{27}BrN_2O$ 426.1, found MH^+ 427.2.

General Procedure for Batch Dione Synthesis (12a−l). Twelve conical polypropylene cell culture tubes (20 mL) were charged with 400 mg of ketone resin (**4** and **11**, approximately 0.38 mmol, six tubes per ketone), p-nitrophenyl esters (5.76 mmol, **5a−c**), and 15 mL of THF. Each tube was then purged with a nitrogen atmosphere using a 14/20 septa and then chilled in an ice bath. A 1.0 M THF solution of LHMDS (3.84 mmol) was added dropwise via syringe to each tube; the reaction was then sealed with a screw cap and shaken vigorously. Esters **5d−f** could not be present during enolate formation due to their reactivity toward LHMDS and thus were added in one portion 30 min after addition of LHMDS. All 12 reaction tubes were then

loaded into a homemade reaction block, which was slowly rotated within a 40 °C oven using a modified rotary evaporator motor. After 5 h, the resins were transferred to coarse sintered glass filters using CH_2Cl_2. A rinse procedure followed involving methanol/DMF 1:1 (1 × 30 mL), DMF (3 × 20 mL), CH_2Cl_2 (3 × 20 mL), and methanol (2 × 20 mL). The resins were then dried in vacuo, and the level of product formation was determined by nanoprobe ^1H NMR-MAS. In all 12 cases, disappearance of the ketone α-protons occurred, and a new signal at approximately δ 5−5.3 was observed for the α/α′ methine proton, indicating successful dione formation. Diagnostic chemical shifts are reported below (note: aromatic resonances from dione which overlap with polystyrene backbone in addition to the resin backbone signals themselves are not listed; for purposes of naming, polystyrene is abbreviated "PS"; integration values are approximately ±15%).

1-PS-(4-Benzyloxyphenyl)-2-ethyl-3-phenyl-propane-1,3-dione (12a): δ 1.02 (3H, CH_3CH$_2$), 2.15 (2H, CH$_3$CH_2), 4.95 and 5.05 (two overlapping s, 3H, PS-ArCH_2O and α/α′-CH), 7.95 (4H, ArCH ortho-C=O).

1-PS-(4-Benzyloxyphenyl)-2-ethyl-3-(4-methoxyphenyl)-propane-1,3-dione (12b): δ 1.01 (3H, CH_3CH$_2$), 2.15 (2H, CH$_3$CH_2), 3.74 (3H, OCH_3), 4.98 (s, 3H, ArCH_2 and α/α′-CH), 7.95 (4H, ArCH ortho-C=O).

1-PS-(4-Benzyloxyphenyl)-2-ethyl-3-(3-methoxyphenyl)-propane-1,3-dione (12c): δ 1.02 (3H, CH_3CH$_2$), 2.14 (2H, CH$_3$CH_2), 3.72 (3H, OCH_3), 5.05 (two overlapping s, 3H, PS-ArCH_2O and α/α′-CH), 7.51 (2H, ArCH), 7.96 (2H, ArCH).

1-PS-(4-Benzyloxyphenyl)-2-ethyl-3-(4-bromophenyl)-propane-1,3-dione (12d): δ 1.01 (3H, CH_3CH$_2$), 2.13 (2H, CH$_3$CH_2), 4.97 (s, PS-ArCH_2O and α/α′-CH); 7.50 (ArCH), 7.79 (ArCH), 7.95 (ArCH).

1-PS-(4-Benzyloxyphenyl)-2-ethyl-3-(4-fluorophenyl)-propane-1,3-dione (12e): δ 1.01 (3H, CH_3CH$_2$), 2.14 (2H, CH$_3$CH_2), 4.97 (s, PS-ArCH_2O and α/α′-CH), 7.97 (4H, ArCH).

1-PS-(4-Benzyloxyphenyl)-2-ethyl-3-(3-fluorophenyl)-propane-1,3-dione (12f): δ 1.01 (3H, CH_3CH$_2$), 2.13 (2H, CH$_3$CH_2), 4.97 (s, PS-ArCH_2O and α/α′-CH), 7.64, 7.69, 7.95 (three s, 4H, ArCH).

1-PS-(4-Benzyloxyphenyl)-2-iso-butyl-3-phenyl-propane-1,3-dione (12g): δ 0.96 (6H, (CH_3)$_2$), 2.01 (β-CH_2), 4.95 (2H, PS-ArCH_2O), 5.24 (1H, α/α′-CH), 7.39 (3H, ArCH), 7.48 (ArCH), 7.97 (3H, ArCH).

1-PS-(4-Benzyloxyphenyl)-2-iso-butyl-3-(4-methoxyphenyl)-propane-1,3-dione (12h): δ 0.95 (6H, (CH_3)2), 2.02 (β-CH_2), 3.76 (3H, OCH_3), 4.93 (2H, PS-ArCH_2O), 5.17 (1H, α/α′-CH), 7.97 (4H, ArCH).

1-PS-(4-Benzyloxyphenyl)-2-iso-butyl-3-(3-methoxyphenyl)-propane-1,3-dione (12i): δ 0.96 (6H, (CH_3)$_2$), 2.00 (β-CH_2), 3.74 (3H, OCH_3), 4.95 (2H, PS-ArCH_2O), 5.23 (1H, α/α′-CH), 7.29 (ArCH), 7.52 (2H, ArCH), 7.97 (2H, ArCH).

1-PS-(4-Benzyloxyphenyl)-2-iso-butyl-3-(4-bromophenyl)-propane-1,3-dione (12j): δ 0.95 (6H, (CH_3)$_2$), 1.97 and 2.05 (overlapping s, β-CH_2), 4.95 (2H, PS-ArCH_2O), 5.14 (1H, α/α′-CH), 7.51 (2H, ArCH), 7.81 (2H, ArCH), 7.96 (3H, ArCH).

1-PS-(4-Benzyloxyphenyl)-2-*iso*-butyl-3-(4-fluorophenyl)-propane-1,3-dione (12k): δ 0.95 (6H, (CH_3)$_2$), 1.99 and 2.05 (overlapping s, β-CH_2), 4.95 (2H, PS-ArCH_2O), 5.16 (1H, α/α'-CH), 7.98 (4H, ArCH).

1-PS-(4-Benzyloxyphenyl)-2-*iso*-butyl-3-(3-fluorophenyl)-propane-1,3-dione (12l): δ 0.95 (6H, (CH_3)$_2$), 1.95 and 2.07 (overlapping s, β-CH_2), 4.97 (2H, PS-ArCH_2O), 5.18 (1H, α/α'-CH), 7.66 (ArCH), 7.73 (ArCH), 7.97 (4H, ArCH).

General Solid-Phase Conditions Used To Prepare 96-Member Pyrazole Library. Pyrazole Formation: Each of the above diones (**12a—l**) were divided into eight approximately 50 mg portions and distributed across each row of an 8 × 12 Polyfiltronics Unifilter plate. After charging each well with the appropriate dione, the 12 commercially available hydrazine components (Figure 4) were carefully added as preweighed solids to the appropriate wells while carefully blocking off neighboring wells in order to avoid cross-contamination. The bottom of the plate was then secured in a reaction clamp (Polyfiltronics Combiclamp) with two Viton gaskets. To each well was added 1.5 mL of EtOH and approximately 100 μL of TEA. The top of the plate was sealed and the assembly agitated and heated to 65 °C in an oscillating cell culture oven. The reaction was monitored by FT-IR using several suspected "worst-case" scenarios (**H-2**, **F-2**, and **E-5** and our lead compound, **A-2**) by observing the diminishing intensity of the C=O signal at 1670 cm^{-1}. After 38 h, the plate was cooled to room temperature, and the crude mixtures were filtered within the reaction block by vacuum aspiration (Polyfiltronics filter/collection vacuum manifold). The resin-bound pyrazoles were then rinsed with methanol/DMF 1:1 (2 × 2 mL), DMF (3 × 2 mL), CH$_2$Cl$_2$ (3 × 2 mL), and methanol (3 × 2 mL) and then dried in vacuo overnight in a desiccator.

Deprotection/Cleavage: In a N$_2$-charged glovebag at room temperature, the resins were suspended in 0.5 mL of CH$_2$Cl$_2$ and treated dropwise with a 1.0 M CH$_2$Cl$_2$ solution of BBr$_3$ (500 μL). The reaction block was sealed as before and allowed to stand at room temperature with occasional mixing. After 8 h, the resins were carefully quenched with cold MeOH (0.5 mL), and then approximately 100 mg of bicarbonate resin **10c** was added to each well. After 20 min, when most of the CO$_2$ evolution ceased, the reaction top was resealed and the block heated to 50—60 °C for 1 h. Upon cooling to room temperature, the released library members were collected in a 96-well 2 mL collection plate, and the solvent evaporated to dryness (a 96-pin manifold capable of providing a gentle overhead stream of N$_2$ to each well in addition to gentle warming using a hot plate allowed for the removal of most of the MeOH; the remaining residual volatiles were removed in vacuo). Each member was then reconstituted in 1 mL of MeOH and analyzed by RP-HPLC.

Characterization of 96-Member Pyrazole Library. RP-HPLC analysis was performed on an analytical HPLC system with an autosampler. UV detection was performed at 254 nm and a flow rate of 1.0 mL/min using a C-18 CombiScreen analytical column (YMC, Inc., 4.6 mm × 50 mm) with a MeOH:H$_2$O gradient solvent system (40—90% MeOH, 0—5 min, total run time = 10 min). A fluorometer HPLC flow

detector was used to aid in identification of the expected pyrazole peak. An excitation wavelength of 306 nm and emission wavelength of 364 nm were used, based on the fluorescence properties of pyrazole **1**. After RP-HPLC analysis, the library members were transferred from autosampler vials to tared 7 × 40 mm flat bottom vials (8 mm crimp tops), and the solvent was then removed using a Savant vacuum centrifuge. After further drying in vacuo the sample weight was recorded, and a modified three-point competitive binding assay was then performed. Authentic HPLC traces obtained for **8a—l** (Table 1) were used to help confirm their later synthesis in the 96-member library. These controls represent 13% of the total library members produced. The RBA values of these "controls" from this library were equivalent to those obtained for the same compounds in the 12-membered library, within the statistical limits of the binding assay (coefficient of variation is 0.3).

References and Notes

(1) Dolle, R. E.; Nelson, K. H. J. Comprehensive Survey of Combinatorial Library Synthesis. *J. Comb. Chem.* **1999**, *1*, 235—282.

(2) Grese, T. A.; Dodge, J. A. Selective Estrogen Receptor Modulators (SERMS) [Review]. *Curr. Pharm. Des.* **1998**, *4*, 71—92.

(3) Grese, T. A.; Sluka, J. P.; Bryant, H. U.; Cullinan, G. J.; Glasebrook, A. L.; Jones, C. D.; Matsumoto, K.; Palkowitz, A. D.; Sato, M.; Termine, J. D.; Winter, M. A.; Yang, N. N.; Dodge, J. A. Molecular determinants of tissue selectivity in estrogen receptor modulators. *Proc. Natl. Acad. Sci. U.S.A.* **1997**, *94*, 14105—14110.

(4) Willard, R.; Jammalamadaka, V.; Zava, D.; Benz, C. C.; Hunt, C. A.; Kushner, P. J.; Scanlan, T. S. Screening and characterization of estrogenic activity from hydroxystilbene library. *Chem. Biol.* **1995**, *2*, 45—51.

(5) Brown, D. S.; Armstrong, R. W. Synthesis of tetrasubstituted ethylenes on solid support via resin capture. *J. Am. Chem. Soc.* **1996**, *118*, 6331—6332.

(6) Fink, B. E.; Mortensen, D. S.; Stauffer, S. R.; Aron, Z. D.; Katzenellenbogen, J. A. Novel structural templates for estrogen-receptor ligands and prospects for combinatorial synthesis of estrogens. *Chem. Biol.* **1999**, *6*, 205—219.

(7) Sun, J.; Meyers, M. J.; Fink, B. E.; Rajendran, R.; Katzenellenbogen, J. A.; Katzenellenbogen, B. S. Novel ligands that function as selective estrogens or antiestrogens for estrogen receptor-α or estrogen receptor-β. *Endocrinology* **1999**, *140*, 800—804.

(8) Nilsson, S.; Kuiper, G.; Gustafsson, J. A. ER beta: a novel estrogen receptor offers the potential for new drug development [Review]. *Trends Endocrinol. Metab.* **1998**, *9*, 387—395.

(9) Marzinik, A. L.; Felder, E. R. Solid support synthesis of highly functionalized pyrazoles and isoxazoles; scaffolds for molecular diversity. *Tetrahedron Lett.* **1996**, *37*, 1003—1006.

(10) Marzinzik, A. L.; Felder, E. R. Key intermediates in combinatorial chemistry: access to various heterocycles from α,β-unsaturated ketones on the solid phase. *J. Org. Chem.* **1998**, *63*, 723—727.

(11) Watson, S. P.; Wilson, R. D.; Judd, D. B.; Richards, S. A. Solid-phase synthesis of 5-aminopyrazoles and derivatives. *Tetrahedron Lett.* **1997**, *38*, 9065−9068.

(12) Wilson, R. D.; Watson, S. P.; Richards, S. A. Solid-phase synthesis of 5-aminopyrazoles and derivatives. *Tetrahedron Lett.* **1998**, *39*, 2827−2830.

(13) Green, J. Solid-Phase synthesis of lavendustin analogues. *J. Org. Chem.* **1995**, *60*, 4287−4290.

(14) Boojamra, C. G.; Burow, K. M.; Ellman, J. A. An Expedient and High-Yielding Method for the Solid-Phase Synthesis of Diverse 1,4-Benzodiazepine-2,5-Diones. *J. Org. Chem.* **1995**, *60*, 5742−5743.

(15) Cardillo, G.; Orena, M.; Porzi, G.; Sandri, S. Carbonate ion on a polymeric support: hydrolysis of alkyl halides and cyclic iodocarbonates. *Synthesis* **1981**, 793−794.

(16) Still, W. C.; Kahn, M.; Mitra, A. Rapid chromatographic technique for preparative separations with moderate resolution. *J. Org. Chem.* **1978**, *43*, 2923−2926.

(17) Katzenellenbogen, J. A.; Johnson, H. J., Jr.; Myers, H. N. Photo-affinity labels for estrogen binding proteins of rat uterus. *Biochemistry* **1973**, *12*, 4085−4092.

(18) Kuiper, G. G. J. M.; Carlsson, B.; Grandien, K.; Enmark, E.; Häggblad, J.; Nilsson, S.; Gustafsson, J.-Å. Comparison of the ligand binding specificity and transcript tissue distribution of estrogen receptor α and β. *Endocrinology* **1997**, *138*, 863−870.

(19) Mosselman, S.; Polman, J.; Dijkema, R. ERβ: identification and characterization of a novel human estrogen receptor. *FEBS* **1996**, *392*, 49−53.

(20) O'Connor, C. J.; Lomax, T. D. The reactivity of *p*-nitrophenyl esters with surfactants in apolar solvents. VII* substituent effects on the reactivity of 4′-nitrophenyl 4-substituted benzoates in benzene solutions of dodecylammonium propionate and butane-1,4-diamine bis(dodecanoate). *Aust. J. Chem.* **1983**, *36*, 917−925.

Pyrazole Ligands: Structure–Affinity/Activity Relationships and Estrogen Receptor-α-Selective Agonists

Shaun R. Stauffer, Christopher J. Coletta, Rosanna Tedesco,
Gisele Nishiguchi, Kathryn Carlson, Jun Sun,
Benita S. Katzenellenbogen, and John A. Katzenellenbogen

Departments of Chemistry, Physiology, and Cell and Structural
Biology, University of Illinois and University of Illinois College
of Medicine, Urbana, Illinois 61801

JOURNAL OF

MEDICINAL CHEMISTRY®

Articles

Pyrazole Ligands: Structure–Affinity/Activity Relationships and Estrogen Receptor-α-Selective Agonists

Shaun R. Stauffer,[†] Christopher J. Coletta,[†] Rosanna Tedesco,[†] Gisele Nishiguchi,[†] Kathryn Carlson,[†] Jun Sun,[‡] Benita S. Katzenellenbogen,[‡,#] and John A. Katzenellenbogen[*,†]

Departments of Chemistry, Physiology, and Cell and Structural Biology, University of Illinois and University of Illinois College of Medicine, Urbana, Illinois 61801

Received June 9, 2000

We have found that certain tetrasubstituted pyrazoles are high-affinity ligands for the estrogen receptor (ER) (Fink et al. *Chem. Biol.* **1999**, *6*, 205–219) and that one pyrazole is considerably more potent as an agonist on the ERα than on the ERβ subtype (Sun et al. *Endocrinology* **1999**, *140*, 800–804). To investigate what substituent pattern provides optimal ER binding affinity and the greatest enhancement of potency as an ERα-selective agonist, we prepared a number of tetrasubstituted pyrazole analogues with defined variations at certain substituent positions. Analysis of their binding affinity pattern shows that a C(4)-propyl substituent is optimal and that a *p*-hydroxyl group on the N(1)-phenyl group also enhances affinity and selectivity for ERα. The best compound in this series, a propylpyrazole triol (PPT, compound **4g**), binds to ERα with high affinity (ca. 50% that of estradiol), and it has a 410-fold binding affinity preference for ERα. It also activates gene transcription only through ERα. Thus, this compound represents the first *ERα-specific agonist*. We investigated the molecular basis for the exceptional ERα binding affinity and potency selectivity of pyrazole **4g** by a further study of structure–affinity relationships in this series and by molecular modeling. These investigations suggest that the pyrazole triols prefer to bind to ERα with their C(3)-phenol in the estradiol A-ring binding pocket and that binding selectivity results from differences in the interaction of the pyrazole core and C(4)-propyl group with portions of the receptor where ERα has a smaller residue than ERβ. These ER subtype-specific interactions and the ER subtype-selective ligands that can be derived from them should prove useful in defining those biological activities in estrogen target cells that can be selectively activated through ERα.

Introduction

The estrogen receptor (ER) displays a remarkable capacity for binding nonsteroidal ligands with high affinity.[1] Many of these ligands have been developed into hormonal agents having mixed agonist–antagonist and tissue-selective activities that are useful in menopausal hormone replacement, in fertility regulation, and in the prevention and treatment of breast cancer. Because of their unusual pharmacology, some of these agents have been termed **s**elective **e**strogen **r**eceptor **m**odulators (SERMs).[2] To understand the molecular basis of the tissue selectivity of these SERMs, it would be helpful to know in detail how they are interacting with the ER. However, short of performing X-ray crystallographic analysis of ER complexes with each ligand, it can be a challenge to obtain such information.

If the nonsteroidal ligand bears a reasonable structural relationship with steroidal estrogens, it is generally quite easy to imagine the orientation that this ligand is likely to adopt when it is bound by ER.[3,4] ER mutagenesis studies,[5] and the recent X-ray crystallographic structures of ER complexed with both estradiol and three nonsteroidal ligands (raloxifene, hydroxytamoxifen, and diethylstilbestrol), provide additional guidance in the selection of reasonable binding orientations for ligands of this type.[4,6] However, when the nonsteroidal estrogens have structures that are more divergent from those of steroidal estrogens, it becomes a greater challenge to predict ligand-binding orientation.[7]

The recent characterization of a second ER gene, encoding ERβ, places a further premium on our understanding of the details of ligand–receptor interaction,[8,9] because it would be especially interesting to have ligands that could activate or inhibit each of the ER subtypes with high selectivity. Such ligands would be valuable tools to define the biological effects that are mediated by ERα and ERβ. So far, however, there have been only a few reports of ER subtype-selective estrogens, and in many cases, the selectivity has been relatively modest.[10]

Recently, we investigated various heterocyclic diazole structures as core elements for nonsteroidal estrogens
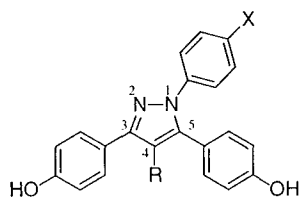
**Figure 1.** Pyrazole core optimized for high-affinity ER binding (X = H, OH; R = alkyl).

of novel design.[11,12] Our aim was to identify systems that would be amenable to combinatorial assembly and library synthesis. From among the several systems we studied that included imidazoles, oxazoles, thiazoles, and isoxazoles, we found that high-affinity ER ligands could be obtained by appropriate substitution on a pyrazole core. Subsequently, we used a parallel, solid-phase synthesis approach to prepare some combinatorial pyrazole libraries of moderate size.[13] In the cases we investigated, high-affinity binding required tetrasubstitution of the pyrazole core and an appropriate display of aromatic, phenolic, and aliphatic groups.[11,12] An example of this optimal pattern of substitution that we have thus far delineated for pyrazoles includes three aromatic groups at the 1-, 3-, and 5-positions, specifically phenols at the 3- and 5-positions, and an alkyl group at the 4-position (Figure 1). Initial studies on one of these compounds (Figure 1; X = H, R = Et) showed that it acted as an agonist on both ER subtypes, but it was considerably more potent on ERα than on ERβ.[14] Thus, this pyrazole was termed an ERα potency-selective agonist.[14]

In this report, we have investigated structure–activity relationships in these tetrasubstituted pyrazoles to delineate two aspects of their behavior: (1) the C(4)-alkyl substituent and phenol hydroxyl pattern that provide optimal ER subtype selectivity and (2) the extent to which the ERα-selective binding affinity and potency of these pyrazoles can be understood in the context of crystal structures of the ERα ligand-binding domain (LBD) and models for ERβ derived from these structures. Our studies provide new information on these issues, and in the process, we have identified a pyrazole that shows complete ERα selectivity in transcription activation by the receptor.

Results and Discussion

Chemical Syntheses. The compounds we have studied have various C(4)-alkyl substituents and have either a phenyl or 4-hydroxylphenyl substituent on N(1). Shown in Scheme 1 is the route used for the synthesis of the pyrazoles **4a–i**. The starting alkylphenones **1a–f** were readily prepared in good yields by Friedel–Crafts acylation of anisole. The requisite β-diketones **2a–e** were then produced in moderate to good yields by acylation of the corresponding lithium enolates with 4-nitrophenyl 4-methoxybenzoate. Because the pyrazoles are sterically crowded, rather harsh conditions were required for their formation (>16 h at reflux at 110–120 °C in DMF/THF solution). Nonetheless, these conditions served quite well for pyrazole formation in solution. Several of the pyrazole intermediates protected as methyl ethers were isolated in good yield. However, with the trimethoxy pyrazoles **3g–i**, it was difficult to

Scheme 1. Synthesis of C(4)-Alkylpyrazole Analogues
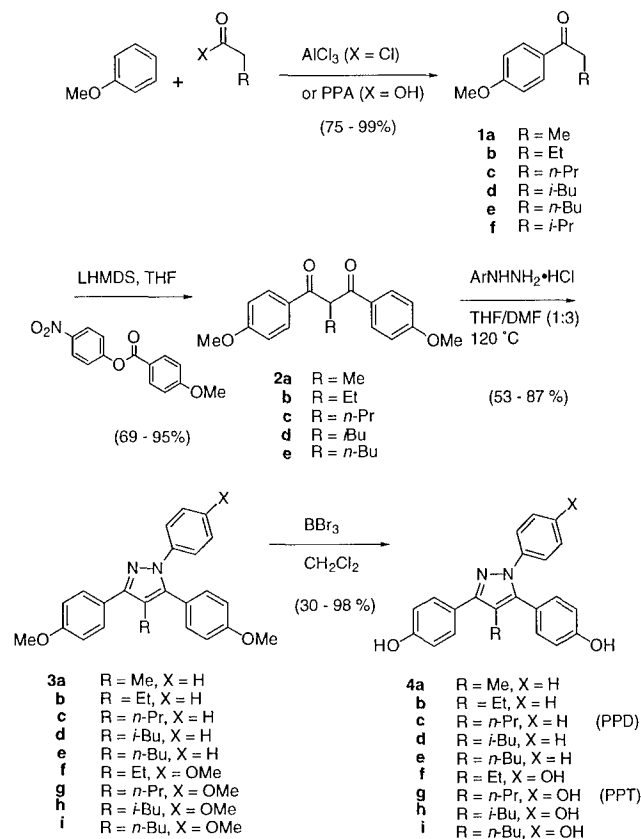
separate the protected product from traces of the diketone precursor by chromatography. So, in these cases the crude material was passed through a short silica gel column and, without further purification, was then deprotected using BBr$_3$. Pyrazoles **3d,e** were also treated in this manner. The final phenolic pyrazoles **4a–i** were isolated in 30–98% yield after purification by recrystallization and/or chromatography.

In addition to the final pyrazole products **4a–i**, we wished to prepare the isopropyl analogue derived from ketone **1f**. However, we encountered difficulties in the preparation of this hindered dione because of significant O-acylation that occurred during the Claisen condensation. Separation of the O-acylated byproduct from the desired dione proved to be difficult. Moreover, once the dione was isolated, the pyrazole condensation failed using the conditions described above, which had been optimized for solution-phase synthesis. To avoid these problems, we utilized a solid-phase synthesis according to the methodology that we had previously developed,[13] and in this manner we were able to obtain the isopropylpyrazole **6** starting from the resin-bound ketone **5**, as shown in Scheme 2, although the overall yield was relatively low.

To prepare a complete series of all of the possible diphenol and monophenol analogues of the C(4)-ethyl triphenol **4f**, we also synthesized monophenols **7a–c** and the remaining diphenols **8a,b** (all mono- and diphenols are shown in Scheme 3, top). Monophenol **7a** was prepared from dibenzoylmethane (**9**) and 4-methoxyphenylhydrazine by the usual sequence[11] (Scheme 3, middle). The synthesis of the remaining two monophenols (**7b,c**) by a regioselective route has been described elsewhere (not shown).[15] The two remaining

Scheme 2. Synthesis of C(4)-Isopropylpyrazole **6** by Solid-Phase Methodology[13]

6 (11%, three steps from ketone)
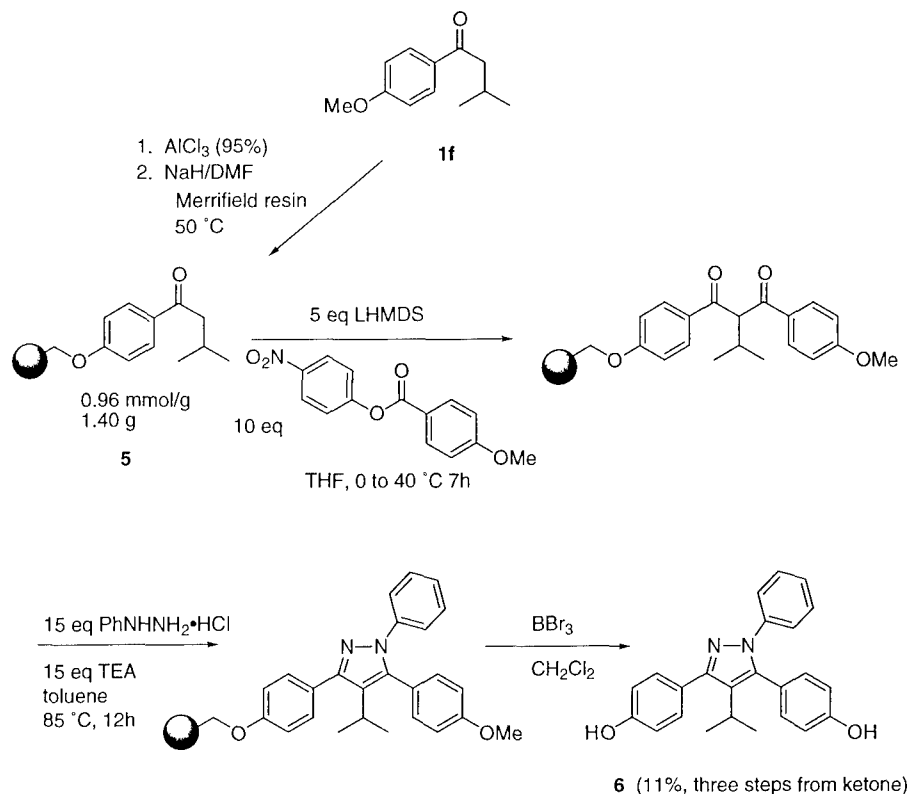
diphenols (**8a,b**) were also prepared by this regio-selective method, as shown in Scheme 3 (bottom). The two chalcones (**12a,b**) are treated with p-methoxy-phenylhydrazine under anerobic conditions to give the pyrazolines **13a,b**. The corresponding anions, generated by treatment with LDA, were ethylated, and the C(4)-ethylpyrazolines **14a,b** were then oxidized to the pyrazoles **15a,b** and deprotected to the desired bisphenols **8a,b**.

ER Binding Affinity of Tetrasubstituted Pyrazoles. The ER binding affinity of pyrazoles **4a–i**, **6**, **7a–c**, and **8a,b** was determined in a competitive radiometric binding assay using purified full-length human ERα and ERβ, as previously described.[16,17] The affinities are expressed as relative binding affinity (RBA) values and are presented in two tables: Table 1, which is discussed here, covers the effect of the nature of the C(4)-alkyl substituent on the binding affinity and ER subtype selectivity of pyrazoles in the triphenol and the principal 3,5-diphenol series; the data in Table 2, which compares the affinity of the three possible mono- and diphenols with the triphenol in the C(4)-ethylpyrazole series, relates to the issue of ligand orientation and is discussed in a later section.

Two interesting trends are notable in the binding affinity data presented in Table 1. In both the diphenol series (X = H, **4a–e**, **6**) and the triphenol series (X = OH, **4f–i**), optimal binding affinity for ERα requires a C(4)-alkyl substituent that is not too long (n-Bu: **4e,i**) or too short (Me: **4a**), the highest affinity being found with the intermediate size substituents: Et (**4b,f**), n-Pr (**4c,g**), and i-Bu (**4d,h**). Thus, it appears that the subpocket that is accommodating this group has a limited size and relatively narrow shape. A more significant trend evident in this series has to do with

the effect of the phenolic substituent on the N(1)-phenyl group. In each case where a comparison can be made (namely, Et, Pr, i-Bu, or n-Bu), the triphenols (X = OH, **4f–i**) have higher affinity on ERα and/or lower affinity on ERβ than do the diphenols (X = H, **4a–e**). As a result, the triphenols consistently have higher ERα affinity selectivity than do the corresponding 3,5-diphenols.[18] In fact, some of the members show a remarkable selectivity in their binding affinity for ERα vs ERβ, which is 30–40 for some of the pyrazole diols (**4c,d**) and as high as 200–400 for some of the pyrazole triols (**4f,g**).

The increased ERα binding affinity of the triphenols is not expected, because additional polar substituents are generally poorly tolerated in the center of the ligand-binding pocket of ER, at least in most nonsteroidal ligand systems that have been examined, such as the benzo[b]thiophenes[19] and 2,3-diarylindans.[7] One exception is found with certain triphenylacrylonitriles, where addition of a third hydroxyl increases binding affinity.[20]

We have previously reported binding affinities for one of these pyrazoles (**4b**), using receptor preparations containing only the *LBDs* of human ERα and ERβ, rather than *full-length* human ERα and ERβ.[14] The values obtained previously were higher but less ERα-selective (60 ± 16 for ERα and 18 ± 4 for ERβ). At this point, the reasons for these affinity differences between full-length ER and the ER LBD are not clear, although they have been seen, as well, in a structurally different class of ER ligands.[17] However, it is of note that the higher ERα/ERβ affinity ratio that we obtain for pyrazole **4b** with the full-length ERs is more consistent with the 120-fold potency ratio we described in transcription assays than was the 3-fold ERα/ERβ affinity ratio obtained with ERs containing only the LBDs.[14]

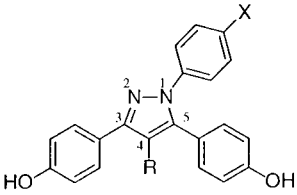**Transcriptional Activity and Potency of Tetra-**

Scheme 3. Synthesis of the Remaining Mono- and Diphenolic C(4)-Ethylpyrazoles

		X	Y	Z
Monophenols:	7a	OH	H	H
	7b	H	OH	H
	7c	H	H	OH
Diphenols:	4b	H	OH	OH
	8a	OH	H	OH
	8b	OH	OH	H
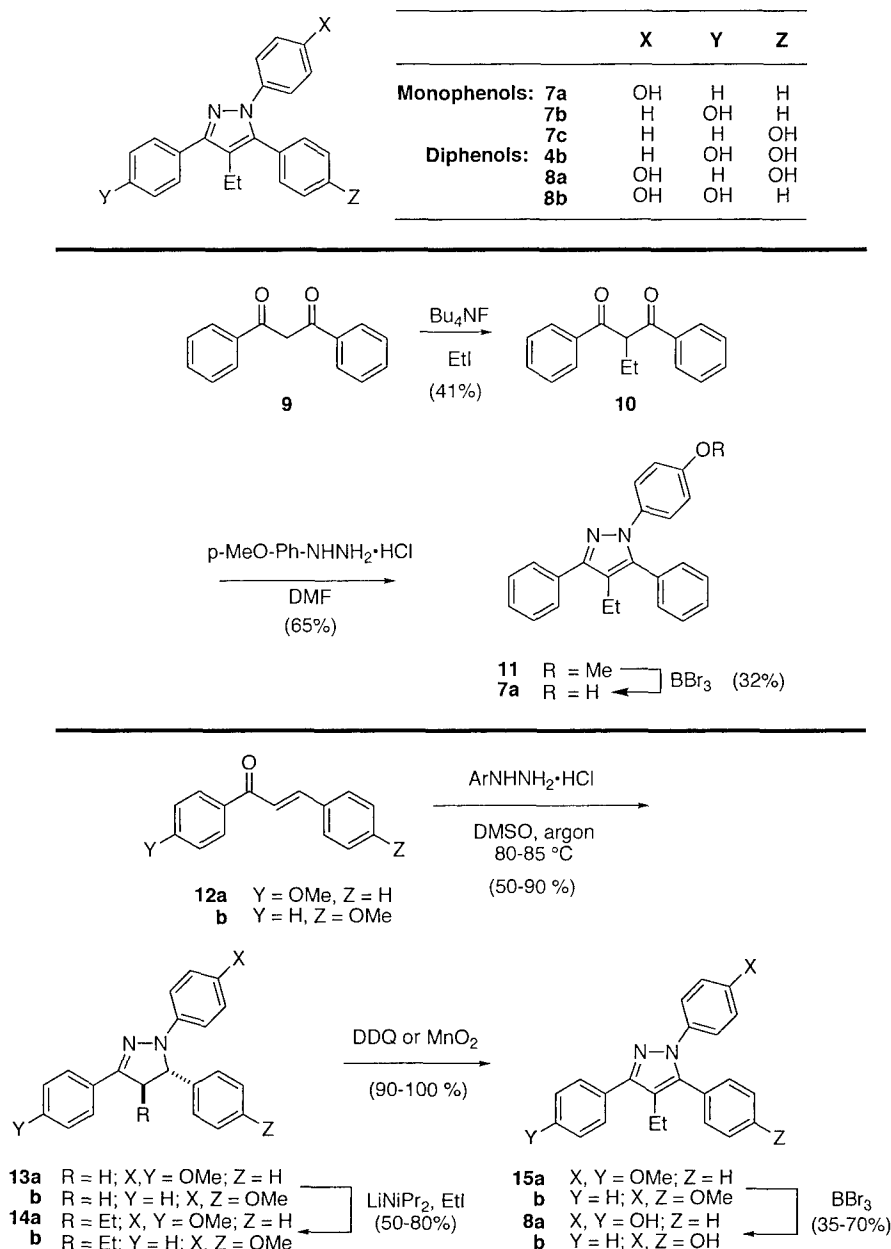
substituted Pyrazoles. For investigation of transcription activation ability, we selected two compounds: the pyrazole having the highest ERα/ERβ affinity selectivity (410-fold, the propylpyrazole triol **4g**, called PPT for convenience) and the corresponding pyrazole in the diol series (**4c**, called propylpyrazole diol or PPD). These two pyrazoles were assayed for estrogen agonist activity in transactivation assays using human endometrial cancer (HEC-1) cells transfected with expression plasmids for ERα and ERβ and an estrogen-responsive reporter gene plasmid. The dose–response curves for these compounds are shown in Figure 2.

Both compounds are potent in activating gene transcription through ERα, but the PPD (**4c**) is weak in transcriptional activation through ERβ and PPT (**4g**) is completely inactive in stimulating transcription via ERβ. Thus, PPT (**4g**) is an ERα-specific agonist. This pharmacological profile is reminiscent of the behavior of the C(4)-ethyl analogue of pyrazole **4c** (namely, pyrazole **4b**), that we have previously described as an

agonist that is more potent on ERα than on ERβ. This compound (**4b**) had an EC$_{50}$ of ca. 1 nM on ERα and showed a 120-fold potency selectivity for this ER subtype.[14] However, in cell transfection assays both PPT and PPD are nearly 10-fold more potent than the original pyrazole **4b** on ERα, and they are much more ERα-selective.

As we had noted in our earlier study on pyrazole **4b**,[14] and is clearly evident here as well, the ERα selectivity of these pyrazoles in terms of their *potency* in transcription assays is substantially greater than their *affinity* selectivity in binding assays. For example, the ERα affinity selectivity of PPD (**4c**) is 32, yet its potency selectivity is ca. 1000 (cf. Figure 2). Likewise, the ERα affinity selectivity of PPT (**4g**) is 410, and its potency selectivity, which although is difficult to accurately evaluate (cf. Figure 2), is probably greater than 10000. Such a discordance between affinity and potency might be explained in the context of "tripartite receptor pharmacology", a concept that we advanced some time

Table 1. Relative Binding Affinity Data for C(4)-Alkyl Triphenol and 3,5-Diphenol Pyrazole Analogues[a]

compd	R	X	RBA ERα[b]	RBA ERβ[b]	ERα/ERβ RBA ratio
			3,5-Diphenols		
4a	Me	H	0.76 ± 0.18	0.28 ± 0.16	2.7
4b	Et	H	31 ± 15	1.1 ± 0.2	28
6	i-Pr	H	5.6 ± 2	0.86 ± 0.11	6.5
4c (PPD)	n-Pr	H	16.8 ± 0.3	0.52 ± 0.03	32
4d	i-Bu	H	56 ± 6	1.4 ± 0	40
4e	n-Bu	H	8.7 ± 2.0	0.47 ± 0.1	19
			1,3,5-Triphenols		
4f	Et	OH	36 ± 6	0.15 ± 0.014	240
4g (PPT)	n-Pr	OH	49 ± 12	0.12 ± 0.04	410
4h	i-Bu	OH	75 ± 6	0.89 ± 0.06	84
4i	n-Bu	OH	14 ± 4	0.18 ± 0.09	77

[a] Relative binding affinity (RBA), where estradiol is 100%. Values are the mean of at least 2 and more typically 3 or more independent determinations (±SD).[33] [b] Competitive radiometric binding assays were done with purified full-length human ERα and ERβ (PanVera Inc.), using 10 nM [³H]E₂ as tracer and HAP for adsorption of the receptor—tracer complex.[16,17]

ago.[21] Binding measured in vitro with purified ERs involves only the interaction between ligand and receptor, whereas transcription measured in cells involves the additional interaction of the ligand—receptor complex with coactivators and other cellular components. Thus, compared to their relative affinities for ERα and ERβ, the relative potency of two ligands can be modulated by differences in the strength with which their respective ligand—receptor complexes bind to coactivators or are modified by other cellular elements, although other factors, as well, might be involved. In this case, it appears that the pyrazole complexes with ERα are better able to bind coactivators than are the ERβ—pyrazole complexes, as we have documented in a recent study.[22]

A Model for the Binding of Pyrazoles with the ER Subtypes. The high affinity, and particularly the high selectivity, with which these pyrazoles bind to ERα raises the important issue of what molecular features underlie the differences in their interaction with ERα vs ERβ. Without crystal structures available for the comparison of any of these pyrazoles complexed with both ERα and ERβ, we are currently limited to investigating this issue by molecular modeling.

1. Structure—Affinity Relationships and the Orientation of Pyrazoles in the Ligand-Binding Pocket of ERα. Because the pyrazoles we have studied here are rather symmetrical and are polyphenolic, it is not obvious which orientation these ligands might prefer to adopt within the ligand-binding pocket of ER. In principle, the triphenolic pyrazoles could adopt six orientations (see Figure 4): Each of the three phenolic rings could play the role of the A-ring of estradiol, and in each case the remainder of the pyrazole could adopt two orientations about the bond connecting the A-ring phenol mimic to the pyrazole core (darkened bond).

These six binding modes are given the designations: N(1), N(1)′, C(3), C(3)′, C(5), and C(5)′.

A classical approach that has been used to try to ascertain which orientation di- and triphenolic compounds adopt within the ER binding pocket has been to systematically delete the phenolic hydroxyl group and examine the effect of this deletion on the binding affinity.[7] Because the hydroxy group on the phenol that corresponds to the A-ring of estradiol is thought to make the major contribution to ligand-binding affinity, the greatest reduction in binding should occur when this hydroxyl group is the one deleted.[3] We have undertaken such an analysis by comparing the affinities of pyrazoles in which the three phenols in the triphenol **4f** were each singly deleted (diphenol set: **4b, 8a,b**) or were deleted in three pairs (monophenol set: **7a–c**). The affinities of these three diphenols and three monophenols, together with the triphenol parent **4f**, are listed in Table 2. Because we had prepared the most pyrazoles in the C(4)-ethyl series, we chose to do this structure—affinity study in this series.

The simplest analysis we can make of the structure—binding affinity pattern shown in Table 2 is the following: In the monophenol set (**7a–c**), the N(1)- and C(3)-phenols (**7a,b**) have comparable affinities, but the C(5)-phenol (**7c**) binds ca. 100-fold less well. Because of the very low affinity of the C(5)-monophenol (**7c**), we believe that the C(5)-phenol cannot function as the mimic of the A-ring of estradiol, in essence, eliminating orientations C(5) and C(5)′ as possibilities. (It is of note that these two "eliminated" binding modes project bulky groups simultaneously in directions that correspond to C(7) and C(11) of estradiol; cf. Figure 3.) Elimination of the C(5)-phenol leaves the N(1)- and C(3)-phenols as potential estradiol A-ring mimics, but the very similar affinities of both of these monophenols suggest that each one may function as the A-ring mimic.

Analysis of the binding affinity pattern of the bisphenols is somewhat more ambiguous, but suggestive, nevertheless: Deletion of the N(1)-phenol from the triphenol has only a minor effect on the binding affinity (**4b** vs triphenol **4f**), which means that in the context of the triphenol in ERα, the N(1)-phenol is not contributing significantly to binding affinity. Thus, one would expect that the C(3)-phenol is likely to be the more important of the two and thus that the orientations C(3) and C(3)′ are more likely than the orientations N(1) and N(1)′. Deletion of either the C(3)-phenol or the C(5)-phenol results in a 4–5-fold decrease in binding (**8a,b** vs **4f**). The fact that the N(1),C(3)-bisphenol (**8b**) still binds quite well is not surprising, because the C(3)-phenol is still available to be the estradiol A-ring mimic. However, the fact that the N(1),C(5)-phenol (**8a**) also binds quite well might seem surprising, because this diphenol lacks the important C(3)-hydroxyl.

We believe that the reasonably good affinity of diphenol **8a** suggests that this pyrazole can bind with the N(1) group as the estradiol A-ring mimic, meaning that the N(1) and N(1)′ ligand orientations are also possible, though, based on the minimal effect of the N(1)-phenol deletion, they are probably not significantly populated when a C(3)-phenol is available. (It seems unlikely that diphenol **8a** would bind with the C(5)-phenol in the A-ring pocket, because of the very low affinity of the
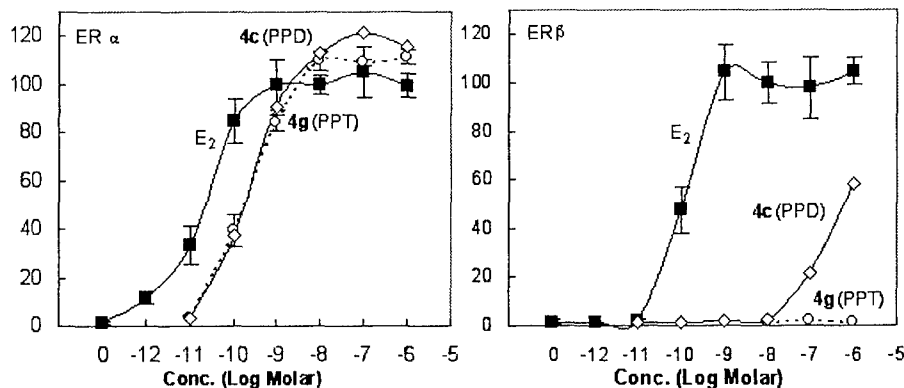
Figure 2. Transcription activation by ERα (left) and ERβ (right) in response to pyrazoles **4c** (PPD) and **4g** (PPT). Human endometrial cancer (HEC-1) cells were transfected with expression vectors for ERα or ERβ and an (ERE)3-pS2-CAT reporter gene and were treated with the indicated concentrations of ligand for 24 h. CAT activity was normalized for β-galactosidase activity from an internal control plasmid. Values are expressed as a percent of the ERα or ERβ response with 1 nM E_2, which is set at 100%.[32]
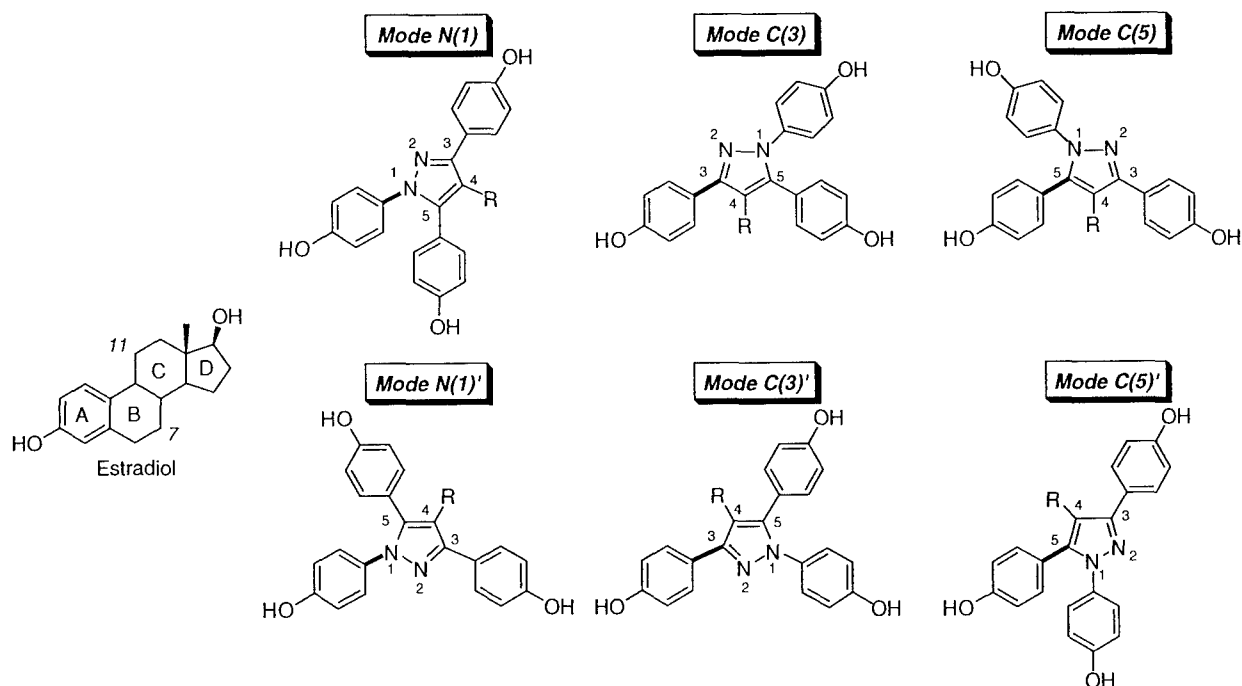

Figure 3. Potential pyrazole binding relative to estradiol. Both modes A and A′ have the C(3)-phenol oriented to project in to the estradiol A-ring binding pocket. Modes A and A′ are related to one another by rotation of the pyrazole core around the darkened bond.

C(5)-monophenol **7c**.) Thus, the phenol deletion/binding affinity approach has only reduced the number of possible ligand orientations in the binding pocket from six to four, with a suggested preference for two orientations, C(3) and C(3)′. As described in the section below, we have tried to narrow down the possible ligand orientations even further by molecular modeling.

The conclusions thus far that the C(3)-phenol is the preferred A-ring mimic but that the N(1)-phenol is a possible alternative are consistent with two other studies that we have recently completed. In a related but more limited investigation of the orientation of ligand binding in two isomeric pyrazole series, we concluded that the orientation with the C(3)-phenol as the A-ring mimic was most likely in the pyrazole series that is the same as the one studied here and that in the isomeric series the phenol that occupied topologically congruent substituent position also functioned as the A-ring mimic.[23] In another investigation in which we worked

to convert these pyrazoles from agonists to antagonists by appending a basic side chain onto the four substituents on these pyrazoles, we found that high affinity was retained only when this group was attached to the C(5)-hydroxyl.[24] On the basis of this structure–affinity pattern, as well as some molecular modeling and consideration of the structure of the ER LBD complexes with antagonists, we concluded in that study that the most likely orientation of these basic side chain-substituted pyrazoles was N(1).[24] In this orientation, the basic side chain could project outward through the 11β-channel that forms in the ER LBD complexes with antagonists.[4,6]

2. Molecular Modeling of the Orientation of Pyrazole Triols in the Ligand-Binding Pocket of the ERs. We have previously done modeling of the pyrazole ligands in the ER LBDs, first in our initial study on these ligands[11] and, more recently, in connection with a study of the orientation of these ligands in
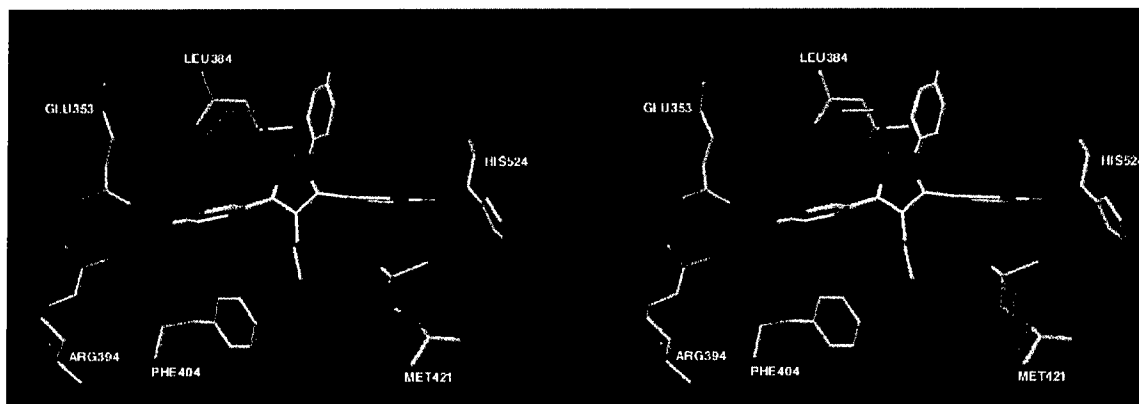
Figure 4. Crossed-stereoview of propylpyrazole triol (PPT, **4g**) docked and minimized in ERα LBD pocket according to binding mode A, showing selected residues close to the ligand. The pyrazole ligand is shown with standard atom colors. The residues in ERα are identified and shown in yellow. At the two positions where the ERβ sequence differs from ERα, the ERβ residues are shown in red (Met in ERβ in place of ERα Leu384 and Ile in ERβ in place of ERα Met421).

Table 2. Relative Binding Affinity Data for C(4)-Ethylpyrazole Tri-, Di-, and Monophenols[a]

compd	X N(1)	Y C(3)	Z C(5)	RBA ERα[b]	RBA ERβ[b]	ERα/ERβ RBA ratio
				Monophenols		
7a	OH	H	H	3.1 ± 0.5	1.5 ± 0.2	2.1
7b	H	OH	H	2.6 ± 0.1	0.61 ± 0.2	4.3
7c	H	H	OH	0.04 ± 0.11	0.06 ± 0.01	0.67
				Diphenols		
4b	H	OH	OH	31 ± 15	1.1 ± 0.2	28
8a	OH	H	OH	7.0 ± 0.6	0.80 ± 0.09	9
8b	OH	OH	H	8.9 ± 0.6	0.32 ± 0.01	28
				Triphenols		
4f	OH	OH	OH	36 ± 6	0.15 ± 0.014	240

[a] Relative binding affinity (RBA), where estradiol is 100%. Values are the mean of at least 2 and more typically 3 or more independent determinations (±SD).[33] [b] Competitive radiometric binding assays were done with purified full-length human ERα and ERβ (PanVera Inc.), using 10 nM [³H]E₂ as tracer and HAP for adsorption of the receptor–tracer complex.[16,17]

the binding pocket.[23] As a result of this latter study,[23] we have come to appreciate that there are some ambiguities in how polyphenolic ligands such as these pyrazoles might be accommodated by ER, at least at the level at which we are currently able to model. Such ambiguity is echoed in the results of the structure–binding affinity considerations discussed above. Therefore, for the purposes of this paper, we have chosen to illustrate a binding mode for these pyrazoles in which the C(3)-phenyl group is placed in the ER LBD pocket that normally binds the A-ring of estradiol (Figure 3, see C(3) and C(3)′), as this appeared to be the most likely orientation for these polyphenolic systems (see above and ref 23). We have, however, also examined the other four possible orientations.

We conducted a ligand docking/binding minimization routine by placing PPT (**4g**) in ERα in both orientations: mode C(3) and mode C(3)′ (Flexidock routine within Sybyl; see Experimental Section, Molecular

Modeling). During the course of the ligand docking routine, the PPT that began in orientation mode C(3)′ became reoriented into mode C(3), whereas the one that began in mode C(3) remained in mode C(3). Therefore, mode C(3)′ was not considered further. After the docking/minimization routine, the PPT in mode C(3) was nicely accommodated in this orientation, with only minimal changes in the side chain conformations of some of the residues that line the ligand-binding pocket. We also modeled the four other possible orientations of this pyrazole using the same routine (not shown), but we found that none of them gave a fit as good as that of the pyrazole orientation illustrated as mode C(3) in Figure 3. The fact that the N(1) and N(1)′ modes did not score well in our modeling, although they seemed possible on the basis of the structure–affinity considerations above, suggests either limitations in our modeling method or the fact that these modes are not important in the triphenolic pyrazoles and only become important when certain phenols are missing (see above) or a basic side chain is appended.[24]

In Figure 4, we show a crossed-stereoview skeletal model illustrating PPT (**4g**) in the ERα structure, oriented in binding mode C(3), after the ligand docking/minimization routine. For clarity and for the ERα and ERβ comparison below, only selected residues from ER are shown. In this orientation, the N(1)-phenyl group of PPT (**4g**) projects into a region of the binding pocket which represents the C/D-subpocket that is normally occupied by portions of the C- and D-rings and the 18-methyl substituent on estradiol (E₂). Despite the importance of the N(1)-phenol in enhancing ERα binding selectivity (see above and Table 1), there are no obvious sites for its interaction in this subpocket. The N(1)- and C(5)-aryl groups of PPT project somewhat more deeply into the C/D-subpocket than do the corresponding regions of estradiol. However, this region is known to tolerate a variety of substituents,[3] and certain residues have been repositioned by the docking/minimization routine to make additional space for the pyrazole ligand. It is of note that these residue conformational changes, which allow for PPT binding in this mode, involve relatively minimal alteration in the total protein energy.

3. Analysis of Interactions Between Pyrazole Substituents and Amino Acid Residues in ERα and ERβ. We have used the C(3) orientation mode
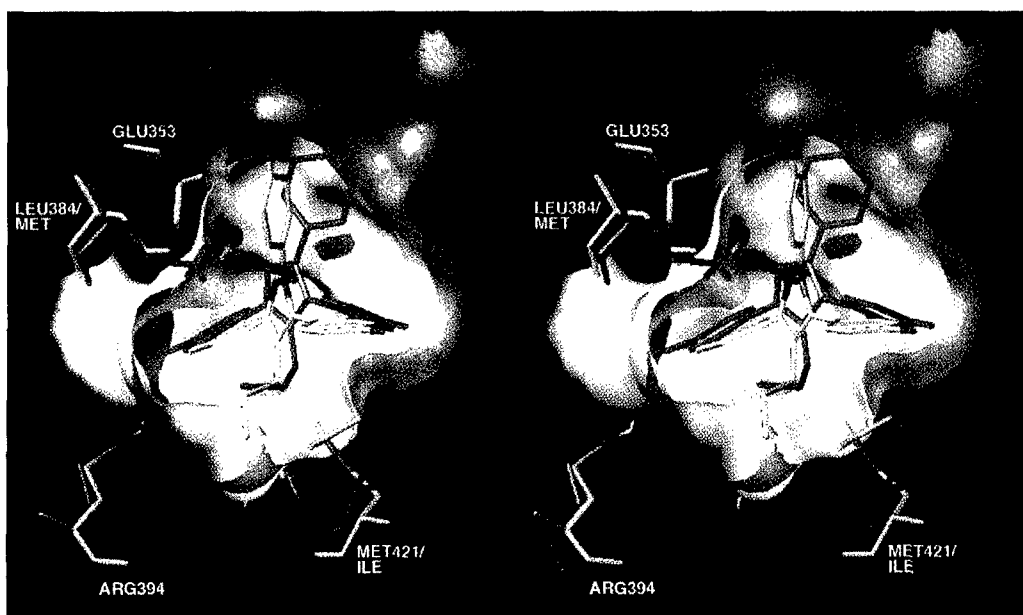
Figure 5. Crossed-stereoview of ligand skeletal structures and receptor molecular surfaces for the ERα— and ERβ—propylpyrazole triol (PPT, **4g**) complexes. The PPT in ERα is shown with standard atom colors, and the ERα receptor surface is shown in yellow; in the ERβ—PPT complex, both the ligand and receptor surface are shown in red. For further details, see text.

model derived above to try to understand the origins of the high ERα affinity selectivity of PPT (**4g**), and to do this, we have constructed a model for ERβ that is derived from ERα LBD—diethylstilbestrol (DES) structure (see Experimental Section for details).[6] Although the LBDs of ERα and ERβ have only 56% amino acid identity, the residues that line the ligand-binding pocket are nearly identical.[25] In fact, of the 22—24 residues that are considered to be in contact with the ligand (i.e., within 4 Å), all but two are identical in ERα and ERβ.[25] The only differences are at ERα position 384, where ERα has a leucine but ERβ has a methionine, and at ERα position 421, where ERα has a methionine but ERβ has an isoleucine. It has been speculated that these sequence differences, in particular, may underlie the differences in the ERα and ERβ binding affinities of ligands that have been studied so far.[25] For clarity, we have distinguished these residues in Figure 4 by color: The residues common to ERα and ERβ are illustrated in yellow, but at the two positions where the ERβ residues are different, the ERβ residues, colored in red, are superimposed over the ERα residues in yellow (see Figure 4 and legend).

In this model with the most ERα potency-selective ligand PPT (**4g**), we can see that the pyrazole core itself has the closest contact with Leu384 in the case of ERα and Met384 in the case of ERβ. For the Met/Ile discriminating residues at ERα position 421, the C(4)-propyl group as well as the C(5)-aryl group appear to have close contacts, although this interaction seems less severe.

A model for PPT (**4g**) binding to ERβ was generated by changing the two residues in the ERα ligand-binding pocket to those found in ERβ, inserting the ligand according to mode C(3), and then conducting the ligand docking/minimization routine as was done before with ERα (see Experimental Section). The comparative fit of this pyrazole in the ligand-binding pocket of ERα and ERβ can be appreciated by the composite receptor surface model shown in Figure 5 in crossed-stereoview.

In this figure, we have displayed the pyrazoles in both of the receptors as skeletal structures, and the two pockets as colored surfaces. The ligand in the ERα model is shown with standard atom colors and the ERα surface in yellow; both the ligand and receptor in the ERβ model are shown in red. In this figure, the view has been rotated, twisting the C(3)-phenol away from the viewer; this orientation is the best we have found to display differences between the two models.

The principal difference in the surface of the ligand-binding pocket is at the site where ERα has a smaller residue (Leu384) than ERβ (Met384). This is illustrated by the sharp red interpenetrating surface in the middle left region of the pocket. The increased steric bulk in ERβ at this site makes contact with the pyrazole core of this ligand, displacing it relative to the pyrazole position in the ERα model. Because the C(3)-phenol remains relatively fixed in the rather rigid A-ring binding pocket, this pyrazole core displacement causes a large shift in the position of the N(1)-phenol and a significant but somewhat smaller shift of the C(5)-phenol and the propyl group. The large shift of the N(1)-phenol is intriguing, because this group contributes significantly to the ERα affinity and potency selectivity of these pyrazoles. However, we have been unable to identify any interaction in the N(1)-phenol subpocket that would favor the presence of a hydroxyl in ERα and disfavor it in ERβ.

The shift of the propyl group forces this substituent to adopt a gauche conformation in ERβ (vs an anti orientation in ERα); this is a change that would most likely increase ligand internal energy and reduce binding affinity. The shift of the pyrazole position in the ERβ model moves the C(5)-phenol toward the site where the smaller Ile residue in ERβ replaces the bulkier Met421 in ERα. Thus, the different shape of the ligand-binding pocket in ERβ, in particular the increased bulk of the ERβ Met residue where ERα has a Leu, appears to interfere with the optimal binding of the pyrazole ligand and is therefore thought to account for its lowered

binding affinity. It is interesting to note that even after extensive minimization, there is a substantial energy difference between the two complexes, with the ERα complex having greater stabilization by ca. 30 kcal/mol.

Conclusions

A series of C(4)-alkyl tetrasubstituted pyrazole analogues have been prepared and their RBA values determined for the ER. These compounds show an interesting binding affinity pattern, including high-affinity selectivity for ERα, which for the propylpyrazole triol (PPT, **4g**) reaches 410-fold. This compound also has very high potency selectivity for ERα in reporter gene transcription assays in cells, and it is the first ERα-specific agonist. Structure–affinity relationships in a series of mono-, di-, and triphenolic pyrazoles and molecular modeling suggests that these pyrazoles bind to the ER with the C(3)-phenol in the A-ring binding pocket. A model of PPT (**4g**) docked in the ERα LBD–DES crystal structure in the most likely binding orientation suggests that the very high ERα binding selectivity of this pyrazole derives from particular interactions between the pyrazole core and the C(4)-propyl group with a region on the ligand-binding pocket where ERα has a smaller residue (Leu384) than ERβ (Met384). These interactions may serve as the basis for future structure-based design of ERα- and ERβ-specific ligands.

Experimental Methods

General. All reagents and solvents were obtained from Aldrich, Fisher, or Mallinckrodt. Tetrahydrofuran was freshly distilled from sodium/benzophenone. Dimethylformamide was vacuum distilled prior to use and stored over 4 Å molecular sieves. Melting points were determined on a Thomas-Hoover UniMelt capillary apparatus and are uncorrected. All reactions were performed under a dry N_2 atmosphere unless otherwise specified. Reaction progress was monitored by analytical thin-layer chromatography using GF silica plates purchased from Analtech. Visualization was achieved by short-wave UV light (254 nm) or potassium permanganate stain. Radial preparative-layer chromatography was performed on a Chromatotron instrument (Harrison Research, Inc., Palo Alto, CA) using EM Science silica gel Kieselgel 60 PF_{254} as adsorbent. Flash column chromatography was performed using Woelm 32–63 μm silica gel packing.[26] Synthetic procedures for **1a**–**f** and spectral data for **1d,f** are described below. Compounds **1a**,[27] **1b**,[28] **1c**,[29] and **1e**[30] were spectroscopically identical to the reported compounds. The synthesis of compounds **7b,c** has been described elsewhere.[15]

^{1}H and ^{13}C NMR spectra were recorded on either a Varian Unity 400 or 500 MHz spectrometers using $CDCl_3$ or MeOD-d_4 as solvent. Chemical shifts are reported as parts per million downfield from an internal tetramethylsilane standard (δ 0.0 for ^{1}H) or from solvent references. NMR coupling constants are reported in hertz (Hz). ^{13}C NMR were determined using either the attached proton test (APT) or standard ^{13}C pulse sequence parameters. Low- and high-resolution electron impact mass spectra were obtained on Finnigan MAT CH-5 or 70-VSE spectrometers. Low- and high-resolution fast atom bombardment (FAB) were obtained on a VG ZAB-SE spectrometer. Elemental analyses were performed by the Microanalytical Service Laboratory of the University of Illinois. Those final components that did not give satisfactory combustion analysis (i.e., **4b**–**d**, **6**, **8a**) gave satisfactory exact mass determinations and were found to be at least 98% pure by HPLC analysis under normal and reversed-phase conditions.

RBA Assays. Purified ERα and ERβ binding affinities were determined using a competitive radiometric binding assay using 10 nM [^{3}H]estradiol as tracer, commercially available ERα and ERβ preparations (PanVera Inc., Madison, WI), and

hydroxylapatite (HAP) to adsorb bound receptor–ligand complex.[16,17] HAP was prepared following the recommendations of Williams and Gorski.[31] All incubations were done at 0 °C for 18–24 h. Binding affinities are expressed relative to estradiol (RBA = 100%) and are reproducible with a coefficient of variation of 0.3.

Transcription Activation Assays. Human endometrial cancer (HEC-1) cells were maintained in culture and transfected as described previously.[32] Transfection of HEC-1 cells in 60-mm dishes used 0.4 mL of a calcium phosphate precipitate containing 2.5 μg of pCMVβGal as internal control, 2 μg of the reporter gene plasmid, 100 ng of the ER expression vector, and carrier DNA to a total of 5 μg DNA. CAT activity, normalized for the internal control β-galactosidase activity, was assayed as previously described.[32]

Molecular Modeling for Pyrazole 4g. The starting conformation for **4g** used for receptor docking studies was generated from a random conformational search performed using the MMFF94 force field as implemented in Sybyl 6.6. The resulting lowest-energy conformer was then used for docking studies. Charge calculations were determined using the MMFF94 method and molecular surface properties displayed using MOLCAD module in Sybyl 6.6.

Pyrazole **4g**, generated as noted above, was prepositioned in the DES–ERα LBD crystal structure (Protein Data Bank code 3ERD)[6] using a least-squares multifitting of select atoms within the DES ligand. Once prepositioned, DES was deleted and ligand **4g** optimally docked in the ERα binding pocket using the Flexidock routine within Sybyl (Tripos). Both hydrogen-bond donors and acceptors within the pocket surrounding the ligand (Glu353, Arg394, and His524), the ligand itself, and select torsional bonds were defined. The best docked receptor–ligand complex from Flexidock then underwent a three-step minimization: first nonring torsional bonds of the ligand were minimized in the context of the receptor using the torsmin command, followed by minimization of the side chain residues within 8 Å of the ligand while holding the backbone and residues Glu353 and Arg394 fixed. A final third minimization of both the ligand and receptor was conducted using the Anneal function (hot radius 8 Å, interesting radius 16 Å from pyrazole **4g**) to afford the final model.

The ERβ molecular model was generated within Sybyl by first modifying residues Leu384 to Met384 and Met421 to Ile421 in the DES–ERα LBD crystal structure[6] and conducting an initial minimization of these two residues while holding the remaining atoms fixed. This was followed by a final minimization using the Anneal function (hot radius 4 Å, interesting radius 8 Å from Met384 and Ile421) using conditions similar to above. The pyrazole **4g** was introduced into this ERβ model and the Flexidock routine implemented as for the ERα model (see above). All minimizations were done using the MMFF94 force field with the Powell gradient method (final rms < 0.02 kcal/mol·Å).

Chemical Syntheses. General Procedure for Preparation of Alkylphenones Using $AlCl_3$ (1a–c,f): Method A. To a stirred solution of $AlCl_3$ (46.8 mmol) in 1,2-dichloroethane (10 mL) at 0 °C was added the commercial acid chloride (39.0 mmol) dropwise over 10 min. The resulting solution was allowed to come to room temperature for 20 min until all of the $AlCl_3$ had dissolved. The reaction mixture was cooled to 0 °C and a solution of anisole (5.1 mL, 46.8 mmol) in 1,2-dichloroethane (20 mL) was then added dropwise over 30 min. Upon completion, the reaction was allowed to reach room temperature and stir for 8–15 h. The mixture was then quenched by pouring over 100 g of ice and extracted with CH_2Cl_2 (3 × 25 mL). The combined organic layers were washed with water, $NaHCO_3$ (satd), brine, then dried over $MgSO_4$ and concentrated under reduced pressure. Excess anisole was removed in vacuo and then the ketone product distilled.

General Procedure for Preparation of Alkylphenones Using PPA (1d,e): Method B. A mechanically stirred mixture consisting of carboxylic acid (1.0 equiv), anisole (1.1 equiv) and polyphosphoric acid (PPA; 6.15 g/mL of anisole) was heated to 90–100 °C for 1.5 h. Upon cooling to near room

temperature, the dark mixture was poured over ice (100 g/0.1 mol) and extracted repeatedly with EtOAc. The organic layers were then washed with satd NaHCO₃ followed by brine. After drying the extract over Na₂SO₄ and removal of solvent, a crude oil was obtained. The final products were purified by bulb-to-bulb distillation.

1-(4-Methoxyphenyl)-4-methylpentan-1-one (1d). Prepared according to method B outlined above to afford the title compound as a pale yellow oil (75%): ¹H NMR (CDCl₃, 500 MHz) δ 0.94 (d, 6H, J = 6.0), 1.60 (m, 3H, overlapping methine and β-CH₂), 2.90 (t, 2H, J = 6.8), 3.87 (s, 3H), 6.92 (d, 2H, J = 8.8), 7.90 (d, 2H, J = 8.8); ¹³C NMR (CDCl₃, 125 MHz) δ 22.6, 28.5, 33.9, 36.4, 55.2, 113.5, 130.2, 163.6, 198.7; MS (EI, 70 eV) *m/z* 206.1 (M⁺). Anal. (C₁₃H₁₈O₂) C, H.

1-(4-Methoxyphenyl)-3-methylbutan-1-one (1f). Prepared according to general method A outlined above to afford the title compound as a pale yellow oil (84%): ¹H NMR (CDCl₃, 500 MHz) δ 0.95 (d, 6H, J = 6.7), 2.24 (sept, 1H, J = 6.6), 2.73 (d, 2H, J = 6.7), 3.81 (s, 3H), 6.88 (d, 2H, J = 8.9), 7.90 (d, 2H, J = 9.2); ¹³C NMR (CDCl₃, 125 MHz) δ 22.6, 25.2, 46.2, 55.2, 113.5, 130.2, 130.3, 163.1, 198.7; HRMS (EI, M⁺) calcd for C₁₂H₁₆O₂ 192.1150, found 192.1153.

2-Methyl-1,3-bis(4-methoxyphenyl)propane-1,3-dione (2a). To a solution of **1a** (160 mg, 0.97 mmol) and 4-nitrophenyl 4-methoxybenzoate (prepared from *p*-nitrophenol and 4-methoxybenzoic acid using diisopropylcarbodiimide and 4-(dimethyamino)pyridine in THF (35 mL) at 0 °C was added a 1.0 M solution of lithium hexamethyldisilamide (3.03 mL, 3.03 mmol) dropwise over 5 min. The reaction was warmed to room temperature and allowed to stir for 1.5 h. At this time the reaction was quenched by the addition of H₂O (25 mL). The mixture was then repeatedly extracted with diethyl ether. The organic layers were combined and washed with H₂O, then dried over Na₂SO₄ and concentrated under reduced pressure to afford a crude solid. Unreacted ester was removed by adding a solution of 40% ethyl acetate/hexanes and filtering off the insoluble ester. The remaining filtrate was concentrated and subjected to flash chromatography (40% ethyl acetate/hexanes) to afford the title compound as a light yellow oil (266 mg, 92%): ¹H NMR (CDCl₃, 500 MHz) δ 1.58 (d, 3H, J = 7.3), 3.85 (s, 3H), 5.13 (q, 1H, J = 7.2), 6.92 (d, 2H, J = 6.8), 7.93 (d, 2H, J = 7.0).

2-Ethyl-1,3-bis(4-methoxyphenyl)propane-1,3-dione (2b).[11] Prepared according to the procedure outlined above from **1b** and purified by flash chromatography (ethyl acetate/hexanes) to afford a viscous oil (95%): ¹H NMR (CDCl₃, 500 MHz) δ 1.01 (t, 3H, J = 7.4), 2.12 (quint, 2H, J = 7.1), 3.80 (s, 6H), 4.98 (t, 1H, J = 6.6), 6.87 (AA′XX′, 2H, J = 8.8, 2.1), 7.94 (AA′XX′, 2H, J = 8.5, 2.3); APT ¹³C NMR (CDCl₃, 125 MHz) δ 12.9 (CH₃), 23.2 (CH₂), 55.6 (CH), 58.8 (CH₃O), 114.0 (ArCH), 129.3 (ArC), 131.0 (ArCH), 163.8 (ArC), 195.0 (C=O); MS (EI, 70 eV) *m/z* 312.3 (M⁺).

2-Propyl-1,3-bis(4-methoxyphenyl)propane-1,3-dione (2c). Prepared according to the procedure outlined above from **1c** and purified by flash chromatography (ethyl acetate/hexanes) to afford product as a clear viscous oil (76%): ¹H NMR (CDCl3, 500 MHz) δ 0.95 (t, 3H, J = 7.4), 1.36−1.47 (m, 2H), 2.06−2.11 (m, 2H), 3.83 (s, 6H), 5.05 (t, 1H, J = 6.7) 6.90 (AA′XX′, 2H, J = 9.0, 2.5), 7.95 (AA′XX′, 2H, J = 9.0, 2.5); ¹³C NMR (CDCl₃, 125 MHz) δ 14.0, 21.5, 31.6, 55.4, 57.1, 113.8, 129.0, 130.8, 163.5, 194.8; HRMS (EI, M⁺) calcd for C₂₀H₂₂O₄ 326.1518, found 326.1512.

2-Isobutyl-1,3-bis(4-methoxyphenyl)propane-1,3-dione (2d). Prepared according to the procedure outlined above from **1d** and purified by flash chromatography (ethyl acetate/hexanes) to afford product as a clear viscous oil (77%): ¹H NMR (CDCl₃, 500 MHz) δ 0.96 (d, 3H, J = 6.5), 1.70 (m, 1H, J = 6.7), 2.00 (br t, 2H, J = 6.9), 3.82 (s, 6H), 5.18 (t, 1H, J = 6.5), 6.89 (d, 2H, J = 8.6), 7.97 (d, 2H, J = 9.0); ¹³C NMR (CDCl₃, 125 MHz) δ 22.8 (CH₃), 27.2 (CH), 38.5 (CH₂), 55.7 (CH₃O), 55.8 (CH), 114.2 (ArCH), 129.4 (ArC), 131.2 (ArCH), 163.2 (C=O); HRMS (EI, M⁺) calcd for C₁₃H₁₈O₄ 340.1674, found 340.1679. Anal. (C₂₁H₂₄O₄) C, H.

2-*n*-Butyl-1,3-bis(4-methoxyphenyl)propane-1,3-di-

one (2e). Prepared according to the procedure outlined above from **1e** and purified by flash chromatography (ethyl acetate/hexanes) to afford product as a light yellow oil (69%): ¹H NMR (CDCl₃, 500 MHz) δ 0.89 (t, 3H, J = 7.0), 1.37 (m, 4H), 2.11 (q, 2H, J = 7.1), 3.85 (s, 6H), 6.91 (d, 4H, J = 9.0), 7.98 (d, 4H, J = 9.0); ¹³C NMR (CDCl₃, 125 MHz) δ 14.0 (CH₃), 22.9 (CH₂), 22.7 (CH₂), 30.7 (CH₂), 55.7 (CH₃O), 57.7 (CH), 114.2 (ArCH), 129.5 (ArC), 131.2 (ArCH), 163.2 (C=O); HRMS (EI, M⁺) calcd for C₁₃H₁₈O₄ 340.1674, found 340.1675. Anal. (C₁₃H₁₈O₄) C, H.

General Procedure for Pyrazole Synthesis. To a DMF (30 mL) and THF (10 mL) solution containing diketone (1.0 mmol) was added phenylhydrazine hydrochloride (3−5 equiv). The mixture was brought to reflux (oil bath temperature 120 °C) until disappearance of diketone as evident by TLC analysis (8−20 h). The reaction mixture was then allowed to cool to room temperature and diluted with H₂O (30 mL). The product was extracted repeatedly with ethyl acetate (3 × 25 mL) and the organic layers combined and washed sequentially with a satd LiCl solution (25 mL), satd NaHCO₃ (25 mL), and brine (25 mL). The oganic layer was dried over Na₂SO₄ and concentrated under reduced pressure to afford the crude product in the form of an oil, which was purified by flash chromatography or by passage through a short silica plug eluting with an ethyl acetate/hexane solvent system.

3,5-Bis(4-methoxyphenyl)-4-methyl-1-phenyl-1*H*-pyrazole (3a). The diketone **2a** (250 mg, 0.84 mmol) was reacted with phenylhydrazine hydrochloride (423 mg, 2.94 mmol) according to the general procedure above. Upon purification by flash chromatography (40% ethyl acetate/hexanes) the title compound was obtained as a tan solid (220 mg, 71%): mp 142−143 °C; ¹H NMR (CDCl₃, 500 MHz) δ 2.21 (s, 3H), 3.83 (s, 3H), 3.86 (s, 3H), 6.89 (AA′XX′, 2H, J = 8.9, 2.5), 6.99 (AA′XX′, 2H, J = 8.9, 2.5), 7.15 (AA′XX′, 2H, J = 8.8, 2.5), 7.19−7.32 (m, 5H), 7.74 (AA′XX′, 2H, J = 8.9, 2.5); ¹³C NMR (CDCl₃, 125 MHz) δ 10.2, 55.2, 55.3, 113.6, 113.9, 113.9, 123.1, 124.7, 126.5, 126.6, 128.7, 129.1, 131.3, 140.4, 141.2, 150.9, 159.2, 159.4; MS (EI, 70 eV) *m/z* 370 (M⁺). Anal. (C₂₄H₂₂N₂O₂) C, H, N.

4-Ethyl-3,5-bis(4-methoxyphenyl)-1-phenyl-1*H*-pyrazole (3b).[11] Diketone **2b** and phenylhydrazine hydrochloride were reacted as outlined above to afford **3b** as an orange solid after flash chromatography purification (87%): ¹H NMR (CDCl₃, 400 MHz) δ 1.04 (t, 3H, J = 7.6), 2.63 (q, 2H, J = 7.6), 3.83 (s, 3H), 3.86 (s, 3H), 6.90 (AA′XX′, 2H, J = 8.8, 2.4), 6.99 (AA′XX′, 2H, J = 8.8, 2.6), 7.17 (AA′XX′, 2H, J = 8.8, 2.4), 7.20 (m, 2H), 7.24 (m, 3H), 7.72 (AA′XX′, 2H, J = 9.0, 2.4); ¹³C NMR (CDCl₃, 100 MHz) δ 15.8, 17.3, 55.4, 55.5, 114.1, 114.2, 120.7, 123.5, 124.8, 126.8, 127.0, 128.8, 129.3, 131.5, 140.5, 141.2, 150.8, 159.4, 159.6; HRMS (EI, M⁺) calcd for C₂₅H₂₄N₂O₂ 384.1835, found 384.1837.

3,5-Bis(4-methoxyphenyl)-1-phenyl-4-propyl-1*H*-pyrazole (3c). Diketone **2c** (200 mg, 0.61 mmol) was reacted with phenylhydrazine hydrochloride (444 mg, 3.07 mmol) according to the general procedure to afford **3c** as an orange oil (130 mg, 53%) after purification by flash chromatography (40% ethyl acetate/hexanes): ¹H NMR (CDCl₃, 500 MHz) δ 0.79 (t, 3H, J = 7.4), 1.42 (sext, 2H, J = 7.7), 2.57 (t, 2H, J = 8.0), 3.83 (s, 3H), 3.86 (s, 3H), 6.90 (AA′XX′, 2H, J = 8.6, 2.5), 6.99 (AA′XX′, 2H, J = 8.8, 2.5), 7.18−7.32 (m, 5H), 7.15 (AA′XX′, 2H, J = 8.6, 2.5), 7.72 (AA′XX′, 2H, J = 8.8, 2.5); ¹³C NMR (CDCl₃, 125 MHz) δ 14.05, 23.79, 25.86, 55.09, 55.15, 113.74, 113.85, 118.87, 118.86, 122.86, 124.60, 126.52, 129.49, 131.17, 139.66, 141.31, 150.36, 159.14, 159.33; HRMS (EI, M⁺) calcd for C₂₆H₂₆N₂O₂ 398.1994, found 398.2000.

4-Isobutyl-3,5-bis(4-methoxyphenyl)-1-phenyl-1*H*-pyrazole (3d). Diketone **2d** was reacted with phenylhydrazine hydrochloride according to the general procedure to afford **3d** as an orange oil (85%) after a short silica plug (20% ethyl acetate/hexanes). The purified material was then directly used in the subsequent deprotection step.

4-Butyl-3,5-bis(4-methoxyphenyl)-1-phenyl-1*H*-pyrazole (3e). Diketone **2e** was reacted with phenylhydrazine hydrochloride according to the general procedure to afford **3e** as a reddish oil (86%) after purification by flash chromatog-

raphy (20% ethyl acetate/hexanes). This material was then directly used in the subsequent deprotection step.

4-Ethyl-1,3,5-tris(4-methoxyphenyl)-1H-pyrazole (3f). Diketone **2b** (400 mg, 1.28 mmol) was reacted with 4-methoxyphenylhydrazine hydrochloride (1.11 g, 6.40 mmol) according to the general procedure. The crude product was purified by flash chromatography (2% acetone/CH$_2$Cl$_2$) to afford **3f** as an oil (351 mg, 66%): ^{1}H NMR (CDCl$_3$, 500 MHz) δ 1.06 (t, 3H, J = 7.5), 2.65 (q, 2H, J = 7.5), 3.73 (s, 3H), 3.79 (s, 3H), 3.83 (s, 3H), 6.78 (AA'XX', 2H, J = 9.0, 2.8) 6.89 (AA'XX', 2H, J = 8.8, 2.4), 6.69 (AA'XX', 2H, J = 8.8, 2.4), 7.16 (AA'XX', 2H, J = 8.8, 2.4), 7.21 (AA'XX', 2H, J = 9.0, 2.7), 7.74 (AA'XX', 2H, J = 8.7, 2.4); ^{13}C NMR (CDCl$_3$, 125 MHz) δ 15.52, 17.09, 55.05, 55.10, 55.22, 113.65, 113.80, 113.83, 119.78, 123.11, 125.96, 126.78, 128.95, 131.18, 133.45, 140.84, 149.94, 158.99, 157.97, 159.22; HRMS (EI, M$^+$) calcd for C$_{26}$H$_{26}$N$_2$O$_3$ 414.1943, found 414.1942.

1,3,5-Tris(4-methoxyphenyl)-4-propyl-1H-pyrazole (3g). Diketone **2c** (500 mg, 1.52 mmol) was reacted with 4-methoxyphenylhydrazine hydrochloride (800 mg, 4.59 mmol) according to the general procedure to afford 362 mg of **3g** as a red oil (67%) after a short silica plug (20% ethyl acetate/hexanes). This material was then directly used in the subsequent deprotection step.

4-Isobutyl-1,3,5-tris(4-methoxyphenyl)-1H-pyrazole (3h). Diketone **2d** was reacted with 4-methoxyphenylhydrazine hydrochloride according to the general procedure to afford **3h** as a light orange oil (85%) after a short silica plug (20% ethyl acetate/hexanes). The purified material was then directly used in the subsequent deprotection step.

4-Butyl-1,3,5-tris(4-methoxyphenyl)-1H-pyrazole (3i). Diketone **2e** was reacted with 4-methoxyphenylhydrazine hydrochloride according to the general procedure to afford **3i** as a light orange oil (87%) after a short silica plug (20% ethyl acetate/hexanes). The purified material was then directly used in the subsequent deprotection step.

General Demethylation Procedure. To a stirred solution of methyl-protected pyrazole (1 equiv) in CH$_2$Cl$_2$ at −78 °C was added dropwise a 1 M BBr$_3$ solution in CH$_2$Cl$_2$ (3–5 equiv). Upon complete addition of BBr$_3$, the reaction was maintained at −78 °C for 1 h and then allowed to reach room temperature and stir for an additional 16 h. The mixture was cooled to 0 °C and carefully quenched with H$_2$O (15–25 mL). The product was then repeatedly extracted with EtOAc and the organic layers dried over Na$_2$SO$_4$. Upon solvent removal the crude phenolic products were purified by flash chromatography and/or recrystallization from MeOH/CH$_2$Cl$_2$ mixtures.

3,5-Bis(4-hydroxyphenyl)-4-methyl-1-phenyl-1H-pyrazole (4a). A stirred CH$_2$Cl$_2$ solution of **3a** (200 mg, 0.54 mmol) was deprotected using BBr$_3$ according to the general demethylation procedure. Purification by flash chromatography (5% CH$_3$OH/CH$_2$Cl$_2$) afforded the title compound as a tan solid (54 mg, 30%): mp 225–230 °C; ^{1}H NMR (MeOD-d_4, 500 MHz) δ 2.13 (s, 3H), 6.76 (AA'XX', 2H, J = 8.4, 2.7), 6.93 (AA'XX', 2H, J = 8.7, 2.5), 7.01 (AA'XX', 2H, J = 8.8, 2.5), 7.54 (AA'XX', 2H, J = 8.6, 2.4), 7.35–7.22 (m, 5H); ^{13}C NMR (MeOD-d_4, 125 MHz) 8.7, 112.8, 114.7, 114.8, 120.9, 124.4, 124.8, 126.7, 128.3, 128.9, 130.9, 139.8, 151.4, 157.1, 157.4; MS (EI, 70 eV) m/z 342. Anal. (C$_{22}$H$_{18}$N$_2$O$_2$·H$_2$O) C, H, N.

4-Ethyl-3,5-bis(4-hydroxyphenyl)-1-phenyl-1H-pyrazole (4b).[11] A stirred CH$_2$Cl$_2$ solution of **3b** (100 mg, 0.26 mmol) was deprotected using BBr$_3$ according to the general demethylation procedure. Purification by flash chromatography (5% CH$_3$OH/CH$_2$Cl$_2$) afforded the title compound as a white solid (50 mg, 54%): mp 247–248 °C; ^{1}H NMR (MeOD-d_4, 400 MHz) δ 0.98 (t, 3H, J = 7.4), 2.60 (q, 2H, J = 7.5), 6.78 (AA'XX', 2H, J = 8.8, 2.4), 6.88 (AA'XX', 2H, J = 8.7, 2.5), 7.05 (AA'XX', 2H, J = 8.8, 2.4), 7.24–7.42 (m, 5H), 7.51 (AA'XX', 2H, J = 8.7, 2.5); HRMS (EI, M$^+$) calcd for C$_{23}$H$_{21}$N$_2$O$_2$ 357.1611, found 357.1603.

3,5-Bis(4-hydroxyphenyl)-1-phenyl-4-propyl-1H-pyrazole (4c). A stirred CH$_2$Cl$_2$ solution of **3c** (107 mg, 0.27 mmol) was deprotected using BBr$_3$ according to the general demeth-

ylation procedure. The crude product was purified by flash chromatography (10% CH$_3$OH/CH$_2$Cl$_2$) to afford **4c** as a tan solid (85 mg, 86%): mp 240–245 °C; ^{1}H NMR (MeOD-d_4, 500 MHz) δ 0.72 (t, 3H, J = 7.4), 1.35 (sext, 2H, J = 7.5), 2.55 (t, 2H, J = 7.7), 6.77 (AA'XX', 2H, J = 8.7, 2.5), 6.88 (AA'XX', 2H, J = 8.5, 2.4), 7.03 (AA'XX', 2H, J = 8.5, 2.4), 7.32–7.27 (m, 5H), 7.50 (AA'XX', 2H, J = 8.8, 2.5); ^{13}C NMR (MeOD-d_4, 400 MHz) δ 12.73, 13.28, 25.28, 114.75, 114.89, 118.26, 121.13, 124.78, 124.82, 126.69, 128.26, 128.99, 131.02, 139.71, 142.12, 151.30, 157.08, 157.49; HRMS (EI, M$^+$) calcd for C$_{24}$H$_{22}$N$_2$O$_2$ 370.1681, found 370.1676.

4-Isobutyl-3,5-bis(4-hydroxyphenyl)-1-phenyl-1H-pyrazole (4d). A stirred CH$_2$Cl$_2$ solution of **3d** (100 mg, 0.24 mmol) was deprotected using BBr$_3$ according to the general demethylation procedure. The crude product was purified by flash chromatography (10% CH$_3$OH/CH$_2$Cl$_2$) to afford **4d** as a tan powder (70 mg, 76%): mp 225 °C dec; ^{1}H NMR (MeOD-d_4, 500 MHz) δ 0.63 (d, 6H, J = 6,5), 1.51 (m, 1H, J = 7.0), 2.51 (d, 2H, J = 7.5), 6.76 (AA'XX', 2H, J = 9.0, 2.3), 6.87 (AA'XX', 2H, J = 8.9, 2.3), 7.02 (AA'XX', 2H, J = 8.5, 2.4), 7.26 (m, 5H), 7.49 (AA'XX', 2H, J = 8.0, 2.3); ^{13}C NMR (MeOD-d_4, 125 MHz) δ 22.8, 29.9, 33.8, 116.4, 116.6, 119.1, 123.0, 126.6, 126.8, 128.4, 129.9, 130.9, 132.9, 141.5, 144.2, 153.4, 158.8, 159.2; FAB-HRMS (M + 1) calcd for C$_{25}$H$_{25}$N$_2$O$_2$ 385.1916, found 385.1916.

4-Butyl-3,5-bis(4-hydroxyphenyl)-1-phenyl-1H-pyrazole (4e). A stirred CH$_2$Cl$_2$ solution of **3e** (100 mg, 0.24 mmol) was deprotected using BBr$_3$ according to the general demethylation procedure. The crude product was purified by flash chromatography (30% EtOAc/hexanes) to afford a tan solid. This material was subsequently recrystallized from 5–10% MeOH/CH$_2$Cl$_2$ to afford the title compound as small off-white crystals (59 mg, 64%): mp 205.5–207.5 °C; ^{1}H NMR (MeOD-d_4, 400 MHz) δ 0.72 (t, 3H, J = 7.2), 1.16 (sext, 2H, J = 7.2), 1.34 (quint, 2H, J = 7.2), 2.60 (t, 2H, J = 7.2), 4.95 (br s, 2H exchange with D$_2$O), 6.78 (d, 2H, J = 9.0), 6.91 (d, 2H, J = 8.0), 7.02 (d, 2H, J = 8.8), 7.26 (m, 5H), 7.53 (d, 2H, J = 8.4); ^{13}C NMR (MeOD-d_4, 125 MHz) δ 14.6, 23.9, 24.8, 34.3, 116.8, 116.9, 120.5, 123.2, 126.8, 128.7, 130.3, 131.0, 131.1, 133.1, 141.7, 144.0, 153.3, 159.0, 159.4. Anal. (C$_{25}$H$_{24}$N$_2$O$_2$·0.1H$_2$O) C, H, N.

4-Ethyl-1,3,5-tris(4-hydroxyphenyl)-1H-pyrazole (4f). A stirred CH$_2$Cl$_2$ solution of **3f** (200 mg, 0.48 mmol) was deprotected using BBr$_3$ according to the general demethylation procedure. A crude oil was isolated which was triturated with a 10% CH$_3$OH/CH$_2$Cl$_2$ solution from which the desired product precipitated. The white powder was collected by filtration and recrystallized from CH$_3$OH/CH$_2$Cl$_2$ to afford the title compound **4f** (175 mg, 98%): mp 210–215 °C; ^{1}H NMR (MeOD-d_4, 400 MHz): δ 0.96 (t, 3H, J = 7.5) 2.58 (q, 2H, J = 7.5) 6.70 (AA'XX', 2H, J = 8.8, 2.6), 6.77 (AA'XX', 2H, J = 8.6, 2.3), 6.87 (AA'XX', 2H, J = 8.8, 2.3), 7.10 (m, 4H), 7.48 (AA'XX', 2H, J = 8.6, 2.4); ^{13}C NMR (MeOD-d_4, 100 MHz) δ 14.5, 16.6, 114.8, 114.9, 114.9, 119.2, 121.4, 125.0, 126.8, 129.1, 131.2, 131.9, 142.1, 150.5, 156.7, 157.1, 157.5. Anal. (C$_{23}$H$_{20}$N$_2$O$_3$·0.7H$_2$O) C, H, N.

1,3,5-Tris(4-hydroxyphenyl)-4-propyl-1H-pyrazole (4g). A stirred CH$_2$Cl$_2$ solution of **3g** (200 mg, 0.48 mmol) was deprotected using BBr$_3$ according to the general demethylation procedure. A crude oil was isolated which was triturated with a 10% CH$_3$OH/CH$_2$Cl$_2$ solution from which the desired product precipitated. The white powder was collected by filtration and recrystallized from CH$_3$OH/CH$_2$Cl$_2$ to afford the title compound **4g** (125 mg, 68%): mp 230 °C dec; ^{1}H NMR (MeOD-d_4, 400 MHz) δ 0.72 (t, 3H, J = 7.2), 1.33 (sext, 2H, J = 7.6), 2.54 (t, 2H, J = 8), 6.70 (AA'XX', 2H, J = 8.8, 2.4), 6.76 (AA'XX', 2H, J = 6.8, 2.0), 6.87 (AA'XX', 2H, J = 8.8, 2.4), 7.02 (AA'XX', 2H, J = 8.8, 2.4), 7.05 (AA'XX', 2H, J = 9.2, 2.4), 7.47 (AA'XX', 2H, J = 8.8, 2.0); ^{13}C NMR (MeOD-d_4, 100 MHz) δ 25.8 (CH$_3$), 36.4 (CH$_2$), 38.4 (CH$_2$), 127.0 (C), 128.0 (C), 128.5 (C), 130.5 (CH), 134.3 (CH), 137.9 (CH), 138.9 (C), 140.3 (C), 141.3 (C), 142.8 (C), 143.3 (C), 144.1 (C),144.7 (CH), 155.3 (CH), 163.6 (CH), 169.5 (CH), 170.3 (CH). Anal. (C$_{24}$H$_{22}$N$_2$O$_3$·0.6H$_2$O) C, H, N.

4-Isobutyl-1,3,5-tris(4-hydroxyphenyl)-1H-pyrazole (4h). A stirred CH$_2$Cl$_2$ solution of **3h** (250 mg, 0.56 mmol) was

deprotected using BBr$_3$ according to the general demethylation procedure. Recrystallization from CH$_3$OH/CH$_2$Cl$_2$ afforded the title compound **4h** as an off-white powder (80 mg, 37%): mp 226−228 °C; ^{1}H NMR (MeOD-d_4, 500 MHz) δ 0.61 (d, 6H, J = 6.5), 1.50 (m, 1H, J = 7.0), 2.50 (d, 2H, J = 7.5), 4.87 (s, 3H, OH), 6.70 (AA'XX', 2H, J = 8.5, 2.0), 6.75 (AA'XX', 2H, J = 8.5, 2.3), 6.85 (AA'XX', 2H, J = 9.0, 2.3), 7.01 (AA'XX', 2H, J = 9.0, 2.3), 7.05 (AA'XX', 2H, J = 9.0, 2.3), 7.45 (AA'XX', 2H, J = 8.5, 2.3); ^{13}C NMR (MeOD-d_4, 125 MHz) δ 22.9, 29.9, 33.9, 116.4, 116.5, 116.6, 118.3, 123.2, 126.9, 128.3, 130.9, 132.9, 133.5, 144.3, 152.7, 158.2, 158.6, 158.9. Anal. (C$_{25}$H$_{24}$N$_2$O$_3$· 0.7H$_2$O) C, H, N.

4-Butyl-1,3,5-tris(4-hydroxyphenyl)-1*H***-pyrazole (4i).** A stirred CH$_2$Cl$_2$ solution of **3i** (200 mg, 0.45 mmol) was deprotected using BBr$_3$ according to the general demethylation procedure. Recrystallization from CH$_3$OH/CH$_2$Cl$_2$ afforded the title compound **4i** as an off-white powder (90 mg, 50%): mp 214−230 °C dec; ^{1}H NMR (MeOD-d_4, 500 MHz) δ 0.71 (t, 3H, J = 7.5), 1.13 (sext, 2H, J = 7.0), 1.30 (quint, 2H, J = 8.5), 2.57 (t, 2H, J = 8.0), 6.70 (AA'XX', 2H, J = 9.0, 2.4), 6.76 (AA'XX', 2H, J = 8.5, 2.3), 6.86 (AA'XX', 2H, J = 9.0, 2.5), 7.02 (AA'XX', 2H, J = 8.5, 2.3), 7.05 (AA'XX', 2H, J = 8.5, 2.3), 7.46 (AA'BB', 2H, J = 8.5, 2.3); ^{13}C NMR (MeOD-d_4, 400 MHz) δ 14.1, 23.5, 24.4, 33.9, 116.3, 116.4, 116.5, 119.3, 123.0, 126.7, 128.3, 130.7, 132.8, 133.5, 143.9, 152.4, 158.3, 158.7, 159.0. Anal. (C$_{25}$H$_{24}$N$_2$O$_3$·0.3H$_2$O) C, H, N.

4-Isopropyl-3,5-bis(4-methoxyphenyl)-1-phenyl-1*H***-pyrazole (6).**[13] Upon solid support cleavage and solvent removal, the crude solid was recrystallized from 25% ethyl acetate/hexane to afford **6** as small cubic crystals (30 mg, 11% over three steps): mp 225−230 °C; ^{1}H NMR (MeOD-d_4, 400 MHz) δ 1.09 (d, 6H, J = 7.0 Hz) 2.98 (septet, 1H, J = 7.11 Hz), 6.76 (AA'XX', 2H, J = 9.1, 2.6), 6.88 (AA'XX', 2H, J = 9.0, 2.6), 7.1 (AA'XX', 2H, J = 8.7, 2.5), 7.20−7.30 (m, 5H), 7.39 (AA'XX', 2H, J = 8.8, 2.40); ^{13}C NMR (MeOD-d_4, 100 MHz) δ 22.5, 24.5, 114.5, 114.6, 121.6, 124.6, 125.0, 126.7, 128.2, 130.2, 131.8, 139.6, 141.3, 151.3, 157.2, 157.6; HRMS (EI, M$^+$) calcd for C$_{24}$H$_{22}$N$_2$O$_2$ 370.1681, found 370.1674.

1,3-Bisphenylpropane-1,3-dione (10). To a stirred solution of diketone **9** (2g, 8.9 mmol) in freshly distilled THF (50 mL), was added 8.9 mL (8.9 mmol) of tetrabutylammonium fluoride (1 M in THF) and stirred for 30 min. The solution was concentrated under reduced pressure and dissolved in 50 mL of CHCl$_3$. Ethyl iodide (1.4 mL, 17.8 mmol) was added in one portion and stirred at room temperature overnight. The solution was concentrated and the crude was purified by flash chromatgraphy (petroleum ether/CH$_2$Cl$_2$, 1:1) to give 920 mg of **19** as a white solid in 41% yield: ^{1}H NMR (CDCl$_3$, 400 MHz) δ 1.05 (t, 3H, J = 7.4), 2.17 (quint, 2H, J = 7.4), 5.12 (t, 1H, J = 6.5) 7.42−7.58 (m, 6H), 7.94−7.98 (m, 4H); ^{13}C NMR δ 12.8, 22.9, 58.7, 128.5, 128.8, 133.4, 136.1, 196.1; MS (EI, 70 eV) m/z 252.1 (M$^+$).

4-Ethyl-1-(4-methoxyphenyl)-3,5-bisphenyl-1*H***-pyrazole (11).** The diketone **10** (300 mg, 1.2 mmol) was reacted with 4-methoxyphenylhydrazine hydrochloride (830 mg, 4.7 mmol) according to the general procedure for pyrazole synthesis. The crude product was purified by flash chromatography (petroleum ether/CH$_2$Cl$_2$, 1:1) to afford 276 mg of **11** as a yellow oil (65%): ^{1}H NMR (CDCl$_3$, 400 MHz) δ 1.04 (t, 3H, J = 7.5), 2.67 (q, 2H, J = 7.5), 3.77 (s, 1H), 6.77 (AA'XX', 2H, J = 1.0, 2.2), 7.19 (AA'XX', 2H, J = 9.1, 2.2), 7.23−7.48 (m, 9H), 7.78 (AA'XX', 2H, J = 8.2, 2.5); ^{13}C NMR δ 15.6, 17.1, 55.4, 113.8, 120.4, 126.1, 127.5, 127.9, 128.1, 128.41, 128.45, 130.1, 130.9, 133.4, 134.1, 141.2, 150.4, 158.2; MS (EI, 70 eV) m/z 354.2 (M$^+$).

4-Ethyl-1-(4-hydroxyphenyl)-3,5-bisphenyl-1*H***-pyrazole (7a).** A stirred CH$_2$Cl$_2$ solution of **11** (274 mg, 0.77 mmol) was deprotected with BBr$_3$ according to the general demethylation procedure. The crude was purified by flash chromatography (CH$_2$Cl$_2$/acetone, 3:1) to give 84 mg of **7a** as a white solid (32%): mp 184−185 °C; ^{1}H NMR (CD$_3$OD, 400 MHz) δ 1.03 (t, 3H, J = 7.5), 2.66 (q, 2H, J = 7.5), 6.65 (AA'XX', 2H J = 8.8, 2.2), 7.09 (AA'XX', 2H, J = 9.0, 2,1), 7.2−7.5 (m, 8H), 7.77 (AA'XX', 2H, J = 8.4); ^{13}C NMR δ 15.5, 17.0, 115.8, 120.2,

126.6, 127.7, 128.0, 128.2, 128.4, 128.5, 130.0, 130.6, 132.6, 133.8, 141.6, 150.5, 155.2; MS (EI, 70 eV) m/z 340.2 (M$^+$). Anal. (C$_{23}$H$_{20}$ON$_2$) C, H, N.

1,3-Bis(4-methoxyphenyl)-5-phenyl-4,5-dihydro-1*H***-pyrazole (13a).** A mixture of commercially available 4′-methoxychalcone (**12a**; 253 mg, 1.1 mmol) and 807 mg of 4-methoxyphenylhydrazine (4.6 mmol) in 10 mL of anhydrous DMF was heated to 85 °C overnight. The reaction solution was cooled to room temperature and partitioned with diethyl ether and water. The organic layer was washed with water, dried (MgSO$_4$), and concentrated. The crude was then recrystallized from a mixture of ethyl acetate and hexanes to give 198 mg of **13a** as light yellow crystals (48%): ^{1}H NMR (CDCl$_3$, 400 MHz) δ 3.12 (dd, 1H, J = 16.7, 8.4), 3.74 (s, 3H), 3.86 (s, 3H), 3.74−3.88 (m, 1H), 5.14 (dd, 1H, J = 11.9, 8.6), 6.8 (AA'XX', 2H, J = 9.0), 6.94 (AA'XX', 2H, J = 9.0), 7.04 (AA'XX', 2H, J = 9.0), 7.26−7.42 (m, 5H), 7.68 (d, 2H, J = 9.0); ^{13}C NMR δ 43.9, 55.3, 55.6, 65.8, 114.0, 114.4, 114.8, 126.1, 127.5, 127.8, 128.0, 129.1, 140.1, 142.9, 146.9, 153.2, 160.0; HRMS (EI, M$^+$) calcd for C$_{23}$H$_{22}$N$_2$O$_2$ 358.1688, found 358.1681.

1,5-Bis(4-methoxyphenyl)-3-phenyl-4,5-dihydro-1*H***-pyrazole (13b).** A mixture of commercially available 4-methoxychalcone (**12b**; 2 g, 8.4 mmol) and 7.3 g of 4-methoxyphenylhydrazine (42 mmol) in 80 mL of anhydrous DMF was heated to 85 °C overnight. The reaction solution was cooled to room temperature and partitioned with diethyl ether and water. A yellow solid precipitated and was collected by filtration to give 2.6 g of **13b** (86%): ^{1}H NMR (CDCl$_3$, 400 MHz) δ 3.1 (dd, 1H, J = 15.6,7.8), 3.72 (s, 3H), 3.78 (s, 3H), 3.8 (d, 1H, J = 5.6), 5.13 (dd, 1H, J = 12.0, 9.0), 6.76 (AA'XX', 2H, J = 9.1, 2.3), 6.87 (AA'XX', 2H, J = 8.7, 2.1), 7.01 (d, 2H, J = 9.0), 7.2−7.4 (m, 5H), 7.7 (d, 2H, J = 7.3); ^{13}C NMR δ 43.7, 55.2, 55.6, 65.2, 114.4, 114.4, 114.9, 125.6, 127.3, 128.3, 128.5, 132.9, 134.7, 139.7, 146.3, 153.3, 158.9; MS (EI, 70 eV) m/z 358.2 (M$^+$).

4-Ethyl-1,3-bis(4-methoxyphenyl)-5-phenyl-4,5-dihydro-1*H***-pyrazole (14a).** To a solution of lithium diisopropylamide in 20 mL of THF [prepared by dropwise addition of 0.88 mL of n-BuLi (1.41 mmol) to 0.21 mL (1.5 mmol) of diisopropylamine in 18 mL of THF at −78 °C] was added a solution of 317 mg (0.88 mmol) of pyrazoline **13a** in 8 mL of THF dropwise via syringe at −78 °C and stirred for 1 h. To the dark red solution was added iodoethane (0.11 mL, 1.31 mmol) in one portion and the resulting yellow solution was warmed to room temperature overnight. The reaction was quenched with 5 mL of brine, the aqueous layer was separated and extracted with CH$_2$Cl$_2$, the organic layer was dried (MgSO$_4$) and concentrated in vacuo. The residue was purified by flash chromatography (ether/hexanes, 3:2) to afford 262 mg of **14a** as a yellow foam (77%): ^{1}H NMR (CDCl$_3$, 400 MHz) δ 0.8 (t, 3H, J = 7.3), 1.45 (tq, 1H, J = 4, 2), 1.55 (m, 1H), 3.2 (m, 1H), 3.25 (s, 3H), 3.3 (s, 3H), 4.8 (d, 1H, 3.4), 6.77 (AA'XX', 2H, J = 8.9), 6.82 (AA'XX', 2H, J = 8.5), 7.0 (AA'XX', 2H, J = 8.7), 7.13 (AA'XX', 2H, J = 8.5), 7.25−7.40 (m, 3H), 7.70 (AA'XX', 2H, J = 7.3); ^{13}C NMR δ 10.5, 25.4, 54.8, 55.1, 57.8, 69.7, 114.4, 114.4, 115.0, 125.8, 126.0, 127.5, 127.7, 129.3, 139.3, 142.8, 148.4, 153.6, 160.2; HRMS (EI, M$^+$) calcd for C$_{25}$H$_{26}$N$_2$O$_2$ 386.1999, found 386.1994.

4-Ethyl-1,5-bis(4-methoxyphenyl)-3-phenyl-4,5-dihydro-1*H***-pyrazole (14b).** Prepared from lithium diisopropylamide (4.65 mmol), pyrazoline **13b** (1 g, 2.8 mmol), and ethyl iodide (0.45 mL, 5.6 mmol) by the procedures used to prepare pyrazoline **14a**. The crude product was purified by flash chromatography (hexanes/ether 3:2) to give 0.33 g (38%) of **14b** a yellow foam: ^{1}H NMR (CDCl$_3$, 400 MHz) δ 1.03 (t, 3H, J = 7.3), 1.69 (tq, 1H, J = 4, 2), 1.85 (m, 1H), 3.37 (m, 1H), 3.73 (s, 3H), 3.75 (s, 3H), 4.91 (d, 1H, 3.4), 6.77 (AA'XX', 2H, J = 8.9), 6.82 (AA'XX', 2H, J = 8.5), 7.0 (AA'XX', 2H, J = 8.7), 7.13 (AA'XX', 2H, J = 8.5), 7.25−7.40 (m, 3H), 7.70 (AA'XX', 2H, J = 7.3); ^{13}C NMR δ 10.5, 25.1, 55.2, 55.6, 57.3, 68.9, 113.9, 114.4, 114.5, 125.8, 126.8, 127.9, 128.5, 132.6, 134.1, 138.5, 148.5, 152.8, 158.8; MS (EI, 70 eV) m/z 386.2 (M$^+$).

4-Ethyl-1,3-bis(4-methoxyphenyl)-5-phenyl-1*H***-pyrazole (15a).** To a stirred solution of **14a** (27.8 mg, 0.07 mmol)

in 3 mL of benzene was added 78 mg (0.9 mmol) of MnO_2. The solution was heated to 100 °C with a Dean–Stark trap for 2 h, cooled to room temperature, filtered through Celite and concentrated. The crude was chromatographed (EtOAc/hexanes, 1:10) to afford 28 mg of **15a** (100%): ^1H NMR ($CDCl_3$, 400 MHz) δ 1.12 (t, 3H, $J = 7.5$), 2.65 (q, 2H, $J = 7.5$), 3.78 (s, 3H), 3.85 (s, 3H), 6.77 (AA'XX', 2H, $J = 9.0, 2.0$), 7.0 (AA'XX', 2H, $J = 8.8, 2.0$), 7.2 (AA'XX', 2H, $J = 9.0, 2.0$), 7.22–7.40 (m, 5H), 7.71 (d, 2H, $J = 8.6, 2.0$); ^{13}C NMR δ15.5, 17.1, 55.2, 55.4, 113.8, 113.8, 120.1, 126.1, 126.8, 128.1, 128.4, 129.1, 130.1, 131.1, 133.5, 141.1, 150.2, 158.2, 159.1; HRMS (EI, M^+) calcd for $C_{25}H_{24}N_2O_2$ 385.1912, found 385.1916.

4-Ethyl-1,5-bis(4-methoxyphenyl)-3-phenyl-1H-pyrazole (15b). A mixture of 147 mg (0.37 mmol) of pyrazoline **14b** and 127 mg (0.56 mmol) of dichlorodicyanoquinone in 10 mL of benzene was heated to reflux for 5 h. The mixture was cooled to room temperature and filtered through a plug of Celite with diethyl ether. The filtrate was concentrated in vacuo and the residue was chromatographed (hexanes/ethyl acetate, 4:6) to give 130 mg (90%) of **15b** as a white solid: ^1H NMR ($CDCl_3$, 400 MHz) δ 1.04 (t, 3H, $J = 7.5$), 2.65 (q, 2H, $J = 7.5$), 3.78 (s, 3H), 3.83 (s, 3H), 6.79 (AA'XX', 2H, $J = 8.9, 2.0$), 6.89 (AA'XX', 2H, $J = 8.5, 2.0$), 7.16 (AA'XX', 2H, $J = 8.3, 1.8$), 7.20 (AA'XX', 2H, $J = 8.7, 2.1$), 7.3–7.5 (m, 3H), 7.77 (AA'XX', 2H, $J = 8.8, 1.8$); ^{13}C NMR δ 15.6, 17.12, 55.2, 55.4, 113.7, 113.9, 120.2, 123.2, 126.1, 127.4, 127.9, 128.4, 131.3, 133.5, 134.27, 141.07, 150.3, 158.1, 159.3; MS (EI, 70 eV) m/z 384.2 (M^+).

4-Ethyl-1,3-bis(4-hydroxyphenyl)-5-phenyl-1H-pyrazole (8a). A stirred CH_2Cl_2 solution of **15a** (26 mg, 0.068 mmol) was deprotected with BBr_3 according to the general demethylation procedure. The crude was purified by flash chromatography (CH_2Cl_2/MeOH, 10:1) to give 17 mg of **8a** as a tan solid (70%): mp 225–227 °C; ^1H NMR (CD_3OD, 500 MHz) δ 0.8 (t, 3H, $J = 7.5$), 2.5 (q, 2H, $J = 7.5$), 6.58 (AA'XX', 2H, $J = 9.0, 2.2$), 6.78 (AA'XX', 2H, $J = 8.5, 2.0$), 6.94 (AA'XX', 2H, $J = 8.9, 2.0$), 7.1–7.3 (m, 5H), 7.39 (AA'XX', 2H, $J = 8.9, 2.0$); ^{13}C NMR δ 15.8, 17.9, 116.3, 116.4, 121.0, 122.6, 128.2, 128.9, 129.3, 129.6, 132.6, 133.2, 135.3, 143.8, 151.7, 158.2, 159.0; HRMS (EI, M^+) calcd for $C_{23}H_{20}N_2O_2$ 356.1598, found 356.1603.

4-Ethyl-1,5-bis(4-hydroxyphenyl)-3-phenyl-1H-pyrazole (8b). A stirred CH_2Cl_2 solution of **15b** (130 mg, 0.34 mmol) was deprotected with BBr_3 according to the general demethylation procedure. The crude was purified by flash chromatography (CH_2Cl_2/acetone, 3:1) to give 42 mg of **8b** as a white solid (35%): mp 225–226 °C; ^1H NMR (CD_3OD, 500 MHz) δ 0.96 (t, 3H, $J = 7.5$), 2.62 (q, 2H, $J = 7.5$), 6.71 (AA'XX', 2H, $J = 9.1, 2.2$), 6.77 (AA'XX', 2H, $J = 8.5, 2.0$), 7.06 (AA'XX', 2H, $J = 8.9, 2.1$), 7.07 (AA'XX', 2H, $J = 9.1, 2.2$), 7.35–7.47 (m, 3H), 7.67 (AA'XX', 2H, $J = 8.9, 2.0$); ^{13}C NMR δ 15.8, 17.9, 116.3, 116.4, 121.0, 122.6, 128.2, 128.9, 129.3, 129.6, 132.6, 133.2, 135.3, 143.8, 151.7, 158.2, 159.0; HRMS (EI, M^+) calcd for $C_{23}H_{20}N_2O_2$ 356.151939, found 356.152478 Anal. ($C_{23}H_{20}N_2O_2\cdot0.75H_2O$) C, H, N.

References

(1) Gao, H.; Katzenellenbogen, J. A.; Garg, R.; Hansch, C. Comparative QSAR Analysis of Estrogen Receptor Ligands. *Chem. Rev.* **1999**, *99*, 723–744.

(2) Grese, T. A.; Dodge, J. A. Selective Estrogen Receptor Modulators (SERMs) [Review]. *Curr. Pharm. Des.* **1998**, *4*, 71–92.

(3) Anstead, G. M.; Carlson, K. E.; Katzenellenbogen, J. A. The estradiol pharmacophore: ligand structure-estrogen receptor binding affinity relationships and a model for the receptor binding site. *Steroids* **1997**, *62*, 268–303.

(4) Brzozowski, A. M.; Pike, A. C.; Dauter, Z.; Hubbard, R. E.; Bonn, T.; Engström, O.; Öhman, L.; Greene, G. L.; Gustafsson, J.-A.; Carlquist, M. Molecular basis of agonism and antagonism in the oestrogen receptor. *Nature* **1997**, *389*, 753–758.

(5) Ekena, K.; Weis, K. E.; Katzenellenbogen, J. A.; Katzenellenbogen, B. S. Different residues of the human estrogen receptor are involved in the recognition of structurally diverse estrogens and antiestrogens. *J. Biol. Chem.* **1997**, *272*, 5069–5075.

(6) Shiau, A. K.; Barstad, D.; Loria, P. M.; Cheng, L.; Kushner, P. J.; Agard, D. A.; Greene, G. L. The structural basis of estrogen receptor/coactivator recognition and the antagonism of this interaction by tamoxifen. *Cell* **1998**, *95*, 927–937.

(7) Anstead, G. M.; Peterson, C. S.; Katzenellenbogen, J. A. Hydroxylated 2,3-diarylindenes: Synthesis, estrogen receptor binding affinity, and binding orientation considerations. *J. Steroid Biochem.* **1989**, *33*, 877–887.

(8) Kuiper, G. G. J. M.; Enmark, E.; Pelto-Huikko, M.; Nilsson, S.; Gustafsson, J. Å. Cloning of a novel receptor expressed in rat prostate and ovary. *Proc. Natl. Acad. Sci. U.S.A.* **1996**, *93*, 5925–5930.

(9) Mosselman, S.; Polman, J.; Dijkema, R. ERβ: identification and characterization of a novel human estrogen receptor. *FEBS Lett.* **1996**, *392*, 49–53.

(10) Kuiper, G. G. J. M.; Carlsson, B.; Grandien, K.; Enmark, E.; Häggblad, J.; Nilsson, S.; Gustafsson, J.-Å. Comparison of the ligand binding specificity and transcript tissue distribution of estrogen receptor α and β. *Endocrinology* **1997**, *138*, 863–870.

(11) Fink, B. E.; Mortensen, D. S.; Stauffer, S. R.; Aron, Z. D.; Katzenellenbogen, J. A. Novel Structural Templates for Estrogen-Receptor Ligands and Prospects for Combinatorial Synthesis of Estrogens. *Chem. Biol.* **1999**, *6*, 205–219.

(12) Katzenellenbogen, J. A.; Katzenellenbogen, B. S.; Fink, B. S.; Stauffer, S. R.; Mortensen, D. S.; Sattigeri, V. J.; Huang, Y. Estrogen Receptor Ligands. Patent WO 00/19994, Apr 13, 2000.

(13) Stauffer, S. R.; Katzenellenbogen, J. A. Solid-Phase Synthesis of Tetrasubstituted Pyrazoles, Novel Ligands for the Estrogen Receptor. *J. Comb. Chem.* **2000**, *2*, 318–329.

(14) Sun, J.; Meyers, M. J.; Fink, B. E.; Rajendran, R.; Katzenellenbogen, J. A.; Katzenellenbogen, B. S. Novel Ligands that Function as Selective Estrogens or Antiestrogens for Estrogen Receptor-α or Estrogen Receptor-β. *Endocrinology* **1999**, *140*, 800–804.

(15) Huang, Y.; Katzenellenbogen, J. A. Regioselective synthesis of 1,3,5-triaryl-4-alkylpyrazoles: Novel ligands for the estrogen receptor. *Org Lett.* **2000**, *2*, 2833–2836.

(16) Carlson, K. E.; Choi, I.; Gee, A.; Katzenellenbogen, B. S.; Katzenellenbogen, J. A. Altered ligand binding properties and enhanced stability of a constitutively active estrogen receptor: Evidence that an open pocket conformation is required for ligand interaction. *Biochemistry* **1997**, *36*, 14897–14905.

(17) Meyers, M. J.; Sun, J.; Carlson, K. E.; Katzenellenbogen, B. S.; Katzenellenbogen, J. A. Estrogen receptor subtype-selective ligands: Asymmetric synthesis and biological evaluation of cis- and *trans*-5,11-dialkyl-5,6,11,12-tetrahydrochrysenes. *J. Med. Chem.* **1999**, *42*, 2456–2468.

(18) We are grateful to a referee for noting this relationship.

(19) Grese, T. A.; Cho, S.; Finley, D. R.; Godfrey, A. G.; Jones, C. D.; Lugar, C. W., III; Martin, M. J.; Matsumoto, K.; Pennington, L. D.; Winter, M. A.; Adrian, M. D.; Cole, H. W.; Magee, D. E.; Phillips, D. L.; Rowley, E. R.; Short, L. L.; Glasebrook, A. L.; Bryant, H. U. Structure–activity relationships of selective estrogen receptor modulators: Modifications at the 2-arylbenzothiophene core of raloxifene. *J. Med. Chem.* **1997**, *40*, 146–167.

(20) Pons, M.; Michel, F.; Crastes de Paulet, A.; Gilbert, J.; Miquel, J.-F.; Precgoux, G.; Hospital, M.; Ojasoo, T.; Raynaud, J.-P. Influence of new hydroxylated triphenylethylene (TPE) derivatives on estradiol binding to uterine cytosol. *J. Steroid Biochem.* **1984**, *20*, 137–145.

(21) Katzenellenbogen, J. A.; O'Malley, B. W.; Katzenellenbogen, B. S. Tripartite steroid hormone receptor pharmacology: Interaction with multiple effector sites as a basis for the cell- and promoter-specific action of these hormones. *Mol. Endocrinol.* **1996**, *10*, 119–131.

(22) Kraichely, D. M.; Sun, J.; Katzenellenbogen, J. A.; Katzenellenbogen, B. S. Conformational Changes and Coactivator Recruitment by Novel Ligands for Estrogen Receptor-α and Estrogen Receptor-β: Correlations with Biological Character and Distinct Differences among SRC Coactivator Family Members. *Endocrinology* **2000**, *141*, 3534.

(23) Stauffer, S. R.; Huang, Y.; Coletta, C. J.; Katzenellenbogen, J. A. Estrogen Pyrazoles: Defining the Pyrazole Core Structure and Orientation of Substituents in the Ligand Binding Pocket of the Estrogen Receptor. *Biorg. Med. Chem.* **2000**, in press.

(24) Stauffer, S. R.; Huang, Y.; Aron, Z. D.; Coletta, C. J.; Sun, J.; Katzenellenbogen, B. S.; Katzenellenbogen, J. A. Triarlpyrazoles with basic side chains: Development of pyrazole-based estrogen receptor antagonists. *Biorg. Med. Chem.* **2000**, in press.

(25) Pike, A. C.; Brzozowski, A. M.; Hubbard, R. E.; Bonn, T.; Thorsell, A. G.; Engstrom, O.; Ljunggren, J.; Gustafsson, J.; Carlquist, M. Structure of the ligand-binding domain of oestrogen receptor beta in the presence of a partial agonist and a full antagonist. *EMBO J.* **1999**, *18*, 4608−4618.

(26) Still, W. C.; Kahn, M.; Mitra, A. Rapid chromatographic technique for preparative separations with moderate resolution. *J. Org. Chem.* **1978**, *43*, 2923−2926.

(27) Hachiya, I.; Moriwaki, M.; Kobayashi, S. Hafnium (IV) Trifluoromethanesulfonate, An Efficient Catalyst for the Friedel−Crafts Acylation and Alkylation Reactions. *Bull. Chem. Soc. Jpn.* **1995**, *68*, 2053−2060.

(28) Wang, D.; Chen, D.; Haberman, J.; Li, C. J. Ruthenium-Catalyzed Isomerization of Homoallylic Alcohols in Water. *Tetrahedron* **1998**, *54*, 5129−5142.

(29) Horiuchi, Y.; Oshima, K.; Utimoto, K. Titanium Tetrachloride-Induced Three-Component Coupling Reaction of α-Haloacylsilane, Allysilane, and Carbonyl Compound. *J. Org. Chem.* **1996**, *61*, 4483−4486.

(30) Narasaka, K.; Kusama, H. Friedel−Crafts Acylation of Arenes Catalyzed by Bromopentacarbonylrhenium (I). *Bull. Chem. Soc. Jpn.* **1995**, *68*, 2379−2383.

(31) Williams, D.; Gorski, J. Equilibrium binding of estradiol by uterine cell suspensions and whole uteri in vitro. *Biochemistry* **1974**, *13*, 5537−5542.

(32) McInerney, E. M.; Tsai, M. J.; O'Malley, B. W.; Katzenellenbogen, B. S. Analysis of estrogen receptor transcriptional enhancement by a nuclear hormone receptor coactivator. *Proc. Natl. Acad. Sci. U.S.A.* **1996**, *93*, 10069−10073.

(33) Katzenellenbogen, J. A.; Johnson, H. J., Jr.; Myers, H. N. Photoaffinity labels for estrogen binding proteins of rat uterus. *Biochemistry* **1973**, *12*, 4085−4092.

Estrogen Pyrazoles: Defining the Pyrazole Core Structure and the Orientation of Substituents in the Ligand Binding Pocket of the Estrogen Receptor

Shaun R. Stauffer, Ying Huang, Christopher J. Coletta, Rosanna Tedesco and John A. Katzenellenbogen*

Department of Chemistry, University of Illinois, 600 South Mathews Avenue, Urbana, IL 61801, USA

Abstract—Previously, we reported that certain tetrasubstituted 1,3,5-triaryl-4-alkyl-pyrazoles bind to the estrogen receptor (ER) with high affinity (Fink, B. E.; Mortenson, D. S.; Stauffer, S. R.; Aron, Z. D.; Katzenellenbogen, J. A. *Chem. Biol.* **1999**, *6*, 205–219; Stauffer, S. R.; Katzenellenbogen, J. A. *J. Comb. Chem.* **2000**, *2*, 318–329; Stauffer, S. R.; Coletta, C. J.; Sun, J.; Tedesco, R.; Katzenellenbogen, B. S.; Katzenellenbogen, J. A. *J. Med. Chem.* **2000**, submitted). To investigate how cyclic permutation of the two nitrogen atoms of a pyrazole might affect ER binding affinity, we prepared a new pyrazole core isomer, namely a 1,3,4-triaryl-5-alkyl-pyrazole (**2**), to compare it with our original pyrazole (**1**). We also prepared several peripherally matched core pyrazole isomer sets to investigate whether the two pyrazole series share a common binding orientation. Our efficient, regioselective synthetic route to these pyrazoles relies on the acylation of a hydrazone anion, followed by cyclization, halogenation, and Suzuki coupling. We found that the ER accommodates 1,3,4-triaryl-pyrazoles of the isomeric series only somewhat less well than the original 1,3,5-triaryl series, and it appears that both series share a common binding mode. This preferred orientation for the 1,3,5-triaryl-4-alkyl-pyrazoles is supported by binding affinity measurements of analogues in which the phenolic hydroxyl groups were systematically removed from each of the three aryl groups, and the orientation is consistent, as well, with molecular modeling studies. These studies provide additional insight into the design of heterocyclic core structures for the development of high affinity ER ligands by combinatorial methods. © 2000 Elsevier Science Ltd. All rights reserved.

Introduction

The estrogen receptor (ER) binds a remarkably wide range of non-steroidal ligands,[1] and the diverse core structures of these ligands span a wide range of synthetic accessibility.[2] We have been intrigued, in particular, by the design of non-steroidal ligand cores that might be easily prepared and thus would be well suited to combinatorial expansion. As part of this investigation, we identified pyrazoles as favorable heterocyclic core building blocks,[3] and we found that by attaching a sufficient number of appropriate substituents onto this core system, we could obtain high affinity ligands for the ER.[3–5]

An issue which had interested us initially about these systems was whether the heterocyclic core structure itself plays an active role in ligand–receptor interaction, or whether it acts merely as a inert scaffold, simply displaying groups in a geometry appropriate for filling the

various subpockets that make up the ligand cavity of ER.[3] Interestingly, we found that there were large differences in binding affinity (up to 50-fold) for ligands that had identical peripheral substitution patterns but different core structures (e.g. the two diazoles, imidazoles versus pyrazoles; Figure 1).[3] Clearly, our initial thought that the ligand core structure might be acting as a passive entity—simply to position peripheral substituents—was not true. In the case shown below, the lower ER binding affinity for the imidazoles compared to the pyrazoles was attributed, at least in part, to the significantly greater dipole moment of the imidazoles.[3]

In further consideration, we wondered whether the distribution of heteroatoms within the same heterocyclic system would also have a significant effect on ER binding affinity. In the two *imidazoles* shown in Figure 1, the different position of the nitrogen atoms had little effect on their binding affinity. However, we were curious whether the related cyclic permutation of the two nitrogen atoms of a *pyrazole* might have a more significant effect on ER binding affinity.

*Corresponding author. Tel.: +1-217-333-6310; fax: +1-217-333-7325; e-mail: jkatzenc@uiuc.edu

RBA = 14 %

[Pyrazole]

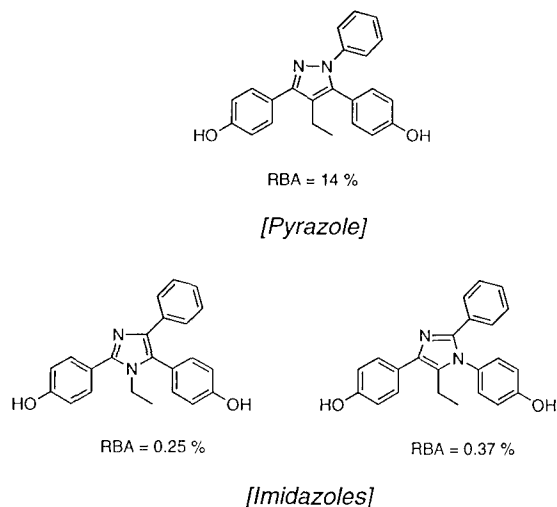RBA = 0.25 %   RBA = 0.37 %

[Imidazoles]

Figure 1. Effect of different core structures of selected five-member heterocycles (diazoles) on their estrogen receptor relative binding affinity (RBA).

To investigate this issue, we have prepared a new pyrazole core isomer, namely a 1,3,4-triaryl-5-alkyl-pyrazole (2), to compare it with our original 1,3,5-triaryl-4-alkyl-pyrazole (1) (Fig. 2). This new compound (2) represents the only other possible pyrazole system capable of displaying the same relative substitution pattern of aryl, alkyl, aryl, and phenyl groups as does our original pyrazole 1. To extend this investigation further, we synthesized several other peripherally matched core pyrazole isomer

1
(Series I)

2
(Series II)
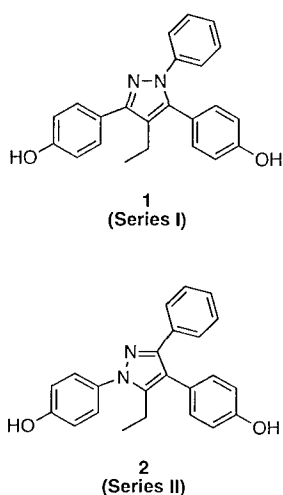
Figure 2. Original 1,3,5-triaryl-pyrazole 1 (the basis of Series I) and the new 1,3,4-triaryl-pyrazole isomer 2 (the basis of Series II).

sets, in which some of the phenolic hydroxyl groups are systematically deleted, to establish more definitively which core isomer is most favored and to investigate whether they share a common binding orientation.

Results and Discussion

Synthesis of 1,3,4-triaryl-5-alkyl-pyrazoles

Our initial attempts to synthesize the pyrazole isomer 2 involved conditions similar to those used in previous studies (Scheme 1).[3] We first prepared diketone 3 in high yield, starting from the deoxybenzoin and propionic anhydride. However, our attempts to generate the pyrazole by condensation of the dione with 4-methoxyphenylhydrazine were unsuccessful and resulted in a complex mixture that contained the two possible retro-Claisen condensation products from cleavage of the 1,3-dione.

Because of these difficulties and the fact that this route was not likely to be regioselective, we investigated an alternative, potentially regioselective approach that involved a one-pot acylation and cyclization procedure starting from an appropriate hydrazone, as illustrated in Figure 3. Unfortunately, we could not isolate the hydrazone (4), because it rapidly underwent Fischer indole cyclization to the 2,3-diaryl-indole product (5). Even under mild conditions, we obtained only starting material or indole product, but no hydrazone. Apparently, the 4-methoxyphenyl substituent in the deoxybenzoin starting material facilitates the [3,3]-sigmatropic cyclization of the ene-phenylhydrazole intermediate by stabilizing the transition state through a stilbene-like structure (Fig. 3).

We wondered whether we could avoid this competing cyclization by omitting the 4-methoxyphenyl substituent during the synthesis of the pyrazole (Fig. 4). Of course, this approach would entail adding an aryl group later to the completed heterocycle, but this could presumably be done using an appropriate Pd(0)-mediated coupling reaction. This synthetic strategy was also attractive because it allows for the introduction of additional structural diversity into these systems at a late stage, just before phenol deprotection, an attractive feature for combinatorial library expansion.[5]

According to this approach, we were able to successfully synthesize pyrazole 2 as well as analogues 10a–d (Scheme 2). Initial formation of hydrazones 6a–c by reaction of

3, (78 %)
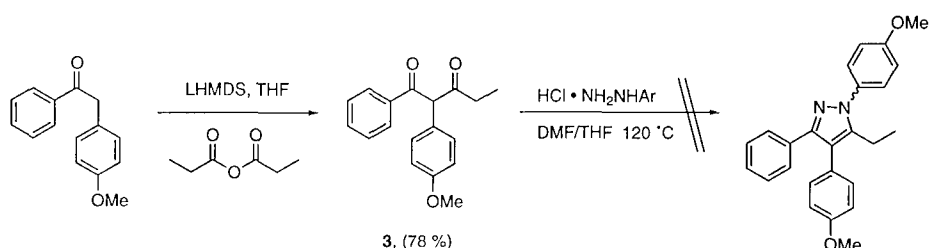
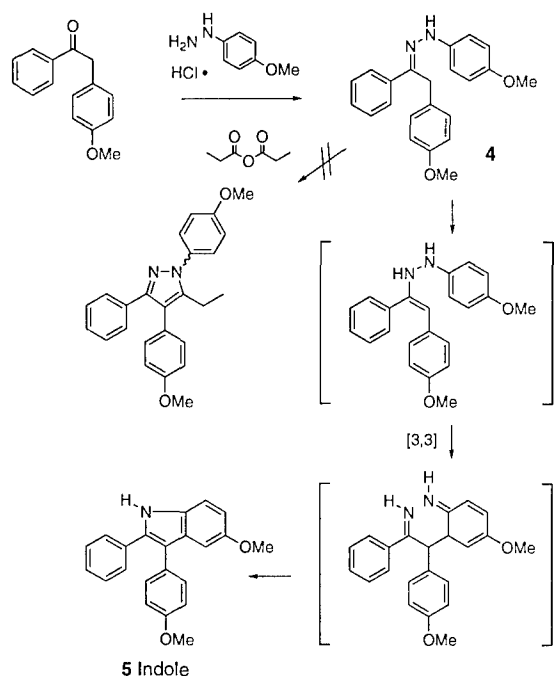Scheme 1. Attempted synthesis of MeO-protected pyrazole isomer.

Figure 3. Attempted synthesis of pryazole isomer using an acylation–cyclization.
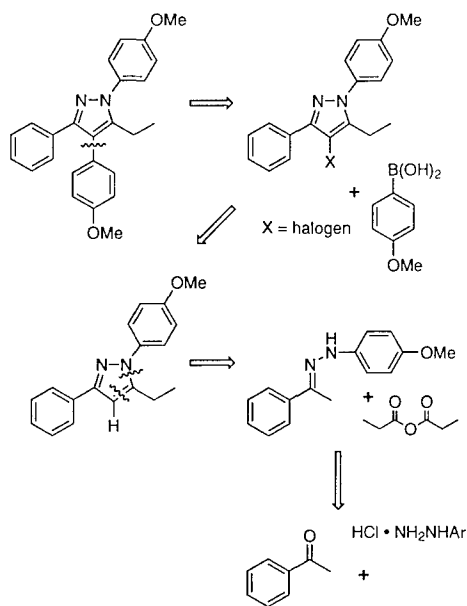

Figure 4. Retro-synthetic strategy for Pd(0)-mediated coupling approach to pyrazoles.

the acetophenone compounds with either the hydro-chloride salt of 4-methoxyphenylhydrazine or phenylhydrazine occurred in moderate yields, and as we had hoped, no competing cyclization to the indole occurred with this less stabilized system. Hydrazones **6a–c** were then treated with butyllithium to form the corresponding dianion, which was acylated with an alkyl anhydride and then cyclized upon addition of HCl.[6] The yields shown for pyrazole formation are based on the anhydride and are typical for this reaction.

To introduce the last aromatic substituent, the tri-substituted pyrazoles **7a–d** were iodinated by treatment with a solution of KI and I_2,[7] and then subjected to Suzuki coupling conditions with either phenylboronic acid or p-methoxyphenylboronic acid. Initial conditions involved using $Pd(PPh_3)_4$ as a Pd(0) catalyst and DME/H_2O as solvent (**9c** 52%, 72 h); however, by using $Pd(OAc)_2$ as a pre-catalyst and an n-PrOH/H_2O solvent mixture, we were able to obtain the tetra-substituted pyrazoles (**9a,b,d,e**) with slightly improved yields (60–71%) and shorter reaction times (1–14 h).[8] The protected pyrazole isomers were subsequently demethylated using BBr_3 to afford the desired phenolic products **10a–d** and **2**.

Comparison of the estrogen receptor binding affinities of the isomeric 1,3,4-triaryl-pyrazoles (Series II) and the original 1,3,5-triaryl-pyrazoles (Series I)

The binding affinities of the pyrazoles for ER were assayed in a competitive radiometric binding assay; this assay has been described previously,[9] and affinities are expressed as relative binding affinity (RBA) values, where estradiol has an affinity of 100% (Table 1). The 1,3,4-triaryl-pyrazole **2**, which is the nitrogen ring isomer of our original 1,3,5-triaryl-pyrazole **1**, has a very significant affinity of 5.8%, but is 2.6-fold less than the original pyrazole **1**. To determine whether the 1,3,4-triaryl-pyrazole binds to ER in the same mode as pyrazole **1**, we investigated the binding affinity of several other 1,3,4-triaryl-pyrazoles (**10a–d**) and compared their affinities with those of their corresponding 1,3,5-triaryl-pyrazole isomers (**11a,b**[4] and **11c,d**[10]).

When examining the first three sets of isomeric pyrazoles (the other two are discussed below), the pyrazoles in the new isomeric Series II (1,3,4-triaryl-pyrazoles) have somewhat lower affinity than those in the original Series I (1,3,5-triaryl-pyrazoles), but only by an average of 2-fold. Within the original pyrazole series (Series I), certain changes to the peripheral substituents resulted in an increase in RBA. For example, when a hydroxyl group is added to the N(1)-phenyl substituent (i.e. from pyrazole **1** to **11a**), a slight increase in affinity occurs. A similar increase in RBA upon hydroxyl substitution is observed in the isomeric Series II, going from pyrazole **2** to **10a**.

Previously, we also showed that modification of the alkyl chain at C(4)-position of the initial pyrazole Series I from an ethyl **1** to a propyl substituent **11b** results in a 1.6-fold increase in affinity, indicating a more favorable hydrophobic interaction. However, this favorable interaction ended at propyl, as the n-butyl isomer experienced a significant drop in binding affinity.[4] In Series II, going from $R_3 = $ Et (**2**) to n-propyl (**10b**) results in a similar but somewhat larger increase in affinity than it does in Series I (2.7-fold versus 1.6-fold).

Because the structure–binding affinity patterns observed for both pyrazole isomers (Series I and II) are quite similar, we postulated that these distinct core structure pyrazole isomers would be binding in the same orientation in the ER binding pocket.
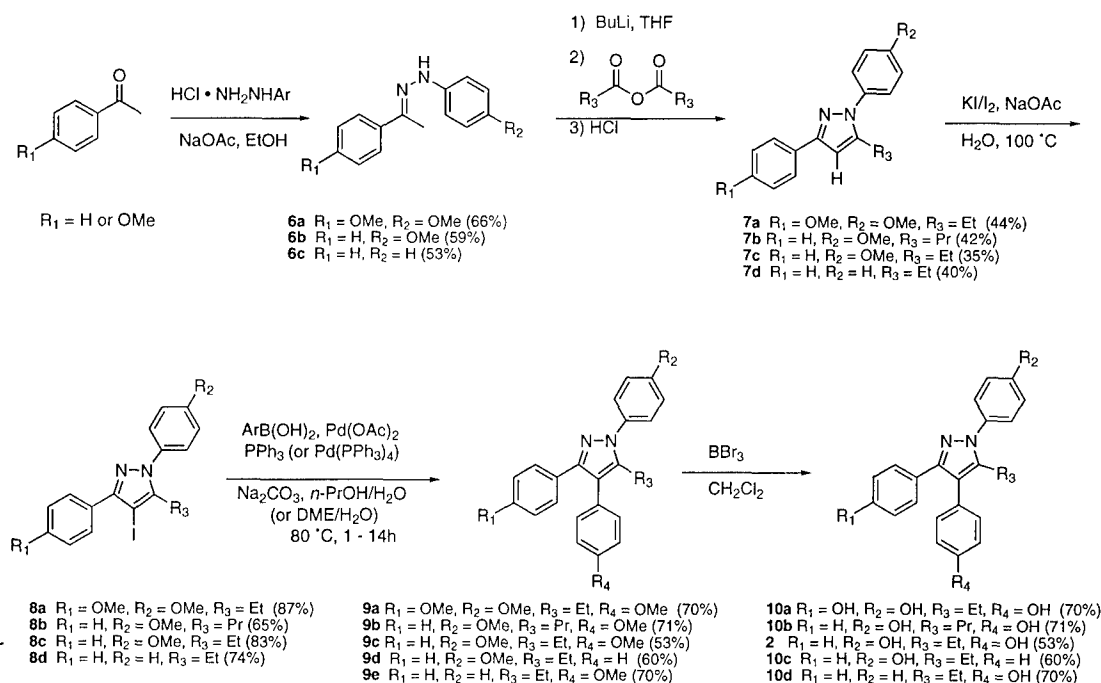
Scheme 2. Synthesis of 1,3,4-triaryl-5-alkyl-pyrazoles.

Table 1. Binding affinity data for pyrazole isomers and original pyrazole series

R_1	R_2	R_3	R_4	Compound (I)	RBA (I)[a]	Compound (II)	RBA (II)[a]
H	OH	Et	OH	1	15.3±3	2	5.8±0.3
OH	OH	Et	OH	11a	20.3±3	10a	7.8±4
H	OH	n-Pr	OH	11b	25±0.01	10b	16.0±1
H	OH	Et	H	11c	0.46	10c	0.43±0.07
H	H	Et	OH	11d	0.007	10d	0.008±0.005

[a]Competitive radiometric binding assays were done using 10 nM [³H]E₂ as tracer and lamb uterine cytosol as receptor source; for details, see Experimental. Compounds 11a–d were prepared as described elsewhere.[4,10]

Elucidation of the aryl group in the pyrazole that mimics the A-ring of estradiol: Inferring pyrazole orientation in the ligand binding pocket from the binding affinity of isomeric monophenols

To further support the hypothesis that both pyrazole isomers have the same binding mode and to more confidently establish which phenolic group is playing the role of the A-ring phenol in estradiol, we prepared the individual monophenolic derivatives of pyrazole 1 (Table 1, Series I, 11c and 11d) and pyrazole 2 (Table 1, Series II, 10c and 10d). Systematic phenol deletion is a standard approach that has been used in the past to determine which phenol in an unsymmetrical bisphenolic non-steroidal ER ligand mimics the crucial A-ring phenol of estradiol (E_2).[11,12] The monophenolic analogue having the highest affinity is then presumed to have preserved the phenol that is acting as the estradiol A-ring mimic, because the hydroxyl substituent at this position is known to be essential for high affinity binding to the ER.[13] (At the outset, it is of note that removal of one of the phenols from the R_1 position (pyrazole 1 versus 11a in Series I, and pyrazole 2 versus 10a in Series II) has little effect

on binding affinity, suggesting that these rings are not the ones that correspond to the A-ring of estradiol.)

The route in Scheme 2 was used to prepare both the N(1) and the C(4) monophenolic pyrazole Series II analogues 10c and 10d, regioselectively and in good yield. The RBA of pyrazole isomer 10c is 0.43%, whereas that of pyrazole isomer 10d is only 0.008%. When these affinities are compared to that of the bisphenolic pyrazole 2 (5.8%) (Table 1), one can see that removal of the phenolic hydroxyl from the N(1) phenyl ring results in a 725-fold decrease in affinity, whereas removal of the hydroxyl from the C(4) phenyl group results in only a 13-fold decrease. Thus, the 56-fold greater decrease in affinity that results from deleting the phenolic hydroxyl from the N(1) phenyl group versus from the C(4) phenyl group strongly suggests that the N(1)-phenolic substituent in the Series II pyrazoles is acting as the A-ring mimic (Fig. 5).

Initial attempts to prepare the C(3) and C(5) monophenol pyrazole analogues for Series I (11c and 11d) regioselectively using the acylation–cyclization strategy were unsuccessful. However, these compounds could successfully be prepared via the corresponding pyrazolines by a new regioselective route (not shown) that will be described elsewhere.[10] The binding affinities for the Series I monophenolic isomers 11d and 11c are 0.007% and 0.46%, respectively. Compared to the corresponding bisphenolic pyrazole 1 (15.3%) (Table 1), a much greater decrease in binding affinity results when the hydroxyl group is removed from C(3) phenol (2185-fold, 11d) than from the C(5) phenol (33-fold, 11c). The difference in affinity loss that results from the alternative hydroxy group deletion in this series (i.e. 2185/33- or 66-fold) is comparable to that found in Series II (56-fold). This result indicates that in Series I the C(3) phenol is
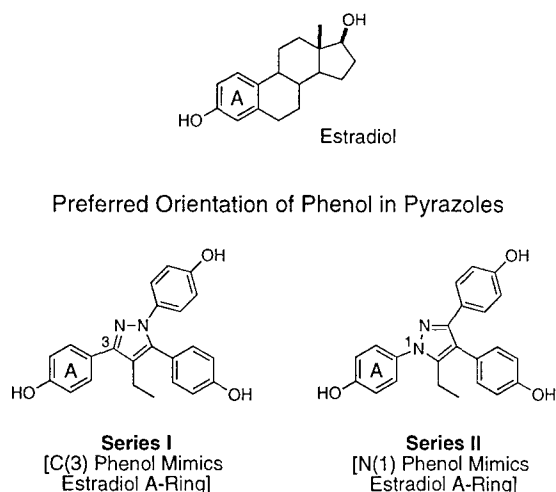
Estradiol

Preferred Orientation of Phenol in Pyrazoles

Series I
[C(3) Phenol Mimics
Estradiol A-Ring]

Series II
[N(1) Phenol Mimics
Estradiol A-Ring]

Figure 5. Preferred orientation and proposed A-ring mimic for Series I and Series II pyrazoles.
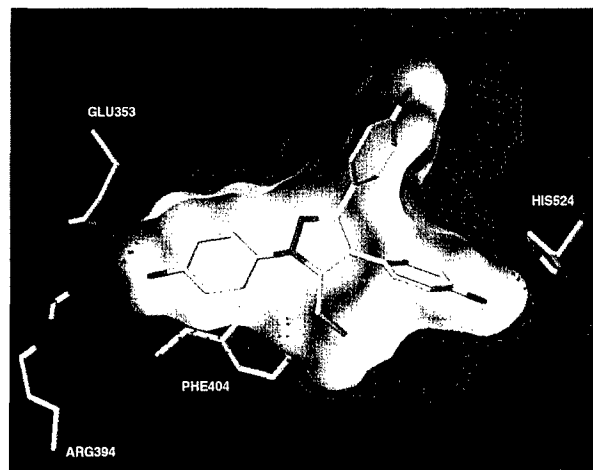

Figure 6. A model for pyrazole **10a** docked and minimized in the DES-ERα-LBD. The surface of the ligand is shown in yellow, and the solvent accessible surface of ER as purple dots.

mimicking the A-ring of E_2. Thus, because the C(3) phenol in Series I and the N(1) phenol in Series II are positioned in a congruent fashion, we believe that the pyrazoles of both Series I and II share a single common binding mode, as illustrated in Figure 5. According to this mode, the other two aryl groups are displayed within a region of the binding pocket resembling the C/D region of E_2, which is known to tolerate a large number of substituents.[13]

Modeling pyrazole orientation in the ligand binding pocket

In our original study of pyrazole **1**, we used molecular modeling to show that this compound could bind in an orientation in which the C(5) phenol mimicked the A-ring of estradiol;[3] this is different from that shown in Figure 5. However, in this earlier study, we had based our model on the ERα crystal structure with the antagonist ligand raloxifene.[14] Upon further consideration, we now think that the ERα crystal structure we used previously was not an appropriate one for modeling ligands like pyrazole **1**, because unlike raloxifene, these pyrazoles are ERα agonists, not antagonists.[4,15]

We have recently completed a more extensive modeling of a pyrazole triphenol that corresponds to pyrazole *di*phenol **11b**,[4] using as a starting point an X-ray structure of ERα complexed with the agonist diethylstilbestrol, a nonsteroidal estrogen agonist with an RBA of 98%.[16] In this study, we considered six possible starting orientations (the three phenols placed in the A-ring pocket and in each case the two alternative orientations of the remaining two phenols that come from rotation about the bond linking the A-ring phenol and the pyrazole core). From this recent study,[4] the orientation in which the C(3) phenol of the Series I pyrazole mimics the A-ring of estradiol gave the lowest energy structure and appeared to be quite reasonable on steric grounds, although it is difficult to rigorously eliminate some of the other possible orientations. This is the orientation shown in Figure 5 for the Series I pyrazole.

In the present study, we have used this approach to examine the six possible binding orientations of the ethyl triphenol Series II pyrazole **10a**. Again, the orientation in which the N(1) phenol is the mimic of the A-ring of estradiol (cf. Fig. 5) is well accommodated by the structure and has a reasonable binding energy, although an alternative orientation with the C(4) phenol in this position cannot be ruled out by binding energy considerations. Nevertheless, this latter orientation seems unlikely, given the much higher experimental binding affinity of monophenol **10c** versus **10d** (Table 1).

Thus, on the basis of the experimental determinations of monophenol binding affinities and molecular modeling, we suggest that the preferred binding modes of the pyrazoles in the estrogen receptor correspond to those illustrated in Figure 5. A pictorial representation of pyrazole **10a** in this orientation is shown in Figure 6.

Conclusions

To explore the effect of core structure on the ability of pyrazole ligands to bind to ER, we developed an efficient, regioselective, and flexible route to a new isomeric series of pyrazoles (1,3,4-triaryl-5-alkyl-pyrazoles), and we evaluated their binding affinity to ER. The synthesis relies on the acylation of a hydrazone anion, followed, after cyclization and halogenation, by a Pd(0) Suzuki coupling strategy. We found that the ER accommodates 1,3,4-triaryl-pyrazoles of the new isomeric series (Series II) only slightly less well than the original 1,3,5-triaryl series (Series I), and on the basis of the binding affinity of the corresponding monophenols and molecular modeling studies, both isomers appear to share a common binding mode. In this binding mode, the putative A-ring mimic is the C(3) phenol in Series I and the N(1) phenol in Series II. Thus, as in the case of the imidazoles discussed earlier (Fig. 1), it does appear possible to permute the position of heteroatoms in the azole ring without having a major effect on the ER binding

affinity, provided that the peripheral substituents remain disposed with the same geometry and provided that one remains in the same azole series (i.e. 1,2-azoles [pyrazoles] not 1,3-azoles [imidazoles]), so that compounds with equivalent dipole moments and polarities are being compared. These studies provide additional insight into the design of heterocyclic core structures for the development of high affinity ER ligands by combinatorial methods.

Experimental

General

Melting points were determined on a Thomas-Hoover UniMelt capillary apparatus and are uncorrected. All reagents and solvents were obtained from Aldrich, Fisher or Mallinckrodt. Tetrahydrofuran was freshly distilled from sodium/benzophenone. Dimethylformamide was vacuum distilled prior to use, and stored over 4 Å molecular sieves. *n*-Butyllithium and *t*-butyllithium were titrated with *N*-pivaloyl-*o*-toluidine. Et_3N was stirred with phenylisocyanate, filtered, distilled, and stored over 4 Å molecular sieves. All reactions were performed under a dry N_2 atmosphere unless otherwise specified. Reaction progress was monitored by analytical thin-layer chromatography using GF silica plates purchased from Analtech. Visualization was achieved by short wave UV light (254 nm) or potassium permanganate. Flash column chromatography was performed using Woelm 32–63 µm silica gel packing.[17]

^1H and ^{13}C NMR spectra were recorded on either a Varian Unity 400 MHz or 500 MHz spectrometer using $CDCl_3$, MeOD or $(CD_3)_2SO$ as solvent. Chemical shifts were reported as parts per million downfield from an internal tetramethylsilane standard (δ 0.0 for ^1H) or from solvent references. NMR coupling constants are reported in Hertz. ^{13}C NMR spectra were determined using either the Attached Proton Test (APT) or standard ^{13}C pulse sequence parameters. Low resolution and high resolution electron impact mass spectra were obtained on Finnigan MAT CH-5 or 70-VSE spectrometers. Elemental analyses were performed by the Microanalytical Service Laboratory of the University of Illinois. Hydrazones **6a–c** are prone to decomposition and therefore could only be stored for 2–3 days at 0 °C. Once the hydrazone products were confirmed by ^1H NMR they were typically used directly in the acylation cyclization step without further characterization.

Biological procedures: relative binding affinity assay

Ligand binding affinities (RBAs) using lamb uterine cytosol as a receptor source were determined by a competitive radiometric binding assay using 10 nM [^3H]estradiol as tracer and dextran-coated charcoal as an adsorbent for free ligand.[9] All incubations were done at 0 °C for 18–24 h. Binding affinities are expressed relative to estradiol (RBA = 100%) and are reproducible with a coefficient of variation of 0.3.

Molecular modeling of pyrazole 10a

The protocol for modeling followed that recently described for a related pyrazole triphenol.[4] The starting conformation for pyrazole **10a** used for receptor docking studies was generated from a random conformational search performed using the MMFF94 force field as implemented in Sybyl 6.6. The resulting lowest energy conformer was then used for docking studies. Charge calculations were determined using the MMFF94 method and molecular surface properties displayed using MOLCAD module in Sybyl 6.6.

Pyrazole **10a**, generated as noted above, was pre-positioned in the DES-ERα-LBD crystal structure[16] using a least squares multifitting of select atoms within the DES ligand. Once pre-positioned, DES was deleted and ligand **10a** was optimally docked in the ERα binding pocket in six orientations (as specified in the text) using the Flexidock routine within Sybyl (Tripos). Both hydrogen-bond donors and acceptors within the pocket surrounding the ligand (Glu_{353}, Arg_{394}, and His_{524}), the ligand itself and select torsional bonds were defined. The docked receptor ligand complexes from Flexidock then underwent a three step minimization. First, non-ring torsional bonds of the ligand were minimized in the context of the receptor using the torsmin command. This was followed by minimization of the side chain residues within 8 Å of the ligand, while holding the backbone and residues Glu_{353} and Arg_{394} fixed. A final third minimization of both the ligand and receptor was conducted using the Anneal function (hot radius 8 Å, interesting radius 16 Å from pyrazole **10a**) to afford the final model.

Chemical syntheses

5-Ethyl-1,4-bis-(4-methoxyphenyl)-3-phenyl-1H-pyrazole (2). A stirred solution of **9c** (46 mg, 0.16 mmol) in CH_2Cl_2 (15 mL) was treated with BBr_3 (1.62 mL, 1.62 mmol) according to the general demethylation procedure. After work up and an SiO_2 plug (30% EtOAc/hexanes) a white solid was isolated (40 mg, 94%): mp 220–225 °C; ^1H NMR (MeOD-d_4, 400 MHz) δ 0.90 (t, 3H, $J = 7.5$), 2.62 (q, 2H, $J = 7.5$), 6.79 (XX′ of AA′XX′, 2H, $J_{AX} = 8.3$, $J_{XX} = 2.3$), 6.94 (XX′ of AA′XX′, 2H, $J_{AX} = 8.6$, $J_{XX} = 2.7$), 7.04 (AA′ of AA′XX′, 2H, $J_{AX} = 8.2$, $J_{AA'} = 2.4$), 7.20–7.27 (m, 2H), 7.34 (AA′ of AA′XX′, 2H, $J_{AX} = 8.8$, $J_{AA'} = 2.6$), 7.37–7.44 (m, 3H); ^{13}C NMR (MeOD-d_4, 100 MHz) δ 12.4, 17.2, 114.8, 115.2, 118.5, 124.3, 126.9, 127.4, 127.5, 127.6, 131.0, 131.0, 132.9, 144.1, 148.9, 156.2, 157.8; MS (EI, 70 eV) m/z (relative intensity, %): 356 (M^+, 100); Anal calcd for $C_{23}H_{20}N_2O_2 \cdot H_2O$: C, 73.78; H, 5.92; N, 7.48. Found: C, 73.82; H, 5.95; N, 7.69.

4′-Methoxyacetophenone-4-methoxyphenylhydrazone (6a). An EtOH (40 mL) solution of 4-methoxyacetophenone (1 g, 6.67 mmol), sodium acetate (1.09 g, 13.34 mmol), and 4-methoxyphenylhydrazine hydrochloride (1.74 g, 10.0 mmol) was heated to 80 °C for 3.0 h. The reaction mixture was cooled to room temperature and concentrated under reduced pressure. The residue was dissolved in ethyl

acetate (30 mL) and washed with water (40 mL) and brine (2×40 mL). After drying over $MgSO_4$ and solvent concentration a red and white heterogeneous solid formed. The product was collected by filtration and rinsed with cold ethanol (20 mL) to afford **6a** as a white solid (1.18 g, 66%) which was used directly in the next step.

Acetophenone-4-methoxyphenylhydrazone (6b). A solution of acetophenone (250 mg, 2.00 mmol) and 4-methoxyphenylhydrazine hydrochloride (349 mg, 2.00 mmol) was reacted similarly to conditions used for **6a** to afford a red and white heterogeneous sold. Cold ethanol (20 mL) was added and the remaining solid collected via vacuum filtration to afford **6b** as a white solid (1.41 g, 59%) which was used directly in the next step.

Acetophenonephenylhydrazone (6c). A solution of acetophenone (1.8 g, 15 mmol), phenylhydrazine hydrochloride (2.17 g, 15 mmol), and sodium acetate (1.23 g, 15.0 mmol), in anhydrous ethanol (40 mL), was reacted similarly to conditions used for **6a** to afford a yellow and white heterogeneous solid. Cold ethanol (20 mL) was added to the solid and the product collected via vacuum filtration to afford **6c** as a white solid (1.67 g, 53%) which was used directly in the next step.

General acylation–cyclization procedure (7a–d). To a stirred solution of hydrazone (3.05 mmol) in THF (10 mL) at 0 °C was added 1.29 M BuLi (4.73 mL, 6.10 mmol) dropwise. The resulting deep red solution was allowed to stir at 0 °C for 0.25 h, then room temperature for 0.25 h, and re-cooled to 0 °C, whereupon a THF solution (2.0 mL) of the appropriate alkyl anhydride (1.53 mmol) was added dropwise. This mixture was stirred at 0 °C for 0.25 h, then treated with 3 M HCl (6 mL, 18 mmol) and refluxed for 1.5 h. The biphasic mixture was cooled to room temperature and the aqueous layer separated and neutralized with saturated $NaHCO_3$. The neutralized solution was extracted with ethyl acetate (3×20 mL) and the organic layers combined with the THF layer from the reaction mixture. The final organic layers were washed with satd $NaHCO_3$ (3×20 mL), dried over $MgSO_4$, and concentrated to afford a red oil. The crude oil was purified by flash chromatography.

5-Ethyl-1,3-bis-(4-methoxyphenyl)-1H-pyrazole (7a). Following the general procedure above hydrazone **6a** (824 mg, 3.05 mmol) was acylated with propionic anhydride (198 mg, 0.20 mL, 1.53 mmol) and cyclized with HCl. Flash chromatography (25% EtOAc/hexanes) afforded an inseparable mixture of 4-methoxyacetophenone and **7a** (474 mg). The phenone was reduced by the dropwise addition of a solution of $NaBH_4$ (27.3 mg, 0.72) in H_2O (5 mL) to a solution of the product mixture in ethanol (5 mL). The solution was stirred for 18 h at room temperature and poured over 1 M HCl (20 mL). Upon product isolation (EtOAc, satd $NaHCO_3$, brine) and solvent removal under reduced pressure an orange oil was isolated, which upon addition of 25% EtOAc/hexanes resulted in selective crystallization of pyrazole **7a** as fine white crystals (200 mg, 44%): ^1H NMR (CDCl$_3$, 400 MHz) δ 1.24 (t, 3H, $J = 7.6$), 2.64 (q, 2H, $J = 7.5$),

3.83 (s, 3H) 6.45 (s, 1H), 3.85 (s, 3H), 6.98 (XX' of AA'XX', 2H, $J_{AX} = 8.9$, $J_{XX} = 2.4$), 7.09 (XX' of AA'XX', 2H, $J_{AX} = 9.0$, $J_{XX} = 2.7$), 7.39 (AA' of AA'XX', 2H, $J_{AX} = 8.9$, $J_{AA'} = 2.7$), 7.79 (AA' of AA'XX', 2H, $J_{AX} = 8.9$, $J_{AA'} = 2.8$); ^{13}C NMR (CDCl$_3$, 100 MHz) δ 13.0, 19.6, 55.1, 55.4, 101.2, 113.7, 114.1, 126.2, 126.8, 126.8, 133.0, 146.5, 150.8, 158.9, 159.1.

1-(4-Methoxyphenyl)-3-phenyl-5-propyl-1H-pyrazole (7b). Following the general procedure above hydrazone **6a** (1.37 g, 5.71 mmol) was acylated with butyric anhydride (452 mg, 0.47 mL, 2.86 mmol) and cyclized with HCl. Flash chromatography (30% EtOAc/hexanes) afforded the title compound as a yellow oil (710 mg, 42%): ^1H NMR (CDCl$_3$, 400 MHz) δ 0.96 (t, 3H, $J = 7.5$) 1.66 (sext, 2H, $J = 7.5$), 2.61 (t, 2H, $J = 7.7$), 3.85 (s, 3H), 6.54 (s, 1H), 6.99 (XX' of AA'XX', 2H, $J_{AX} = 8.7$, $J_{XX} = 2.7$), 7.31 (app tt, 1H, $J = 7.3$, 1.5), 7.38–7.43 (m, 4H), 7.89 (AA' of AA'XX', 2H, $J_{AX} = 7.2$, $J_{AA'} = 1.3$); ^{13}C NMR (CDCl$_3$, 100 MHz) δ 13.7, 21.9, 27.1, 55.4, 102.2, 114.1, 125.5, 126.9, 127.5, 128.4, 132.9, 133.4, 145.2, 150.9, 159.1; HRMS (EI, M$^+$) calcd for $C_{19}H_{20}N_2O$: 292.1576. Found: 292.1569.

5-Ethyl-1-(4-methoxyphenyl)-3-phenylpyrazole (7c). Following the general procedure above hydrazone **6b** (4.50 g, 18.75 mmol) was acylated with propionic anhydride (1.22 g, 1.20 mL, 9.38 mmol) and cyclized with HCl. Upon solvent removal a crude orange solid was isolated. The crude solid was recrystallized from 20% ethyl acetate/hexanes to afford the title compound as pale yellow needles (1.82 g, 35%): mp 70–75 °C; ^1H NMR (CDCl$_3$, 400 MHz) δ 1.25 (t, 3H, $J = 7.5$), 2.65 (q, 2H, $J = 7.5$), 6.53 (s, 1H), 3.86 (s, 3H), 6.99 (AA'XX', 2H, $J = 8.6$, 2.6), 7.28–7.33 (m, 1H), 7.37–7.43 (m, 4H), 7.85–7.90 (m, 2H); ^{13}C NMR (CDCl$_3$, 125 MHz) δ 13.0, 19.6, 55.4, 101.6, 114.2, 125.5, 126.8, 127.5, 128.4, 132.9, 133.3, 146.6, 151.0, 159.0; MS (EI, 70 eV) m/z (relative intensity, %): 278 (M$^+$, 100). Anal. calcd for $C_{18}H_{18}N_2O$: C, 77.67; H, 6.52; N, 10.06. Found: C, 77.62; H, 6.49; N, 10.05.

1,3-Diphenyl-5-propyl-1H-pyrazole (7d). Following the general procedure above hydrazone **6c** (1.30 g, 6.19 mmol) was acylated with propionic anhydride (403 mg, 0.40 mL, 3.10 mmol) and cyclized with HCl. Flash chromatography (20% diethyl ether/hexanes) afforded the title compound as a yellow oil (600 mg, 40%): ^1H NMR (CDCl$_3$, 500 MHz) δ 1.28 (t, 3H, $J = 7.4$), 2.72 (q, 2H, $J = 7.4$), 6.58 (s, 1H), 7.32–7.53 (m, 8H), 7.91 (d, 2H, $J = 7.5$); ^{13}C NMR (CDCl$_3$, 100 MHz) δ 13.2, 19.9, 102.3, 125.7, 127.8, 127.9, 128.8, 129.1, 133.4, 140.0, 146.7, 151.5; HRMS (EI, M$^+$) calcd for $C_{17}H_{16}N_2$: 248.1313. Found: 248.1312.

General iodination procedure (8a–d). To a refluxing solution of pyrazole (0.59 mmol) and sodium acetate (107 mg, 1.13 mmol) in H_2O (4.00 mL) was added a solution of KI (591 mg, 3.56 mmol) and I_2 (301 mg, 1.19 mmol) in H_2O (4 mL) dropwise. The resulting dark brown solution was allowed to reflux for 3 h and then was cooled to room temperature and the product extracted with diethyl ether (3×25 mL). The organic

layers were combined, washed with NaS_2O_2 (3×20 mL), $NaHCO_3$ (2×20 mL), brine (2×20 mL) and then dried over $MgSO_4$ and concentrated under reduced pressure to afford the crude iodo-pyrazoles. The products were purified by recrystallization from hexanes or by flash chromatography on silica gel.

5-Ethyl-4-iodo-1,3-bis-(4-methoxyphenyl)-1H-pyrazole (8a).
Pyrazole **7a** (153 mg, 0.59 mmol) was iodinated according to the general procedure above. A crude tan solid was isolated and recrystallized from hexanes to afford the title compound as a white solid (224 mg, 87%): ^{1}H NMR ($CDCl_3$, 400 MHz) δ 1.13 (t, 3H, $J = 7.4$), 2.73 (q, 2H, $J = 7.5$), 3.84 (s, 3H), 3.85 (s, 3H), 6.94–7.02 (m, 4H), 7.36 (AA′XX′, 2H, $J = 9.0$, 2.7), 7.83 (AA′XX′, 2H, $J = 8.8$, 2.5); ^{13}C NMR ($CDCl_3$, 125 MHz) δ 13.1, 20.1, 55.1, 55.4, 60.1, 113.4, 114.2, 125.4, 126.9, 129.4, 132.6, 147.2, 151.4, 159.4, 159.5.

4-Iodo-1-(4-methoxyphenyl)-3-phenyl-5-propylpyrazole (8b).
Pyrazole **7b** (660 mg, 2.26 mmol) was iodinated according to the general procedure above. A crude oil was isolated and purified by flash chromatography (25% ethyl acetate/hexanes) to afford a mixture of unreacted pyrazole **7b** and product **8b** as a pale-yellow oil (yield as determined by NMR: 65%; resonances listed for product only): ^{1}H NMR ($CDCl_3$, 400 MHz) δ 0.90 (t, 3H, $J = 7.4$) 1.56 (sext, 2H, $J = 7.6$), 2.70 (t, 2H, $J = 7.8$), 3.86 (s, 3H), 6.99 (XX′ of AA′XX′, 2H, $J_{AX} = 8.7$, $J_{XX'} = 2.8$), 7.90 (AA′ of AA′XX′, 2H, $J_{AX} = 8.3$, $J_{AA'} = 1.6$), 7.26–7.46 (m, 5H); ^{13}C NMR ($CDCl_3$, 100 MHz) δ 13.8, 21.9, 28.4, 55.4, 60.9, 114.2, 127.1, 128.0, 128.0, 128.2, 132.8, 146.2, 151.5, 159.5; HRMS (EI, M^+) calcd for $C_{19}H_{19}N_2OI$: 418.0542. Found: 418.0550.

5-Ethyl-4-iodo-1-(4-methoxyphenyl)-3-phenyl-1H-pyrazole (8c).
Pyrazole **7c** (500 mg, 1.80 mmol) was iodinated according to the general procedure above to afford the title compound as a white solid (603 mg, 83%): mp 70–73 °C; ^{1}H NMR ($CDCl_3$, 500 MHz) δ 1.14 (t, 3H, $J = 7.5$), 2.74 (q, 2H, $J = 7.5$), 3.86 (s, 3H), 6.99 (AA′XX′, 2H, $J = 8.6$, 2.9), 7.34–7.47 (m, 5H), 7.86–7.92 (m, 2H); MS (EI, 70 eV) m/z (relative intensity, %): 404 (M^+, 100). Anal. calcd for $C_{18}H_{17}N_2OI$: C, 53.48; H, 4.24; N, 6.93. Found: C, 53.66; H, 4.24; N, 6.89.

5-Ethyl-4-iodo-1,3-diphenyl-1H-pyrazole (8d).
Pyrazole **7d** (248 mg, 1.13 mmol) was iodinated according to the general procedure above to afford a crude orange solid. Recrystallization from hexanes afforded **8d** as small white crystals (312 mg, 74%): mp 82–85 °C; ^{1}H NMR ($CDCl_3$, 500 MHz) δ 1.61 (t, 3H, $J = 7.5$), 2.78 (q, 2H, $J = 7.5$), 7.35–7.55 (m, 8H), 7.86–7.91 (m, 2H); ^{13}C NMR ($CDCl_3$, 125 MHz) δ 13.3, 20.3, 61.1, 125.6, 128.2, 128.3, 128.4, 128.6, 129.3, 132.9, 139.9, 147.3, 152.1; HRMS (EI, M^+) calcd for $C_{17}H_{15}N_2I$: 374.0280. Found: 374.0277.

General procedure for Suzuki coupling (9a,b,d,e).
To a stirred solution of iodo-pyrazole (0.43 mmol) in n-propanol (2 mL) were added the appropriate boronic acid (0.45 mmol), $Pd(OAc)_2$ (3 mg, 0.013 mmol), PPh_3 (10 mg, 0.039 mmol), 2 M Na_2CO_3 (0.47 mL, 0.95 mmol), and

H_2O (0.5 mL). The heterogeneous solution was heated to reflux for 5 h, cooled to room temperature, and filtered through Celite (EtOAc 4×5 mL). The filtrate was concentrated and partitioned in diethyl ether and water and the aqueous layer separated and extracted twice more with ether. The combined organic layers were washed with brine, dried over $MgSO_4$ and concentrated under reduced pressure. The tetrasubstituted pyrazoles were subsequently purified by flash chromatography.

5-Ethyl-1,3,4-tris-(4-methoxyphenyl)-1H-pyrazole (9a).
Iodo-pyrazole **8a** (187 mg, 0.43 mmol) was coupled with 4-methoxyphenylboronic acid (68 mg, 0.45 mmol) according to the general procedure above to afford a crude brown oil. Flash chromatography (40% ethyl acetate/hexanes) furnished the title compound as a clear oil (124 mg, 70%): ^{1}H NMR ($CDCl_3$, 400 MHz) δ 0.93 (t, 3H, $J = 7.5$), 2.63 (q, 2H, $J = 7.5$), 3.77 (s, 3H), 3.85 (s, 3H), 3.87 (s, 3H), 6.78 (AA′XX′, 2H, $J = 8.9$, 2.5), 6.93 (AA′XX′, 2H, $J = 8.7$, 2.5), 7.01 (AA′XX′, 2H, $J = 8.9$, 2.6), 7.20 (AA′XX′, 2H, $J = 8.6$, 2.5), 7.43 (AA′XX′, 2H, $J = 8.8$, 2.4), 7.46 (AA′XX′, 2H, $J = 8.9$, 2.6); ^{13}C NMR (CD_3OD, 100 MHz) δ 13.7, 17.8, 54.9, 55.0, 55.4, 113.3, 113.8, 114.1, 125.9, 126.4, 127.1, 127.4, 128.9, 131.3, 133.1, 143.5, 148.7, 158.3, 158.7, 159.1; HRMS (EI, M^+) calcd for $C_{26}H_{26}N_2O_3$: 414.1943. Found: 414.1937.

1,4-Bis-(4-methoxyphenyl)-3-phenyl-5-propyl-1H-pyrazole (9b).
Iodo-pyrazole **8b** (300 mg, 0.72 mmol) was coupled with 4-methoxyphenylboronic acid (115 mg, 0.75 mmol) according to the general procedure above. Flash chromatography (25% EtOAc/hexanes) afforded the title compound as a glassy solid (203 mg, 71%): ^{1}H NMR ($CDCl_3$, 500 MHz) δ 0.70 (t, 3H, $J = 7.4$), 1.31 (sext, 2H, $J = 7.6$), 2.59 (t, 2H, $J = 7.9$), 3.84 (s, 3H), 3.86 (s, 3H), 6.92 (AA′XX′, 2H, $J = 8.4$, 2.4), 7.00 (AA′XX′, 2H, $J = 8.5$, 2.5), 7.16–7.27 (m, 5H), 7.45 (AA′XX′, 2H, $J = 8.7$, 2.4), 7.48–7.54 (m, 2H); ^{13}C NMR (MeOD-d_4, 100 MHz) δ 13.8, 22.2, 26.5, 55.2, 55.5, 113.9, 114.3, 114.6, 126.4, 127.2, 127.3, 127.9, 128.1, 131.5, 133.3, 133.4, 142.6, 149.0, 158.5, 159.3; HRMS (EI, M^+) calcd for $C_{26}H_{27}N_2O_2$: 398.1994. Found: 398.1991.

5-Ethyl-1,4-bis-(4-methoxyphenyl)-3-phenyl-1H-pyrazole (9c).
To a degassed solution of 2 M Na_2CO_3 (0.55 mL, 1.09 mmol; 0.5 mL H_2O), and DME (3.0 mL) was added 4-methoxyphenylboronic acid (83 mg, 0.55 mmol) and pyrazole **8c** (200 mg, 0.45 mmol). To this solution $Pd(Ph_3P)_4$ (27 mg, 0.025 mmol) was added and the mixture heated to 80 °C for 72 h. The reaction mixture was then cooled to room temperature and filtered through Celite. The filtrate was transferred to a separatory funnel and the aqueous layers extracted with Et_2O (3×5 mL). The organic layers were combined and concentrated under reduced pressure. Flash chromatography (25% EtOAc/hexanes) afforded **9c** as a white solid (100 mg, 53%): ^{1}H NMR ($CDCl_3$, 400 MHz) δ 0.93 (t, 3H, $J = 7.5$), 2.64 (q, 2H, $J = 7.6$), 3.85 (s, 3H), 3.86 (s, 3H), 6.93 (AA′XX′, 2H, $J = 8.7$, 2.4), 7.00 (AA′XX′, 2H, $J = 9.2$, 2.7), 7.18–7.27 (m, 5H), 7.46 (AA′XX′, 2H, $J = 9.0$, 2.7), 7.49–7.53 (m, 2H); HRMS (EI, M^+) calcd for $C_{25}H_{24}N_2O_3$: 384.1834. Found: 384.1838.

5-Ethyl-1-(4-methoxyphenyl)-3,4-diphenyl-1H-pyrazole (9d).

Iodo-pyrazole **8c** (400 mg, 0.99 mmol) was coupled with phenylboronic acid (144 mg, 1.04 mmol) according to the general procedure above to afford a crude brown oil. Flash chromatography (15% THF/hexanes) furnished the product and a mixture of the product and unreacted starting material. The mixture was treated to a second column under the same conditions to afford additional **9d** (50 mg combined, 14% isolated yield; 217 mg for remaining mixture, 60% total yield as determined by NMR): ^{1}H NMR (MeOD-d_4, 500 MHz) δ 0.94 (t, 3H, J = 7.4), 2.66 (q, 2H, J = 7.5), 7.02 (AA'XX', 2H, J = 8.9, 2.7), 7.17–7.53 (m, 12H); ^{13}C NMR (MeOD-d_4, 100 MHz) δ 13.7, 17.8, 55.4, 114.1, 118.7, 126.6, 127.2, 127.9, 127.9, 128.3, 130.2, 132.8, 133.1, 133.9, 143.7, 148.8, 159.3.

5-Ethyl-4-(4-methoxyphenyl)-1,3-diphenyl-1H-pyrazole (9e).

Iodo-pyrazole **8d** (244 mg, 0.65 mmol) was coupled with 4-methoxyphenylboronic acid (105 mg, 0.69 mmol) according to the general procedure above to afford a yellow oil. Flash chromatography (15% EtOAc/hexanes) was performed to afford a pale yellow oil which was then recrystallized from hexanes to afford the title compound as white crystals (160 mg, 70%): ^{1}H NMR (MeOD-d_4, 500 MHz) δ 0.94 (t, 3H, J = 7.5), 2.70 (q, 2H, J = 7.5), 3.85 (s, 3H), 6.94 (AA'XX', 2H, J = 8.8, 2.6), 7.19–7.28 (m, 5H), 7.43 (app tt, 1H, J = 7.4, 1.7), 7.48–7.55 (m, 4H), 7.55–7.60 (m, 2H); ^{13}C NMR (MeOD-d_4, 125 MHz) δ 13.7, 17.9, 55.1, 113.8, 118.8, 125.7, 126.1, 127.2, 127.8, 127.9, 129.0, 131.3, 133.2, 140.0, 143.6, 149.3, 158.4.

General procedure for demethylation using BBr₃ (2, 10a–d).

To a stirred solution of pyrazole (**9a–e**, 0.28 mmol) in CH₂Cl₂ (10 mL) at −78 °C was added BBr₃ (2.82 mL, 2.82 mmol) dropwise as a 1 M solution in CH₂Cl₂. The mixture was allowed to warm to room temperature and stirred for 3 h. The reaction was quenched at 0 °C by the addition of H₂O (10 mL). The resulting solid was solubilized by the addition of ethyl acetate and the resulting biphasic solution transferred to a separatory funnel and the aqueous layer isolated. The aqueous layer was acidified with 3 M HCl (3 mL) and extracted with ethyl acetate (2×15 mL). The combined organic layers were washed with brine and dried over MgSO₄. The solvent was removed under reduced pressure and the phenolic products purified by flash chromatography and/or crystallization.

5-Ethyl-1,3,4-tris-(4-hydroxyphenyl)-1H-pyrazole (10a).

A stirred solution of **9a** (46 mg, 0.11 mmol) in CH₂Cl₂ (5 mL) was treated with BBr₃ (1.10 mL, 1.10 mmol) according to the general demethylation procedure. After work up a reddish brown oil isolated. The oil was dissolved in methanol and concentrated under reduced pressure. No effort was made to remove trace amounts of methanol remaining in the sample. The residue was triturated by adding CH₂Cl₂ dropwise until a precipitate formed. The precipitate was isolated by vacuum filtration to afford **10a** as a white solid (40 mg, 93%): ^{1}H NMR (MeOD-d_4, 400 MHz) δ 0.89 (t, 3H, J = 7.6) 2.59 (q, 2H, J = 7.5), 6.65 (d, 2H, J = 8.4), 6.79 (d, 2H,

J = 8.4), 6.93 (d, 2H, J = 8.8), 7.03 (d, 2H, J = 8.8), 7.21 (d, 2H, J = 8.4), 7.32 (d, 2H, J = 8.8); ^{13}C NMR (MeOD-d_4, 100 MHz) δ 12.4, 17.2, 114.3, 114.8, 115.1, 118.0, 124.2, 124.6, 127.4, 128.9, 131.0, 131.2, 143.9, 149.1, 156.0, 156.6, 157.7; HRMS (EI, M$^+$) calcd for C₂₃H₂₀N₂O₃: 372.1474. Found: 372.1468.

1,4-Bis-(4-hydroxyphenyl)-3-phenyl-5-propyl-1H-pyrazole (10b).

A stirred solution of **9b** (100 mg, 0.25 mmol) in CH₂Cl₂ (10 mL) was treated with BBr₃ (2.50 mL, 2.50 mmol) according to the general demethylation procedure. After work up a red solid was isolated. The solid was recrystallized from 10% CH₃OH/CHCl₃ to afford **10b** as small white crystals (75 mg, 81%): mp 233–236 °C; ^{1}H NMR (MeOD-d_4, 400 MHz) δ 0.67 (t, 3H, J = 7.3), 1.29 (sext, 2H, J = 7.5), 2.59 (t, 2H, J = 7.9), 6.79 (AA'XX', 2H, J = 8.4, 2.2), 6.94 (AA'XX', 2H, J = 8.6, 2.5), 7.03 (AA'XX', 2H, J = 8.3, 2.1), 7.20–7.26 (m, 3H), 7.31–7.43 (m, 4H); ^{13}C NMR (MeOD-d_4, 100 MHz) δ 12.4, 21.5, 25.9, 114.9, 115.2, 119.1, 124.4, 127.0, 127.4, 127.5, 127.6, 131.1, 131.2, 132.9, 142.8, 148.9, 156.2, 157.8; HRMS (EI, M$^+$) calcd for C₂₄H₂₂N₂O₂: 370.1681. Found: 370.1685.

5-Ethyl-1-(4-hydroxyphenyl)-3,4-diphenyl-1H-pyrazole (10c).

A stirred solution of **9c** (37 mg, 0.10 mmol) in CH₂Cl₂ (5 mL) was treated with BBr₃ (1.00 mL, 1.00 mmol) according to the general demethylation procedure. After work up a brown oil was afforded. The crude oil was purified by flash chromatography (5% CH₃OH/CH₂Cl₂) to afford **10c** as a white solid (30 mg, 86%): mp 210–220 °C; ^{1}H NMR (MeOD-d_4, 400 MHz) δ 0.90 (t, 3H, J = 7.60 Hz), 2.65 (q, 2H, J = 7.4), 6.95 (AA'XX', 2H, J = 9.1, 2.7), 7.19–7.26 (m, 5H), 7.31–7.42 (m, 7H); ^{13}C NMR (MeOD-d_4, 100 MHz) δ 13.8, 17.8, 116.5, 118.8, 126.8, 127.5, 127.6, 128.1, 128.1, 128.5, 130.3, 132.1, 132.9, 133.9, 144.2, 149.1, 156.5; HRMS (EI, M$^+$) calcd for C₂₃H₂₀N₂O: 340.1576. Found: 340.1576.

5-Ethyl-4-(4-hydroxyphenyl)-1,3-diphenyl-1H-pyrazole (10d).

A stirred solution of **9e** (100 mg, 0.28 mmol) in CH₂Cl₂ (10 mL) was treated with BBr₃ (2.82 mL, 2.82 mmol) according to the general demethylation procedure. After work up a crude brown solid was isolated. The solid was purified by flash chromatography (5% CH₃OH/CH₂Cl₂) to afford **10d** as a white solid (89 mg, 93%): ^{1}H NMR (MeOD-d_4, 500 MHz) δ 0.93 (t, 3H, J = 7.5), 2.68 (q, 2H, J = 7.6), 6.78 (XX' of XX'AA', 2H, J_{AX} = 8.4, $J_{XX'}$ = 2.5), 7.10 (AA' of AA'XX', 2H, J_{AX} = 8.4, $J_{AA'}$ = 2.5), 7.21–7.28 (m, 3H), 7.40–7.52 (m, 6H), 7.53–7.58 (m, 2H); ^{13}C NMR (MeOD-d_4, 100 MHz) δ 13.7, 17.9, 115.6, 119.1, 125.8, 125.9, 127.4, 128.0, 128.1, 128.2, 129.2, 131.5, 133.0, 139.8, 143.9, 149.5, 154.9; HRMS (EI, M$^+$) calcd for C₂₃H₂₀N₂O: 340.1576. Found: 340.1571.

Acknowledgements

References and Notes

1. Gao, H.; Katzenellenbogen, J. A.; Garg, R.; Hansch, C. Chem. Rev. 1999, 99, 723.

2. Magarian, R. A.; Overacre, L. B.; Singh, S.; Meyer, K. L. Curr. Med. Chem. 1994, 1, 61.

3. Fink, B. E.; Mortensen, D. S.; Stauffer, S. R.; Aron, Z. D.; Katzenellenbogen, J. A. Chem. Biol. 1999, 6, 205.

4. Stauffer, S. R.; Coletta, C. J.; Sun, J.; Tedesco, R.; Katzenellenbogen, B. S.; Katzenellenbogen, J. A. J. Med. Chem. 2000, submitted.

5. Stauffer, S. R.; Katzenellenbogen, J. A. J. Comb. Chem. 2000, 2, 318.

6. Foote, R. S.; Beam, C. F.; Hauser, C. R. Heterocycle Chem. 1970, 7, 589.

7. Holzer, W.; Gruber, H. Heterocycle Chem. 1995, 32, 1351.

8. Huff, B. E.; Koenig, T. M.; Staszak, M. A. Org. Synth. 1998, 75, 53.

9. Katzenellenbogen, J. A.; Johnson, H. J. Jr; Myers, H. N. Biochemistry 1973, 12, 4085.

10. Huang, Y.; Katzenellenbogen, J. A. Org. Lett. 2000, 2, 2833.

11. Anstead, G. M.; Wilson, S. R.; Katzenellenbogen, J. A. J. Med. Chem. 1989, 32, 2163.

12. Anstead, G. M.; Peterson, C. S.; Katzenellenbogen, J. A. J. Steroid Biochem. 1989, 33, 877.

13. Anstead, G. M.; Carlson, K. E.; Katzenellenbogen, J. A. Steroids 1997, 62, 268.

14. Brzozowski, A. M.; Pike, A. C.; Dauter, Z.; Hubbard, R. E.; Bonn, T.; Engström, O.; Öhman, L.; Greene, G.L.; Gustafsson, J.-A.; Carlquist, M. Nature 1997, 389, 753.

15. Sun, J.; Meyers, M. J.; Fink, B. E.; Rajendran, R.; Katzenellenbogen, J. A.; Katzenellenbogen, B. S. Endocrinology 1999, 140, 800.

16. Shiau, A. K.; Barstad, D.; Loria, P. M.; Cheng, L.; Kushner, P. J.; Agard, D. A.; Greene, G. L. Cell 1998, 95, 927.

17. Still, W. C.; Kahn, M.; Mitra, A. J. Org. Chem. 1978, 43, 2923.

Pergamon

Triarylpyrazoles with Basic Side Chains: Development of Pyrazole-Based Estrogen Receptor Antagonists

Shaun R. Stauffer,[a] Ying R. Huang,[a] Zachary D. Aron,[a] Christopher J. Coletta,[a] Jun Sun,[b] Benita S. Katzenellenbogen[b,c] and John A. Katzenellenbogen[a,*]

[a]*Department of Chemistry, University of Illinois and University of Illinois College of Medicine, Urbana, IL 61801, USA*
[b]*Department of Physiology, University of Illinois and University of Illinois College of Medicine, Urbana, IL 61801, USA*
[c]*Department of Cell and Structural Biology, University of Illinois and University of Illinois College of Medicine, Urbana, IL 61801, USA*

Abstract—Recently, we developed a novel triaryl-substituted pyrazole ligand system that has high affinity for the estrogen receptor (ER) (Fink, B. E.; Mortenson, D. S.; Stauffer, S. R.; Aron, Z. D.; Katzenellenbogen, J. A. *Chem. Biol.* **1999**, *6*, 205). Subsequent work has shown that some analogues in this series are very selective for the ERα subtype in terms of binding affinity and agonist potency (Stauffer, S. R.; Coletta, C. J.; Tedesco, R.; Sun, J.; Katzenellenbogen, J. A. *J. Med. Chem.* **2000**, submitted). We now investigate how this pyrazole ER agonist system might be converted into an antagonist or a selective estrogen receptor modifier (SERM) by incorporating a basic or polar side chain like those typically found in antiestrogens and known to be essential determinants of their mixed agonist/antagonist character. We selected an *N*-piperidinyl-ethyl chain as a first attempt, and introduced it at the four possible sites of substitution on the pyrazole core structure to determine the orientation that the pyrazole might adopt in the ER ligand binding pocket. Of these four, the C(5) piperidinyl-ethoxy-substituted pyrazole **5** had by far the highest affinity. Also, it bound to the ER subtype alpha (ERα) with 20-fold higher affinity than to ERβ. In cell-based transcription assays, pyrazole **5** was an antagonist on both ERα and ERβ, and it was also more potent on ERα. Based on structure-binding affinity relationships and on molecular modeling studies of these pyrazoles in a crystal structure of the ERα–raloxifene complex, we propose that pyrazoles having a basic substituent on the C(5) phenyl group adopt a binding mode that is different from that of the pyrazole agonists that lack this group. The most favorable orientation appears to be one which places the N(1) phenol in the A-ring binding pocket so that the basic side chain can adopt an orientation similar to that of the basic side chain of raloxifene. © 2000 Elsevier Science Ltd. All rights reserved.

Introduction

The term SERM, or selective estrogen receptor modifier, is used to describe ligands for the estrogen receptor (ER) that display an interesting balance of agonist and antagonist activity that can vary from tissue to tissue.[1] SERMs have particular utility in menopausal hormone replacement and in the treatment and prevention of breast cancer, although the pharmacological profiles of the currently available agents are not optimal.

SERMs typically consist of a non-steroidal core structure onto which is attached a side chain bearing a basic or polar function. X-ray crystal structures of the ER ligand binding domain (LBD) complexed with the SERMs raloxifene[2] or hydroxytamoxifen[3] show that the large side chains of these ligands displace the C-terminal helix (helix-12) from the position it normally occupies in ER-LBD complexes with agonists. In this antagonist conformation, helix-12 moves into a position where it occludes a hydrophobic groove on the surface of the receptor that normally functions as a tethering site for the interaction of ER with coactivator proteins, an interaction that is important in mediating agonist activity.[3,4]

It is clear, however, that more subtle changes in the conformation of ER must underlie some of the pharmacological differences among various SERMs.[5,6] Recently, conformation-sensitive peptides have been used to discriminate among these different ligand-induced ER conformations.[7–9] Nevertheless, it is not completely clear how the ligand structure of the various SERMs determines ER conformation, at least at this level of detail. In addition, differential interaction of SERMs with the two ER subtypes, ERα and ERβ, might also underlie certain aspects of their tissue-selective activity.[10–12]

*Corresponding author at Department of Chemistry, University of Illinois, 600 South Mathews Avenue, Urbana, IL 61801, USA. Tel.: +1-217-333-6310; fax: +1-217-333-7325; e-mail: jkatzene@uiuc.edu

In recent studies of novel, heterocyclic non-steroidal estrogens amenable to combinatorial assembly and library synthesis, we identified tetrasubstituted pyrazoles as a system that afforded high affinity ligands for ER.[13] Subsequently, we used parallel synthesis, as well as directed synthesis, to characterize structure affinity relationships in this series.[14,15] In the process, we found several high affinity compounds, and in particular, some that show very high binding affinity and transcriptional efficacy for the ER alpha subtype (ERα).[15] Although some of these compounds were also agonists on the ER beta subtype (ERβ), their potency and binding affinity on this ER subtype was much lower.[15] The high difference in ER-subtype binding affinities shown by some of these pyrazoles raised an interesting prospect that this system might be a favorable starting point for the development of ERα potency-selective antagonists or SERMs. This would depend, of course, on whether these ligands could be converted to antagonists by appropriate substitution of basic or polar side chains.

In this report, we describe the preparation of several analogues of an ERα high-affinity pyrazole which embody the type of basic or polar side chain that is typically found in SERMs. We evaluate how this substitution is tolerated in terms of ER binding affinity, and in some selected cases, we show it affects the transcriptional efficacy and potency of these ligands. We also develop a model for how these basic side chain-substituted pyrazoles are likely to be orientated in the ligand-binding pocket of ER.

Results and Discussion

An example of a favorable pattern of substitution for high affinity ER pyrazoles ligands consists of three phenols at the 1-, 3- and 5-positions and an alkyl group at the 4-position, and is shown in Figure 1 (pyrazole 1).[13,16] The piperidinyl-ethyl substituent, which is widely represented in many SERM classes (see, for example, Raloxifene, Figure 1),[1,17] was chosen in this study as a typical basic side chain that might be expected to confer the characteristic mixed agonist/antagonist activity of these compounds. The question at hand, however, is at which position on a pyrazole such as 1 should this basic substituent be attached. Molecular modeling studies using the LBD crystal structures provided a starting point towards answering this question.

From published crystal structures, it is known that the ER-LBD adopts a different conformation when complexed with agonists (E_2, DES) versus antagonists (hydroxytamoxifen, raloxifene).[2,3] In our initial molecular modeling studies, we examined various binding modes for the pyrazole core structure (i.e. without a basic side chain) based on the larger ligand binding pocket in the ER-LBD–raloxifene (antagonist) complex.[13] However, in a subsequent publication,[15] knowing now that these pyrazoles were agonists, we reexamined our initial predictions, this time using the ER-LBD–DES (agonist) structure. As a result of this additional modeling work, as well as further structure activity relationship studies we have done in this series of compounds,[15] we now believe that these core
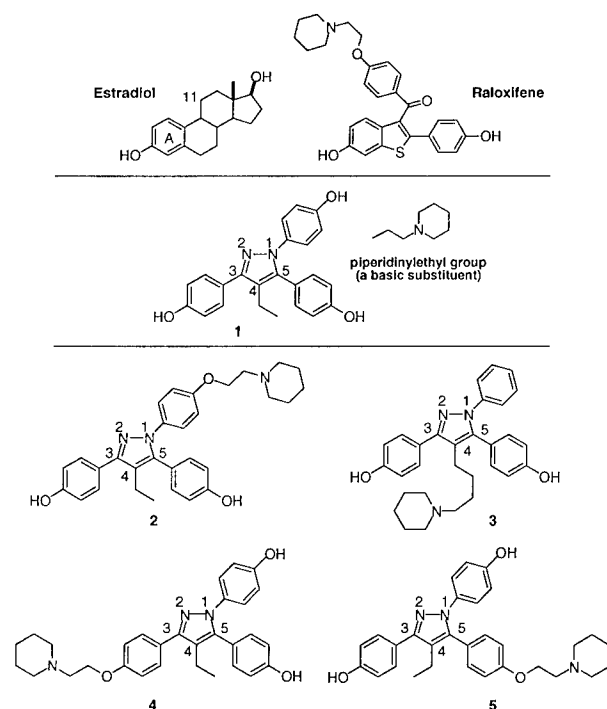

Figure 1. Pyrazole triol core structure (1) and basic side chain-containing pyrazoles (2–5).

pyrazoles, which behave as agonists, bind in an orientation in which the C(3) phenol plays a role analogous to the critical A-ring of estradiol.[15] We have illustrated this binding orientation with the relative positions we have chosen for pyrazole 1 and estradiol in Figure 1. The orientation of the SERM raloxifene relative to estradiol, known from X-ray crystallography,[2] is also displayed in Figure 1. In this orientation, the benzothiophene ring system of raloxifene mimics the AB ring system of estradiol, so that the basic side chain is directed roughly in the estradiol 11β direction (Fig. 1), where it extends outward to displace helix-12, as noted above.[2]

On the basis of our current model, we might have considered it unlikely that the pyrazole ligand could even accommodate a basic side chain. When bound with the ER-LBD in the agonist conformation, there is no position on the pyrazole analogue where such a side chain could be disposed so as to occupy a region of the ligand binding pocket that is normally occupied by this group in other SERMs (i.e. the estradiol 11β region, Figure 1).[2,3] However, because of the near symmetry of these triaryl pyrazoles and the known flexibility of the ligand-binding pocket of the ER,[2,3] we were not convinced that the binding orientation preferences of the smaller core pyrazole agonist ligands would be retained. The additional bulk and polarity of the basic side chain that we were adding to engender antagonist activity might cause the ligand to adopt an entirely different orientation in the binding pocket.

Therefore, as an initial effort to develop pyrazole-based SERMs, we prepared four pyrazoles in which the basic piperidinyl-ethyl side chain is attached at four different positions (2–5, Fig. 1), and we determined the binding affinity of these derivatives for the ER. Each of these

isomers serves as a model to determine which position on the heterocycle scaffold can best accommodate the SERM-defining basic side chain in the ER-LBD. Once identified, such a site would obviously be a prime target for further study through a series of pyrazoles in which the structure of this basic substituent is varied.[18]

The four basic side chain-containing pyrazoles (2–5) shown in Figure 1 are designed to probe several potential ligand orientations within the binding pocket. For example, pyrazole 2 was proposed on the basis of our initial docking study of the N-aryl pyrazole 1 in the ERα-raloxifene X-ray crystal structure[13] (now revised, as noted above[15]), which placed the C(5) phenol in the subpocket corresponding to the A-ring of E_2. In this mode, the N(1) basic side chain group resides in what would be the estradiol 11β direction. Pyrazole 3 was envisioned to undergo a ligand "flipping" around the bond between the pyrazole core and the C(3) phenol, to place the C(4)-linked basic side chain in the estradiol 11β direction. Pyrazoles 4 and 5 are regioisomers that have the basic side chain at the 3- and 5-positions, respectively. Pyrazole 5, a C(5)-substituted analogue, was predicted to have a potentially favorable interaction with ER by way of a ca. 120° counterclockwise rotation about an axis perpendicular to the pyrazole ring, resulting in a binding mode that would make the N(1) phenol the mimic of the A-ring in estradiol. Pyrazole 4, a regioisomer of pyrazole 5, was considered unlikely to have a favorable interaction with the ER, because the phenols and the basic side chain groups are displayed in a "long" orientation. This leaves the remaining two free phenols too close to one another for proper interaction with the A-ring and D-ring subpockets in ER. Nevertheless, it was prepared for the sake of completeness.

Chemical syntheses

The synthesis of pyrazole 2 is shown in Scheme 1. For the preparation of the required piperidinyl-ethoxy-substituted phenylhydrazine, we initially investigated the classical diazotization–reduction route, starting from the corresponding substituted aniline 6. However, we had difficulty isolating the desired hydrazine precursor. Fortunately, we found the approach of Demers and Klaubert,[19] involving metallation of the corresponding aromatic bromide (7) followed by reaction with an azodicarboxylate ester, conveniently afforded the di-Boc protected hydrazine 8. Because isolation of the free hydrazine proved to be problematic, we performed the Boc deprotection and pyrazole cyclization in one-pot, which gave pyrazole 9 in 65% yield. Selective demethylation using either $AlCl_3$–EtSH or BBr_3 afforded pyrazole 2 in 55–75% yield.

The synthesis of the C(4) basic side chain-containing pyrazole 3 is shown in Scheme 2. Introduction of a basic side chain into the pyrazole structure at the 4-position was done early in the synthesis, starting with Freidel–Crafts acylation of anisole with 6-bromohexanoyl chloride. For this transformation, the temperature had to be carefully maintained at $-10\,°C$ to avoid reaction of the product ketone 10 with a second equivalent of anisole, a side reaction that results in the formation of a 1,1-diaryl-alkene by-product upon dehydration. The bromoketone 10 was then aminated with excess piperidine in DMF to afford amino-ketone 11 in high yield. Condensation with the p-nitrophenyl benzoate furnished the β-diketone 12, which was cyclized with phenyl hydrazine hydrochloride to give the desired protected pyrazole 13. Deprotection using $AlCl_3$–EtSH yielded the final pyrazole 3.

The final pyrazoles 4 and 5 were initially prepared as an approx. 1:1 mixture of regioisomers by the route shown in Scheme 3. Starting from 4-hydroxybutryophenone, we used a Mitsunobu reaction to prepare the piperidinyl-ethoxy-substituted ketone 14. Claisen condensation afforded the requisite β-diketone 15. Treatment with phenylhydrazine hydrochloride followed by BBr_3 deprotection afforded the desired pyrazoles 4 and 5 as a
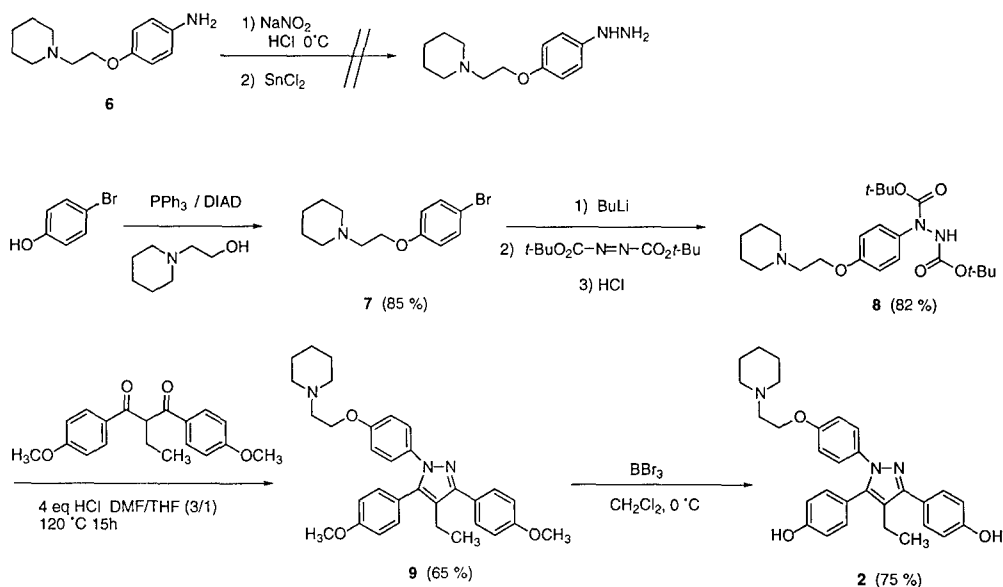
Scheme 1. Synthesis of N(1) basic side chain-containing pyrazole 2.
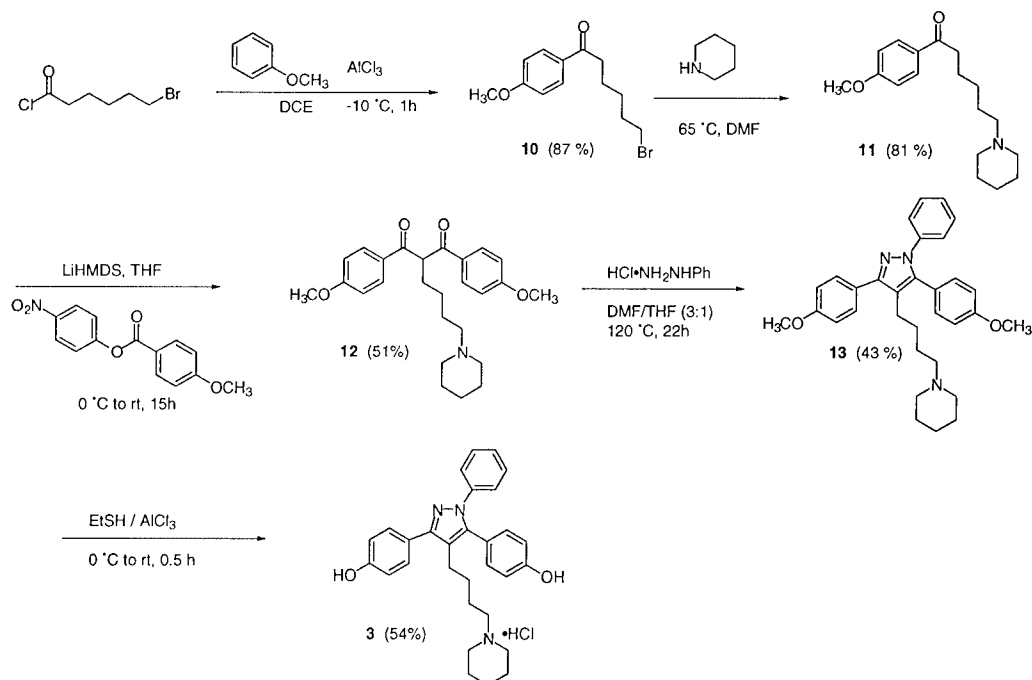
Scheme 2. Synthesis of C(4) basic side chain-containing pyrazole **3.**
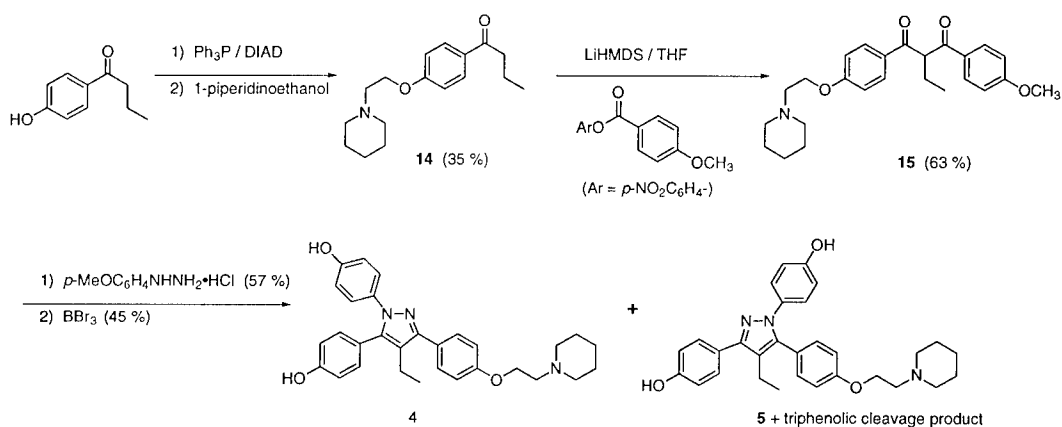
Scheme 3. Synthesis of C(3) and C(5) basic side chain-containing pyrazoles **4** and **5.**

1:1 mixture that could be separated by chromatography. Pyrazole **4** was further purified by recrystallization from MeOH, and definitive regiochemical assignment of this isomer was made on the basis of a single crystal X-ray analysis. An ORTEP diagram of this compound is shown in Figure 2.

Isolation of the last pyrazole (**5**) proved to be more problematical because we found that the basic side chain of these pyrazoles undergoes partial cleavage when BBr$_3$ is used as a deprotection reagent. This is a significant problem, because the triphenolic by-product resulting from this cleavage was difficult to separate from the desired C(5) basic side chain isomer by chromatography and it has distinctly different biological activity.[15] Later, we found that we could do this deprotection selectively, without this side reaction, using the milder AlCl$_3$ EtSH reagent. Ultimately, however, we used a regioselective route (described elsewhere in detail[18]) to produce the desired pyrazole **5.**

Estrogen receptor binding affinity of pyrazoles 2–5

The binding affinity of pyrazoles **2–5** for ER was assayed in a competitive radiometric binding assay as described previously,[20,21] and affinities are expressed as relative binding affinity (RBA) values, where the affinity of estradiol is considered to be 100% (Table 1). The affinity of all compounds was tested both in a natural ER preparation from lamb uterine cytosol,[21] which is predominantly ERα,[10,11] as well as with purified recombinant human ERα and ERβ (see Experimental).[20]

When uterine cytosol was used as a source of estrogen receptor, pyrazole **2** had a relatively low binding affinity, just 1.5% that of estradiol, a value which is 10-fold lower than that of the parent N(1) aryl pyrazole (**1**).[13,15] Pyrazole **3** with the basic side chain on C(4) also displayed very low affinity for the receptor. Apparently, even with the reorientation proposed above, this analogue, in which the basic side chain is attached to the pyrazole
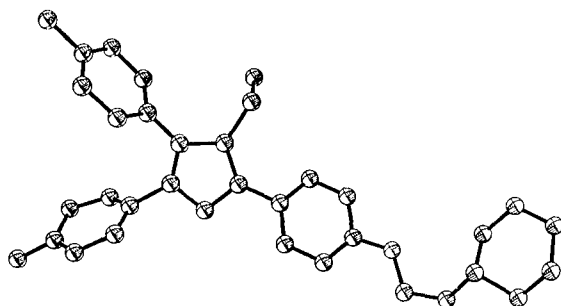
Figure 2. X-ray crystal structure for 4 (ORTEP: ellipsoids drawn at the 35% probability level).

core solely through aliphatic linkages, does not fit well in the ligand binding pocket of ER. More intriguing are the two regioisomeric pyrazoles 4 and 5; they display very distinctive preferences for binding to the ER, pyrazole 5 having a 65- to 90-fold higher affinity than pyrazole 4 in all three test systems. As noted previously, the higher affinity of isomer 5 versus 4 was expected.

Pyrazole 5 has the highest affinity of all basic side chain pyrazoles investigated thus far, and, in fact, is among the highest affinity of all pyrazoles we have reported as ER ligands.[13-15] When we evaluated the binding affinity of these pyrazoles with pure human ERα and ERβ (Table 1),[20] pyrazole 5 showed a distinctive preference for binding to ERα (ca. 20-fold), a characteristic that it shares with the parent pyrazole triol 1 (ca. 230-fold).[15] Pyrazole 2 shows only a 5-fold affinity preference for ERα. Pyrazoles 3 and 4 had very low affinity for both ERα and ERβ, and they were not investigated further either for binding affinity or transcriptional activity.

Transcription activity of pyrazole 5

Based on the promising ERα binding selectivity of pyrazole 5 and because of its piperidine side chain, we were interested in whether this compound had antagonistic properties, and in particular, whether it might function as an antagonist on one or both of the ER subtypes in a potency selective manner. Figure 3 shows the transcriptional activity profiles of pyrazole 5 assayed in HEC-1 cells with either ERα or ERβ. Cells were transfected with an expression plasmid for ERα or ERβ, together with an estrogen-responsive reporter gene construct ((ERE)$_3$-pS2-CAT), and reporter gene expression was determined at different concentrations of ligand. Antagonism was
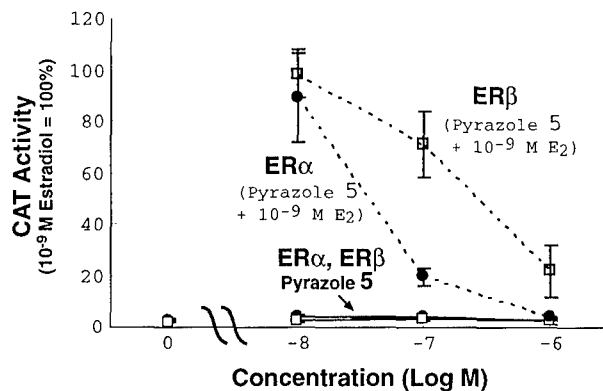

Figure 3. Transcription activation profile for pyrazole 5 with ERα and ERβ. Human endometrial cancer (HEC-1) cells were transfected with expression vectors for ERα or ERβ and an (ERE)$_3$-pS2-CAT reporter gene and were treated with indicated concentrations of pyrazole 5 alone (solid lines) or pyrazole 5 in the presence of 10^{-9} M estradiol (E$_2$) (dashed lines) for 24 h. CAT activity was normalized for β-galactosidase activity from an internal control plasmid. Values are the mean ±SD for three separate experiments, and are expressed as a percent of the ERα or ERβ response with 10^{-9} M E$_2$, which is set at 100%. For some values, error bars are too small to be visible.

assayed at different concentrations of ligand in the presence of 10^{-9} M E$_2$.

Pyrazole 5 showed no stimulation of transcriptional activity of ERα or ERβ, and it was a full antagonist on ERα and ERβ, completely antagonizing activity stimulated by estradiol (Fig. 3). Thus, introduction of the type of basic side chain typically found in the mixed agonist/antagonist SERMs at the proper site on the parent pyrazole 1, which is an agonist, converts this pyrazole system into an antagonist (pyrazole 5). The relatively good ERα binding affinity selectivity of pyrazole 5 (ca. 20-fold; cf. Table 1) is preserved to a considerable degree in its potency as a transcriptional antagonist. Its IC$_{50}$ value is ca. 20 nM on ERα and ca. 160 nM on ERβ, which gives an ERα antagonist potency selectivity of ca. 10-fold (Fig. 3).

In work to be presented elsewhere, we have prepared additional analogues of pyrazole 5 having other basic and polar side chains as substituents on the C(5) phenyl group.[18] Some of these have very high affinity selectivity for ERα over ERβ, and they act as ERα potency selective antagonists (J. Sun et al., in preparation).

Binding models for pyrazoles 2 and 5 in the ERα–raloxifene crystal structure

As previously mentioned, the low binding affinity of pyrazole 4 was not surprising. The low affinity of pyrazole 3, however, was unexpected, because, as mentioned earlier, when the pyrazole core is flipped, the basic side chain attached to C(4) appears to be oriented properly for this substituent to project through the 11β channel.

Pyrazole 2, in which the basic side chain is substituted on the N(1) phenyl group, was initially believed to be the most favorable candidate for interacting with ER. However, this turned out not to be the case; pyrazole 5 has the

Table 1. Estrogen receptor binding affinity of pyrazoles 1–5

Compound	Site of basic side chain	RBA lamb uterine cytosol[a]	RBA hERα[a]	RBA hERβ[a]
1	[none]	20.3±3	35.7±6	0.15±0.01
2	N(1)	1.5±0.4	0.65±0.13	0.13±0.03
3	C(4)	0.017±0.006	0.05[b]	0.019[b]
4	C(3)	0.29±0.26	0.13[b]	0.01[b]
5	C(5)	24.5±1	11.5±1	0.65±0.02

[a]Relative binding affinity (RBA) where estradiol = 100%. Values are the average of repeat determinations±SD (n≥3) or ±range (n = 2). For details of the assay procedure, see Experimental.
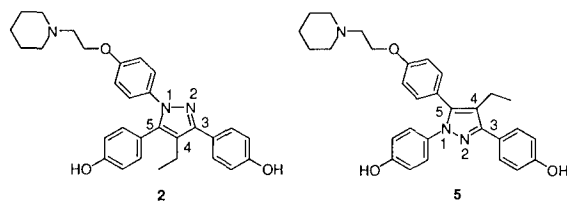[b]Single determinations.

Figure 4. Pyrazoles **2** and **5** oriented with corresponding aryl rings oriented in a congruent fashion.

highest affinity. These two pyrazoles have somewhat related structures (cf. Fig. 1); the three aryl groups (two unsubstituted and one side chain-substituted) can be superimposed in a congruent fashion, as illustrated in Figure 4. When oriented in this fashion, the only difference between these two isomers is the position of the two ring nitrogen atoms and the C(4) ethyl substituent.

In an attempt to understand the 16-fold higher affinity of pyrazole **5** than pyrazole **2**, we performed some docking studies of these two ligands with the ERα-raloxifene

crystal structure.[2] Both ligands were docked in the ERα–raloxifene crystal structure in a similar manner, and they were subjected to a three-step minimization protocol to generate the final receptor–ligand model complexes shown (see Experimental, Molecular Modeling for details). Residue side chains that were close to each ligand in its initial position were allowed to undergo torsional movement during the docking operation, in order to obtain an optimal fit, prior to minimization. A crossed-stereo view of pyrazoles **2** and **5** is shown in Figure 5(A) and (B). The final models have similar energies, which at least at this level of refinement, simply indicates that they have no bad contacts or unfavorable conformations.

In both of the views shown in Figure 5, the three aryl groups displayed peripherally from the pyrazole core are accommodated comfortably and in a very similar manner within the ligand binding pocket. This was achieved with only minimal and energetically favorable movement of a few residues that were initially in close contact with the ligand.
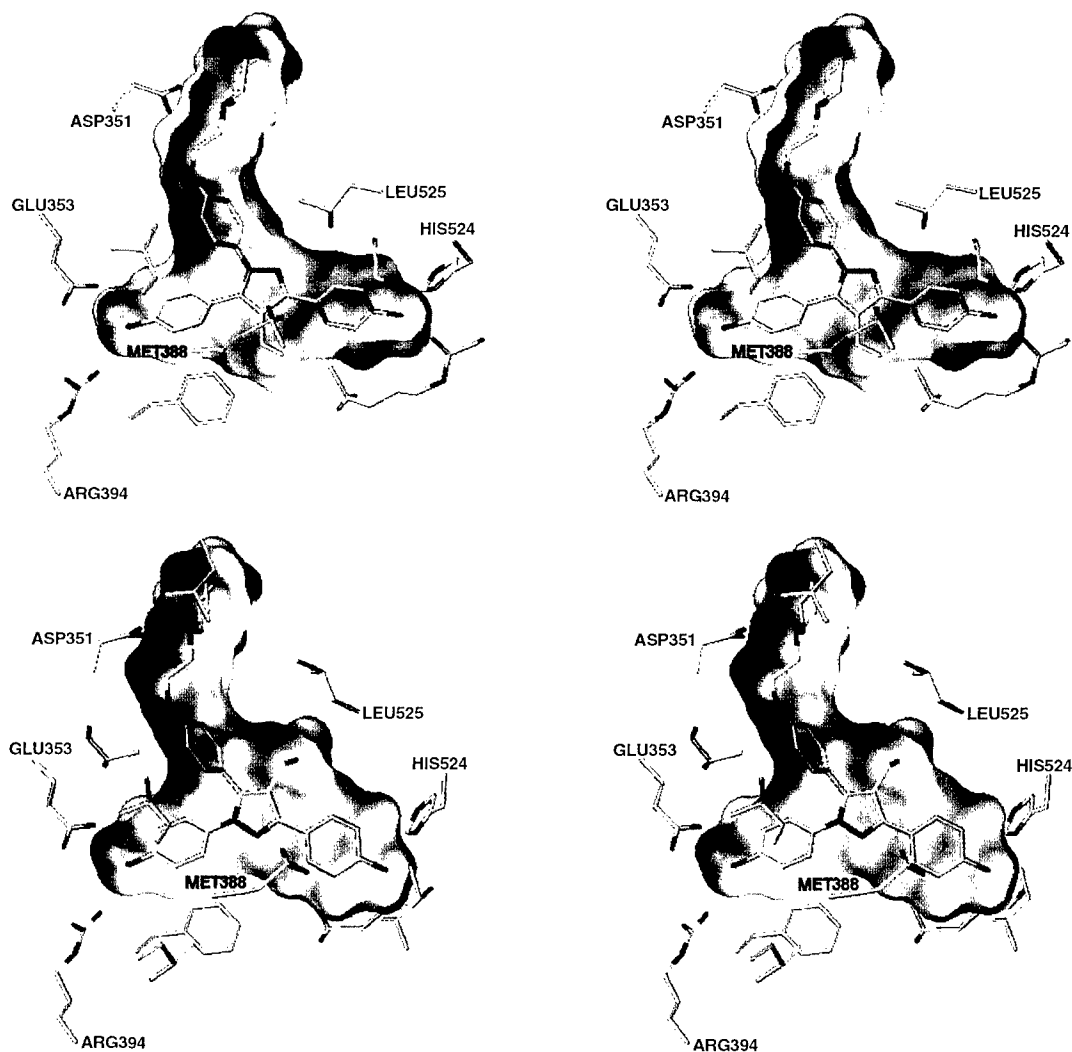

Figure 5. Crossed-stereo views of pyrazole **2** (top) and **5** (bottom) docked and minimized in ERα–raloxifene structure ligand binding pocket showing residues within 2.5 Å of ligand. The pyrazoles were initially positioned with respect to certain reference atoms of the ligand raloxifene, and then minimized together with the same contact residues in the protein using the Flexidock routine within SYBYL. For details, see Experimental. The yellow surface is a cutaway of the Connolly surface of the protein ligand-binding pocket.

The most significant difference between the complexes with pyrazoles **2** and **5** is the position of the ethyl group (cf. Fig. 4). In Figure 5(B), the C(4) ethyl group of pyrazole **5** projects into a region of ER that accommodates the 18-methyl of estradiol in the ER–E$_2$ complex.[2] In this subpocket, the favorable van der Waals interaction that normally occurs between Leu525 and the 18-methyl group of E$_2$ is conveniently replaced by a similar interaction with the ethyl substituent of pyrazole **5** (Fig. 5(B)).

By contrast, in the complex with pyrazole **2**, the ethyl substituent is oriented in a different position (downward), where it no longer benefits as much from a favorable hydrophobic–hydrophobic interaction, as was the case in the complex with pyrazole **5**. Leu525 is somewhat closer to the pyrazole core, where it interacts with the N(1) phenyl ring. The closest residue for interaction with the C(4) ethyl of pyrazole **2** (Fig. 5(A)) is Met388. This residue is a somewhat "softer" partner for interaction than Leu525, and may be less stabilizing. Other differences between the ER complexes with pyrazoles **2** and **5** which could account for their differing binding affinity may have to do with electronic effects and are not considered in these models. As noted earlier (Fig. 4), the positions of the nitrogen atoms are different between the two binding modes, so the electronic molecular surfaces that are presented to the receptor are predicted to be quite different.

Conclusions

We have prepared a series of basic side chain-substituted pyrazoles as potential selective antagonists for ER subtypes. The initial four analogues were designed to explore the four possible orientations that the pyrazole core structure might adopt in the ER ligand binding pocket, and thereby to identify which site on the pyrazole could best accommodate the rather large, basic side chain substituent. Of the four analogues, the C(5) piperidinyl-ethoxy-substituted pyrazole **5** was found to have the highest affinity for ERα, with an affinity among the highest observed for all ER ligands of the pyrazole type. It also shows considerable affinity selectivity for ERα versus ERβ. Through cell-based transfection assays, we found that pyrazole **5** was an antagonist on both ERα and ERβ, and that its potency on ERα was somewhat higher, reflecting its ERα affinity selectivity. Modeling studies using the crystal structure of the ERα–raloxifene complex were used to compare potential binding modes for pyrazoles **2** and **5**. The binding modes appear to be quite similar, and the origin of the higher affinity for pyrazole **5** versus **2** may result from a more favorable positioning of the ethyl group in the binding pocket in the complex with pyrazole **5**. In work to be presented elsewhere, we have prepared additional analogues of pyrazole **5** having other basic and polar side chains as substituents on the C(5) phenyl group.[18] Some of these have very high affinity selectivity for ERα over ERβ, and they act as ERα potency selective antagonists (J. Sun et al., in preparation). This work is the first effort towards developing a novel SERM based on a pyrazole core structure.

Experimental

General

Melting points were determined on a Thomas-Hoover UniMelt capillary apparatus and are uncorrected. All reagents and solvents were obtained from Aldrich, Fisher or Mallinckrodt. Tetrahydrofuran was freshly distilled from sodium/benzophenone. Dimethylformamide was vacuum distilled prior to use, and stored over 4 Å molecular sieves. n-Butyllithium was titrated with N-pivaloyl-o-toluidine. Et$_3$N was stirred with phenylisocyanate, filtered, distilled, and stored over 4 Å molecular sieves. All reactions were performed under a dry N$_2$ atmosphere unless otherwise specified. Reaction progress was monitored by analytical thin-layer chromatography using GF silica plates purchased from Analtech. Visualization was achieved under illumination with short wave UV light (254 nm) or with a potassium permanganate indicator spray. Radial preparative-layer chromatography was performed on a Chromatotron instrument (Harrison Research, Inc., Palo Alto, CA) using EM Science silica gel Kieselgel 60 PF$_{254}$ as adsorbent. Flash column chromatography was performed using Woelm 32–63 μm silica gel packing. The preparation of pyrazole **5** by a regioselective route is described elsewhere.[18]

^{1}H and ^{13}C NMR spectra were recorded on either a Varian Unity 400 or 500 MHz spectrometers using CDCl$_3$ or MeOD-d_4 as solvent. Chemical shifts were reported as parts per million downfield from an internal tetramethylsilane standard (δ 0.0 for ^{1}H) or relative to solvent peaks. NMR coupling constants are reported in Hertz. ^{13}C NMR spectra were determined using either the Attached Proton Test (APT) or standard ^{13}C pulse sequence parameters. Low-resolution and high-resolution electron impact mass spectra were obtained on Finnigan MAT CH-5 or 70-VSE spectrometers. Elemental analyses were performed by the Microanalytical Service Laboratory of the University of Illinois. Single crystal X-ray analysis on pyrazole **4** was performed to determine connectivity. A rigorous analysis was not performed because of the presence of a disordered solvent molecule in the unit cell. However, for the purposes of regiochemical assignment, the analysis was satisfactory.

Biological procedures

Relative binding affinity assay. Ligand binding affinities (RBAs) using lamb uterine cytosol as a receptor source were determined by a competitive radiometric binding assay using 10 nM [^{3}H]estradiol as tracer and dextran-coated charcoal as an adsorbent for free ligand, as previously described.[21] Binding affinities with purified recombinant human ERα and ERβ were determined by a competitive radiometric binding assay using 10 nM [^{3}H]estradiol as tracer, commercially available ERα and ERβ preparations (PanVera Inc. Madison, WI), and hydroxylapatite (HAP) to adsorb bound receptor–ligand complex.[20] HAP was prepared following the recommendations of Williams and Gorski.[22] All incubations were done at 0 °C for 18–24 h. Binding affinities are expressed relative to estradiol (RBA = 100%) and are reproducible with a coefficient of variation of 0.3.

Transcriptional activation assay. Human endometrial cancer (HEC-1) cells were maintained in culture and transfected as described previously.[23,24] Transfection of HEC-1 cells in 60 mm dishes used 0.4 mL of a calcium phosphate precipitate containing 0.5 µg of pCMVβGal as internal control, 2 µg of the reporter gene plasmid, 100 ng of the ER expression vector, and carrier DNA to a total of 5 µg DNA. Compounds were added to the cell culture media as ethanol solutions so as to yield a final ethanol concentration of 0.1%. CAT activity, normalized for the internal control β-galactosidase activity, was assayed as previously described.[23,24]

Molecular modeling

Small molecule modeling. The starting structures of pyrazoles **2** and **5** used for the ER-LBD docking studies were generated from random conformational searches using the TRIPOS force field as implemented in Sybyl 6.5.2. Low energy conformers then underwent full minimization until a convergence criterion of 0.001 kcal/mol was met using the AM1 semi-empirical force field. Charge calculations were done using Gasteiger–Huckel method and molecular surface properties displayed using MOLCAD module in Sybyl 6.5.2.

Receptor docking studies. The lowest energy conformers for pyrazoles **2** and **5**, generated as indicated above, were used for docking studies. Prior to docking, a +1 formal charge and a proton were added to each piperidinyl nitrogen. Ligands were then pre-positioned in the crystal structure of the ERα raloxifene complex,[2] using a least squares multifitting of the most congruent atoms of the pyrazole and raloxifene. In raloxifene this included the A-ring carbon atoms and the 1,4-carbon atoms in both the 2- and 3-substituted phenyl groups. The same fitting strategy was used in the pyrazoles, all six carbon atoms in the ring corresponding to the A-ring and the 1,4-carbon atoms of the other two aryl rings. Once pre-positioned, the raloxifene structure was deleted and then the pyrazole ligand was optimally docked in the ERα binding pocket using the TRIPOS Flexidock routine. Hydrogen bond donors (Arg394, His524) and hydrogen bond acceptors (Glu353, His524, and Asp351) in ER were indicated in Flexidock, as well as the hydrogen bond donors and acceptors in the ligand. Side chains that were allowed to rotate during docking of the pyrazoles **2** and **5** included Met543, Leu539, Leu536, Leu354, Asp351, Trp383, all of which are near the basic side chain group; Phe404, Leu387, and Met388, which are near the A-ring mimic; Leu384, Leu346, Leu428, and Trp383, which are near the B/C ring region; and Ile424, His524, and Leu525, which are near the D-ring subpocket. Arg394 and Glu353, the hydrogen bonding partners of the critical A-ring phenol mimic, were kept fixed during the entire docking and minimization.

The best docked ligand ER-LBD complex from the Flexidock routine then underwent a three-step minimization: First, non-ring torsional bonds of the ligand were minimized in the context of the receptor, using the torsmin command. This was followed by minimization

of the side chain residues within 8 Å of the ligand while holding the backbone and residues Glu353 and Arg394 fixed. A final, third minimization of both the ligand and receptor was conducted using the Anneal function (hot radius 8 Å, interesting radius 16 Å), again holding residues Glu353 and Arg394 fixed. The result of this was considered to be the final model. Minimizations were done using the TRIPOS Forcefield (MAXIMIN) with the Powell gradient method and default settings (final RMS < 0.05 kcal/mol·Å). The total energy for the ERα complex with pyrazole **2** was −806 kcal/mol and for the complex with pyrazole **5** was −868 kcal/mol. At this level of refinement, these numbers cannot be used to predict relative binding affinities. However, they indicate that there are no serious errors or unfavorable contacts in the ER-LBD ligand models.

Chemical synthesis

1-[4-(2-N-Piperidinyl-ethoxy)-phenyl]-3,5-di-(4-hydroxyphenyl)-4-ethyl-pyrazole (2). To a stirred solution of the protected pyrazole **9** (100 mg, 0.19 mmol) in CH_2Cl_2 (1.0 mL) at 0 °C was added BBr_3 (1.0 M CH_2Cl_2, 5 equiv, 0.95 mL) dropwise. The reaction was kept at 0 °C for 4 h and then quenched with water. The solution was neutralized with satd $NaHCO_3$ and then repeatedly extracted with EtOAc. The combined organic layers were washed with brine, dried over Na_2SO_4 and concentrated to afford a tan residue. Purification by flash chromatography (5% TEA and 5% MeOH in CH_2Cl_2) afforded **2** as an off-white powder (75%): mp 125–130 °C (decomposed); ^{1}H NMR ($CDCl_3$, 400 MHz) δ 0.98 (t, 3H, $J = 7.3$), 1.51 (br s, 2H), 1.62 (quint, 4H, $J = 5.5$), 2.58 (q, 2H, 7.5), 2.67 (br s, 4H), 2.89 (t, 2H, $J = 5.5$), 4.13 (t, 2H, $J = 5.5$), 6.76 (d, 2H, $J = 8.5$), 6.87 (d, overlapping, 2H, $J = 8.5$), 6.88 (d, overlapping, 2H, $J = 9$), 7.03 (d, 2H, $J = 8.5$), 7.16 (d, 2H, $J = 9.0$), 7.49 (d, 2H, $J = 8.5$); APT ^{13}C NMR ($CDCl_3$, 100 MHz) δ 9.9 (CH_3), 18.5 (CH_2), 24.8 (CH_2), 26.2 (CH_2), 54.1 (CH_2), 56.1 (CH_2), 58.8 (CH_2), 116.1 (CH), 116.8 (CH), 116.9 (CH), 121.4 (C), 123.1 (C), 126.8 (C), 128.5 (CH), 130.9 (CH), 133.0 (CH), 135.2 (C), 144.0 (C), 152.6 (C), 159.1 (C), 159.4 (C), 159.5 (C); MS (EI, 70 eV) m/z 483.3 (M); HRMS (EI) calcd for $C_{30}H_{33}N_3O_2$ (M^+−HBr): 483.2522. Found: 481.2365 (M^+−HBr−2).

4-(4-N-Piperdinyl-butyl)-3,5-di-(4-hydroxyphenyl)-1-phenylpyrazole hydrochloride (3). To a stirred CH_2Cl_2 (1.0 mL) solution of the protected pyrazole **13** (72 mg, 0.15 mmol) was added $AlCl_3$ (116 mg, 0.87 mmol). The mixture was cooled to 0 °C and EtSH (55 µL, 0.73 mmol) added dropwise. The mixture was then allowed to reach rt and stirred for an additional 0.5 h. At this time the reaction was concentrated under a stream of nitrogen in a fume hood, brought up in CH_2Cl_2 and concentrated once again. The crude mixture was re-dissolved in CH_2Cl_2 and a mixture of THF (1 mL), water (1 mL), and 6 M HCl (0.25 mL) added. The resulting precipitate was isolated by vacuum filtration and was washed with four 5 mL portions of water followed by four 5 mL portions of ether to afford pyrazole **3** as a white solid (37 mg, 54%): ^{1}H NMR (McOD-d_4, 500 MHz) δ 1.30–1.60 (m, 6H), 1.75 (br s, 6H), 2.73 (t, 2H, $J = 7.2$), 2.78

(t, 4H, $J = 8.1$), 6.90 (XX' of AA'XX', 2H, $J_{AX} = 8.8$, $J_{XX''} = 2.5$), 7.07 (AA' of AA'XX', 2H, $J_{AX} = 8.8$, $J_{AA'} = 2.5$), 7.23–7.36 (m, 5H), 7.32 (XX' of AA'XX', 2H, $J_{AX} = 8.6$, $J_{XX'} = 2.4$), 7.52 (AA' of AA'XX', 2H, $J_{AX} = 8.6$, $J_{AA'} = 2.2$); ^{13}C NMR (McOD-d_4, 125 MHz) δ 21.5, 22.5, 22.3, 23.0, 27.0, 52.8, 56.6, 115.1, 115.2, 117.4, 121.1, 124.8, 124.9, 127.0, 127.3, 128.5, 131.2, 139.8, 142.4, 151.5, 157.5, 157.9; MS (EI, 70 eV) m/z (relative intensity, %): 467 (M$^+$–HCl, 21); HRMS (EI, M$^+$) calcd for $C_{30}H_{33}N_3O_2$: 467.2573. Found: 467.2579.

1-(4-Hydroxyphenyl)-3-[4-(2-N-piperidinyl-ethoxy)-phenyl]-4-ethyl-5-(4-hydroxy-phenyl)-1H-pyrazole (4).

A CH_2Cl_2 solution (10 mL) of the crude protected pyrazole isomers (300 mg, 0.60 mmol) prepared from the 1,3-dione 15 was cooled to 0 °C and treated dropwise with BBr$_3$ (1 M in hexane, 5 equiv, 3 mmol). The reaction was allowed to reach temperature and stir overnight. The mixture was re-cooled to 0 °C and quenched with 5 mL of MeOH and the solvent removed under reduced pressure. To the crude mixture 8 mL of H_2O was added and the aqueous layer neutralized with a satd aqueous NaHCO$_3$ solution and extracted repeatedly with EtOAc (5×20 mL). The organic layers were washed with brine, dried over Na$_2$SO$_4$ and concentrated in vacuo to afford a brown residue. Pyrazole 4 was cleanly separated from the regioisomer 5 and other byproducts by flash chromatography (7% Et$_3$N and 7% MeOH in CH_2Cl_2). It was further purified by recrystallization from MeOH to afford the C(3) isomer (4) as small white crystals whose structure was verified by X-ray analysis (23%). Pyrazole 4: mp 151–153 °C; ^{1}H NMR ((CD$_3$)$_2$SO, 400 MHz) δ 1.01 (t, 3H, $J = 7.6$), 1.43 (m, 2H), 1.55 (m, 4H), 2.49 (br s, 4H), 2.59 (q, 2H, $J = 7.6$), 2.72 (t, 2H, $J = 5.6$), 4.15 (t, 2H, $J = 6.0$), 6.74 (d, 2H, $J = 8.4$), 6.83 (d, 2H, $J = 8.4$), 7.08 (apparent triplet due to three overlapping doublets, 6H, $J = 7.6$), 7.67 (d, 2H, $J = 8.4$), 9.71 (br s, 2H, OH exchangeable with D$_2$O); APT ^{13}C NMR ((CD$_3$)$_2$SO, 100 MHz) δ 15.4 (CH$_3$), 16.8 (CH$_2$), 23.9 (CH$_2$), 25.6 (CH$_2$), 54.5 (CH$_2$), 57.5 (CH$_2$), 65.6 (CH$_2$), 114.5 (CH), 115.1 (CH), 115.4 (CH), 118.7 (C), 120.9 (C), 126.1 (CH), 126.5 (C), 128.5 (CH), 131.2 (CH), 131.8 (C), 141.2 (C), 148.5 (C), 156.2 (C), 157.4 (C), 157.9 (C); HRMS (EI, M$^+$) calcd for $C_{30}H_{33}N_3O_3$: 483.2521. Found: 483.2516.

As was noted in the text, isolation of the other regioisomer (pyrazole 5) from this reaction mixture was complicated by the fact that it could not be separated effectively from the triphenolic byproduct that resulted from partial cleavage of the basic side chain during the BBr$_3$ deprotection. This compound was prepared in a regioselective fashion by another route that is described elsewhere.[18]

1-Bromo-4-(2-N-piperidinyl-ethoxy)benzene (7).

In a 250 mL flask charged with Ph$_3$P (35 mmol) in 60 mL of THF at 0 °C was added di-iso-propyl-azodicarboxylate (DIAD, 35 mmol) reagent dropwise. The solution was kept at 0 °C and stirred for 50 min. At this time N-(2-hydroxyethyl)-piperidine was added dropwise via syringe. After 10 min, p-bromophenol (35 mmol) and TEA (86.7 mmol) in 20 mL THF were added dropwise via an addition funnel. After 1 h at 0 °C the reaction was warmed to rt and stirred for 6 h. The crude mixture was then concentrated in vacuo and the Ph$_3$PO byproduct removed by vacuum filtration. The filtrate was again concentrated and the product purified by gradient flash chromatography using 5% TEA and 30% EtOAc in hexanes up to 5% TEA and 50% EtOAc in hexanes to afford 7 as a clear oil (85%).[25] ^{1}H NMR (CDCl$_3$, 500 MHz) δ 1.41 (m, 2H), 1.58 (m, 4H), 2.47 (br s, 4H), 2.72 (d, 2H, $J = 7.2$), 4.05 (d, 2H, $J = 7.6$), 6.79 (d, 2H, 8.3), 7.82 (d, 2H, $J = 8.1$); ^{13}C NMR (CDCl$_3$, 125 MHz) δ 22.1, 38.0, 67.5, 113.0, 116.5, 121.8, 123.8, 132.3, 136.6, 149.6, 158.0, 158.3; MS (EI, 70 eV) m/z 284 (M$^+$).

N,N-di-tert-Butoxycarbonyl-N-[4-(2-N-piperidinyl-ethoxy)phenyl]hydrazine (8).

To a THF solution at −70 °C containing the substituted bromobenzene 7 (10.56 mmol) was added n-BuLi (1.3 equiv) dropwise over 10 min. After 30 min, tert-butoxycarbonyl-azodicarboxylate (15.84 mmol) was added as a solid in one portion. The mixture was then slowly warmed to rt and 1 equiv of dilute AcOH added. After stirring the quenched mixture for 30 min, the reaction was partitioned between water (30 mL) and Et$_2$O (50 mL). The layers were separated and the aqueous layer extracted twice more with Et$_2$O (2×50 mL). The combined organic layers were washed with brine and dried over Na$_2$SO$_4$. Subsequent solvent removal afforded 6.8 g of a crude red oil. Flash chromatography (5% TEA and 25% EtOAc in hexanes) produced 8 as a white solid (75%): mp 50–55 °C; (note: spectrum complicated by Boc rotamers); ^{1}H NMR (CDCl$_3$, 400 MHz) δ 1.38 (s, 9H), 1.40 (overlapping s, 11H), 1.61 (m, 4H), 2.45 (m, 4H), 2.73 (t, 2H, $J = 5.6$), 4.05 (t, 2H, $J = 5.3$), 6.82 (d, 2H, $J = 7.8$), 7.25 (br s, 2H); ^{13}C NMR (CDCl$_3$, 100 MHz) δ 24.2 (CH$_2$), 24.8 (CH$_2$), 28.2 (CH$_3$), 28.3 (CH$_3$), 36.8 (CH$_2$), 46.0 (CH$_2$), 46.7 (CH$_2$), 55.1 (CH$_2$), 57.8 (CH$_2$), 60.4 (CH$_2$), 65.7 (CH$_2$), 66.0 (CH$_2$), 81.0 (CH$_2$), 81.8 (CH$_2$), 113.9 (CH), 114.6 (CH), 120.7 (CH), 129.4 (CH), 156.7 (C), 158.7 (C), 171.2 (C); MS (EI, 70 eV) m/z 435.4 (M, 35%). Anal. ($C_{23}H_{37}N_3O_5$): C, 63.42; H, 8.56; N, 9.65. Found: C, 63.20; H, 8.72; N, 9.47.

1-[4-(2-N-Piperidinyl-ethoxy)-phenyl]-3,5-bis-(4-methoxy-phenyl)-4-ethyl-1H-pyrazole (9).

To a stirred solution of DMF (14 mL), THF (6 mL), and 1,3-bis-(4-methoxy-phenyl)-2-ethyl-propane-1,3-dione (500 mg, 1.52 mmol)[15] was added hydrazine 8 in 3-fold excess (800 mg, 4.59 mmol). The mixture was brought to reflux for 5 h and then recooled to rt. The THF was removed under reduced pressure and the remaining residue diluted with H_2O (30 mL) and extracted repeatedly with EtOAc. The organic layers were washed with brine, dried over Na$_2$SO$_4$ and concentrated to produce a crude red–orange oil. Flash chromatography using 10% TEA and 20% EtOAc in hexanes afforded the pure product 9 as an orange oil (65%): ^{1}H NMR (CDCl$_3$, 400 MHz) δ 1.03 (t, 3H, $J = 8.1$), 1.42 (m, 2H), 1.58 (quin, 4H, $J = 6$); 2.47 (br s, 2H), 2.61 (q, 2H, $J = 6.2$), 2.72 (t, 2H, $J = 6$), 3.79 (s, 3H), 3.82 (s, 3H), 4.04 (t, 2H, $J = 6.2$), 6.76 (d, 2H, $J = 9.0$), 6.86 (d, 2H, $J = 9.0$), 6.96 (d, 2H, $J = 9.1$), 7.13 (d, 2H, $J = 9.1$), 7.16 (d, 2H, $J = 9.1$), 7.69 (d, 2H, $J = 9.0$); ^{13}C NMR (CDCl$_3$, 100 MHz) δ 15.6 (CH$_3$),

17.2 (CH$_2$), 24.3 (CH$_2$), 26.0 (CH$_2$), 55.1 (CH$_3$), 55.2 (CH$_3$), 57.9 (CH$_2$), 66.2 (CH$_2$), 113.8 (CH), 113.9 (CH), 114.5 (CH), 119.9 (C), 123.3 (C), 126.0 (CH), 126.9 (C), 129.0 (CH), 131.3 (CH), 133.6 (C), 141.0 (C), 150.1 (C), 157.4 (C), 159.1 (C), 159.4 (C); HRMS (EI, M$^+$) calcd for C$_{32}$H$_{37}$N$_3$O$_2$: 511.2834. Found: 511.2825.

6-Bromo-1-(4-methoxy-phenyl)-hexan-1-one (10). To a stirred solution of AlCl$_3$ (12.40 g, 92.75 mmol) in 1,2-dichloroethane (30 mL) at 0 °C was added 6-bromohex-anoyl chloride (23.70 g, 17 mL, 111.30 mmol) dropwise over 10 min. The resulting solution was stirred at rt for 0.5 h, cooled to −15 °C and a solution of anisole (10.00 g, 10.05 mL, 92.75 mmol) in 1,2-dichloroethane (10 mL) was added dropwise over 20 min. The reaction mixture was allowed to stir at −15 °C for 1 h, then quenched with H$_2$O (50 mL). The aqueous layer was isolated and extracted with CH$_2$Cl$_2$ (2×50 mL), and the organic layers were combined and washed with H$_2$O (2×50 mL), saturated NaHCO$_3$ (2×50 mL), and brine (2×50 mL). Subsequent drying over Na$_2$SO$_4$ and solvent removal in vacuo afforded a crude orange oil. Upon standing at rt, large crystals formed after 48 h. The crystals were isolated and rinsed with cold hexane to afford 10 (23 g, 87%): mp 50–52 °C; ^{1}H NMR (CDCl$_3$, 400 MHz) δ 1.52 (quint, 2H, J = 7.6), 1.76 (quint, 2H, J = 7.5), 1.91 (quint, 2H, J = 7.1), 2.94 (t, 2H, J = 7.3), 3.42 (t, 2H, J = 6.7), 3.87 (s, 3H), 6.93 (d, 2H, J = 8.8), 7.94 (d, 2H, J = 9.0); ^{13}C NMR (CDCl$_3$, 100 MHz) δ 23.39, 27.79, 32.51, 33.59, 37.80, 55.34, 113.56, 129.88, 130.13, 163.24, 198.48; HRMS (EI, M$^+$) calcd for C$_{13}$H$_{17}$O$_2$Br: 286.0391. Found: 286.0394.

1-(4-Methoxy-phenyl)-6-(N-piperidinyl)-hexan-1-one (11). To a stirred solution of ketone 10 (248 mg, 1.00 mmol) in DMF (30 mL) at 0 °C was added piperidine (170 mg, 0.20 mL, 2.00 mmol) dropwise over 5 min. The solution was placed in a 70 °C oil bath for 4 h and then cooled to rt. The crude mixture was concentrated under reduced pressure to remove a majority of the DMF and excess piperidine to afford an orange residue. The residue was taken up in CH$_2$Cl$_2$ (30 mL), washed with brine (2×20 mL), dried over MgSO$_4$ and concentrated under reduced pressure to afford 11 as a white solid (227 mg, 79%): mp 163–165 °C; ^{1}H NMR (CDCl$_3$, 500 MHz) δ 1.35–1.45 (m, 2H), 1.65–2.00 (m, 8H), 2.26 (br q, 2H, J = 8), 2.59 (br q, 2H, J = 7), 2.88–2.96 (m, 4H), 3.51 (br d, 2H), 3.88 (s, 3H), 6.93 (d, 2H, J = 8.9), 7.93 (d, 2H, J = 8.9); ^{13}C NMR (CDCl$_3$, 100 MHz) δ 22.1, 22.3, 23.3, 23.4, 26.4, 37.5, 53.1, 55.5, 57.2, 113.8, 129.9, 130.3, 163.5, 198.5; MS (EI, 70 eV) m/z (relative intensity, %): 289 (M$^+$, 3); HRMS (EI, M$^+$) calcd for C$_{19}$H$_{27}$NO$_2$: 289.2042. Found: 289.2060.

1,3-Bis-(4-methoxy-phenyl)-2-(4-N-piperidinyl-butyl)-pro-pane-1,3-dione (12). To a solution of ketone 11 (350 mg, 1.21 mmol) and TMEDA (140.6 mg, 0.18 mL, 1.21 mmol) in THF (15 mL) at 0 °C was added a 1.0 M solution of LiHMDS (3.02 mL, 3.02 mmol) dropwise. The solution was allowed to stir at rt for 0.5 h, then was cooled back to 0 °C. At this time a solution of 4-nitro-phenyl 4-methoxybenzoate (990 mg, 3.63 mmol; prepared from p-nitrophenol and 4-methoxybenzoic acid using

DIC and DMAP coupling conditions) in THF (5 mL) was added dropwise. The resulting solution was allowed to stir for 15 h at rt and 4 h at reflux (oil bath temperature of 70 °C). At this time the mixture was allowed to come to rt and quenched by the addition of H$_2$O (10 mL). The organic layer was isolated and washed with H$_2$O (3×15 mL), dried over Na$_2$SO$_4$, and concentrated under reduced pressure to afford a yellow solid. The remaining ester was removed by warming the crude mixture in 15% ethyl acetate/hexanes and filtering off the excess crystalline ester. The filtrate was concentrated under reduced pressure and purified by flash chromatography (10% TEA and 55% EtOAc in hexanes) to afford 12 as a yellow oil (227 mg, 51%): ^{1}H NMR (CDCl$_3$, 400 MHz) δ 1.22–1.48 (m, 4H), 1.50–1.75 (m, 6H), 2.10 (q, 2H, J = 7.5), 2.34 (t, 2H, J = 9.8), 2.42 (br s, 4H), 3.83 (s, 6H), 5.05 (t, 1H, J = 6.6), 6.89 (d, 4H, J = 8.9), 7.94 (d, 4H, J = 8.9); ^{13}C NMR (CDCl$_3$, 100 MHz) δ 24.0, 25.3, 26.1, 26.3, 29.3, 54.3, 55.4, 57.0, 58.7, 113.9, 128.9, 128.9, 130.8, 130.8, 163.6, 194.6.

3,5-Bis-(4-methoxyphenyl)-4-(4-N-piperidinyl-butyl)-1-phenyl-1H-pyrazole (13). To a stirred solution of DMF (45 mL), THF (20 mL), and β-diketone 12 (170 mg, 0.40 mmol) was added phenylhydrazine hydrochloride (289 mg, 2.00 mmol). The solution was brought to reflux (oil bath temperature between 110 and 120 °C) for 22 h. The reaction mixture was allowed to cool to rt, and the THF was evaporated under reduced pressure. The remaining mixture was diluted with H$_2$O (40 mL) and extracted with EtOAc (3×40 mL). The organic layers were combined and washed with saturated LiCl (3×40 mL), saturated NaHCO$_3$ (2×40 mL), H$_2$O (2×40 mL), and brine (2×40 mL). The organic layer was dried over MgSO$_4$ and concentrated under reduced pressure to afford a crude brown oil. Purification by flash chromatography (10% TEA and 55% EtOAc in hexanes) afforded 13 as a reddish oil (79 mg, 40%). Compound 13 was verified by ^{1}H NMR and used in the next step of the reaction scheme without further characterization.

1-[4-(2-N-Piperidinyl-ethoxy)-phenyl]-butan-1-one (14). To a solution of PPh$_3$ (10.05 g, 38.31 mmol) in THF (150 mL) at 0 °C was added diisopropyl azodicarboxylate (7.5 mL, 38.31 mmol) dropwise. After stirring at 0 °C for 50 min, N-piperidinylethanol (5.09 mL, 38.31 mmol) was added followed 10 min later by addition of a solution of 4-hydroxy-butyrophenone (5.24 g, 31.9 mmol) in Et$_3$N (13.4 mL, 95.8 mmol) and THF (30 mL). The mixture was allowed to warm to rt and stirred overnight and then concentrated in vacuo. To the crude residue was added Et$_2$O (150 mL) and the insoluble Ph$_3$PO by-product removed by filtration. The filtrate was concentrated once again and the residue purified by flash chromatography (10% TEA and 25% EtOAc in hexanes) to afford an oil. This material was dissolved in Et$_2$O (60 mL) and acidified with HCl (4 M in dioxane, 6.3 mL). The precipitate that formed was collected by vacuum filtration and partitioned between saturated NaHCO$_3$ (35 mL) and ether (50 mL). The organic layer was washed with brine, dried over Na$_2$SO$_4$ and concentrated under reduced pressure to give 14 as pale-yellow

crystals (3.05 g, 35%). An analytically pure sample was obtained by recrystallization from hexane: mp 48–50 °C; ^{1}H NMR (CDCl$_3$, 400 MHz) δ 0.99 (t, 3H, $J = 7.5$), 1.43–1.49 (m, 2H), 1.64 (quint, 4H, $J = 5.9$), 1.75 (sext, 2H, $J = 7.6$), 2.55 (br s, 4H), 2.87 (t, 2H, $J = 5.9$), 2.90 (t, 2H, $J = 7.2$), 4.19 (t, 2H, $J = 6.0$), 6.93 (XX' of AA'XX', 2H, $J_{AX} = 8.9$, $J_{XX'} = 2.5$), 7.93 (AA' of AA'XX', 2H, $J_{AX} = 9.0$, $J_{AA'} = 2.5$); ^{13}C NMR δ 14.1, 18.2, 24.2, 26.0, 40.4, 55.3, 57.9, 66.3, 114.4, 130.5, 162.7, 199.2; HRMS calcd for C$_{17}$H$_{26}$NO$_2$: 276.1963. Found: 276.1964.

2-Ethyl-1-(4-methoxyphenyl)-3-[4-(2-*N*-piperidinyl-ethoxy)-phenyl]-propane-1,3-dione (15).

To a THF (25 mL) solution of ketone 14 (500 mg, 1.82 mmol) and 4-nitrophenyl 4-methoxybenzoate (745.3 mg, 2.73 mmol) at 0 °C was added LiHMDS (1 M solution in hexane, 4.55 mL, 4.55 mmol) dropwise. Upon complete addition of LiHMDS the solution was allowed to warm to rt and stir overnight. The reaction mixture was concentrated to near dryness and EtOAc (35 mL) added. The crude mixture was washed sequentially with saturated NaHCO$_3$ and brine. The solvent was dried over Na$_2$SO$_4$, removed in vacuo and the resulting oil purified via flash chromatography (10% TEA and 50% EtOAc in hexanes) to give 15 as a viscous red oil (465 mg, 63%): ^{1}H NMR (CDCl$_3$, 400 MHz) δ 1.03 (t, $J = 7.31$), 1.49 (br s, 2H), 1.70 (br s, 4H), 2.16 (quint, $J = 7.29$ Hz, 2H), 2.63 (br s, 4H), 2.90 (br s, 2H), 3.85 (s, 3H), 4.25 (br s, 2H), 4.96 (t, $J = 6.76$ Hz, 1H), 6.91 (d, $J = 9.05$ Hz, 4H), 7.95 (d, $J = 8.96$ Hz, 2H), 7.96 (d, $J = 8.85$ Hz, 2H); ^{13}C NMR (CDCl$_3$, 125 MHz) δ 12.8, 23.1, 24.0, 25.8, 55.0, 55.4, 57.6, 59.0, 66.2, 113.9, 114.5, 116.5, 129.2, 129.3, 130.9, 131.0, 163.0, 163.7, 194.9; HRMS (EI, M$^+$) calcd for C$_{25}$H$_{31}$NO$_4$: 409.2253. Found: 407.2096 (M$^+$−2).

References and Notes

1. Grese, T. A.; Dodge, J. A. *Curr. Pharm. Design* **1998**, *4*, 71.
2. Brzozowski, A. M.; Pike, A. C.; Dauter, Z.; Hubbard, R. E.; Bonn, T.; Engström, O.; Öhman, L.; Greene, G. L.; Gustafsson, J.-A.; Carlquist, M. *Nature* **1997**, *389*, 753.
3. Shiau, A. K.; Barstad, D.; Loria, P. M.; Cheng, L.; Kushner, P. J.; Agard, D. A.; Greene, G. L. *Cell* **1998**, *95*, 927.
4. Darimont, B. D.; Wagner, R. L.; Apriletti, J. W.; Stallcup, M. R.; Kushner, P. J.; Baxter, J. D.; Fletterick, R. J.; Yamamoto, K. R. *Genes Develop.* **1998**, *12*, 3343.
5. Katzenellenbogen, J. A.; O'Malley, B. W.; Katzenellenbogen, B. S. *Mol. Endocrinol.* **1996**, *10*, 119.
6. McDonnell, D. P.; Clemm, D. L.; Hermann, T.; Goldman, M. E.; Pike, J. W. *Mol. Endocrinol.* **1995**, *9*, 659.
7. Paige, L. A.; Christensen, D. J.; Gron, H.; Norris, J. D.; Gottlin, E. B.; Padilla, K. M.; Chang, C.; Ballas, L. M.; Hamilton, P. T.; McDonnell, D. P.; Fowlkes, D. M. *Proc. Natl. Acad. Sci. USA* **1999**, *96*, 3999.
8. Norris, J. D.; Paige, L. A.; Christensen, D. J.; Chang, C. Y.; Huacani, M. R.; Fan, D.; Hamilton, P. T.; Fowlkes, D. M.; McDonnell, D. P. *Science* **1999**, *285*, 744.
9. Chang, C. Y.; Norris, J. D.; Gron, H.; Paige, L. A.; Hamilton, P. T.; Kenan, D. J.; Fowlkes, D.; McDonnell, D. P. *Mol. Cell Biol.* **1999**, *19*, 8226.
10. Kuiper, G.; Shughrue, P. J.; Merchenthaler, I.; Gustafsson, J. A. *Frontier Neuroendocrinol.* **1998**, *19*, 253.
11. Kuiper, G. G. J. M.; Gustafsson, J.-A. *FEBS Lett.* **1997**, *410*, 87.
12. Kuiper, G. G. J. M.; Carlsson, B.; Grandien, K.; Enmark, E.; Häggblad, J.; Nilsson, S.; Gustafsson, J. Å. *Endocrinology* **1997**, *138*, 863.
13. Fink, B. E.; Mortensen, D. S.; Stauffer, S. R.; Aron, Z. D.; Katzenellenbogen, J. A. *Chem. Biol.* **1999**, *6*, 205.
14. Stauffer, S. R.; Katzenellenbogen, J. A. *J. Combinat. Chem.* **2000**, *2*, 318.
15. Stauffer, S. R.; Coletta, C. J.; Tedesco, R.; Sun, J.; Katzenellenbogen, B. S.; Katzenellenbogen, J. A. *J. Med. Chem.* **2000**, submitted.
16. Stauffer, S. R.; Huang, Y.; Coletta, C. J.; Katzenellenbogen, J. A. *Bioorg. Med. Chem.* **2000**, *9*, 141.
17. Magarian, R. A.; Overacre, L. B.; Singh, S.; Meyer, K. L. *Curr. Med. Chem.* **1994**, *1*, 61.
18. Huang, Y.; Katzenellenbogen, J. A. *Org. Lett.* **2000**, *2*, 2833.
19. Demers, J. P.; Klaubert, D. H. *Tetrahedron Lett.* **1987**, *42*, 4933.
20. Carlson, K. E.; Choi, I.; Gee, A.; Katzenellenbogen, B. S.; Katzenellenbogen, J. A. *Biochemistry* **1997**, *36*, 14897.
21. Katzenellenbogen, J. A.; Johnson, H. J. Jr; Myers, H. N. *Biochemistry* **1973**, *12*, 4085.
22. Williams, D.; Gorski, J. *Biochemistry* **1974**, *13*, 5537.
23. McInerney, E. M.; Weis, K. E.; Sun, J.; Mosselman, S.; Katzenellenbogen, B. S. *Endocrinology* **1998**, *139*, 4513.
24. Sun, J.; Meyers, M. J.; Fink, B. E.; Rajendran, R.; Katzenellenbogen, J. A.; Katzenellenbogen, B. S. *Endocrinology* **1999**, *140*, 800.
25. Grese, T. A.; Pennington, L. D.; Sluka, J. P.; Adrian, M. D.; Cole, H. W.; Fuson, T. R.; Magee, D. E.; Phillips, D. L.; Rowley, E. R.; Shetler, P. K.; Short, L. L.; Venugopalan, M.; Yang, N. N.; Sato, M.; Glasebrook, A. L.; Bryant, H. U. *J. Med. Chem.* **1998**, *41*, 1272.
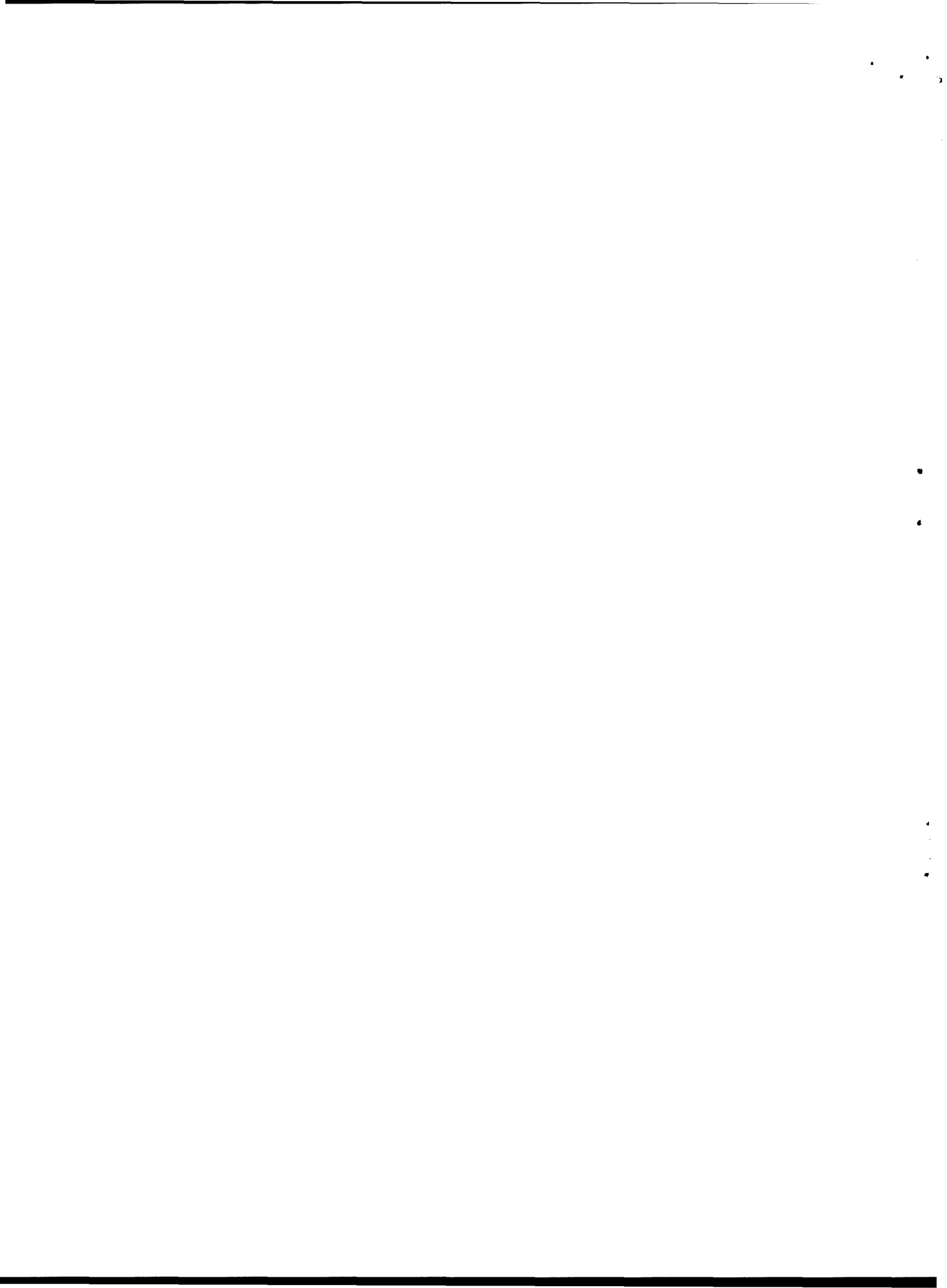
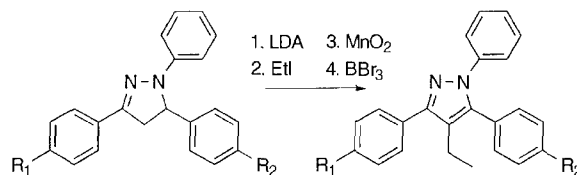# Regioselective Synthesis of 1,3,5-Triaryl-4-alkylpyrazoles: Novel Ligands for the Estrogen Receptor

Ying R. Huang and John A. Katzenellenbogen

Department of Chemistry, University of Illinois,
Urbana, Illinois 61801

Organic
LETTERS

Regioselective Synthesis of 1,3,5-Triaryl-4-alkylpyrazoles: Novel Ligands for the Estrogen Receptor

Ying R. Huang and John A. Katzenellenbogen*

Department of Chemistry, University of Illinois, Urbana, Illinois 61801

jkatzene@uiuc.edu

ABSTRACT

A regioselective synthesis of 4-alkyl-1,3,5-triarylpyrazoles has been developed for the preparation of unsymmetrically substituted systems of interest as ligands for the estrogen receptor.

In our efforts to discover novel ligands for the estrogen receptor (ER) that might act as selective estrogen receptor modifiers (SERMs),[1] we found that 1,3,5-triaryl-4-alkylpyrazoles such as 1 and 2 (Scheme 1) were good ligands for ER, demonstrating high binding affinities and transcriptional efficacy that in some cases were very selective for the ER α subtype (ERα).[2,3] Initially, we synthesized these pyrazoles by condensation of 2-alkyl-1,3-diketones with arylhydrazines.[4–6] Of course, when the 1,3-diketones were unsymmetrical, this approach did not afford any significant regioselectivity. This lack of regioselectivity became of concern when we needed the corresponding monophenols 3 and 4 for structure–activity studies to determine which phenol in pyrazole 2 mimics the A-ring of estradiol. According to a classical approach, the monophenol with the higher affinity can be presumed to be the one that corresponds to the A-ring

of estradiol.[7,8] However, when the original 1,3-dione–hydrazine condensation pyrazole synthesis was used to prepare these monophenols, only an inseparable mixture of the two regioisomers 3 and 4 was afforded (Scheme 1). Thus, a regioselective approach to these and related compounds was needed.

In a related effort, we wanted to develop these novel 1,3,5-triaryl-4-alkylpyrazole ligands into the sort of mixed agonist/antagonists that typically have SERM activity.[9,10] This generally involves incorporating a basic or polar side chain (such as a piperidinylethoxy group) onto either the C(3) or C(5) phenyl groups. However, when pyrazoles 6 and 7 were prepared by condensation of 4-methoxyphenylhydrazine with unsymmetrical 1,3-diketone 5, we obtained the regiosiomeric pyrazoles 6 and 7 in pure form only after exhaustive chromatography, and we had to obtain an X-ray structure of the more crystalline isomer 6 to establish the identity of these regioisomers (Scheme 1).

The results from cell-based transcriptional assays showed that pyrazole 7 has the desired antagonistic character typical for a SERM. However, to examine this series further we

(1) Grese, T. A.; Dodge, J. A. *Curr. Pharm. Des.* **1998**, *4*, 71–92.

(2) Fink, B. E.; Mortensen, D. S.; Stauffer, S. R.; Aron, Z. D.; Katzenellenbogen, J. A. *Chem. Biol.* **1999**, *6*, 205–219.

(3) Stauffer, S. R.; Katzenellenbogen *J Comb. Chem.* **2000**, *2*, 318–329.

(4) Fink, B. E.; Mortensen, D. S.; Stauffer, S. R.; Aron, Z. D.; Katzenellenbogen, J. A. *Chem. Biol.* **1999**, *6*, 205–219.

(5) Stauffer, S. R.; Coletta, C. J.; Tedesco, R.; Sun, J.; Katzenellenbogen, B. S.; Katzenellenbogen, J. A. Submitted.

(6) Stauffer, S. R.; Huang, Y.; Coletta, C. J.; Tedesco, R.; Kazenellenbogen, J. A. *Bioorg. Med. Chem.* In press.

(7) Anstead, G. M.; Carlson, K. E.; Katzenellenbogen, J. A. *Steroids* **1997**, *62*, 268–303.

(8) Anstead, G. M.; Peterson, C. S.; Katzenellenbogen, J. A. *J. Steroid Biochem.* **1989**, *33*, 877–887.

(9) Grese, T. A.; Dodge, J. A. *Curr. Pharm. Des.* **1998**, *4*, 71–92.

(10) Magarian, R. A.; Overacre, L. B.; Singh, S.; Meyer, K. L. *Curr. Med. Chem.* **1994**, *1*, 61–104.

pyrazole **7** and its analogues, we prepared α,β—unsaturated ketone **21** by an aldol condensation of 4-methoxyacetophenone and *p*-hydroxybenzaldehyde, according to a literature procedure[19] with modifications (Scheme 4). Despite numerous attempts, we were unable to obtain good yields in this simple reaction. However, we were able to isolate the highly crystalline enone **21** easily.

Enone **21**, protected as its silyl ether (**22**), reacted with 4-methoxylphenylhydrazine to give pyrazoline **23**. This material was alkylated, as before, with various iodides to give pyrazolines **24**—**26**, which were oxidized with either MnO₂ or DDQ to afford the desired pyrazoles **27**—**29**. Fluoride ion cleavage of the silyl group the gave the C(5) phenolic pyrazoles **30**—**32**. An X-ray structure of one of these pyrazoles (**31**, Scheme 4) secured the structure of this compound, in the process confirming the regioselectivity of this route to pyrazoles. Installation of the piperidinylethoxy side chain was accomplished by a Mitsunobu reaction. Although BBr₃ cleaved all three ether groups, AlCl₃—EtSH selectively cleaved only the methyl ethers, leaving the basic side chain unaffected and giving pyrazoles **33**—**35** in very high yield. A number of other side chain derivatives (**36**—**41**) were prepared in the C(4) ethyl series. Pyrazole **41** was prepared by a closely related route (not shown). We are currently investigating the biological activities of all of the new pyrazole compounds bearing the various polar/basic side chains.

Basis of Regioselectivity. The regioselectivity of this pyrazole synthesis derives from the initial enone—arylhydrazine condensation, which results in the attachment of the aryl-substituted hydrazine nitrogen to the enone β-carbon and the unsubstituted hydrazine nitrogen to the enone carbonyl carbon. Two mechanisms seem plausible for this transformation (Scheme 5), and they differ in the timing of bond formation. In path a, the aryl-substituted nitrogen reacts first, undergoing a Michael-type addition to the β-carbon of the enone which is followed by an intramolecular imine formation between the carbonyl group and the free amine. In path b, imine formation between the unsubstituted nitrogen and the carbonyl group occurs first, this being followed by a cyclization process to a zwitterionic species that undergoes proton tautomerization to furnish the pyrazoline. Whereas pathway b might first appear to be an ionic 5-endo-trig process, it can more reasonably be considered to be a concerted, symmetry-allowed closure of a 1,2-diaza analogue

Scheme 5. Possible Mechanistic Pathways for the Regiospecific Formation of Pyrazolines
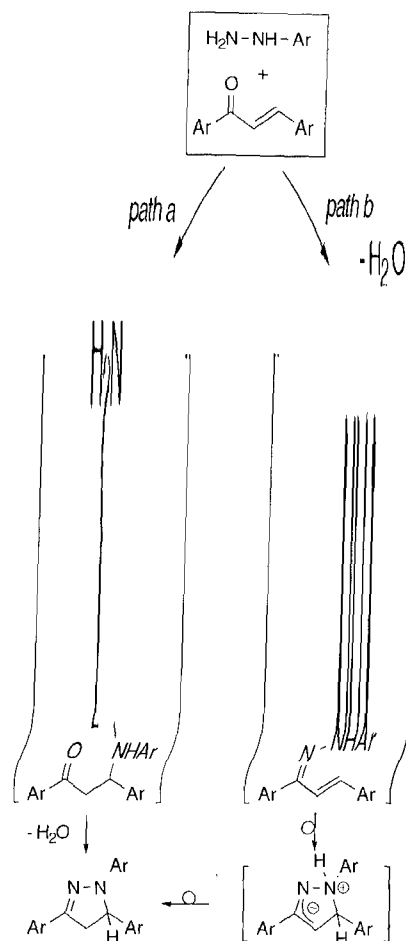
of a pentadienyl anion to a 1-azaallyl anion. No intermediates are observed in this transformation. Thus, at this point, there is no definitive basis for favoring one mechanism over the other. However, the fact that α-substituted unsaturated ketones (e.g., **8**) fail to react under conditions where the unsubstituted congeners (e.g., **10**) react well (see Scheme 2) would be more consistent with mechanism a.

Synthesis and Biological Evaluation of a Novel Series of Furans:

Ligands Selective for Estrogen Receptor Alpha

Deborah S. Mortensen,[a] Alice L. Rodriguez,[a] Kathryn E. Carlson,[a] Jun Sun,[b] Benita S. Katzenellenbogen,[b] and John A. Katzenellenbogen[a,*]

[a]Department of Chemistry

[b]Department of Molecular and Integrative Physiology

University of Illinois

Urbana, IL 61801

To be submitted to: *Journal of Medicinal Chemistry*

*Address Correspondence to:
John A. Katzenellenbogen
Department of Chemistry
University of Illinois
600 S. Mathews Ave.
Urbana, IL 61801
(217) 333-6310 (phone)
(217) 333-7325 (fax)
e-mail: jkatzene@uiuc.edu

Table of Contents graphic

**Synthesis and Biological Evaluation of a Novel Series of Furans:
Ligands Selective for Estrogen Receptor Alpha**

Deborah S. Mortensen, Alice L. Rodriguez, Kathryn E. Carlson,
Jun Sun, Benita S. Katzenellenbogen and John A. Katzenellenbogen

3-Alkyl-2,4,5-triarylfurans are potent
agonists for the estrogen receptor
(ER), having highselectivity for ERα
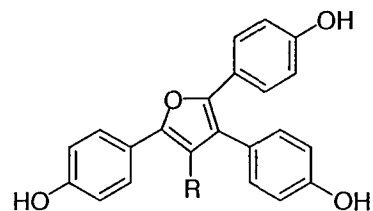
Abstract

A variety of non-steroidal systems can function as ligands for the estrogen receptor (ER), in some cases showing selectivity for one of the two ER subtypes, ERα or ERβ. We have prepared a series of heterocycle-based ligands for the estrogen receptor, furans, thiophenes, and pyrroles, and assessed their behavior as ER ligands. An aldehyde enone conjugate addition approach and an enolate alkylation approach were developed to prepare the 1,4-dione systems that were precursors to the tri-substituted and tetra-substituted systems, respectively. All of the diones were easily converted into the corresponding furans, but formation of the thiophenes and pyrroles from the more highly substituted 1,4-diones was problematical. Of the systems investigated, the tetra-substituted furans proved to be most interesting. They were ERα binding- and potency-selective agents, with the triphenolic 3-alkyl-2,4,5-tris(4-hydroxyphenyl)furans (**15a-d**) displaying generally higher subtype binding selectivity than the bis-phenolic analogs (**15f-i**). Binding selectivity for ERα was a high as 50-70 fold, and transcriptional activation studies showed that several members of this series were ERα selective agonists, with the best compound (3-ethyl-2,4,5-tris(4-hydroxyphenyl)furan, **15b**) having full transcriptional activity on ERα while being inactive on ERβ. Comparative binding affinity analysis and molecular modeling were used to investigate the preferred binding mode adopted by the furan ligands, which appears to have the C(2) phenol mimicking the important role of the A-ring of estradiol. These ligands should be useful in studying the biological roles of both ERα and ERβ, and they might form the basis for the development of novel estrogen pharmaceuticals.

The estrogen receptor (ER) is a ligand-regulated transcription factor whose activity as an inducer or repressor of gene transcription depends upon the nature of the ligand with which it is bound, as well as the nature of the co-regulator proteins with which it associates.[1] Estrogen action is important in many tissues, and ER is involved in the development and function of the reproductive system and plays a role in bone density maintenance,[2-4] regulation of blood-lipid profiles,[3-7] and brain function.[8,9] Not surprisingly, ER is a target for the discovery of new drugs for treating or regulating a variety of hormone-related conditions.

There are two ER genes, the well known gene that produces subtype ERα and the more recently discovered gene that produces the subtype ERβ.[10,11] The tissue distribution of ERα and ERβ differ, though the biological significance of this difference is not yet well understood.[12] A number of previously known ER ligands,[12-15] as well as some recently developed novel ligand systems,[16] have different potencies[17] or are able to effect different response levels through ERα and ERβ.[18] Ligands having very high ER sub-type selectivity would be effective probes of the respective biological roles of ERα and ERβ, and might also function as tissue-selective agents having improved endocrine profiles.

The ER sub-types α and β have only fifty-five percent amino acid identity in the ligand binding domain, yet all but two of the residues that define the ligand binding pocket are the same.[19] The two differences are conservative substitutions, with Met421 in ERα corresponding to an isoleucine in ERβ, and similarly Leu384 in ERα being replaced with a methionine in ERβ. These subtle changes in the ligand-binding pocket of the two ER sub-types do not provide a definitive basis for understanding the selectivity in either binding or potency that is seen with some ligands; so, further structural analyses will be required.

In previous investigations, we found that certain pyrazoles, particularly those displaying a 1,3,5-triaryl-4-alkyl substitution pattern, were very selective for ERα, in terms of affinity, potency and efficacy.[20-25] Pyrazole 1 was found to have the highest ERα binding affinity, but pyrazole 2 had the greatest ERα subtype selectivity (Figure 1). While certain azoles, such as oxazoles, thiazoles, isoxazoles, and imidazoles, did not produce good ER ligands in our hands,[20]

we wondered whether other five-membered ring heterocycles bearing only one heteroatom, namely, furans, thiophenes and pyrroles, might provide ER ligands with interesting biological character. Several furans (**3-5**) and pyrroles (**6-8**) have been described as potential anti-fertility agents.[26-29] Few, however, showed significant activity, the most active being the furans (**3-5**), and binding and transcriptional activity were reported only in one instance.[26]

[Figure 1]

[Figure 2]

In this report we describe an investigation of single heteroatom-containing five-membered ring heterocyclic analogs of the high affinity pyrazole ligands. We find that certain furans are ER ligands that display ERα-selective biological character equivalent to that of the pyrazoles. We have also developed a structure-activity relationship within the furan series to optimize ligand affinity and selectivity, and to investigate the binding mode adopted by this class of ligands.

Results

Synthesis of Ligands

While the literature provides a plethora of approaches to furans, thiophenes, and pyrroles, we wished to prepare all three of these heterocycles from a common precursor, namely, a 1,4-dione. The trisubstituted 1,4-diketones **10a-c** were prepared by the conjugate addition of an aldehyde to an α,β-unsaturated ketone **9a-c** (Scheme 1). Treatment of commercially available acetophenones and aromatic aldehydes with ethanolic KOH afforded chalcones **9a-c**. The α,β-unsaturated ketones **9a-c** then underwent conjugate addition reactions with commercially available aldehydes, utilizing Stetter's thiazolium salt catalysts, either 3-ethyl-5-(2-hydroxyethyl)-4-methyl-thiazolium bromide for aromatic aldehydes or 3-benzyl-5-(2-hydroxyethyl)-4-methyl-thiazolium chloride for aliphatic aldehydes.[30] The Stetter reactions produced the desired 1,2,4-*tri-substituted* butane-1,4-diones **10a-c** in good yields. However, all

of our attempts to use this approach with an α-substituted enone to produce the desired *tetra-substituted* diones were unsuccessful.

[Scheme 1]

The 1,2,3,4-tetrasubstituted butanediones were instead prepared by the alkylation of an enolate with an α-bromoketone (Scheme 2). Treatment of the 1,2-diaryl-ethanones **11a-d** with potassium hexamethyldisilyl amide (KHMDS), followed by the addition of an α-bromoketone **12a-f**, provided the desired 1,3,4-triaryl-2-alkyl-butane-1,4-diones **13a-l**. These reactions afforded the product diones as mixtures of diastereomers, which in some cases were separable by crystallization. Separation was not required, however, because these centers become trigonal in the final products. The α-bromoketones **12a-f** were produced in nearly quantitative yields from the parent ketones upon treatment with bromine and a catalytic amount of aluminum chloride.

[Scheme 2]

Furans: The 1,4-diketones were converted into furans upon treatment with catalytic *p*-toluenesulfonic acid in refluxing toluene. Table 1 lists the yields for conversion of diones **13a-l** and **10a-b** to furans **14a-n**. The methyl ether protecting groups of furans **14a-n** were removed using boron trifluoride-dimethyl sulfide complex, to afford furans **15a-n** as free phenols. The demethylation reactions and yields for conversion of **14a-n** to **15a-n** are listed in Table 2.

[Table 1 and Table 2]

Thiophenes: Upon treatment with Lawesson's reagent, diones **10a-b** were converted into thiophenes **16a-b**.[31,32] Furan formation was found to be a competing process in these reactions, sometimes giving as high as a 1:1 furan to thiophene ratio when the 1,4-diones were treated with Lawesson's reagent alone. Competing furan formation not only reduced yields, but the furan byproducts could not be separated from the corresponding thiophenes by flash column chromatography or recrystallization. Fortunately, the addition of solid potassium carbonate as an acid scavenger minimized furan formation, so the thiophenes could be isolated in pure form. Demethylation of **16a-b** with boron trifluoride-dimethyl sulfide complex afforded the phenolic thiophene analogs **17a-b** in good yields (Scheme 3).

[Scheme 3]

Unfortunately, all attempts to convert the 1,2,3,4-*tetra-substituted* butanediones into thiophenes afforded solely furan products. Even with the addition of potassium carbonate, Lawesson's reagent gave only quantitative yields of the furans. An alternate approach using hydrogen sulfide-hydrogen chloride also failed to give the desired thiophenes, instead producing furan in low yield and leaving unreacted starting material. It is known that these latter reagents can be used to produce *di-substituted* thiophenes either from 1,4-diones[33,34] or directly from the corresponding furans.[33] However, these conditions were reported not to work for the conversion of *tetra-substituted* systems, such 1,4-diaryl-2,3-dibromo-butane-1,4-diones, into the corresponding thiophenes.[34] While our failure to convert tetra-substituted 1,4-diones into thiophenes was disappointing, it is not surprising considering the ample precedent for preferential furan formation from hindered 1,4-diones.[33-36] In fact, to our knowledge, there has been only one report of the formation of thiophenes from 1,2,3,4-tetra-substituted-1,4-dicarbonyl precursors.[37]

Pyrroles: Treatment of diones **10c** with *p*-anisidine and *p*-toluenesulfonic acid produced pyrrole **18** in modest yield; however, unreacted dione may be recycled to increase production of the desired heterocycle. Demethylation of **18** provided the target pyrrole **19** (Scheme 4). As was the case with the thiophenes, all attempts to convert 1,2,3,4-tetrasubstituted-butane-1,4-diones into pyrroles resulted in quantitative furan formation.

[Scheme 4]

Biological Studies

Relative Binding Affinities: The relative binding affinity of the heterocyclic ligands were determined by a competitive radiometric receptor binding assay first using lamb uterine cytosol as a source of receptor.[38] (The uterus is thought to contain almost exclusively ERα.)[12] The higher affinity ligands were then studied further with purified human ERα and ERβ.[18,39] The

7

results of these studies, given as relative binding affinity (RBA) values where the affinity of estradiol is considered to be 100%, are summarized in Table 3.

While the members of these series of heterocycles displayed somewhat lower affinities for uterine cytosol ER than did those of the pyrazole class,[20] they showed good affinity nevertheless, with the highest RBA of 6.5% being observed for the 2,4,5-tris(4-hydroxyphenyl)-3-ethyl furan **15b**. As was the case with the pyrazoles,[20] the tri-substituted ligands, furans **15m,n** and thiophenes **17a,b,** showed very low affinities and thus were not assayed further with ERα and ERβ. The one pyrrole we prepared (**19**) also had low affinity; this was unexpected, considering that it is a tetra-substituted ligand that is a close structural analog to a high affinity pyrazole (cf., Fig 1).[20]

[Table 3]

All of the tetra-substituted furans (**15a-l**) were assayed for binding to ERα and ERβ, and a number of structure-affinity trends are of note. All of these furans had much higher affinity for purified ERα than for ER from lamb uterine cytosol. We believe that this is due to reduced non-specific binding of these relatively lipophilic ligands in the assays with the purified receptor, ERα, which are performed at much lower total protein concentrations than are the assays using uterine cytosol. While all of the furans proved to be ERα binding selective ligands, the data indicates that the presence of a third phenolic hydroxyl is required to achieve the highest binding selectivity for ERα versus ERβ (compare tris-phenols vs the corresponding bis-phenols: **15c** vs **15g**, and **15b** vs **15f,h,i**, respectively). As the size of the 3-alkyl substituent is changed in the triphenols, the highest ERα binding affinity is found with the ethyl and propyl analogs (**15b** and **15c** with of RBAs 100-140), but the highest ERα binding selectivity was found with the methyl furan **15a** (RBA ERα/ERβ = 65). The symmetrical tetra-(4-hydroxyphenyl)furan (**15e**) has respectable ERα affinity and selectivity, but is not as good as the best of the 3-alkyl analogs. The homologous series of bis-phenols (**15f,h,i**) and mono-phenols (**15j-l**) were prepared to investigate the orientation of these furans in the ligand binding pocket of ER; their affinities are lower, and the structure-affinity correlations are considered further in the Discussion section.

8

Transcriptional Activation Assays: Four high affinity tetra-substituted furan ligands (**15a,b,c,g**) were assessed for transcriptional activation activity through both ERα and ERβ. These cotransfection assays are conducted in human endometrial carcinoma (HEC-1) cells, using expression plasmids for full-length human ERα or ERβ and an estrogen-responsive luciferase reporter gene system.[16] The results of these initial screening assays are summarized in Figure 3.

All four ligands tested were more potent on ERα than ERβ, and they were fully efficacious on ERα. On ERβ, however, the three tri-phenols (**15a-c**) were inactive, but the bisphenol (**15g**) showed partial agonist activity. Thus, while having a third phenol on the C(5) phenyl group is not essential for high ERα binding affinity (Table 3), it does appear to be important to ensure that the furans are highly selective for ERα and not efficacious on ERβ.

A full dose-response curve for transcriptional activation through ERα and ERβ for one of the most selective of the ligands assayed, 3-ethyl-2,4,5-tris(4-hydroxyphenyl)furan (**15b**), is shown in Figure 4. This furan is highly selective in its activation of ERα, having an $EC_{50} = 0.33$ nM for ERα and having essentially no agonist or antagonist activity on ERβ at concentrations up to 1 μM.

[Figure 3]

[Figure 4]

Discussion

We have prepared a series of aryl-substituted 5-membered ring heterocycles containing a single heteroatom, namely, furans, thiophenes, and pyrroles, and we have assessed them as ligands for the estrogen receptor (ER). Certain tetra-substituted furans proved to be very selective for ERα, in terms of binding affinity and potency as agonists, with the triphenolic 3-alkyl-2,4,5-tris(4-hydroxyphenyl)furans (**15a-d**) displaying generally higher subtype binding selectivity than the bis-phenolic analogs (**15f-i**)(Table 3). The highest ERα binding selectivity (65 fold) was obtained with the 2,4,5-tris(4-hydroxyphenyl)-3-methyl furan **15a**, but the best overall combination of high affinity and ERα selectivity was given by the corresponding 3-ethyl

9

and 3-propyl analogs, furans **15b** and **15c** (Table 3). The ethyl furan **15b** is sufficiently ERα selective, that it can be used to activate ERα fully at concentrations (10-100 nM) where it has no agonist or antagonist activity on ERβ (Figure 4).

Structure-Activity Relationships in the Triaryl-Furan Series: The heterocycles most closely related to the furans, thiophenes, and pyrroles studied here are the pyrazoles that we have investigated extensively (Fig. 1),[20,22-25] and certain features that we noted in the behavior of the pyrazoles are also found with the new heterocycles. The triaryl-substituted systems have low binding affinity, as was the case with the pyrazoles (and other related heterocycles), and high affinity and ERα selectivity was engendered by having a fourth group that was aliphatic and moderate in size.[20] With the furans, the most favorable substituents at this position were ethyl and propyl, whereas with the pyrazoles it was a propyl substituent. The best furan (RBA 140 for furan **15b**) has considerably higher ERα binding affinity than the best pyrazole (RBA 75 for pyrazole **1**),[24] but in both series, the trend of affinity increasing with substituent size up to a point, beyond which further increase proves detrimental, was noted. Such trends are well precedented in both steroidal and non-steroidal systems, [40,41] and they have been interpreted to indicate the filling of a preformed pocket of limited volume within the receptor.[40]

Where it is possible to make direct comparisons between furans and thiophenes (**15m** vs. **17a** and **15n** vs. **17b**), it appears that the furans might be higher affinity ligands. However, this comparison remains limited by difficulties we encountered in the preparation of tetra-substituted thiophenes. We prepared only one pyrrole (**19**), and though it was tetrasubstituted, its affinity was disappointing. Because it has strong structural analogy to other heterocycles that have high affinity,[20] we have no explanation for this fact.

Investigation of the Orientation of the Triaryl Furans in the ER Ligand Binding Pocket

We have been interested in the manner in which non-steroidal ER ligands having more than one phenol are oriented within the ligand binding pocket of ER.[42] Most of the furans we studied here that show high binding selectivity for ERα (**15a-c**) have three phenols, any one of which could be serving as the analog of the phenolic A-ring of estradiol, a ring that is known to

10

be important for the high affinity of this natural estrogen (see Figure 5).[40] While multiple binding modes could be operative, we used comparative binding affinity considerations and molecular modeling to see whether we could determine which of these three phenols might most likely be functioning as the A-ring mimic. One should note that for each of the three potential A-ring mimics, there are two possible binding modes for the rest of the furan (i.e., the ligands could be bound in the orientations shown in Fig. 4, or in alternative binding modes, flipped 180° around the bond connecting the A-ring mimic phenol to the furan core, not shown, giving a total of six basic binding orientations).[42]

[Figure 5]

Comparative Binding Analysis: In the comparative binding affinity approach, we prepared furan bis-phenols (**15f,h,i**) and monophenols (**15j-l**) to investigate the effect that removing phenolic hydroxyl groups had on binding affinity. We imagined that deletion of the hydroxy group from the furan phenol substituent that was playing the role of the A-ring of estradiol would have the greatest effect on binding affinity.[40] Also, if two phenols were deleted, we imagined that the monophenol having the highest affinity would be the one that retained the hydroxyl on the phenyl substituent in the furan that mimics the estradiol A-ring. The ERα binding affinities of the mono and diphenols were given in Table 3, but are schematized here in Figure 6 for ready analysis.

[Figure 6]

In the monophenols (**15j-l**) (See RBA values shown in boxes in Figure 6) the C(4) monophenol (**15k**) has a very low affinity; so, it is unlikely that the C(4) aryl group is the mimic of the estradiol A-ring. However, it is difficult to choose between the C(2) and C(5) phenols (**15j,l**), because their affinities are quite comparable. So, from the monophenols, it appears that either the C(2) or C(5) phenol rings could be the A-ring mimic. The highest affinity bis-phenol (**15f**) (See RBA values shown in parentheses in Italics, Figure 6) has hydroxyl groups on both the C(2) and C(4) phenyl groups, consistent with the importance of the C(2) phenol, noted above.

11

However, the other two bis-phenols (**15h,i**) again have very similar affinities; so, a definitive distinction cannot be made between the importance of the other two phenols, at C(4) and C(5).

Based on these data, we make the following tentative conclusions: (a) the C(4) phenol is unlikely to be the A-ring mimic (based on the affinity pattern of the monophenols), (b) the C(2) phenol is most likely to be the A-ring mimic (based on the higher affinity of the 2,4-bis-phenol (**15f**) than the 2,5- and 4,5-bis-phenols (**15h,i**), but (c) the C(5) phenol might also function as the A-ring mimic. This tentative conclusion is the same as the one we reached in our analysis of the binding orientations of the pyrazoles,[24] and it is supported by further work we have done, both in the pyrazole and the furan series, to develop ERα-selective antagonists by attaching basic side chains to these heterocyclic systems.[25,43] Thus, we believe that the furan triphenols bind with the C(2) phenol in the A-ring binding pocket, but that the C(5) phenol can play this role in certain analogs (notably furan antagonists).[43]

Molecular Modeling Studies: We have also used molecular modeling to investigate the binding orientation of a furan ligand in ERα. Using the FlexiDock routine in the modeling program SYBYL, according to a modification of the protocol we described previously for the pyrazoles (See Experimental),[24] we docked the ERα-selective furan **15b** into the ligand-binding pocket of ERα, positioning the furan initially in each of six possible orientations (Cf., Fig 5, and earlier discussion). In each case, the FlexiDock routine oriented the molecule so that the C(2) phenol remained or returned to the position so as to be the A-ring mimic. With the C(2) phenol in the A-ring orientation, we obtained the best fit when the C(3) ethyl group projected downward in roughly the direction of a 6α or 7α-substituent in estradiol. The result of this docking-minimization study is shown in Figure 7. The purple dots represent the solvent-accessible surface of the ligand binding pocket, and the green surface is the molecular volume for the furan ligand. At the right of the figure is an overlay of furan **15b** (gray), onto estradiol (purple), illustrating their relative position within the ligand binding pocket.

This final minimized model shows that the hydrogen bond contacts found between the phenol and the Glu353 and Arg394 residues in the ERα/estradiol and ERα/diethylstilbestrol

12

crystal structures[44,45] persist with the C(2) phenol of the furan ligand. However, because of the overall greater length of the furan, we found that the phenol appears to be driven more deeply into the A-ring binding pocket in the furan structure than in the estradiol structure. The second phenol on C(4) of the furan makes a hydrogen bond with His524, as is also found with the distal hydroxyl groups of ligands in the crystal structures.[44,45] The third phenol on C(5) appears to be making a hydrogen bond with the hydroxy group of Thr347, which is the only other polar residue in the ligand binding pocket. As was the case with the pyrazoles, it is not clear what interactions are responsible for the high ERα binding selectivity of this ligand, although this is obviously a very interesting issue.[24]

[Figure 7]

The novel heterocyclic systems we have investigated here, the 3-alkyl-2,4,5-triarylfurans, in particular, are ligands for the estrogen receptor that have very high selectivity for ERα in terms of affinity and potency in transcription assays. These ligands should be useful in studying the biological role of both of the ER subtypes, and they might form the basis for the development of novel estrogen pharmaceuticals.

Experimental Section

General Methods

All reagents and solvents were purchased from Aldrich or Fischer. Solvents were distilled prior to use. THF was distilled over sodium/benzophenone. Methylene chloride was distilled over calcium hydride. Hexane was distilled over calcium sulfate. Triethylamine was distilled over calcium hydride. Reactions were all monitored by TLC, performed on 0.25 mm silica gel glass plates containing F-254 indicator (Merck). Visualization on TLC was achieved by UV light or phosphomolybdic acid indicator. Column chromatography was performed with Woelm 32-63 μm silica gel packing. Melting points were measured using a Thomas Hoover

capillary melting point apparatus and are uncorrected. NMR spectra chemical shifts are reported in parts per million downfield from TMS and referenced with either TMS internal standard for d_1-chloroform or d_6-acetone solvent peak. NMR coupling constants are reported in Hertz. All compounds used in structure-activity relationship considerations gave either satisfactory microanalyses or satisfactory exact mass determinations by high resolution mass spectrometry and were shown to be pure by HPLC under two distinct reversed phase conditions.

Chemical Synthesis

General Procedure for the Preparation of Trisubstituted Butane-1,4-diones by the Stetter Reaction. Aldehyde, α,β unsaturated ketone, triethlyamine, and either 3-benzyl-5-(2-hydroxyethyl)-4-methyl-thiazolium chloride (with aliphatic aldehydes) or 3-ethyl-5-(2-hydroxyethyl)-4-methyl-thiazolium bromide (with aromatic aldehydes) were combined and heated to reflux in ethanol for 60-96 h. Solvent was removed under reduced pressure, the resulting residue was taken up into CH_2Cl_2 and extracted with 3M HCl (aq.), water, sat. NaCl, and dried over sodium sulfate. Solvent was removed under reduced pressure and crude product was purified by flash column chromatography and recrystallization to afford 1,4 diones.

General Procedure for the Preparation of Tetrasubstituted Butane-1,4-diones A solution of KHMDS (1.1 equiv, 0.5 M in toluene) was added to a stirring solution of diarylethanone (1 equiv) in THF (2-5 mL), at -78 °C. The mixture was stirred 1 h followed by the dropwise addition of α-bromoketone (1.1 equiv). The reaction mixture was allowed to stir at -78 °C for 1 h and then allowed to gradually warm to rt, stirring 5 h to overnight (monitored for disappearance of starting material) and then quenched with the addition of H_2O. The reaction was further diluted with EtOAc and washed with H_2O and sat. NaCl. Organic extract was dried over Na_2SO_4, filtered and solvent removed under reduced pressure. Purification by flash column chromatography afforded diones as mixtures of diastereomers (by NMR).

General Procedure for Furans In toluene, the 1,4-dione and *p*-toluenesulfonic acid monohydrate (cat. amount) were heated to reflux for 3-12 h. The reaction was the cooled,

filtered and solvent removed under reduced pressure and the crude product was purified by flash column chromatography.

General Demethylation Procedure Using BF$_3$•SMe$_2$ To a stirring solution of the methyl ether precursor (1 equiv) in CH$_2$Cl$_2$ (~8 mL) at rt was added BF$_3$•SMe$_2$ complex (75 equiv). After stirring for 12-18 h, solvent and excess reagent were evaporated under nitrogen stream in hood. Residue was taken up in EtOAc and washed with H$_2$O and sat NaCl. Organic extract was dried over Na$_2$SO$_4$, filtered and solvent removed under reduced pressure. The resulting residue was purified by silica gel flash column chromatography.

General Demethylation Procedure Using BBr$_3$ The methyl ether protected compound was dissolved in CH$_2$Cl$_2$ and stirred at rt. A solution of 1M boron tribromide in CH$_2$Cl$_2$ was added via syringe, and the reaction was left to stir over-night or until all starting material had been consumed. The reaction poured into separatory funnel and extracted with H$_2$O (3x10 ml), sat NaCl, and dried over sodium sulfate. Solvent was removed under reduced pressure and the resulting crude product was purified by flash column chromatography and recrystallization to afford deprotected phenols.

2,3,5-Tris-(4-hydroxy-phenyl)-4-methyl-furan (15a) Furan **14a** (58.0 mg, 0.14 mmol) was reacted according to the general demethylation procedure using BF$_3$•SMe$_2$ to afford crude **15a**. The crude material was purified by flash column chromatography (1:2 EtOAc:hexanes) and recrystallized from EtOAc:hexanes to give **15a** (40.2 mg, 77% yield). mp 231-233 °C (decomp); ^{1}H NMR (500 MHz, acetone-d_6) δ 2.05 (3H, s, CH_3), 6.74 (2H, AA'XX', J_{AX}= 8.77, $J_{AA'}$ = 2.48, ArH ortho to OH), 6.94 (2H, AA'XX', J_{AX}= 8.46, $J_{AA'}$ = 2.42, ArH ortho to OH), 6.95 (2H, AA'XX', J_{AX}= 8.83, $J_{AA'}$ = 2.49, ArH ortho to OH), 7.16 (2H, AA'XX', J_{AX}= 8.81, $J_{XX'}$ = 2.39, ArH meta to OH), 7.34 (2H, AA'XX', J_{AX}= 8.99, $J_{XX'}$ = 2.50, ArH meta to OH), 7.61 (2H, AA'XX', J_{AX}= 8.77, $J_{XX'}$ = 2.46, ArH meta to OH), 8.44 (1H, bs, OH), 8.48 (1H, bs, OH), 8.51 (1H, bs, OH); ^{13}C NMR (125 MHz, acetone-d_6) δ 10.5, 116.1(2), 116.4(2), 116.6(2), 117.5, 124.1, 124.6, 124.7, 125.8, 127.5(2), 127.7(2), 132.2(2), 147.4, 147.9, 157.4, 157.5, 157.7; MS (EI, 70 eV) m/z 358.1 (M$^+$); HRMS calcd for C$_{23}$H$_{18}$O$_4$: 358.12051, found: 358.12040.

3-Ethyl-2,4,5-tris(4-hydoxyphenyl)furan (15b) Furan **14b** (28.0 mg, 0.07 mmol) was reacted according to the general demethylation procedure using BF$_3$•SMe$_2$ to afford crude **15b**. The crude material was purified by flash column chromatography (1:1 hexane:EtOAc) and recrystallized from EtOAc:hexanes to give **15b** (16.3 mg, 93% yield). mp 219-220 °C; ^{1}H NMR (500 MHz, acetone-d_6) δ 1.01 (3H, t, J=7.52, CH_3CH$_2$), 2.51 (2H, q, J= 7.52,. CH$_3$CH_2), 6.72 (2H, AA'XX', J_{AX}= 8.99, $J_{AA'}$ = 2.52, ArH ortho to OH), 6.95 (2H, AA'XX', J_{AX}= 8.85, $J_{AA'}$ = 2.54, ArH ortho to OH), 6.96 (2H, AA'XX', J_{AX}= 8.67, $J_{AA'}$= 2.55, ArH ortho to OH), 7.17 (2H, AA'XX', J_{AX}= 8.89, $J_{XX'}$ = 2.41, ArH meta to OH), 7.31 (2H, AA'XX', J_{AX}= 9.01, $J_{XX'}$ = 2.47, ArH meta to OH), 7.60 (2H, AA'XX', J_{AX}= 8.95, $J_{XX'}$ = 2.49, ArH meta to OH), 8.39 (1H, bs, OH), 8.46 (1H, bs, OH), 8.49 (1H, bs, OH); ^{13}C NMR (125 MHz, acetone-d_6) δ 14.1, 17.1, 115.2(2), 115.6(2), 115.7(2), 123.2, 123.4, 123.5, 123.6, 125.1, 126.5(2), 126.8(2), 131.3(2), 146.5, 146.7, 156.5, 156.7, 156.9; MS (EI, 70 eV) m/z 372.2 (M$^+$); HRMS calcd for C$_{24}$H$_{20}$O$_4$: 372.136159, found: 370.136761; Anal. calcd for C$_{24}$H$_{20}$O$_4$ (+0.5 H$_2$O), C: 74.43, H: 6.12. Found, C: 74.82, H: 5.86.

2,3,5-Tris(4-hydroxyphenyl)-4-propylfuran (15c) Furan **14c** (40.0 mg, 0.09 mmol) was reacted according to the general demethylation procedure using BF$_3$•SMe$_2$ to afford crude **15c**. The crude material was purified by flash column chromatography (1:1 hexane:EtOAc) to provide **15c** (32.0 mg, 93% yield) as a white powder. ^{1}H NMR (500 MHz, acetone-d_6) δ 0.79 (3H, t, J= 7.24, CH_3CH$_2$CH$_2$), 1.42 (2H, m, CH$_3$CH_2CH$_2$), 2.48 (2H, m, CH$_3$CH$_2$CH_2), 6.73 (2H, AA'XX', J_{AX}= 8.89, $J_{AA'}$= 2.53, ArH ortho to OH), 6.95 (4H, AA'XX', J_{AX}= 8.55, $J_{AA'}$= 2.53, ArH ortho to OH), 7.16 (2H, AA'XX', J_{AX}= 8.82, $J_{XX'}$ = 2.41, ArH meta to OH), 7.31 (2H, AA'XX', J_{AX}= 8.86, $J_{XX'}$ = 2.47, ArH meta to OH), 7.60 (2H, AA'XX', J_{AX}= 9.02, $J_{XX'}$ = 2.42, ArH meta to OH), 8.42 (1H, bs, OH), 8.48 (1H, bs, OH), 8.51 (1H, bs, OH); ^{13}C NMR (125 MHz, acetone-d_6) δ14.4, 23.8, 26.8, 116.0(2), 116.4(2), 116.6(2), 122.9, 124.1, 124.4, 124.5, 126.1, 127.3(2), 127.7(2), 132.2(2), 147.5, 147.7, 157.4, 157.5, 157.7; MS (EI, 70 eV) m/z 386.2 (M$^+$); HRMS calcd for C$_{25}$H$_{22}$O$_4$: 386.15181, found: 386.15274.

3-Butyl-2,4,5-tris(4-hydroxyphenyl)furan (15d) Furan **14d** (50.0 mg, 0.11 mmol) was reacted according to the general demethylation procedure using $BF_3 \cdot SMe_2$ to afford crude **15d**. The crude material was purified by flash column chromatography (1:1 EtOAc:hexanes) to provide **15d** (39.5 mg, 88% yield) as a solid. A small amount of **15d** for biological testing was further purified by reverse phase HPLC; ^1H NMR (500 MHz, acetone-d_6) δ 0.76 (3H, t, J= 7.41, CH_3CH$_2$CH$_2$CH$_2$), 1.22 (2H, sextet, J= 7.39, CH$_3$CH_2CH$_2$CH$_2$), 1.39 (2H, m, CH$_3$CH$_2$CH_2CH$_2$), 2.50 (2H, m, CH$_3$CH$_2$CH$_2$CH_2), 6.72 (2H, AA'XX', J_{AX}= 8.72, $J_{AA'}$ = 2.53, ArH ortho to OH), 6.949 (2H, AA'XX', J_{AX}= 8.83, $J_{AA'}$ = 2.49, ArH ortho to OH), 6.952 (2H, AA'XX', J_{AX}= 8.63, $J_{AA'}$ = 2.53, ArH ortho to OH), 7.16 (2H, AA'XX', J_{AX}= 8.67, $J_{XX'}$ = 2.41, ArH meta to OR), 7.31 (2H, AA'XX', J_{AX}= 9.11, $J_{XX'}$ = 2.45, ArH meta to OR), 7.60 (2H, AA'XX', J_{AX}= 9.01, $J_{XX'}$ = 2.53, ArH meta to OR), 8.47 (1H, bs, OH), 8.52 (1H, bs, OH), 8.56 (1H, bs, OH); ^{13}C NMR (125 MHz, acetone-d_6) δ 13.9, 23.2, 24.3, 32.7, 116.0(2), 116.4(2), 116.6(2), 123.0, 124.1, 124.4, 124.5, 126.1, 127.3(2), 127.7(2), 132.2(2), 147.5, 147.6, 157.4, 157.5, 157.7; MS (EI, 70 eV) m/z 400.2 (M^+); HRMS calcd for $C_{26}H_{24}O_4$: 400.16746, found: 400.16743.

2,3,4,5-Tetrakis-(4-hydroxy-phenyl)-furan (15e) Furan **14e** (40.0 mg, 0.10 mmol) was reacted according to the general demethylation procedure using $BF_3 \cdot SMe_2$ to afford crude **15e**. The crude material was purified by flash column chromatography (1:1 hexane:EtOAc) and recrystallized from EtOAc:hexanes to give **15e** (49.0 mg, 85% yield). mp 247-250 °C (decomp); ^1H NMR (500 MHz, acetone-d_6) δ 6.76 (4H, AA'XX', J_{AX}= 8.72, $J_{AA'}$= 2.45, ArH ortho to OH), 6.77 (4H, AA'XX', J_{AX}= 8.65, $J_{AA'}$ = 2.45, ArH ortho to OH), 7.37 (4H, AA'XX', J_{AX}= 8.62, $J_{XX'}$ = 2.32, ArH meta to OH), 8.38 (4H, AA'XX', J_{AX}= 8.73, $J_{XX'}$ = 2.44, ArH meta to OH), 8.38 (2H, bs, OH), 8.53 (2H, bs, OH); ^{13}C NMR (125 MHz, acetone-d_6) δ 116.08(4), 113.12(4), 123.9(2), 124.2(2), 125.5(2), 127.7(4), 132.4(4), 147.7(2), 157.4(2), 157.6(2); MS (EI, 70 eV) m/z 436.2 (M^+); HRMS calcd for $C_{28}H_{20}O_5$: 436.13107, found: 436.13124.

3-Ethyl-2,4-bis(4-hydroxyphenyl)-5-phenylfuran (15f) Furan **14f** (20.0 mg, 0.05 mmol) was reacted according to the general demethylation procedure using $BF_3 \cdot SMe_2$ to afford crude **15f**. The crude material was purified by flash column chromatography (1:1

hexane:EtOAc) followed by recrystallization from CH_2Cl_2:hexanes to give **15f** as a solid (17.4 mg, 94 % yield). mp 226-230 °C; ^1H NMR (500 MHz, acetone-d_6) δ 1.02 (3H, t, J= 7.49, CH_3CH_2), 2.53 (2H, q, J= 7.49, CH_3CH_2), 6.97 (2H, AA'XX', J_{AX}= 8.74, $J_{AA'}$ = 2.60, ArH ortho to OH), 6.98 (2H, AA'XX', J_{AX}= 8.70, $J_{AA'}$ = 2.45, ArH ortho to OH), 7.16 (1H, m, ArH para to furan), 7.19 (2H, AA'XX', J_{AX}= 8.75, $J_{XX'}$ = 2.48, ArH meta to OH), 7.24 (2H, m, ArH meta to furan), 7.46 (2H, m, ArH ortho to furan), 7.64 (2H, AA'XX', J_{AX}= 8.66, $J_{XX'}$ = 2.53, ArH meta to OH), 8.55 (2H, bs, OH); ^{13}C NMR (125 MHz, acetone-d_6) δ14.9, 17.9, 116.5(2), 116.7(2), 124.2, 124.6, 125.6(2), 125.7, 126.5, 127.5, 127.9(2), 129.2(2), 132.1(2), 132.3, 147.0, 148.4, 157.8, 157.9; MS (EI, 70 eV) m/z 356.1 (M$^+$); HRMS calcd for $C_{24}H_{20}O_3$: 356.14125, found: 328.14129.

2,4-Bis(4-hydroxyphenyl)-5-phenyl-3-propylfuran (15g) Furan **14g** (30.0 mg, 0.075 mmol) was reacted according to the general demethylation procedure using BF_3•SMe_2 to afford crude **15g**. The crude material was purified by flash column chromatography (2:1 hexane:EtOAc) and recrystallized from EtOAc:hexanes to give **15g** (23.2 mg, 86% yield). ^1H NMR (500 MHz, acetone-d_6) δ 0.80 (3H, t, J=7.39, CH_3CH_2), 1.44 (2H, m, $CH_3CH_2CH_2$), 2.49 (2H, m, CH_2-furan), 6.969 (2H, AA'XX', J_{AX}= 8.87, $J_{AA'}$ = 2.55, ArH ortho to OH), 6.972 (2H, AA'XX', J_{AX}= 8.55, $J_{AA'}$ = 2.41, ArH ortho to OH), 7.16 (1H, m, ArH para to furan), 7.18 (2H, AA'XX', J_{AX}= 8.78, $J_{XX'}$ = 2.44, ArH meta to OH), 7.24 (2H, m, ArH meta to furan), 7.45 (2H, m, ArH ortho to furan), 7.64 (2H, AA'XX', J_{AX}= 8.68, $J_{XX'}$ = 2.62, ArH meta to OH), 8.52 (1H, bs, OH), 8.57 (1H, bs, OH); ^{13}C NMR (125 MHz, acetone-d_6) δ14.1, 23.6, 26.6, 116.3(2), 116.5(2), 123.0, 124.0, 125.4(2), 125.5, 126.5, 127.3, 127.7(2), 128.9(2), 131.9(2), 132.1, 146.7, 148.5, 157.6, 157.7; MS (EI, 70 eV) m/z 370.2 (M$^+$); HRMS calcd for $C_{25}H_{22}O_3$: 370.156890, found: 370.15661.

3-Ethyl-2,5-bis(4-hydroxyphenyl)-4-phenylfuran (15h) Furan **14h** (30.0 mg, 0.08 mmol) was reacted according to the general demethylation procedure using BF_3•SMe_2 to afford crude **15h**. The crude material was purified by flash column chromatography (1:1 hexane:EtOAc) to provide **15h** (25.8 mg, 93% yield) as a white powder. mp 127-132 °C

(decomp); ^{1}H NMR (500 MHz, acetone-d_6) δ 1.00 (3H, t, J= 7.47, CH_3CH$_2$), 2.52 (2H, q, J= 7.50, CH$_3$CH_2), 6.72 (2H, AA′XX′, J_{AX}= 8.86, $J_{AA'}$= 2.48, ArH ortho to OH), 6.96 (2H, AA′XX′, J_{AX}= 8.75, $J_{AA'}$= 2.56, ArH ortho to OH), 7.27 (2H, AA′XX′, J_{AX}= 8.91, $J_{XX'}$= 2.47, ArH meta to OH), 7.36 (2H, m, ArH ortho to furan), 7.41 (1H, tt, J= 7.51, 1.34, ArH para to furan), 7.48 (2H, m, ArH meta to furan), 7.62 (2H, AA′XX′, J_{AX}= 8.84, $J_{XX'}$= 2.46, ArH meta to OH), 8.44 (1H, bs, OH), 8.54 (1H, bs, OH); ^{13}C NMR (125 MHz, acetone-d_6) δ 14.9, 17.9, 116.1(2), 116.5(2), 123.8, 123.9, 124.0, 124.3, 127.5(2), 127.8(2), 128.3, 129.7(2), 131.1(2), 135.4, 147.6, 147.7, 157.5, 157.6; MS (EI, 70 eV) m/z 356.2 (M$^+$); HRMS calcd for C$_{24}$H$_{20}$O$_3$: 356.14125, found: 356.14168.

3-Ethyl-4,5-bis(4-hydroxyphenyl)-2-phenylfuran (15i) Furan **14i** (40.0 mg, 0.10 mmol) was reacted according to the general demethylation procedure using BF$_3$•SMe$_2$ to afford crude **15i**. The crude material was purified by flash column chromatography (1:1 hexane:EtOAc) and recrystallized from EtOAc:hexanes to give **15i** (31.3 mg, 84% yield). mp 204-206 °C; ^{1}H NMR (500 MHz, acetone-d_6) δ 1.04 (3H, t, J=7.53, CH_3CH$_2$), 2.57 (2H, q, J= 7.50, CH$_3$CH_2), 6.75 (2H, AA′XX′, J_{AX}= 9.14, $J_{AA'}$= 2.46, ArH ortho to OH), 6.97 (2H, AA′XX′, J_{AX}= 8.59, $J_{AA'}$= 2.40, ArH ortho to OH), 7.18 (2H, AA′XX′, J_{AX}= 8.79, $J_{XX'}$= 2.32, ArH meta to OH), 7.30 (1H, m, ArH para to furan), 7.34 (2H, AA′XX′, J_{AX}= 8.86, $J_{XX'}$= 2.47, ArH meta to OH), 7.47 (2H, m, ArH meta to furan), 7.77 (2H, m, ArH ortho to furan), 8.52 (1H, bs, OH), 8.54 (1H, bs, OH); ^{13}C NMR (125 MHz, acetone-d_6) δ 14.8, 18.0, 116.1(2), 116.6(2), 123.8, 124.4, 125.7, 125.9(2), 126.6, 127.5(2), 127.6, 129.6(2), 132.2(2), 132.7, 146.8, 148.5, 157.7, 157.8; MS (EI, 70 eV) m/z 356.2 (M$^+$); MS (CI, 130 eV) m/z 357.2 (M$^+$+H); HRMS calcd for C$_{24}$H$_{20}$O$_3$: 356.14125, found: 356.14045.

3-Ethyl-2-(4-hydroxyphenyl)-(4,5)-bisphenylfuran (15j) Furan **14j** (40 mg, 0.11 mmol) was reacted according to the general demethylation procedure using BF$_3$•SMe$_2$ to afford crude **15j**. The crude material was purified by flash column chromatography (75:25 hexane:EtOAc) and recrystallized from hexane:EtOAc to give **15j** (21 mg, 55% yield) as a white crystalline solid. mp 159-160 °C; ^{1}H NMR (400 MHz, CDCl$_3$) δ 1.04 (3H, t, J = 7.57, CH_3),

2.53 (2H, q, J = 7.51, CH_2), 4.76 (1H, s, OH), 6.93 (2H, d, J = 8.34, ArH ortho to OH), 7.13-7.47 (10H, m, ArH), 7.65 (2H, d, J = 8.75, ArH meta to OH); ^{13}C NMR (500 MHz, CDCl$_3$) δ 14.6, 17.3, 115.6(2), 124.1, 124.8, 125.1(2), 126.7, 127.2(2), 127.4, 128.2(2), 128.8(2), 130.2(2), 131.1, 134.2, 146.6, 147.2, 154.6, 164.5; MS (EI, 70 EV) m/z 340.2 (M$^+$); HRMS calcd for C$_{24}$H$_{20}$O$_2$: 340.14633, found: 340.14611.

3-Ethyl-4-(4-hydroxyphenyl)-(2,5)-bisphenylfuran (15k) Furan **14k** (42 mg, 0.12 mmol) was reacted according to the general demethylation procedure using BF$_3$•SMe$_2$ to afford crude **15k**. The crude material was purified by flash column chromatography (75:25 hexane:EtOAc) and recrystallized from hexane:EtOAc to give **15k** (28 mg, 70% yield) as a white powder. mp 144-147 °C ^{1}H NMR (400 MHz, CDCl$_3$) δ 1.11 (3H, t, J = 7.45, CH_3), 2.62 (2H, q, J = 7.36, CH_2), 4.92 (1H, s OH), 6.97 (2H, d, J = 8.21, ArH ortho to OH), 7.28-7.49 (10H, m, ArH), 7.8 (2H, d, J = 7.87, ArH meta to OH); ^{13}C NMR (500 MHz, CDCl$_3$) δ 14.6, 17.4, 115.8, 125.1, 125.2(2), 125.4(2), 125.8, 126.4, 126.8, 126.9, 128.3(2), 128.6 (2), 131.1, 131.5(2), 131.6, 147.1, 147.2, 154.9; MS (EI, 70 EV) m/z 340.2 (M$^+$); HRMS calc. for C$_{24}$H$_{20}$O$_2$: 340.14633, found: 340.14649.

3-Ethyl-5-(4-hydroxyphenyl)-(2,4)-bisphenylfuran (15l) Furan **14l** (13.4 mg, 0.04 mmol) was reacted according to the general demethylation procedure using BF$_3$•SMe$_2$ to afford crude **15l**. The crude product was purified by flash column chromatography (95:5 hexane:EtOAc) and recrystallized from hexane:EtOAc to give furan **15l** (10 mg, 78% yield) as a light yellow powder. mp 133-136 °C ^{1}H NMR (400 MHz, CDCl$_3$) δ 1.06 (3H, t, J = 7.35, CH_3), 2.57 (2H, q, J = 7.48, CH_2), 4.65 (1H, s, OH), 6.69 (2H, d, J = 8.47, ArH ortho to OH), 7.26-7.46 (10H, m, ArH), 7.74 (2H, d, J = 7.26, ArH meta to OH); ^{13}C NMR (500 MHz, CDCl$_3$) δ 14.6, 17.4, 115.2(2), 124.7, 124.3, 125.4(2), 125.5, 126.8, 127.0(2), 127.4, 128.5, 128.6(2), 128.8(2), 130.3(2), 131.7, 134.2, 146.6, 154.6; MS (EI, 70 eV) m/z 340.2 (M$^+$); HRMS calcd for C$_{24}$H$_{20}$O$_2$: 340.14633, found: 340.14659.

2,5-Bis(4-hydroxyphenyl)-3-phenylfuran (15m) Furan **14m** (22.0mg, 0.06 mmol) was reacted according to the general demethylation procedure using BF$_3$•SMe$_2$ to afford crude **15m**.

The crude material was purified by flash column chromatography (1:1 EtOAc:hexane) followed by recrystallization from CH_2Cl_2:hexanes to give **15m** as a solid (18.7 mg, 92% yield). mp 167-170 °C; ^{1}H NMR (500 MHz, acetone-d_6) δ 6.82 (2H, AA'XX', J_{AX}= 8.77, $J_{AA'}$= 2.32, Ar*H* ortho to OH), 6.83 (1H, s, furan*H*), 6.92 (2H, AA'XX', J_{AX}= 8.90, $J_{AA'}$ = 2.52, Ar*H* ortho to OH), 7.31 (1H, m, Ar*H* para to furan), 7.39 (2H, m, Ar*H* meta to furan), 7.43 (2H, AA'XX', J_{AX}= 8.817, $J_{XX'}$ = 2.45, Ar*H* meta to OH), 7.46 (2H, m, Ar*H* ortho to furan), 7.67 (2H, AA'XX', J_{AX}= 8.93, $J_{XX'}$ = 2.44, Ar*H* meta to OH), 8.56 (2H, bs, OH); ^{13}C NMR (100 MHz, acetone-d_6) δ 107.3, 115.6(2), 115.9(2), 122.78, 122.81, 123.1, 125.4(2), 127.2, 127.8(2), 128.6(2), 128.8(2), 134.9, 147.5, 152.5, 157.36, 158.38; MS (FAB) m/z 328.2 (M^+), HRMS calcd for $C_{22}H_{16}O_3$: 328.10995, found: 328.10980.

3,5-Bis(4-hydroxyphenyl)-2-phenylfuran (15n) Furan **14n** (65.0 mg, 0.18 mmol) was reacted according to the general demethylation procedure using $BF_3 \cdot SMe_2$ to afford crude **15n**. The crude material was purified by flash column chromatography (1:1 EtOAc:hexane) followed by recrystallization from CH_2Cl_2:hexanes to give **15n** as a solid (46.0 mg, 77% yield). mp 160-163 °C; ^{1}H NMR (400 MHz, acetone-d_6) δ 6.79 (1H, s, furan*H*), 6.89 (2H, AA'XX', J_{AX}= 8.65, $J_{AA'}$ = 2.47, Ar*H* ortho to OH), 6.93 (2H, AA'XX', J_{AX}= 8.82, $J_{AA'}$ = 2.45, Ar*H* ortho to OH), 7.23 (1H, m, Ar*H* para to furan), 7.30 (2H, AA'XX', J_{AX}= 8.67, $J_{XX'}$ = 2.53, Ar*H* meta to OH), 7.32 (2H, m, Ar*H* meta to furan), 7.66 (2H, m, Ar*H* ortho to furan), 7.69 (2H, AA'XX', J_{AX}= 8.81, $J_{XX'}$ = 2.45, Ar*H* meta to OH), 8.58 (2H, bs, OH); ^{13}C NMR (100 MHz, acetone-d_6) δ108.7, 116.5(2), 116.6(2), 123.4, 125.63, 126.3(2), 126.5(2), 128.0, 129.3(2), 130.7(2), 132.4, 147.0, 153.7, 157.9, 158.36 (2); MS (EI, 70 eV) m/z 328.2 (M^+); HRMS calcd for $C_{22}H_{16}O_3$: 328.10995, found: 328.10955.

General Procedure for Thiophenes The 1,4-dione and Lawesson's Reagent were stirred in CH_2Cl_2 at 40 °C until all 1,4-dione had been consumed by TLC (2-3 h). The reaction mixture was then poured into separatory funnel and washed with H_2O, 10% sodium bicarbonate, sat. NaCl, and dried over sodium sulfate. Solvent was removed under reduced pressure, and the

crude product was purified by flash column chromatography and recrystallization to afford cyclized thiophenes.

2,5-Bis(4-hydroxyphenyl)-3-phenylthiophene (17a) Thiophene **16a** (22.6 mg, 0.06 mmol) was reacted according to the general demethylation procedure using BBr_3 to afford crude **17a**. The crude material was purified by flash column chromatography (1:1 hexane:EtOAc) to give **17a** as a solid (18.3 mg, 88% yield). mp 125-130 °C; ^{1}H NMR (500 MHz, acetone-d_6) δ 6.78 (2H, AA′XX′, J_{AX}= 8.73, $J_{AA'}$ = 2.47, ArH ortho to OH), 6.90 (2H, AA′XX′, J_{AX}= 8.78, $J_{AA'}$ = 2.60, ArH ortho to OH), 7.14 (2H, AA′XX′, J_{AX}= 8.52, $J_{XX'}$ = 2.47, ArH meta to OH), 7.26 (1H, m, ArH para to thiophene), 7.32 (4H, m, ArH meta and ortho to thiophene), 7.34 (1H, s, thiophene$H$), 7.56 (2H, AA′XX′, J_{AX}= 8.79, $J_{XX'}$ = 2.52, ArH meta to OH), 8.54 (1H, bs, OH), 8.57 (1H, bs, OH); ^{13}C NMR (125 MHz, acetone-d_6) δ 115.5(2), 115.8(2), 124.9, 125.5, 125.8, 126.7(2), 126.8, 128.3(2), 128.9(2), 130.3(2), 136.6, 136.9, 138.0, 141.9, 157.2, 157.4; MS (EI, 70 eV) m/z 344.1 (M^+); HRMS calcd for $C_{22}H_{16}SO_2$: 344.08710, found: 344.08621.

3,5-Bis(4-hydroxyphenyl)-2-phenylthiophene (17b) Thiophene **16b** (108.0 mg, 0.29 mmol) was reacted according to the general demethylation procedure using $BF_3 \cdot SMe_2$ to afford crude **17b**. The crude material was purified by flash column chromatography (1:1 hexane:EtOAc) followed by recrystallization from CH_2Cl_2:hexanes to give **17b** as a solid (85.1 mg, 85 % yield). mp 198-200 °C; ^{1}H NMR (500 MHz, acetone-d_6) δ 6.79 (2H, AA′XX′, J_{AX}= 8.66, $J_{AA'}$ = 2.47, ArH ortho to OH), 6.90 (2H, AA′XX′, J_{AX}= 8.80, $J_{AA'}$ = 2.60, ArH ortho to OH), 7.17 (2H, AA′XX′, J_{AX}= 8.69, $J_{XX'}$ = 2.47, ArH meta to OH), 7.24-7.34 (5H, m, ArH phenyl), 7.32 (1H, s, thiophene$H$), 7.57 (2H, AA′XX′, J_{AX}= 8.72, $J_{XX'}$ = 2.52, ArH meta to OH), 8.50 (2H, bs, OH); ^{13}C NMR (125 MHz, acetone-d_6) δ115.3(2), 115.8(2), 125.3, 125.7, 126.8(2), 127.2, 127.9, 128.5(2), 128.8(2), 130.1(2), 134.7, 134.9, 139.1, 142.6, 156.7, 157.5; MS (EI, 70 eV) m/z 344.1 (M^+); HRMS calcd for $C_{22}H_{16}SO_2$: 344.08710, found: 344.08620.

General Procedure for N-Substituted Pyrroles In toluene, the 1,4-dione, amine and p-toluene sulfonic acid monohydrate were heated to reflux for 24 h, using a Dean-Stark trap. The

reaction was cooled, filtered, and solvent removed in-vacuo. Crude product was purified by flash column chromatography and recrystallization to afford N-substituted pyrroles.

2-Ethyl-1,3-bis-(4-hydroxyphenyl)-5-phenylpyrrole (19) Methyl-ether protected pyrrole **18** (38.8 mg, 0.10 mmol) and boron tribromide (0.6 mL, 0.6 mmol) were reacted as outlined in general procedure for demethylation to give 29.0 mg brownish solid. Trituration with hexane gave product as off-white solid, (21.8 mg), 60.8% yield. ^{1}H NMR (500 MHz, acetone-d_6) δ 0.90 (3H, t, J=7.42, CH_3), 2.62 (2H, q, J=7.42, CH_2), 6.43 (1, s, pyrrole$H$), 6.88 (2H, AA′XX′, J_{AX}= 8.84, $J_{AA'}$ = 2.63, ArH ortho to OH), 6.90 (2H, AA′XX′, J_{AX}= 8.80, $J_{AA'}$ = 2.76, ArH ortho to OH), 7.07 (1H, m, ArH para to pyrrole), 7.11 (2H, AA′XX′, J_{AX}= 8.70, $J_{XX'}$ = 2.73, ArH meta to OH), 7.15 (4H, m, ArH ortho and meta to pyrrole), 7.32 (2H, AA′XX′, J_{AX}= 8.63, $J_{XX'}$ = 2.51, ArH meta to OH), 8.18 (1H, s, ArOH), 8.67 (1H, s, ArOH);. MS (EI, 70 eV) m/z 355.2 (M$^+$). HRMS calcd. for $C_{24}H_{21}NO_2$: 355.1572, found: 355.1567.

Molecular Modeling

The protein structure used in the docking simulations was based on the X-ray crystallographic structure of the human estrogen receptor ligand binding domain bound to estradiol (entry 1ere in the Protein Data Bank). The crystal structure contains 3 homodimers with 244 residues each. For modeling purposes only one monomer (chain A) was chosen. The monomer contains several residues with missing atoms and five residues with alternate conformations. Missing atoms were added using InsightII, and one conformation was selected for each of the five residues. Several residues that are part of two loops were completely missing. These two loops were modeled based on the crystal structure of the wild type estrogen receptor ligand binding domain complexed to estradiol (entry 1qku) using InsightII. To eliminate bad contacts and constraints due to crystal packing and loop reconstruction, the protein was energy minimized for 1000 steps using the Powell algorithm in the presence of strong harmonic constraints on the backbone, followed by an additional 1000 steps without constraints. Minimization was done with the program SYBYL 6.6 and the MMFF94 force field. Furan **15b**

was docked into the minimized receptor using the FlexiDock routine, and the receptor-ligand complex put through a minimization protocol as previously described.[24]

Biological Procedures

Relative Binding Affinities. Ligand binding affinities (RBAs) using lamb uterine cytosol as a receptor source were determined by a competitive radiometric binding assay using 10 nM [^{3}H]estradiol as tracer and dextran-coated charcoal as an adsorbant for free ligand.[38] Purified ERα and ERβ binding affinities were determined using a competitive radiometric binding assay using 10 nM [^{3}H]estradiol as tracer, commercially available ERα and ERβ preparations (PanVera Inc. Madison, WI), and hydroxylapatite (HAP) to adsorb bound receptor-ligand complex.[39] HAP was prepared following the recommendations of Williams and Gorski.[46] All incubations were done at 0 °C for 18-24h. Unlabeled competitors were prepared in 1:1 DMF:TEA to ensure solubility. Binding affinities are expressed relative to estradiol on a percent scale (i.e., for estradiol, RBA = 100%). All essays were run in separate, duplicate experiments, which were reproducible with a coefficient of variation of less than 0.3.

Transcriptional Activation Studies. Transactivation by ligands on ERα and ERβ was tested in transfected human endometrial cancer (HEC-1) cells. HEC-1 cells, maintained in MEM containing 5% CS and 5% FCS, were seeded into 24-well plates in transfection media (IMEM containing 5% FCS, and transfected at about 50% confluency, using lipofectin-transferrin. For each well, 1 μg 4ERE-TATA-LUC, 2.5 μg of pCMVβGal as internal control, 50-100 ng pCMV5-ERα or pCMV5-ERβ were mixed with 5 μl lipofectin (GIBCO, BRL) and 1.6 μl 1mg/ml transferrin in 150 μl HBSS. The mixture was applied to the cell with 350 μl serum-free IMEM media for each well. The cell was incubated at 37° C in the 5% CO_2 containing incubator for 6 h. Compounds were prepared as solutions in ethanol and were added to medium to give a final ethanol concentration of 0.1%. The cell culture media was replaced by transfection media containing different concentration of ligands. Cell were incubated for 24 h in the presence of

ligand. The luciferase reporter assay system (Promega) was used for the luciferase activity assay. The activity of E_2 (10^{-8} M) on ERα or ERβ was set as 100%, and the relative activity was adjusted based on the transfection efficiency which was monitored by the internal control β-galactosidase activity, as previously described.[16,47]

Supporting Information Available:

Experimental detail for all precursors is available.

References

(1)   Pollard, J. W. Modifiers of estrogen action. *Science & Medicine* **1999**, 38-47.

(2)   Cauley, J. A.; Stelley, D. G.; Ensrud, K.; Ettinger, B.; Black, D. et al. Estrogen replacement therapy and fractures in older women. *Ann. Intern. Med.* **1995**, *122*, 9-16.

(3)   Davidson, N. E. Hormone-replacement therapy- breast versus heart versus bone. *N. Engl. J. Med.* **1995**, *352*, 1638-1639.

(4)   Jordan, V. C. Designer estrogens. *Scientific American* **1998**, 60-67.

(5)   Barrett-Conner, E.; Bush, T. L. Estrogen and coronary heart disease in women. *JAMA* **1991**, *265*, 1861-1867.

(6)   Stampfer, M. J.; Colditz, G. A.; Willett, W. C. Postmenopausal estrogen therapy and cardiovascular Disease -- ten year follow-up from the nurses' health study. *N. Engl. J. Med.* **1991**, *325*, 756-762.

(7)   Tuck, C. H.; Holleran, S.; Berglund, L. Hormonal regulation of lipoprotein(a) levels: effects of estrogen replacement therapy on lipoprotein(a) and actute phase reactants in postmenopausal women. *Arterioscler. Thromb. Vasc. Biol.* **1997**, *17*, 1822-1829.

(8)   Sherwin, B. S. Estrogen effects on cognition in menopausal women. *Neurology* **1997**, *48*, S21-S26.

(9)   Rice, M. M.; Graves, A. B.; McCurry, S. M.; Larson, E. B. Estrogen replacement therapy and cognitive function in postmenopausal women without dementia. *Am. J. Med.* **1997**, *103*, 26S-35S.

(10)   Kuiper, G. G. J. M.; Enmark, E.; Pelto-Huikko, M.; Nilsson, S.; Gustafsson, J.-Å. Cloning of a novel receptor expressed in rat prostate and ovary. *Proc. Natl. Acad. Sci. U.S.A.* **1996**, *93*, 5925-5930.

(11)   Mosselman, S.; Polman, J.; Dijkema, R. ERβ: Identification and charaterization of a novel human estrogen receptor. *FEBS Lett.* **1996**, *392*, 49-53.

(12)   Kuiper, G. G. J. M.; Carlsson, B.; Grandien, K.; Enmark, E.; Haggbald, J. et al. Comparison of the ligand binding specificity and transcipt tissue distribution of estrogen receptors α and β. *Endocrinology* **1997**, *138*, 863-870.

(13)   Barkhem, T.; Carlsson, B.; Nilsson, Y.; Enmark, E.; Gustafsson, J.-Å. et al. Differential Response of Estrogen Receptor α and Estrogen Receptor β to Partial Estrogen Agonists/Antagonists. *Mol. Pharmacol.* **1998**, *54*, 105-112.

(14)   Makela, S.; Savolainen, H.; Aavik, E.; Myllarnieni, M.; Strauss, L. et al. Differentiation between vasculoprotective and uterotrophic effects of ligands with different binding affinities to estrogen receptors α and β. *Proc. Natl. Acad. Sci., USA* **1999**, *96*, 7077-7082.

(15)   Paech, K.; Webb, P.; Kuiper, G. G. J. M.; Nilsson, S.; Gustafsson, J.-Å. et al. Differential ligand activation of estrogen receptors ERα and ERβ at AP1 sites. *Science* **1997**, *277*, 1508-1510.

(16)   Sun, J.; Meyers, M. J.; Fink, B. E.; Rajendran, R.; Katzenellenbogen, J. A. et al. Novel ligands that function as selective estrogens or antiestrogens for estrogen receptor-α or estrogen receptor-β. *Endocrinology* **1999**, *140*, 800-804.

(17)   Stauffer, S. R.; Katzenellenbogen, J. A. Acyclic Amides as Estrogen Receptor Ligands: Synthesis, Binding, Activity, and Receptor Interaction. *Bio. Med. Chem.* **2000**, *8*, 1293-1316.

(18)   Meyers, M. J.; Sun, J.; Carlson, K. E.; Katzenellenbogen, B. S.; Katzenellenbogen, J. A. Estrogen receptor subtype-selective ligands: Asymmetric synthesis and biological evaluation of cis- and trans-5,11-dialkyl- 5,6,11,12- tetrahydrochrysenes. *J. Med. Chem.* **1999**, *42*, 2456-2468.

(19)   Pike, A. C. W.; Brzozowski, A. M.; Hubbard, R. E.; Bonn, T.; Thorsell, A.-G. et al. Structure of the ligand-binding domian of oestrogen receptor beta in the presence of a partial agonist and a full antagonist. *EMBO J.* **1999**, *18*, 4608-4618.

(20)   Fink, B. E.; Mortensen, D. S.; Stauffer, S. R.; Aron, Z. D.; Katzenellenbogen, J. A. Novel structural templates for estrogen-receptor ligands and prospects for combinatorial synthesis of estrogens. *Chem. Biol.* **1999**, *6*, 205-219.

(21)   Stauffer, S. R. Development of combinatorial approaches towards selective estrogen receptor modulators: investigations of acyclic amides and tetra-substituted pyazoles. In *Department of Chemistry*; University of Illinios: Urbana-Champaign, 1999; pp 208.

(22)   Stauffer, S. R.; Huang, Y.; Coletta, C. J.; Tedesco, R.; Katzenellenbogen, J. A. Estrogen pyrazoles: defining the pyrazole core structure and the orientation of substituents in the ligand binding pocket of the estrogen receptor. *Bio. Med. Chem.* **2001**, *9*, 141-150.

(23)   Stauffer, S. R.; Katzenellenbogen, J. A. Solid-phase synthesis of tetrasubstituted pyrazoles, novel ligands for the estrogen receptor. *J. Comb. Chem.* **2000**, *2*, 318-329.

(24)   Stauffer, S. R.; Coletta, C. J.; Tedesco, R.; Sun, J.; Katzenellenbogen, B. S. et al. Pyrazole Ligands: Structure-Affinity/Activity Relationships Of Estrogen Receptor-α Selective Agonists. *J. Med. Chem.* **2000**, *43*, 4934-4947.

(25)   Stauffer, S. R.; Huang, Y. R.; Aron, Z. D.; Coletta, C. J.; Sun, J. et al. Triarlpyrazoles with Basic Side Chains: Development of Pyrazole-Based Estrogen Receptor Antagonists. *Bioorg. Med. Chem.* **2001**, *9*, 151-161.

(26)   Durani, N.; Jain, R.; Saeed, A.; Dikshit, D. K.; Durani, S. et al. Structure-activity relationship of antiestrogens: a study using triarylbutenone, benzofuran, and triarylfuran analogues as a model for triarylethylenes and triarypropenones. *J. Med. Chem.* **1989**, *32*, 1700-1707.

(27)   Dikshit, D. K.; Singh, S.; Singh, M. M.; Kamboj, V. P. Synthesis and biological activity of 2,3- and 3,4-diarylfurans and 2,3,4-triaryl-2,5-dihydrofurans. *Ind. J. Chem.* **1990**, *29B*, 954-960.

(28)   Dikshit, D. K.; Munshi, K. L.; Kapil, R. S.; Kamboj, V. P.; Anand, N. Antifertility agent: Part IX -- Synthesis of 2,3,4-triphenylfurans & 2,3,4-triphenyl-5-methylfurans. *Ind. J. Chem.* **1974**, *12*, 1144-1146.

(29)   Iyer, R. N.; Gopalachari, R. s. Studies in Potential Antifertility Agents: Part VII-Synthesis of Dialkylaminoethyl Derivatives of 2,4,5-Triphenylpyrroles & 2,4,5-Triphenylfurans. *Ind. J. Chem.* **1973**, *11*, 1260-1262.

(30)   Stetter, H. Catalyzed addition of aldehydes to activated double bonds-a new synthetic approach. *Angew. Chem. Int. Ed. Engl.* **1976**, *15*, 639-647.

(31)   Thompson, L. A.; Ellman, J. A. Synthesis and Application of Small Molecule Libraries. *Chem. Rev.* **1996**, *96*, 555-600.

(32)   Shridhar, D. R.; Jogibhukta, M.; Shanthan Rao, P.; Handa, V. K. Reaction of 2,4-Bis(4-methoxyphenyl)-1,3,2,4-dithiadiphosphetane-2,4-disulphide with substituted butane-1,4-diones: Part II -- Novel synthesis of substituted thiophenes & furans. *Ind. J. Chem.* **1983**, *22B*, 1187-1190.

(33)   Wynberg, H.; Wiersum, U. E. Rearrangements and transalkylation of *t*-butylthiophenes. *J. Org. Chem.* **1965**, *30*, 1058-1060.

(34)   Champaigne, E.; Foye, W. O. The synthesis of 2,5-diarylthiophenes. *J. Org. Chem.* **1952**, *17*, 1405-1412.

(35)   Wynberg, H.; Metselaar, J. A convenient route to polythiophenes. *Synthetic Communications* **1984**, *14*, 1-9.

(36)   Ramasseul, R.; Rassat, A. Preparation d'heterocycles encombres: di-*t*-butyl-2,5-furanne, pyrrole et thiophene. *Bull. Soc. Chim. (France)* **1965**, 3136-3140.

(37)   Chakrabarty, M. *J. Chem. Soc.* **1940**, 1385.

(38)   Katzenellenbogen, J. A.; Johnson, H. J.; Myers, H. N. Photoaffinity labels for estrogen binding proteins of rat uterus. *Biochemistry* **1973**, *12*, 4085-4092.

(39)   Carlson, K. E.; Choi, I.; Gee, A.; Katzenellenbogen, B. S.; Katzenellenboge, J. A. Altered ligand binding properties and enhanced stability of a constitutively active estrogen receptor: Evidence that an open pocket conformation is required for ligand interaction. *Biochemistry* **1997**, *36*, 14897-14905.

(40)   Anstead, G. M.; Carlson, K. E.; Katzenellenbogen, J. A. The estradiol pharmacophore: ligand structure-estrogen receptor binding affinity relationships and a model for the receptor binding site. *Steroids* **1997**, *62*, 268-303.

(41)   Gao, H.; Katzenellenbogen, J. A.; Garg, R.; Hansch, C. Comparative QSAR Analysis of Estrogen Receptor Ligands. *Chem. Rev.* **1999**, *99*, 723-744.

(42)   Anstead, G. M.; Wilson, S. R.; Katzenellenbogen, J. A. 2-Arylindenes and 2-arylindenones: molecular structures and considerations in the binding orientation of unsymmetrical nonsteroidal ligands to the estrogen receptor. *J Med Chem* **1989**, *32*, 2163-2171.

(43)   Mortensen, D. S.; Rodriguez, A. L.; Sun, J.; Katzenellenbogen, B. S.; Katzenellenbogen, J. A. Furans with basic side chains: Synthesis and biological evaluation of a novel series

of antagonists with selectivity for the estrogen receptor alpha. *Bio. Med. Chem. Lett.* **2001**, *to be submitted*.

(44) Brzozowski, A. M.; Pike, A. C. W.; Dauter, Z.; Hubbard, R. E.; Bonn, T. et al. Molecular basis of agonism and antagonism in the oestrogen receptor. *Nature* **1997**, *389*, 753-758.

(45) Shiau, A. K.; Barstad, D.; Loria, P. M.; Cheng, L.; Kushner, P. J. et al. The structural basis of estrogen receptor/coactivator recognition and the antagonism of this interaction by tamoxifen. *Cell* **1998**, *95*, 927-937.

(46) Williams, D.; Gorski, J. *Biochemistry* **1974**, *13*.

(47) McInerney, E. M.; Tsai, M. J.; O'Malley, B. W.; Katzenellenbogen, B. S. Analysis of estrogen receptor transcriptional enhancement bya a nuclear hormone receptor coactivator. *Proc. Natl. Acad. Sci. U.S.A.* **1996**, *93*, 10069-10073.

Table 1. Synthesis of furans **14a-n**.

14a-n
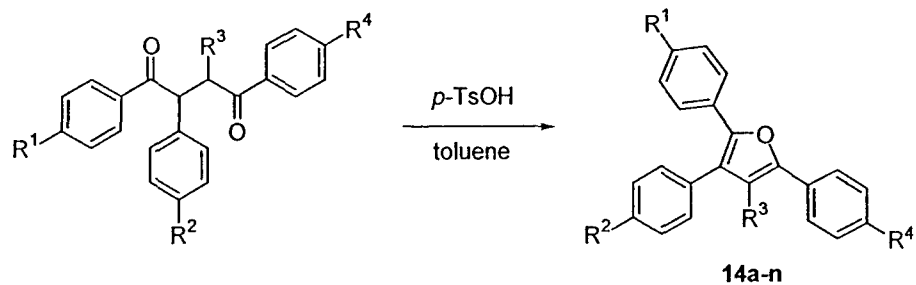
Dione	Furan	R^1	R^2	R^3	R^4	Yield
13a	**14a**	OCH_3	OCH_3	CH_3	OCH_3	74%
13b	**14b**	OCH_3	OCH_3	C_2H_5	OH	70%
13c	**14c**	OCH_3	OCH_3	C_3H_7	OCH_3	85%
13d	**14d**	OCH_3	OCH_3	C_4H_9	OCH_3	98%
13e	**14e**	OCH_3	OCH_3	$pCH_3OC_6H_4$	OCH_3	85%
13f	**14f**	H	OCH_3	C_2H_5	OCH_3	87%
13g	**14g**	H	OCH_3	C_3H_7	OCH_3	83%
13h	**14h**	OCH_3	H	C_2H_5	OCH_3	95%
13i	**14i**	OCH_3	OCH_3	C_2H_5	H	73%
13j	**14j**	H	H	C_2H_5	OCH_3	42%
13k	**14k**	H	OCH_3	C_2H_5	H	75%
13l	**14l**	OCH_3	H	C_2H_5	H	25%
10a	**14m**	OCH_3	H	H	OCH_3	88%
10b	**14n**	H	OCH_3	H	OCH_3	92%

31

Table 2. Demethylation of furans **14a-n** to **15a-n**.
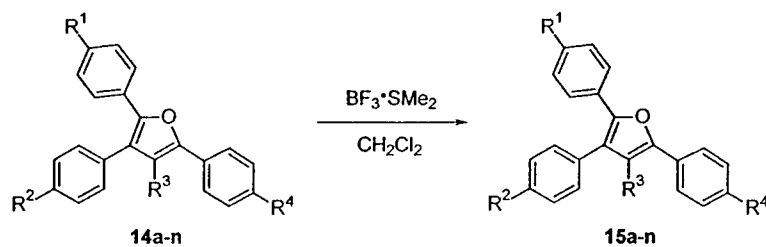
Furan	Deprot. Furan	R^1	R^2	R^3	R^4	Yield
14a	15a	OH	OH	CH$_3$	OH	77%
14b	15b	OH	OH	C$_2$H$_5$	OH	93%
14c	15c	OH	OH	C$_3$H$_7$	OH	93%
14d	15d	OH	OH	C$_4$H$_9$	OH	88%
14e	15e	OH	OH	pHOC$_6$H$_4$	OH	85%
14f	15f	H	OH	C$_2$H$_5$	OH	94%
14g	15g	H	OH	C$_3$H$_7$	OH	88%
14h	15h	OH	H	C$_2$H$_5$	OH	93%
14i	15i	OH	OH	C$_2$H$_5$	H	84%
14j	15j	H	H	C$_2$H$_5$	OH	55%
14k	15k	H	OH	C$_2$H$_5$	H	70%
14l	15l	OH	H	C$_2$H$_5$	H	78%
14m	15m	OH	H	H	OH	75%
14n	15n	H	OH	H	OH	77%

Table 3. Relative Binding Affinity (RBA)[a] data for furans **15a-n**, thiophenes**17a-b**, and pyrrole **19**.

Ligand	Cytosol	ER-α	ER-β	α/β Selectivity
15a	2.9 ± 0.09	40 ± 6.5	0.62 ± 0.02	65 fold
15b	6.5 ± 0.8	140 ± 38	2.9 ± 0.1	48 fold
15c	3.6 ± 0.6	100 ± 14	1.8 ± 0.65	56 fold
15d	1.3 ± 0.7	21 ± 0.6	3.9 ± 1.1	5.4 fold
15e	0.84 ± 0.07	8.7 ± 1.1	0.25 ± 0.01	36 fold
15f	4.6 ± 0.5	82 ± 20	7.1 ± 1.2	12 fold
15g	3.6 ± 0.3	140 ± 13	15 ± 4.1	9.5 fold
15h	0.7 ± 0	16.5 ± 1.9	3.0 ± 0.6	5.5 fold
15i	0.45 ± 0	14.8 ± 3.1	4.5 ± 1.2	3.3 fold
15j	0.44 ± 0.09	10.8 ± 2.6	3.4 ± 1.2	3.8 fold
15k	0.02 ± 0.01	0.15 ± 0.01	0.07 ± 0.02	2.1 fold
15l	0.10 ± 0.04	6.8 ± 2.1	2.0 ± 0.4	3.4 fold
15m	0.13	NA	NA	NA
15n	0.04	NA	NA	NA
17a	0.03	NA	NA	NA
17b	0.04	NA	NA	NA
19	0.50	NA	NA	NA

[a]Determined by a competitive radiometric binding assay with [^{3}H]estradiol using methods described in the Experimental Section. Where indicated, values represent the average ($\pm$ SD or range) of multiple determinations. In our hands, RBA values are reproducible with a coefficient of variation of less than 0.3.
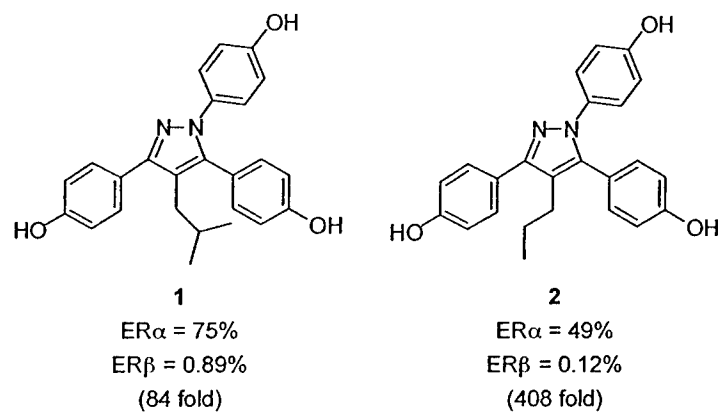
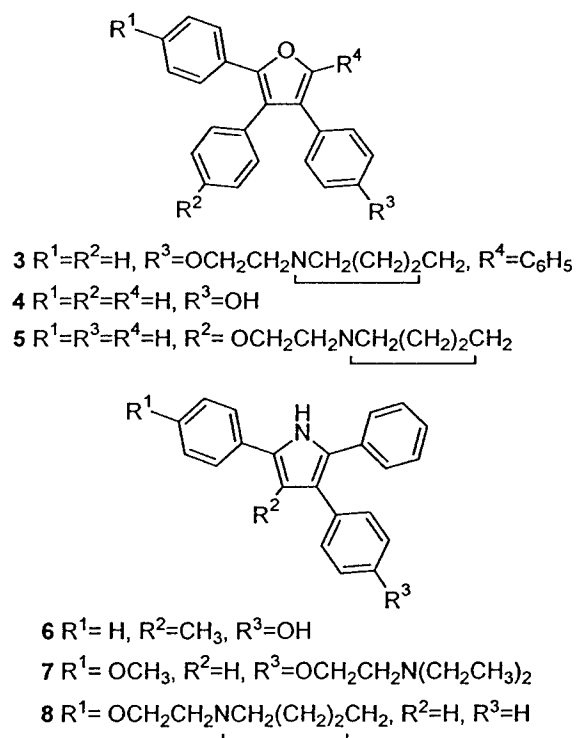**Figure 1.** Structures and binding affinity data pyrazoles **1** and **2**.

3 R^1=R^2=H, R^3=OCH$_2$CH$_2$NCH$_2$(CH$_2$)$_2$CH$_2$, R^4=C$_6$H$_5$

4 R^1=R^2=R^4=H, R^3=OH

5 R^1=R^3=R^4=H, R^2= OCH$_2$CH$_2$NCH$_2$(CH$_2$)$_2$CH$_2$

6 R^1= H, R^2=CH$_3$, R^3=OH

7 R^1= OCH$_3$, R^2=H, R^3=OCH$_2$CH$_2$N(CH$_2$CH$_3$)$_2$

8 R^1= OCH$_2$CH$_2$NCH$_2$(CH$_2$)$_2$CH$_2$, R^2=H, R^3=H

Figure 2. Representative furans and pyrroles explored as antifertility agents[26-29]
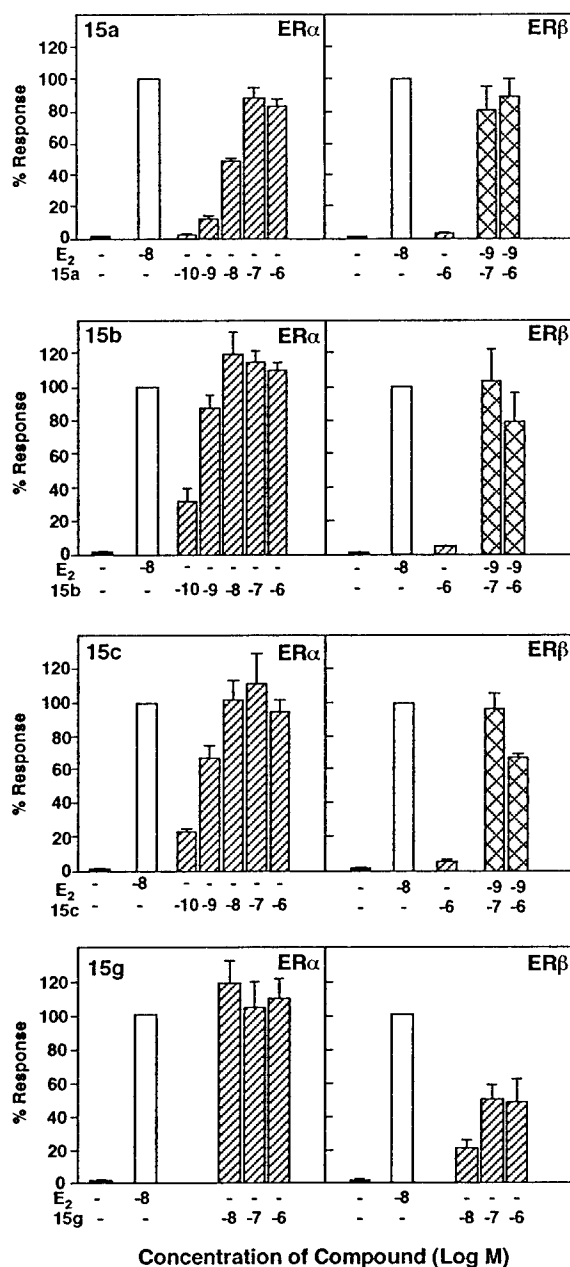
Figure 3. Transcriptional activation data for furans **15a-c** and **15g** through ERα and ERβ. Human endometrial cancer (HEC-1) cells were transfected with expression vectors for ERα or ERβ and an estrogen responsive reporter gene and were treated with indicated concentrations of estradiol or ligand for 24h to assay for agonism (diagonal slashed bars) or antagonism (cross-hatched bars). Transcriptional activity was normalized to an internal β-gal control plasmid using the luciferase reporter assay system. Values are expressed as a percent of the ERα or ERβ response with 10 nM E_2, which is set at 100% (open bars).[29] For details, see Experimental Section.
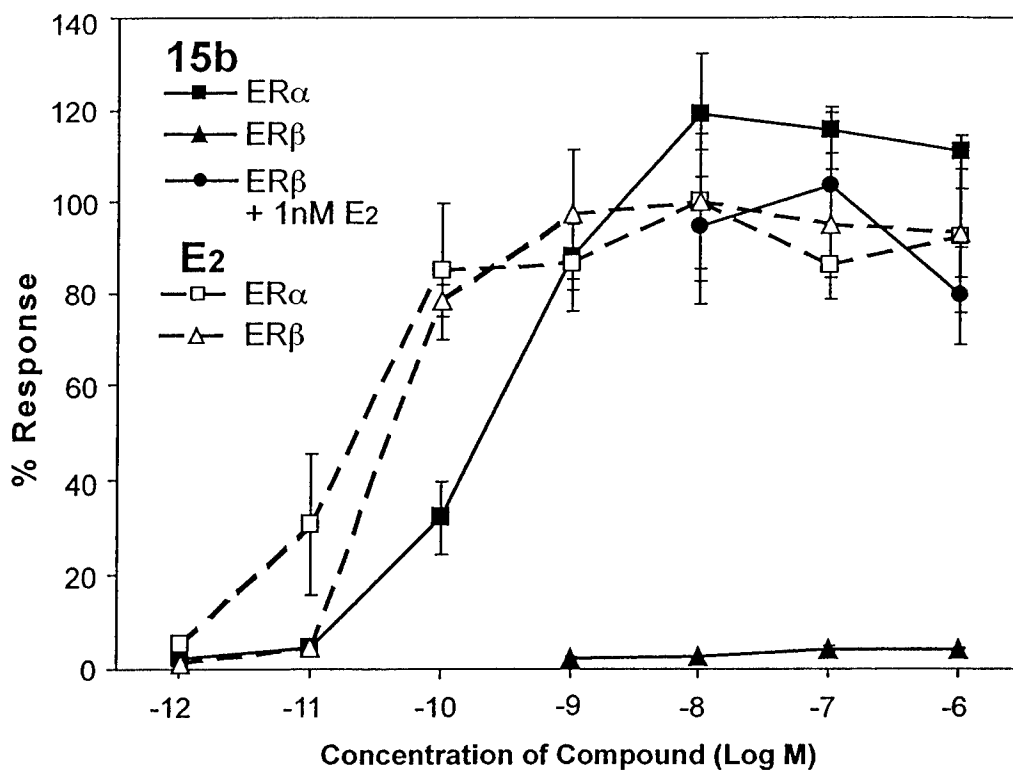
Figure 4. Dose-response curve for transcriptional activation by furan **15b** though ERα (solid squares) and ERβ (solid triangles). Antagonist activity through ERβ (circles) was also assayed. The activation curves for estradiol on those two receptors is shown for reference. (open squares and triangles, respectively; dotted lines) For details, see Experimental Section.
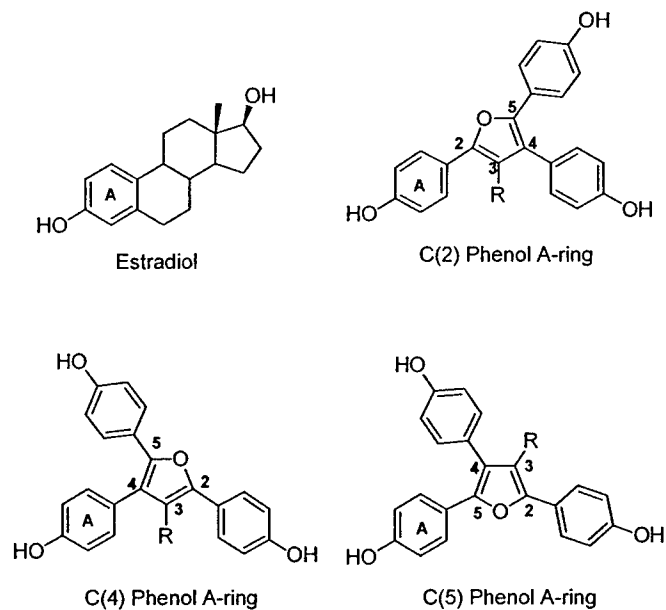
Figure 5. Three possible mimics for the A-ring of estradiol. Note, with each case A-ring mimic, there are two possible orientations of the furan core (only one is shown).
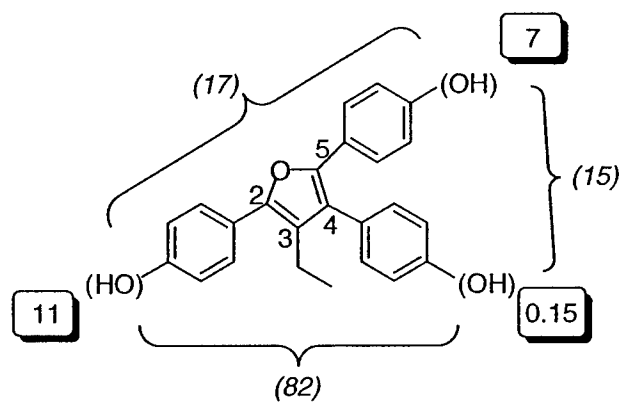
Figure 6. Summary of ERα binding data for furan monophenols and bis-phenols for comparative binding analysis. The binding affinity of the three monophenols is shown in the shadowed box by each of the three hydroxyl groups, and the affinity of the three bis-phenols is indicated by the italicized number in parentheses on braces linking two hydroxyl groups. For a discussion, see text.
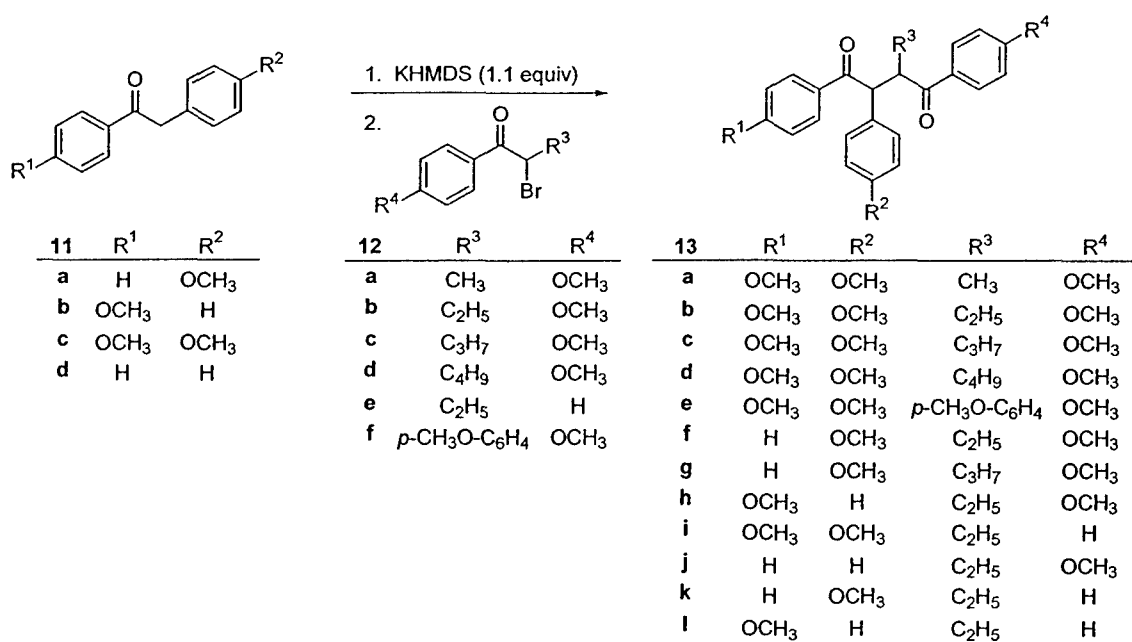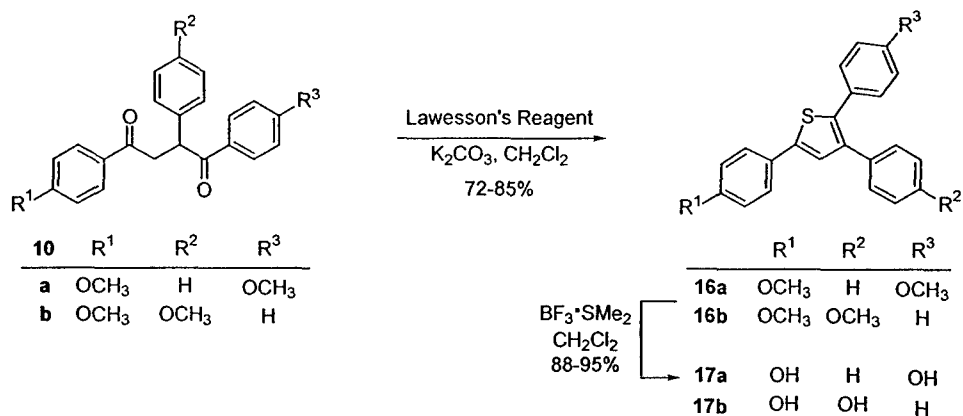
37
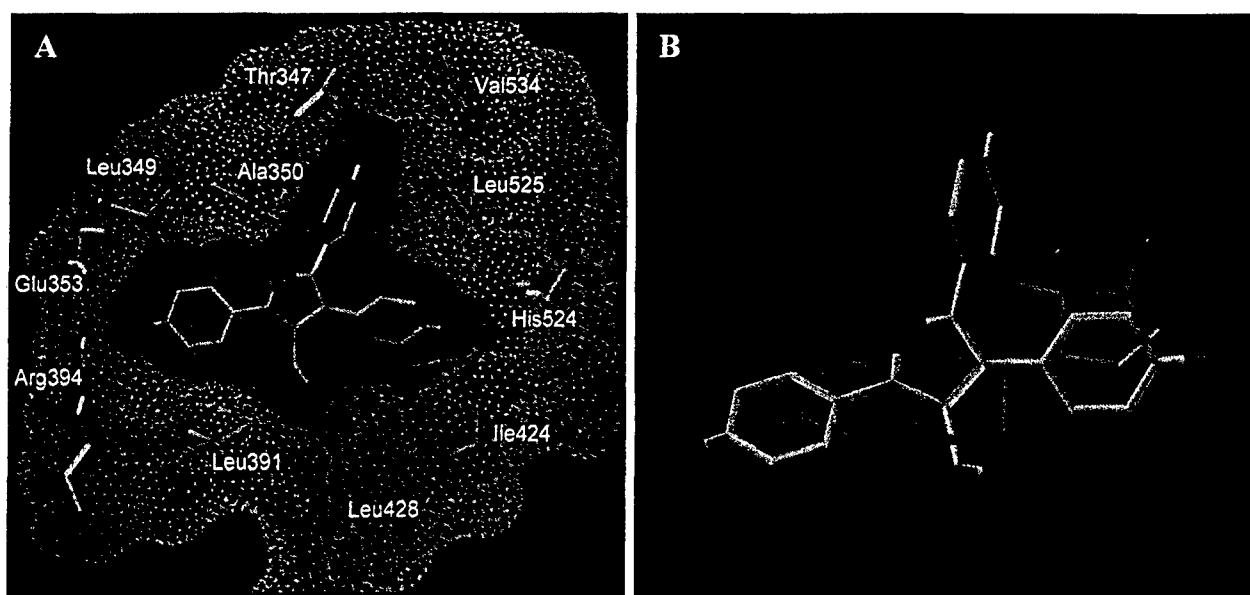
Figure 7. (A) Model of furan **15b** in ERα ligand binding pocket. The surface of the ligand is shown as a continuous green shape; the surface of the ERα pocket is shown as purple dots. (B) Comparison of the orientation of the furan (gray) with respect to that of estradiol (purple) in the ERα ligand binding pocket. For details, see text and Experimental Section.
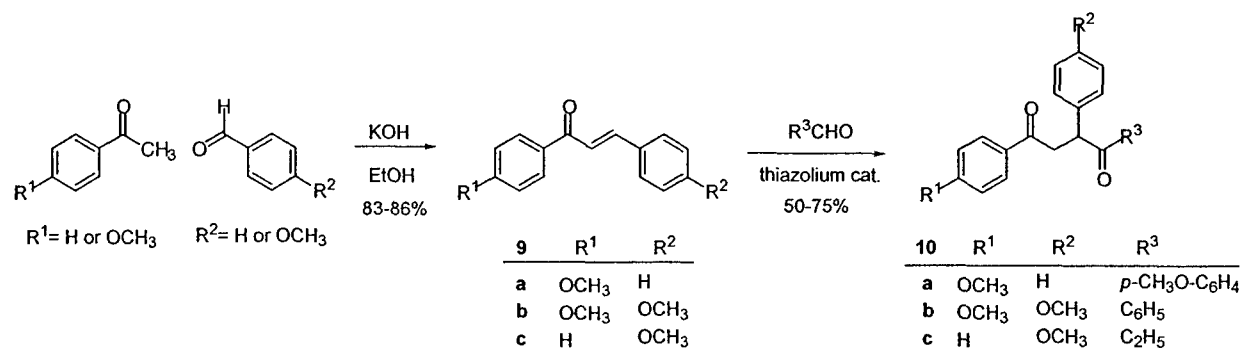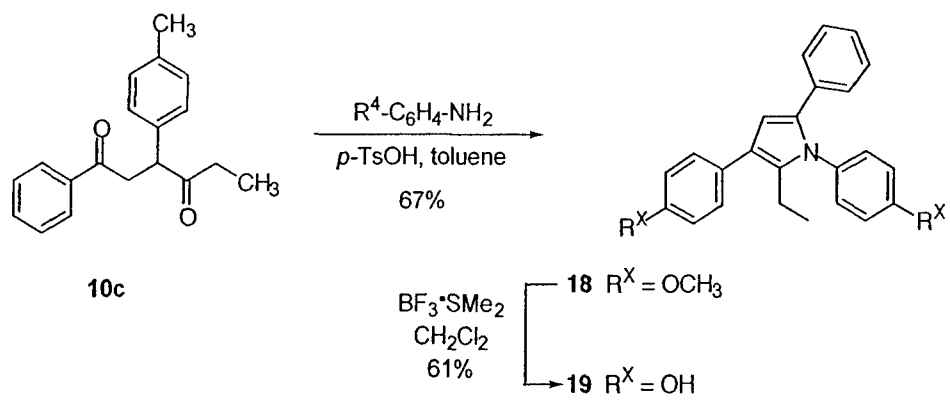
Scheme 1. Preparation of 1,2,4-trisubstituted diones **10a-c**.

9	R¹	R²
a	OCH₃	H
b	OCH₃	OCH₃
c	H	OCH₃

10	R¹	R²	R³
a	OCH₃	H	p-CH₃O-C₆H₄
b	OCH₃	OCH₃	C₆H₅
c	H	OCH₃	C₂H₅

R¹= H or OCH₃   R²= H or OCH₃

1. KHMDS (1.1 equiv)

2.

11	R^1	R^2
a	H	OCH$_3$
b	OCH$_3$	H
c	OCH$_3$	OCH$_3$
d	H	H

12	R^3	R^4
a	CH$_3$	OCH$_3$
b	C$_2$H$_5$	OCH$_3$
c	C$_3$H$_7$	OCH$_3$
d	C$_4$H$_9$	OCH$_3$
e	C$_2$H$_5$	H
f	p-CH$_3$O-C$_6$H$_4$	OCH$_3$

13	R^1	R^2	R^3	R^4
a	OCH$_3$	OCH$_3$	CH$_3$	OCH$_3$
b	OCH$_3$	OCH$_3$	C$_2$H$_5$	OCH$_3$
c	OCH$_3$	OCH$_3$	C$_3$H$_7$	OCH$_3$
d	OCH$_3$	OCH$_3$	C$_4$H$_9$	OCH$_3$
e	OCH$_3$	OCH$_3$	p-CH$_3$O-C$_6$H$_4$	OCH$_3$
f	H	OCH$_3$	C$_2$H$_5$	OCH$_3$
g	H	OCH$_3$	C$_3$H$_7$	OCH$_3$
h	OCH$_3$	H	C$_2$H$_5$	OCH$_3$
i	OCH$_3$	OCH$_3$	C$_2$H$_5$	H
j	H	H	C$_2$H$_5$	OCH$_3$
k	H	OCH$_3$	C$_2$H$_5$	H
l	OCH$_3$	H	C$_2$H$_5$	H

Scheme 2. Preparation of 1,2,3,4-tetrasubstituted diones **13a-l**.

10	R^1	R^2	R^3
a	OCH$_3$	H	OCH$_3$
b	OCH$_3$	OCH$_3$	H

	R^1	R^2	R^3
16a	OCH$_3$	H	OCH$_3$
16b	OCH$_3$	OCH$_3$	H
17a	OH	H	OH
17b	OH	OH	H

Scheme 3. Preparation of thiophenes **17a-b**.

41

Scheme 4. Preparation of pyrrole **19**.

Furans with Basic Side Chains: Synthesis and Biological Evaluation of a Novel Series of Antagonists with Selectivity for the Estrogen Receptor Alpha

Deborah S. Mortensen,[a] Alice L. Rodriguez,[a] Jun Sun,[b] Benita S. Katzenellenbogen,[b] and John A. Katzenellenbogen[a],*

[a]Dept. of Chemistry [b]Dept. Molecular and Integrative Physiology, University of Illinois, Urbana, IL 61801

Abstract – 3-Alkyl-2,4,5-triarylfurans with basic side chain substituents were prepared as ligands for the estrogen receptor. Those analog having the basic side chain on the C(4) phenol were high affinity, ERα-selective antagonists.

We have recently described the synthesis and biological evaluation of a series of 3-alkyl-2,4,5-triaryl-substituted furans, several of which proved to be ligands for the estrogen receptor (ER) with very high selectivity for ERα over ERβ, both in terms of binding affinity and potency of transcriptional activation.[1] Because there is great interest in the development of *antagonists* as well as *agonists* that are ER subtype-selective,[2,3] we have investigated a way to convert these ERα-selective furan agonists into ERα-selective antagonists.

The antagonist character of the antiestrogens raloxifene and hydroxy-tamoxifen (now more properly designated "selective estrogen receptor modifiers" or SERMs)[4] relies on a tertiary amino ethoxy substituent, termed a basic side-chain (BSC). When these ligands are bound to ERα, this bulky BSC projects outward from the ligand binding pocket and effects a structural reorganization of the receptor surface, repositioning helix 12 in a manner that blocks the binding of coactivator proteins important in mediating transcriptional activity.[5,6] Thus, we surmised that we might be able to impart antiestrogenic character to the furan series of agonists ligands, by appending a BSC through one of the three phenols of our furan ligands (Figure 1). It is not immediately evident which attachment site would be preferred, nor that the product BSC-furans would retain the ERα selectivity of the parent furans, because neither raloxifene nor tamoxifen is an ER subtype selective antagonist. We were able to adapt the synthetic route originally used to prepare the tetra-substituted furan systems for the preparation of the BSC-analogs,[1] by differential protection of the phenol functions in the starting materials. We recently used a similar approach to attach BSC groups to pyrazoles.[2] Here we report the results of our efforts to identify the preferred furan position for attachment of the BSC, to obtain ER antagonists that have some selectivity for ERα over ERβ, and to elucidate the orientation with which these furans bind to the receptor.
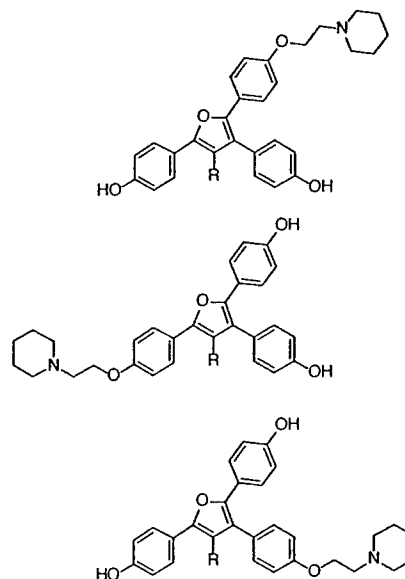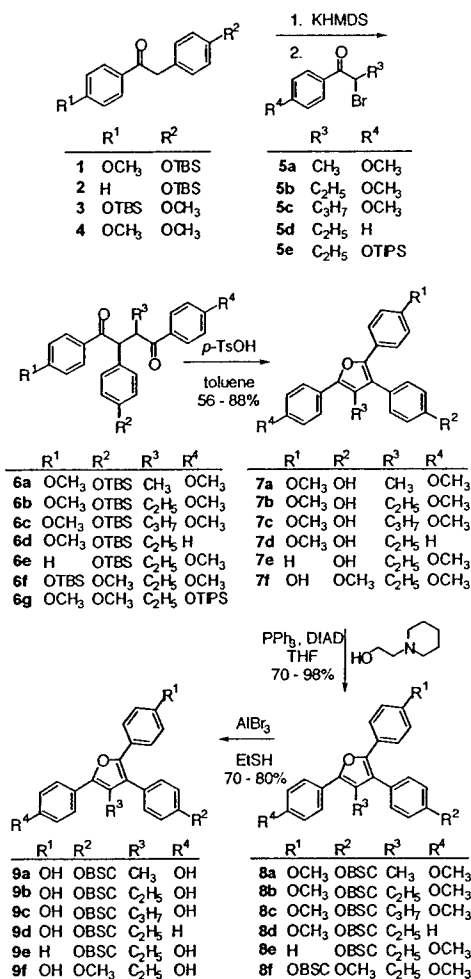

Figure 1. Three potential antiestrogenic furan basic side chain (BSC) derivatives.

Results and Discussion

Synthesis of Ligands

Treatment of the differentially protected 1,2-diaryl-ethanones **1-2**, ketone **3**, or desoxyanisoin (**4**) with potassium hexamethyl-disilyl-amide (KHMDS), followed by the addition of an α-bromoketone **5a-e**, provided the desired, differentially protected 1,3,4-triaryl-2-alkyl-butane-1,4-diones **6a-g** in 66-98% yields (Scheme 1). Although these diones were mixtures of diastereomers, no separation was required, because these stereocenters become trigonal in the furan products.

	R¹	R²			R³	R⁴
1	OCH₃	OTBS		5a	CH₃	OCH₃
2	H	OTBS		5b	C₂H₅	OCH₃
3	OTBS	OCH₃		5c	C₃H₇	OCH₃
4	OCH₃	OCH₃		5d	C₂H₅	H
				5e	C₂H₅	OTPS

	R¹	R²	R³	R⁴			R¹	R²	R³	R⁴
6a	OCH₃	OTBS	CH₃	OCH₃		7a	OCH₃	OH	CH₃	OCH₃
6b	OCH₃	OTBS	C₂H₅	OCH₃		7b	OCH₃	OH	C₂H₅	OCH₃
6c	OCH₃	OTBS	C₃H₇	OCH₃		7c	OCH₃	OH	C₃H₇	OCH₃
6d	OCH₃	OTBS	C₂H₅	H		7d	OCH₃	OH	C₂H₅	H
6e	H	OTBS	C₂H₅	OCH₃		7e	H	OH	C₂H₅	OCH₃
6f	OTBS	OCH₃	C₂H₅	OCH₃		7f	OH	OCH₃	C₂H₅	OCH₃
6g	OCH₃	OCH₃	C₂H₅	OTPS						

	R¹	R²	R³	R⁴			R¹	R²	R³	R⁴
9a	OH	OBSC	CH₃	OH		8a	OCH₃	OBSC	CH₃	OCH₃
9b	OH	OBSC	C₂H₅	OH		8b	OCH₃	OBSC	C₂H₅	OCH₃
9c	OH	OBSC	C₃H₇	OH		8c	OCH₃	OBSC	C₃H₇	OCH₃
9d	OH	OBSC	C₂H₅	H		8d	OCH₃	OBSC	C₂H₅	H
9e	H	OBSC	C₂H₅	OH		8e	H	OBSC	C₂H₅	OCH₃
9f	OH	OCH₃	C₂H₅	OH		8f	OBSC	OCH₃	C₂H₅	OCH₃

Scheme 1. Synthesis of basic side-chain furans **9a-f** (BSC = CH₂CH₂-piperidine).

Diones **6a-f** were refluxed in toluene with a slight excess of p-toluenesulfonic acid (TsOH) to effect furan formation and desilylation, giving mono-deprotected furans **7a-f**. The piperidinyl-ethoxy side-chain was added using Mitsunobu chemistry,[1] and the intermediates **8a-f** were demethylated using AlBr₃/EtSH to afford BSC-furans **9a-f**.[4]

In contrast to the behavior of diones **6a-f**, when refluxed with a catalytic amount of TsOH in toluene, dione **6g**

cyclized to the furan but did not undergo TIPS deprotection (Scheme 2). However, treatment of furan **10** with tetrabutylammonium fluoride at 0 °C did result in desilylation, giving the mono-deprotected furan **11** that was converted to BSC-furan **13**, as described above.

Biological Studies

Binding Affinity and Ligand Orientation Studies: The affinity of the BSC-furans **9a-f** and **13** for the estrogen receptor was assayed by a competitive radiometric binding assay, using purified, full-length human ERα and ERβ from recombinant sources.[7,8] The results of these assays are expressed as relative binding affinity (RBA) values, where the affinity of estradiol is considered to be 100%, and they are summarized in Table 1.

By comparison of the ERα affinities for the isomeric series of 3-ethyl-substituted BSC-furans **9b**, **9f**, and **13**, it appears that the preferred position for the attachment of the BSC is on C(4) phenol (**9b**); much lower affinities were observed when it was attached to the C(2) or C(5) phenols (**13** and **9f**, respectively). The BSC-modified furans did retain much of the selective affinity for ERα shown by their parent furans,[1] the most selective BSC-furan **9a** having a 67-fold ERα/ERβ binding selectivity. Even the analogs with low affinities for ERα maintained some of this selectivity.

The initial series of BSC-furans we prepared have two free phenols, either of which could be serving as the analog of the A-ring of estradiol, a group that functions as a crucial hydrogen-bonding partner in the ligand binding pocket and
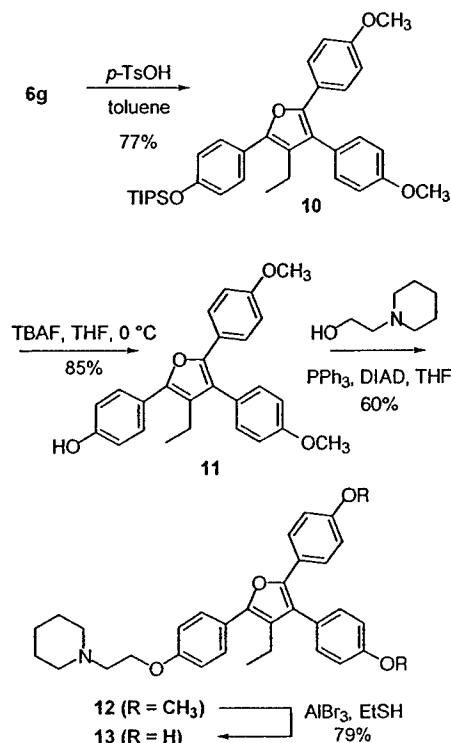
Scheme 2. Synthesis of basic side-chain furan **13**.

Table 1. Estrogen receptor relative binding affinity[a] data for basic side-chain furans 9a-f and 13.

Ligand	ER-α	ER-β	α/β
9a	32 ± 9	0.47 ± 0.1	67.2 fold
9b	75 ± 20	3.1 ± 0.1	24.3 fold
9d	60 ± 1	20 ± 3.5	3.0 fold
9e	3.8 ± 0.9	0.43 ± 0.04	8.8 fold
9f	2.5 ± 0.3	0.91 ± 0.02	2.7 fold
13	0.36 ± 0.11	0.06 ± 0.02	6.1 fold

[a]Determined by a competitive radiometric binding assay with [³H]estradiol.

is essential for the high affinity of the natural estrogen.[9] We sought to determine which of these phenols in the C(4)-BSC-furans was playing this important role in binding by deleting each of them in turn, and then evaluating the effect that this had on their ERα binding affinity.[9]

Estradiol

Raloxifene

Hydroxy-tamoxifen

Binding Mode A
C(2) Phenol A-ring

Binding Mode B
C(5) Phenol A-ring
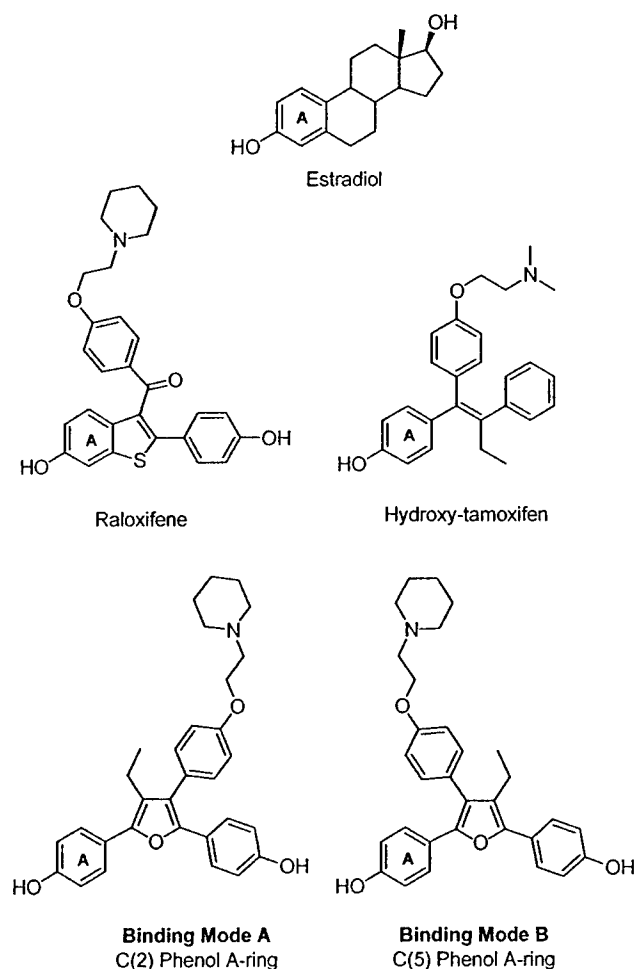
Figure 2. Two possible A-ring mimics of estradiol for furan 9b.

The X-ray crystal structures for ERα complexed with either raloxifene[6] or 4-hydroxy-tamoxifen[5] show that the BSC on these ligands have a common orientation that places them in roughly in the 11β direction with respect to a standard steroid core, where a salt bridge can then form between the teriary amine and aspartate 351 in helix-3.

Thus, as indicated in Figure 2, there are likely to be only two binding modes for a C(4)-BSC-furan, such as 9b, mode A, with the C(2) phenol in the A-ring binding pocket, and mode B, with C(5) phenol mimicking the A-ring.

Comparison of the ERα binding affinity of BSC-furans 9d and 9e, mono-phenol analogs of the high affinity BSC-furan diol 9b (Table 1), clearly shows that the phenol attached at position C(5) serves as the A-ring mimic: There was a 20-fold loss of affinity when this phenol deleted (9e), whereas deletion of the C(2) phenol caused less than a 1.3-fold drop (9d). Thus, we conclude that the highest affinity furan with the basic side chain, ligand 9b, binds to ER in orientation B (Figure 2), and that in this orientation, having a second phenolic hydroxyl on the C(2) phenyl ring, does not seem to be very important for high affinity binding (9b vs 9d); this second phenol does, however, play a significant role in the selective affinity of these BSC-furans for ERα.

Transcriptional Activation Assays: We selected the BSC-furans that combined high affinity with good ERα binding selectivity (namely 9a-c) to be assayed for their capacity to activate transcription through either ERα or ERβ, or to antagonize the transcriptional activity of estradiol through these ERs. These assays were done by cotransfection in human endometrial carcinoma (HEC-1) cells using a luciferase reporter gene system;[10] dose-response studies with the BSC-furans alone were conducted to measure agonist activity, and in the presence of 1 nM estradiol to determine antagonist activity. The results are summarized in Figures 3 and 4.

As expected, none of the three BSC-furans showed appreciable agonist activity on either ERα or ERβ. The methyl analog (9a) was a relatively weak antagonist on both ERs, showing no selectivity; the propyl analog (9c) was somewhat more potent and showed a small degree of selectivity in antagonizing ERα in preference to ERβ. The most potent and selective antagonist was the ethyl BSC-furan, 9b, and a more complete dose response curve for this compound (Figure 4) shows that at 0.1 µM, it almost fully suppresses the transcriptional activity of estradiol through ERα, yet it has no effect on ERβ at this concentration. The IC_{50} values for 9b on ERα and ERβ are approximately 6.5 x 10^{-8} M and 4.8 x 10^{-7} M, respectively, which corresponds to a nearly 10-fold antagonist potency selectivity for ERα over ERβ.

We have shown that one can obtain an ERαselective antagonist by adding a basic side chain (BSC) to the C(4) phenol of 3-ethyl-2,4,5-tris(4-hydroxylphenyl)furan, a ligand we have previously shown to be a very selective ligands.[12] However, the BSC-pyrazoles retained a greater degree of ERα-subtype selectivity in terms of both affinity and antagonist potency than did the BSC-furans.[11] Through binding affinity correlations, we concluded that
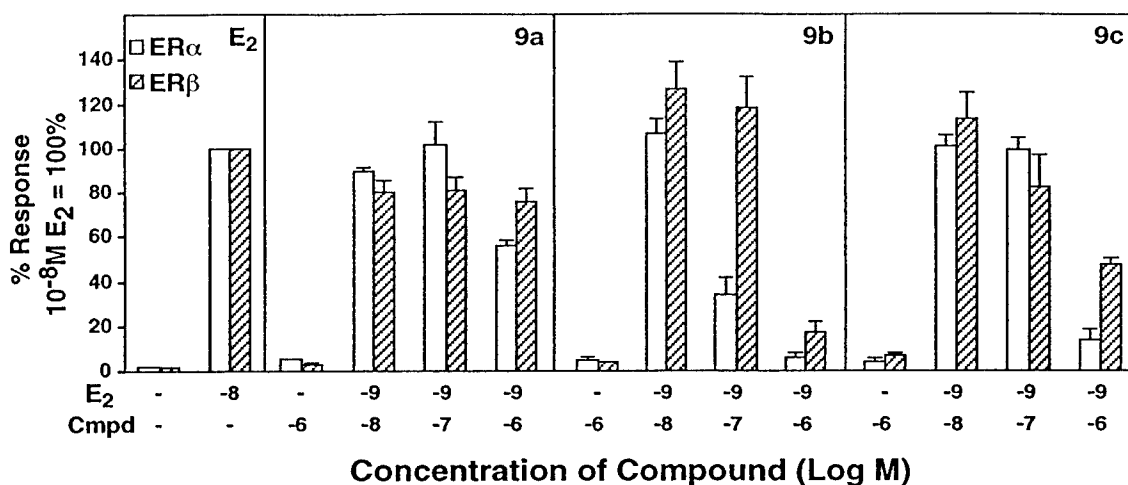
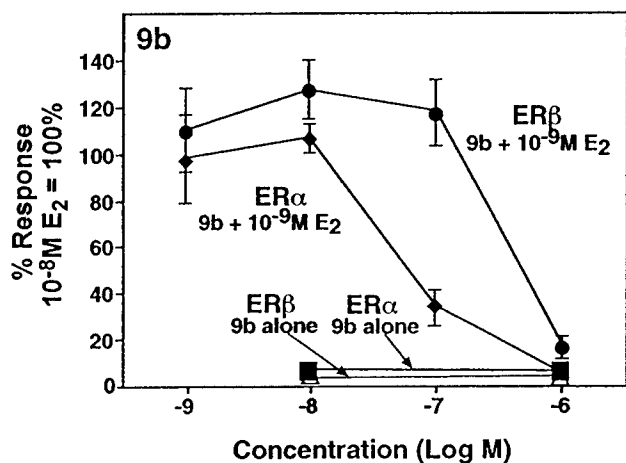**Figure 3.** Transcriptional activity of the BSC-furans 9a-c and their antagonism of estradiol activity through ERα

Figure 4. Full dose-response, showing that the ERα-selective antagonism of BSC-furan **9b**.

these BSC-furans bind to ERα with the C(5) phenol playing the role of the important A-ring of estradiol; we had reached a similar conclusion with the BSC-pyrazoles.[3] It is of note in both the furan and pyrazole series that the parent ligands appear to bind in a different orientation than do the BSC-derivatives, placing the C(2) phenol of the furan (and the corresponding phenol of the pyrazole) in the A-ring binding pocket. The BSC derivatives of ERα-selective ligands should prove to be useful agents to investigate the biological functions of the two ER subtypes.

Acknowledgments

References

1. Mortensen, D. S.; Rodriguez, A. L.; Carlson, K.; Sun, J.; Katzenellenbogen, B. S.; Katzenellenbogen, J. A. *J. Med. Chem.* **2001**, *submitted.*

2. Huang, Y.; Katzenellenbogen, J. A. *Org Lett* **2000**, *2*, 2833-2836.

3. Stauffer, S. R.; Huang, Y. R.; Aron, Z. D.; Coletta, C. J.; Sun, J.; Katzenellenbogen, B. S.; Katzenellenbogen, J. A. *Bioorg. Med. Chem.* **2001**, *9*, 151-161.

4. Grese, T. A.; Dodge, J. A. *Current Pharmaceutical Design* **1998**, *4*, 71-92.

5. Shaiu, A. K.; Barstad, D.; Loria, P. M.; Cheng, L.; Kushner, P. J.; Agard, D. A.; Greene, G. L. *Cell* **1998**, *95*, 927-937.

6. Brzozowski, A. M.; Pike, A. C. W.; Dauter, Z.; Hubbard, R. E.; Bonn, T.; Engstrom, O.; Ohman, L.; Greene, G. L.; Gustafsson, J.-Å.; Carlquist, M. *Nature* **1997**, *389*, 753-758.

7. Carlson, K. E.; Choi, I.; Gee, A.; Katzenellenbogen, B. S.; Katzenellenbogen, J. A. *Biochemistry* **1997**, *36*, 14897-14905.

8. Meyers, M. J.; Sun, J.; Carlson, K. E.; Katzenellenbogen, B. S.; Katzenellenbogen, J. A. *J. Med. Chem.* **1999**, *42*, 2456-2468.

9. Anstead, G. M.; Carlson, K. E.; Katzenellenbogen, J. A. *Steroids* **1997**, *62*, 268-303.

10. Sun, J.; Meyers, M. J.; Fink, B. E.; Rajendran, R.; Katzenellenbogen, J. A.; Katzenellenbogen, B. S. *Endocrinology* **1999**, *140*, 800-804.

11. Sun, J.; Huang, Y. R.; Katzenellenbogen, J. A.; Katzenellenbogen, B. S. *Bioorg. Med. Chem. Lett.* **2001**, *In preparation.*

12. Stauffer, S. R.; Coletta, C. J.; Tedesco, R.; Sun, J.; Katzenellenbogen, B. S.; Katzenellenbogen, J. A. *J. Med. Chem.* **2000**, *43*, 4934-4947.

Publication No. 10

ANTAGONISTS SELECTIVE FOR ESTROGEN RECEPTOR-ALPHA

Jun Sun,[a] Ying R. Huang,[b] William R. Harrington,[a] Shubin Sheng,[a] Benita S. Katzenellenbogen,[a]

and John A. Katzenellenbogen*[b]

[a]Department of Molecular and Integrative Physiology

[b]Department of Chemistry

University of Illinois and University of Illinois College of Medicine

Urbana, IL 61801

(Soon to be) Submitted to: *Endocrinology*

Address Correspondence to:
John A. Katzenellenbogen
Department of Chemistry
University of Illinois
600 South Mathews Avenue
Urbana IL 61801
217 333 6310 (phone)
217 333 7325 (fax)
jkatzene@uiuc.edu

Abstract

By adding basic side chains typically found in non-steroidal antiestrogens, to pyrazoles that are very selective estrogen receptor alpha (ERα) agonists, we have developed compounds that are high affinity, potent antagonists on ERα, and are essentially inactive on ERβ. When such compounds are used together with estradiol, which activates both ERα and ERβ, one can achieve selective stimulation of ERβ. These compounds should be useful in studying the biological functions of ERβ and in selectively blocking responses that are mediated through ERα.

Introduction

The action of estrogens in regulating gene transcription is mediated through two estrogen receptor subtypes, ERα and ERβ.[1,2] While both of these receptors function as ligand-modulated transcription factors, their tissue distributions are quite different,[1,2] and the activity of estrogens of varying structure is not always the same on the two subtypes.[3,4] Thus, it is likely that the biological roles of ERα and ERβ are different, but the nature and importance of these differences are still open questions.

The generation of ERα and ERβ knockout animals has provided much information about the function of these ER subtypes.[5] Another approach has been the development of ER subtype-selective ligands. Coming to a good understanding of the key biological roles of ERα and ERβ will be important for understanding the action of natural estrogens and for developing synthetic selective estrogen receptor modifiers (SERMs)[6,7] that are needed to optimally regulate fertility and menopausal hormone replacement, and to prevent and treat hormone-responsive breast cancer.

We have developed compounds that are capable of stimulating ERα very selectively. Members of the triarylpyrazole class, such as propylpyrazole triol (**PPT**), are more than 1000-fold

1

2

more potent on ERα than on ERβ[8] and certain tetrahydrochrysenes, such as R,R-diethyl-THC that we have developed, are nearly full to full agonists on ERα but pure antagonists on ERβ.[9,10] These two ligands could be classified as "ERα potency selective" and "ERα efficacy selective" compounds, respectively; in both cases, however, these compounds activate ERα in preference to ERβ.

From what has been published, it appears that it is more difficult to develop ligands that stimulate ERβ to a greater extent than ERα. Certain phytoestrogens, such as genistein, are somewhat more potent on ERβ than ERα,[3,4] but their selectivity towards ERβ is more limited than is the selectivity of PPT towards ERα, for example.[8] We have also developed some synthetic ligands, bisbenzylnitriles and related compounds, that have up to 50-fold potency selectivity on ERβ.[10] However, as far as we are aware, no compounds thus far described have higher efficacy on ERβ than ERα, that is, are more agonistic on ERβ than they are on ERα.

In this report, we take a different approach to the development of ERβ-selective ligands, the investigation of *antagonists that are more potent on ERα than on ERβ*. Such compounds, when used together with a subtype non-selective agonist such as estradiol, should result in selective ERβ stimulation, because they would block the agonism of estradiol on ERα, but not on ERβ. The compounds we have investigated are derivatives of the very ERα potency-selective triaryl-substituted pyrazole ligands, of which **PPT** is an example, into which we have introduced basic side chain (BSC) substituents, typical of those found in antiestrogens such as tamoxifen and raloxifene. In this report, we describe the transcriptional activity of these BSC-pyrazoles and the optimization of their selectivity as ERα potency-selective antagonists.

Results

Structure and Synthesis of Basic Side Chain Pyrazoles — In earlier reports, we identified a single position on the triarylpyrazoles where the BSC substitution is well tolerated by the ERs, namely, the C(5) phenol group,[11] and we developed a regioselective route to prepare these compounds efficiently.[12]

The structures of the BSC pyrazoles that we have studied are shown in **Figure 1** (See Fig. 1 legend for a simple nomenclature nemonic for these pyrazole systems). Those that we prepared first (**I-(A-G)-Et**) exemplified various basic side chains placed on our initially discovered 4-ethyl-triaryl ERα-selective pyrazole **I**.[8,13] Once we had identified the most promising basic side chains (**A**, **C**, and **E**, see below), we explored other C(4) substituents on this core system (methyl (**A,C,E**) and in one case propyl (**A**)).

ERα and ERβ Binding Selectivity of Basic Side Chain Pyrazoles — The binding affinities of the BSC-pyrazoles for ERα and ERβ, determined in a radiometric competitive binding assay,[14] are listed in Table 1. All of the affinities are expressed as Relative Binding Affinity (RBA) values, where the RBA of estradiol is 100.

As seen in Table 1, all of the compounds investigated had ERα binding affinity selectivity, with some showing ERα/ERβ selectivity ratios of 100–400. It is instructive to compare the ERα binding affinity and selectivity of these BSC-pyrazoles to those of the parent triaryl pyrazoles (i.e.. R = H instead of the basic side chain): The free phenols have ERα RBA values of 5.4 to 51 and ERα/ERβ ratios of 80 to 390; interestingly, the BSC analogs can reach similar levels of ERα selectivity (ERα/ERβ ratio of 220), and they show similar binding affinity for ERα.

Although we have not explored these series exhaustively, where comparisons can be made, the ERα/ERβ affinity ratio reaches a maximum with a smaller C(4) substituent in the BSC analogs

than in the triphenol series (compare pyrazole triols **I**, where the propyl analog **PPT** has the highest ratio, with BSC-pyrazoles **I-A**, where the methyl analog has the highest). This may reflect differences in the way in which triphenolic and BSC-pyrazoles are oriented in the ligand binding pockets of the ERs (see Discussion).

ERα and ERβ Transcriptional Selectivity of Basic Side Chain Pyrazoles —To evaluate which basic side chains were effective in converting the pyrazoles into ER antagonists, we first screened the activity of the seven BSC-pyrazoles having C(4)-ethyl substituents as agonists or as antagonists of estradiol-induced transcription through ERα and ERβ by a cotransfection assay, using a simple single-concentration regimen. Expression plasmids for ERα and ERβ (pCMV5-ERα and pCMV5-ERβ), together with an estrogen-responsive reporter gene plasmid (3ERE-pS2-CAT) containing three estrogen response elements and the promoter from the pS2 gene, and a control plasmid (pCMV5-βgal), were transfected into human endometrial cancer (HEC-1) cells. The results of these single-concentration assays are summarized in Figure 2.

None of the seven C(4)-ethyl BSC-pyrazoles was a transcriptional agonist on either ERα or ERβ; all were transcriptional antagonists. Several of them showed considerable ER-subtype selectivity, being more potent on ERα than on ERβ, and we selected three of these (piperidinyl (**A**), pyrrolidino (**C**), diethylamino (**E**)) for more extensive dose-response studies, together with their analogs having different C(4)-alkyl substituents. These data are shown in Figures 3 and 4.

Antagonist dose response curves for the three BSC-pyrazoles with C(4)-ethyl and C(4)-methyl substituents are shown in Figures 3A and 3B, respectively. Comparison of the C(4)-ethyl series (Fig. 3A) with the C(4)-methyl series (Fig. 3B), shows, in each case, that the methyl series is more selective. Within the C(4)-methyl series (Fig. 3B), the piperidinyl analog (**A**) appears to be both a more potent and a more complete antagonist with ERα selectivity than the two other analogs.

Thus, of these six compounds, **I-A-Me** appears to be most selective as an ERα antagonist (cf. Fig. 3B). A final evaluation of piperidinyl congeners (**A**) having three different C(4) substituents (methyl, ethyl and propyl), shown in Figure 4, demonstrates again that in terms of both antagonist potency and ERα selectivity, the best compound compound is **I-A-Me**. It is of note that, overall, there is a reasonable correlation between the selectivity of these BSC pyrazoles for ERα in terms of their binding affinity and their potency as antagonists.

The activity of the most ERα-selective antagonist, pyrazole **I-A-Me**, that we have termed **MPP**, as an abbreviation for "methyl-piperidino-pyrazole", was evaluated further in a different estrogen-responsive reporter gene construct, NHERF/EBP50-Luc (which containing the 5'-flanking region of the sodium-hydrogen exchanger regulatory factor/ezrin-radixin-moesin binding protein 50; Fig. 5).[15,16] Even at high (1μM) concentrations, **MPP** had no stimulatory activity on ERα or ERβ, and it fully inhibited ERα activity by estradiol in a concentration-dependent manner. while having little to no suppressive activity on ERβ stimulation by estradiol.

To evaluate the ability of **MPP** to suppress ERα stimulation of an endogenous gene. we monitored its effectiveness in blocking estradiol induction of pS2 mRNA production in MCF-7 breast cancer cells, which are known to contain high levels of ERα and minimal if any ERβ. As seen in Figure 6, **MPP** was effective in suppressing pS2 mRNA induction by 1 nM estradiol. Full suppression required rather high concentrations of MPP (10μM); however, at this concentration. induction was suppressed to the control level and was equivalent to the suppression by 1 μM of ICI 182,780. Thus, MPP is effective in blocking the stimulation of endogenous genes by estradiol through ERα.

Discussion

Typical estrogen antagonists, such as tamoxifen (Nolvadex®), raloxifene (Evista®), and ICI 182,780 (Faslodex®), block estrogen action with equal or rather equal potency through the two estrogen receptor subtypes, ERα and ERβ. We have been able to develop estrogen antagonists that are ERα selective by starting with triarylpyrazoles, a class of ER agonists that we have previously shown to be highly ERα-selective agonists, by introducing basic side chain (BSC) substituents on the C(5) phenol. These BSC-pyrazole antagonists all maintain significant affinity and potency selectivity for ERα, which in the best case (MPP) is very high. Thus, as shown in Figure 3 and 4, with MPP at 1 μM we can antagonize the effect of 1 nM estradiol in activating ERα essentially completely, with only ca. 15% inhibition of the activation of ERβ. The development of these antagonists that are more potent on ERα than on ERβ represents a significant advance in the preparation of ER subtype selective ligands, because when these compounds are used together with estradiol, they would allow estradiol stimulation only via ERβ.

Within the BSC pyrazole series, there is a reasonably good correlation between their ERα selectivity in terms of binding affinity vs antagonist potency. What is interesting in this comparison is that the C(4)-alkyl substituent that gives the highest selectivity for the basic side chain antagonists, namely a *methyl* group as in MPP, is smaller than the C(4)-*propyl* group needed to get the highest ERα/ERβ selectivity in the triarylpyrazole *agonist* series. We believe that this is due to differences in how these two classes of ligands are oriented in the ligand binding pocket of ERα,[8,11,17] so that this alkyl substituents project into different regions of the pocket in the triaryl pyrazoles than in the BSC pyrazoles. As a result, groups of different size are required to obtain the highest selectivity in binding in the agonist vs antagonist series.

It is of note that we also prepared BSC analogs of pyrazoles in an isomeric series (i.e., 1,3,4-triaryl-5-alkyl, with the BSC on the 4-aryl group; not shown)[17]. As was true for parent pyrazoles in this series, the corresponding BSC derivatives were selective for ERα in terms of affinity and antagonist potency, but they are not as selective as MPP (data not shown).

The availability of a compound such as the ERα-selective antagonist MPP provides a new tool for investigating the biological function of the two ER subtypes. It can be used by itself to selectively turn off or block responses that might be mediated through ERα, or it can be used together with an ER-subtype non-selective agonist, such as estradiol, to achieve selective stimulation of ERβ. This compound could also be paired with an ERβ agonist, even if the latter is only moderately selective, to achieve highly selective stimulation via only ERβ. We anticipate that this compound will be useful as an agent to investigate the biological functions of the less well understood estrogen receptor, ERβ, in diverse cells and tissues in which ERβ is expressed.

Materials and Methods

Chemicals, materials, and plasmid constructions

Cell culture media were purchased form Gibco BRL (Grand Island, NY). Calf serum was obtained from Hyclone Laboratories, Inc. (Logan, UT), and FCS was purchased from Atlanta Biologicals (Atlanta, GA). ^{14}C-Chloramphenicol (50-60 Ci/mmol) was from DuPont, NEN Research Products (Boston, MA). ICI 182,780 was kindly provided by Dr. Alan Wakeling, Zeneca Pharmaceuticals, Macclesfield, UK. Luciferase reporter assay system was from Promega (Madison, WI). The expression vector for human ERα (pCMV5-hERα) was constructed previously as described. The expression vector pCMV5-ERβ was constructed by inserting the cDNA encoding the full length human ERβ (530 residues) or the short form of human ERβ (477 residues), into the
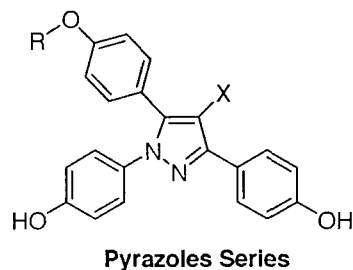
Real-time PCR analysis

The total RNA from MCF-7 cells was isolated using TRIzol® reagent (Life Technologies, Rockville, MD) according to the manufacturer's suggestion. 1 μg of total RNA was reverse transcribed using GeneAmp® RNA PCR kit (Applied Biosystem, Foster City, CA). 1/100 of each cDNA products were subjected to the real-time PCR analysis on ABI PRISM 7700 sequence detection system using TaqMan® universal PCR master mix (Applied Biosystem, Foster City, CA). The pS2 cDNA was amplified with the primers pS2f (5' GCGCCCTGGTCCTGGTGTCCAT 3') and pS2r (5' GAAAACCACAATTCTGTCTTTCAC 3') and was detected by the probe 6FAM-CCCAGACAGAGACGTGTACAGTGGCCC-TAMRA. The GAPDH was used as the internal control which was amplified with the primers GAPDHf (5' GAAGGTGAAGGTCGGAGTC 3') and GAPDHr (5' GAAGATGGTGATGGGATTTC 3'). The signal was detected by the probe 6FAM-CAAGCTTCCCGTTCTCAGCC-TAMRA. Comparative C_T method was used to determine the relative expression level of pS2 mRNA.
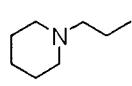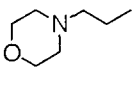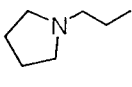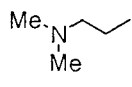
BamHI site of pCMV5. The estrogen responsive reporter plasmids were (ERE)₃-pS2-CAT, constructed as described previously. (ERE)₂-pS2-Luc, constructed by inserting (ERE)₂-pS2 fragment from (ERE)2-pS2-CAT into the *MluI/BglII* sites of pGL3-Basic vector (Promega, Madison, WI). NHERF-Luc, constructed by inserting human NHERF promoter fragment (containing −2985 to +496 bp of human NHERF gene) into the *KpnI/XhoI* sites of pGL3-Basic vector. The plasmid pCMVβ (Clontech, Palo Alto, CA) which contains the β-galactosidase gene, was used as an internal control for transfection efficiency.

Cell culture and transient transfections

Human endometrial cancer (HEC-1) cells were maintained in culture as described. Transfection of HEC-1 cells in 24-well plate used a mixture of 0.35 ml of serum-free IMEM media and 0.15 ml of HBSS containing 5 μl of lipofectin (Life Technologies, Rockville, MD), 1.6 μg of transferrin (Sigma, St. Louis, MO), 0.5 μg of pCMVβ as internal control, 1 μg of the reporter gene plasmid, 100 ng of ER expression vector, and carrier DNA to a total of 2.5 μg DNA, applying them to each well. The cells were incubated at 37°C in a 5% CO_2 containing incubator for 6 h. Fresh media containing desired concentrations of ligands were added to each well. Reporter gene activity was assayed after 24 h incubation. CAT and luciferase activity, normalized for the internal control β-galactosidase activity, were assayed as described.

MCF-7 cells were maintained in culture as described. About 0.3 × 10⁶ cells were seeded into each well of a 6-well plate with phenol red free media. After 3 days, fresh media containing desired concentration of ligands were added to each well. 24 h later, the cells were harvested for RNA extraction.

References

(1) Kuiper, G. G. J. M.; Enmark, E.; Pelto-Huikko. M.; Nilsson. S.; Gustafsson. J. Å. Cloning of a novel receptor expressed in rat prostate and ovary. Proc. Natl. Acad. Sci. U.S.A. **1996.** 93, 5925-5930.

(2) Mosselman. S.; Polman. J.; Dijkema. R. ERβ: identification and characterization of a novel human estrogen receptor. FEBS **1996.** 392, 49-53.

(3) Kuiper, G. G. J. M.; Carlsson, B.; Grandien. K.; Enmark. E.; Häggblad. J.; Nilsson. S.; Gustafsson. J.-Å. Comparison of the ligand binding specificity and transcript tissue distribution of estrogen receptor α and β. Endocrinology **1997.** 138, 863-870.

(4) Barkhem. T.; Carlsson, B.; Nilsson. Y.; Enmark. E.; Gustafsson. J.; Nilsson. S. Differential response of estrogen receptor α and estrogen receptor β to partial estrogen agonists/antagonists. Mol. Pharmacol. **1998.** 54, 105-112.

(5) Couse, J. F.; Korach. K. S. Estrogen receptor null mice: what have we learned and where will they lead us? Endocr. Rev. **1999,** 20, 358-417.

(6) McDonnell. D. P. The molecular pharmacology of SERMs. Trends Endocrinol. Metab. **1999,** 10, 301-311.

(7) Katzenellenbogen, B. S.; Katzenellenbogen. J. A. Estrogen receptor alpha and estrogen receptor beta: Regulation by selective estrogen receptor modulators (SERMs) and importance in breast cancer. Breast Cancer Res. **2000,** 2, 335-344.

(8) Stauffer, S. R.; Coletta, C. J.; Tedesco, R.; Sun, J.; Katzenellenbogen, B. S.; Katzenellenbogen. J. A. Pyrazole Ligands: Structure-Affinity/Activity Relationships Of Estrogen Receptor-α Selective Agonists. J. Med. Chem. **2000,** 43, 4934-4947.

(9) Sun. J.; Meyers. M. J.; Fink. B. E.; Rajendran. R.; Katzenellenbogen. J. A.; Katzenellenbogen, B. S. Novel Ligands that Function as Selective Estrogens or Antiestrogens for Estrogen Receptor-α or Estrogen Receptor-β. Endocrinology **1999.** 140, 800-804.

(10) Meyers. M. J.; Sun, J.; Carlson, K. E.; Katzenellenbogen. B. S.; Katzenellenbogen. J. A. Estrogen Receptor Subtype-Selective Ligands: Asymmetric Synthesis and Biological Evaluation of cis- and trans-5, 11-Dialkyl-5,6,11,12-tetrahydrochrysenes. J. Med. Chem. **1999.** 42, 2456-2468.

(11) Stauffer, S. R.; Huang. Y. R.; Aron. Z. D.; Coletta. C. J.; Sun. J.; Katzenellenbogen. B. S.; Katzenellenbogen. J. A. Triarylpyrazoles with Basic Side Chains: Development of Pyrazole-Based Estrogen Receptor Antagonists. Bio. Med. Chem. **2001,** 9, 151-161.

(12) Huang. Y.; Katzenellenbogen. J. A. Regioselective Synthesis of 1,3,5-Triaryl-4-alkylpyrazoles: Novel Ligands for the Estrogen Receptor. Org Lett **2000.** In press.

(13) Fink. B. E.; Mortensen. D. S.; Stauffer, S. R.; Aron. Z. D.; Katzenellenbogen. J. A. Novel Structural Templates for Estrogen-Receptor Ligands and Prospects for Combinatorial Synthesis of Estrogens. Chem. Biol. **1999,** 6, 205-219.

(14) Carlson. K. E.; Choi, I.; Gee, A.; Katzenellenbogen, B. S.; Katzenellenbogen. J. A. Altered ligand binding properties and enhanced stability of a constitutively active estrogen receptor: Evidence that an open pocket conformation is required for ligand interaction. Biochemistry **1997,** 36, 14897-14905.

(15) Ediger, T. R.; Kraus, W. L.; Weinman. E. J.; Katzenellenbogen. B. S. Estrogen receptor regulation of the Na+/H+ exchange regulatory factor. Endocrinology **1999,** 140, 2976-2982.

(16) Ediger, T. R.; Park, S.-E.; Katzenellenbogen, B. S. In 82nd Annual Meeting of the Endocrine Society Toronto, Canada, 2000, p 120.

Pyrazoles Series

Cpd. No.	R	X		RBA		
				ERα	ERβ	ERα/ERβ
I	H-	Me-		5.4	0.039	140
		Et-		36	0.15	240
		Pr-	[PPT]	51	0.13	390
		Bu-		14	0.18	78
I-A	(piperidinylpropyl)	Me-	[MPP]	11	0.05	220
		Et-		12	0.65	18
		Pr-		6.8	0.54	13
I-B	(morpholinylpropyl)	Et-		9.5	0.08	120
I-C	(pyrrolidinylpropyl)	Me-		1.2	0.05	24
		Et-		16	0.17	94
I-D	Me-N(Me)-propyl	Et-		9.1	0.64	14
I-E	Et-N(Et)-propyl	Me-		7.8	0.05	156
		Et-		17	0.17	100
I-F	(pyrrolidinonylpropyl)	Et-		13	0.43	30
I-G	HO-CH(OH)-propyl	Et-		7.0	0.25	28

Ar = *p*-hydroxyphenyl

Figure 1. Structures and estrogen receptor alpha and beta (ERα and ERβ) binding affinities of pyrazoles and basic side chain (BSC) pyrazoles. Binding affinities are determined in a radiometric competitive binding assay, using [³H]estradiol as tracer and hydroxylapatite to adsorb ligand-receptor complex. Receptor preparations were human ERα and ERβ, expressed in baculovirus and purified (PanVera). Values represent the mean of 2-3 repeat determinations (CV 0.3). Note that a simple compound numbering neumonic is derived from the pyrazole series (designated with a boldface Roman numeral **I**), the nature of the basic side chain (designated as a boldface uppercase letter **A-E**, as noted in the figure), and the nature of the C(4) substituent (boldface **Me, Et, Pr**)

(17)   Stauffer, S. R.; Huang, Y. R.; Coletta, C. J.; Tedesco, R.; Katzenellenbogen, J. A. *Estrogen Pyrazoles: Defining the Pyrazole Core Structure and the Orientation of Substituents in the Ligand Binding Pocket of the Estrogen Receptor. Bio. Med. Chem.* **2001**, *9*, 141-150.

(18)   Cho, H.; Ng, P. A.; Katzenellenbogen, B. S. *Differential regulation of gene expression by estrogen in estrogen growth-independent and -Dependent MCF-7 human breast cancer cell sublines. Mol Endocrinol* **1991**, *5*, 1323-1330.

(19)   Weaver, C. A.; Springer, P. A.; Katzenellenbogen, B. S. *Regulation of pS2 gene expression by affinity labeling and reversibly binding estrogens and antiestrogens: Comparison of effects on the native gene and on pS2-chloramphenicol acetyltransferase fusion genes transfected into MCF-7 human breast cancer cells. Mol. Endocrinol.* **1988**, *2*, 936-945.
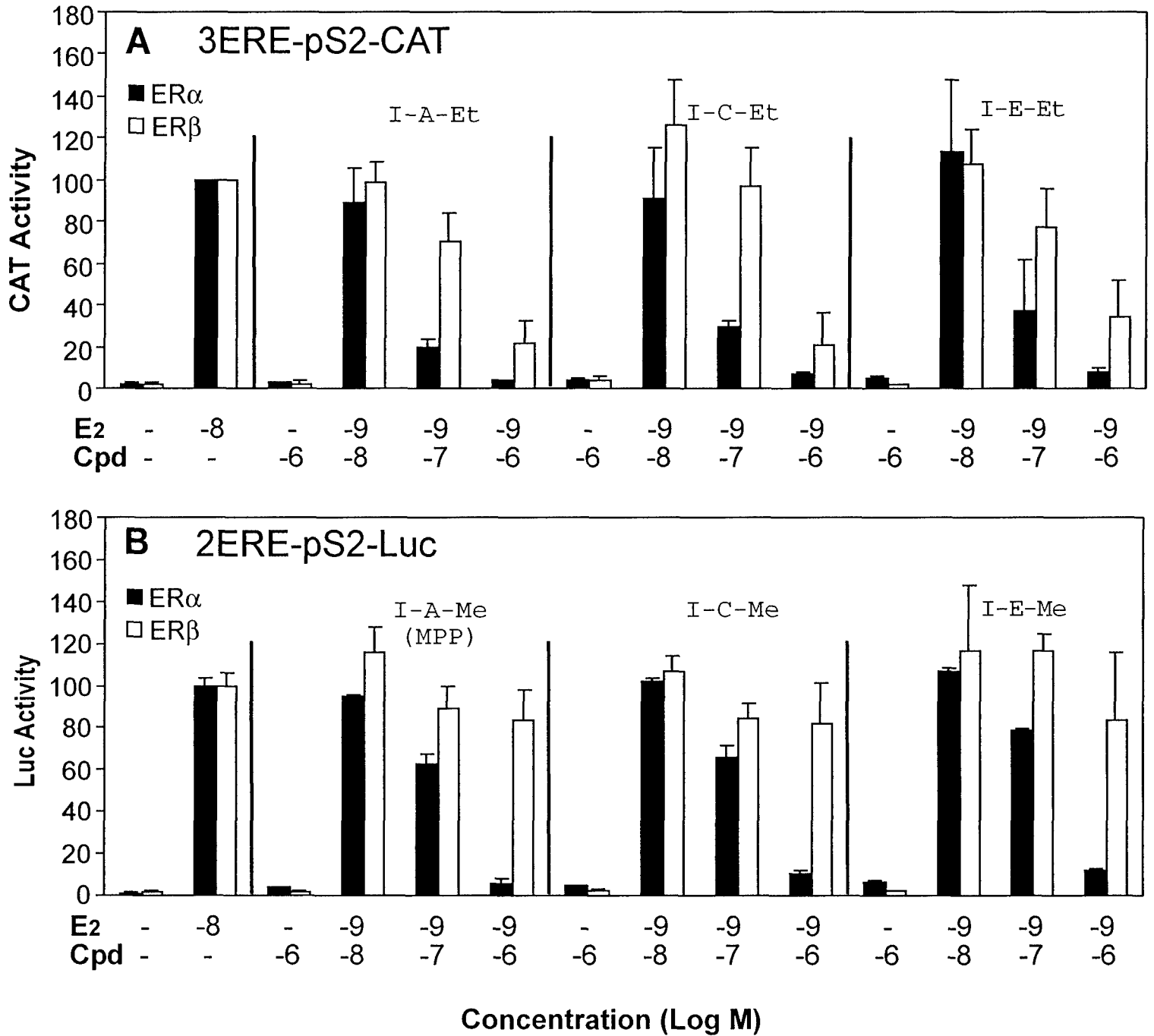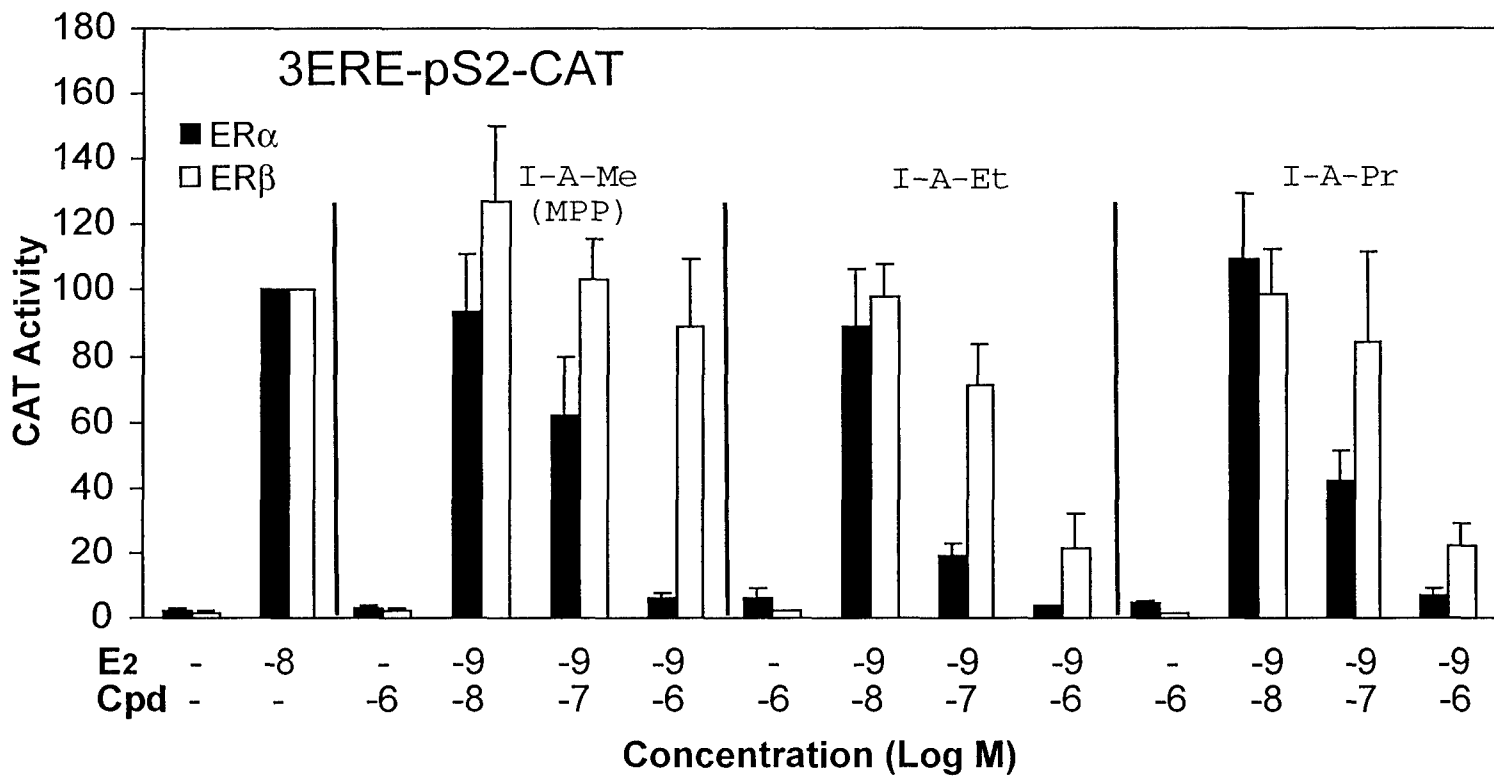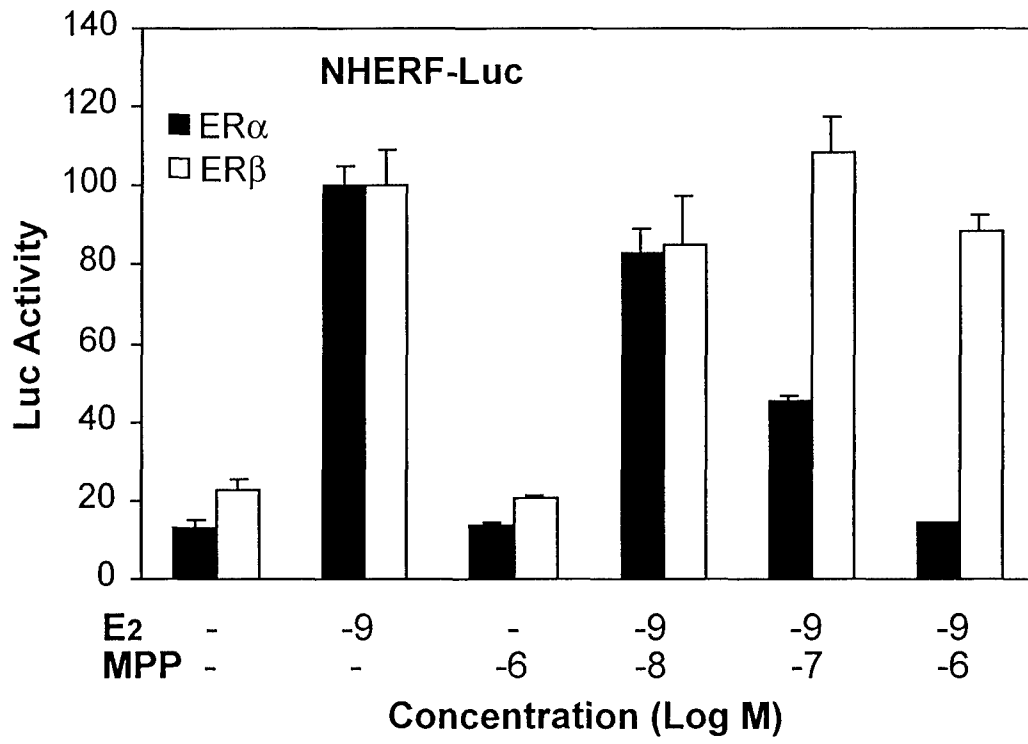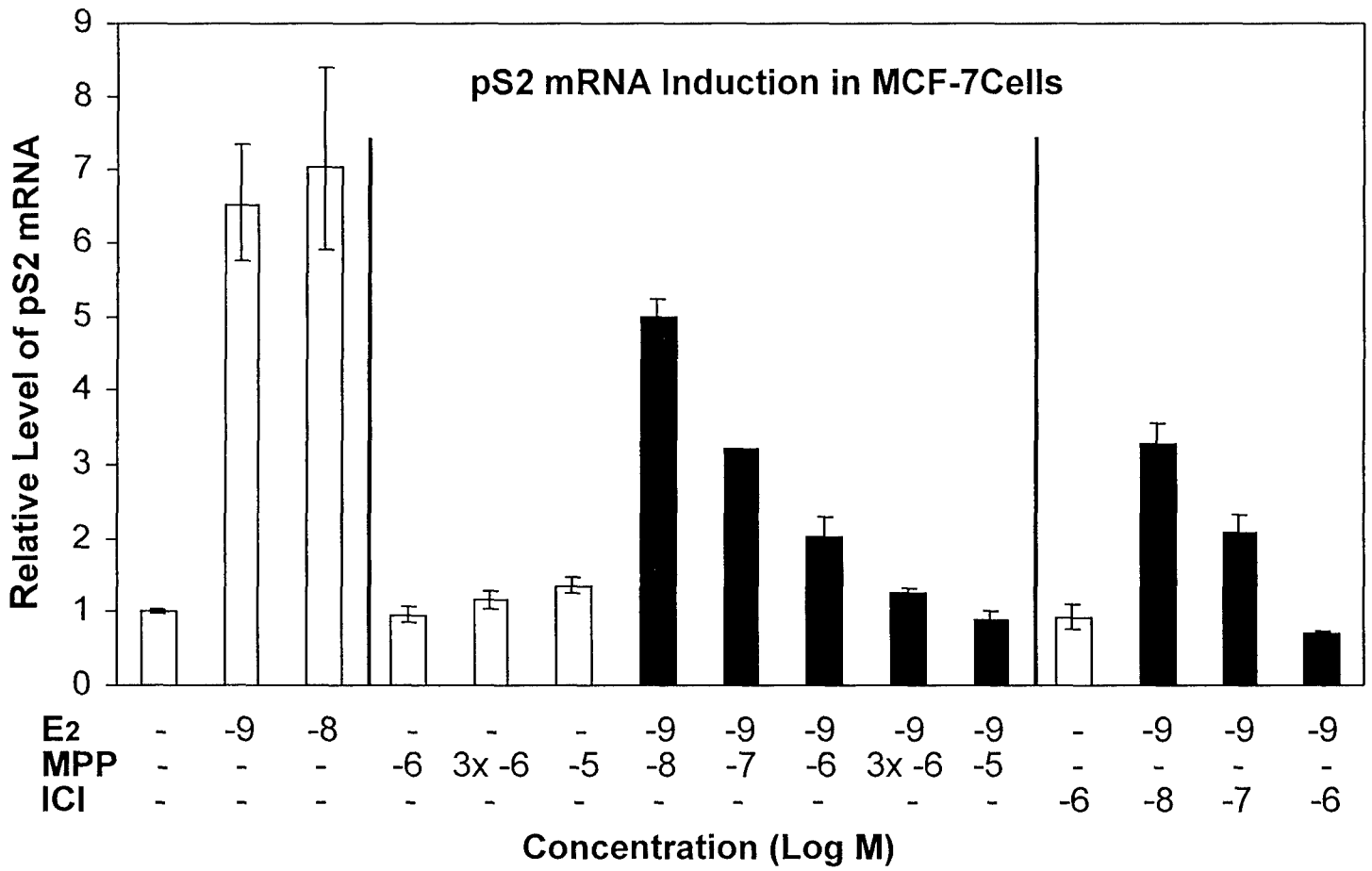
13
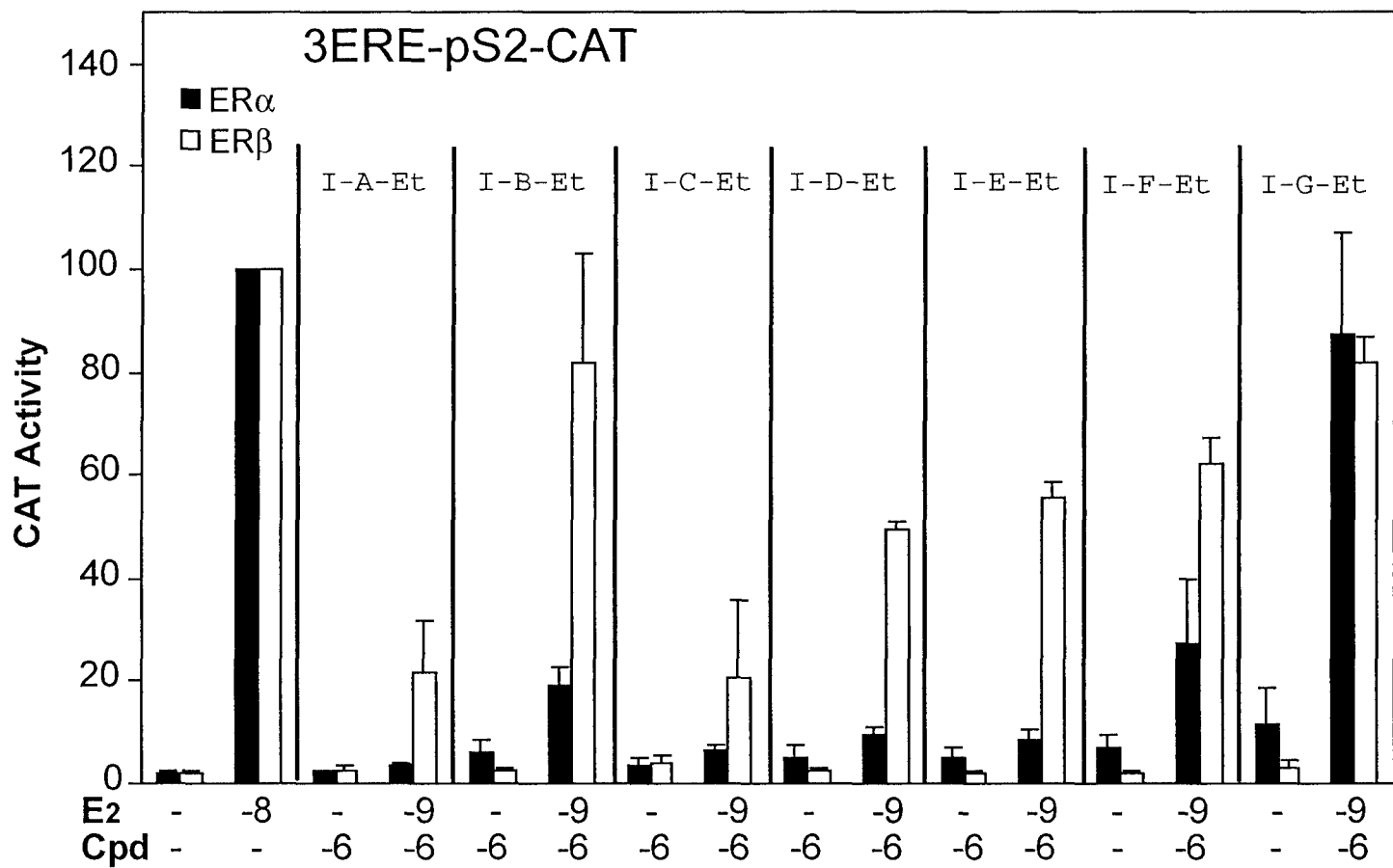
Figure 2.

Figure 3.

Figure 4.

Figure 5.

Figure 6.

MCMR-RMI-S   (70-1y)   26 Aug 02

MEMORANDUM FOR Administrator, Defense Technical Information
Center (DTIC-OCA), 8725 John J. Kingman Road, Fort Belvoir,
VA   22060-6218

SUBJECT: Request Change in Distribution Statement

1.   The U.S. Army Medical Research and Materiel Command has
reexamined the need for the limitation assigned to technical
reports written for this Command. Request the limited
distribution statement for the enclosed accession numbers be
changed to "Approved for public release; distribution unlimited."
These reports should be released to the National Technical
Information Service.

2.   Point of contact for this request is Ms. Kristin Morrow at
DSN 343-7327 or by e-mail at Kristin.Morrow@det.amedd.army.mil.

FOR THE COMMANDER:

Encl   PHYLIS M. RINEHART
                                       Deputy Chief of Staff for
                                          Information Management

ADB274369
ADB256383
ADB264003
ADB274462
ADB266221
ADB274470
ADB266221
ADB274464
ADB259044
ADB258808
ADB266026
ADB274658
ADB258831
ADB266077
ADB274348
ADB274273
ADB258193
ADB274516
ADB259018
ADB231912
ADB244626
ADB256677
ADB229447
ADB240218
ADB258619
ADB259398
ADB275140
ADB240473
ADB254579
ADB277040
ADB249647
ADB275184
ADB259035
ADB244774
ADB258195
ADB244675
ADB257208
ADB267108
ADB244889
ADB257384
ADB270660
ADB274493
ADB261527
ADB274286
ADB274269
ADB274592
ADB274604

ADB274596
ADB258952
ADB265976
ADB274350
ADB274346
ADB257408
ADB274474
ADB260285
ADB274568
ADB266076
ADB274441
ADB253499
ADB274406
ADB262090
ADB261103
ADB274372